

**FORMULATION, OPTIMIZATION AND EVALUATION
OF MICROWAVE ASSISTED ACRYLAMIDE GRAFTED
COPOLYMER AS NOVEL MATRIX FOR SUSTAINED
RELEASE TABLETS**

A Thesis

Submitted in partial fulfillment of the requirements for the
award of the degree of

**DOCTOR OF PHILOSOPHY
IN
PHARMACEUTICAL SCIENCES**

By

Mohit Kumar

(41600044)

Supervised By

Dr. Surajpal Verma

Co-Supervised By

Dr. Narendra Kumar Pandey



LOVELY PROFESSIONAL UNIVERSITY

PUNJAB

2021

DECLARATION

I, declare that the thesis entitled “**FORMULATION, OPTIMIZATION AND EVALUATION OF MICROWAVE ASSISTED ACRYLAMIDE GRAFTED COPOLYMER AS NOVEL MATRIX FOR SUSTAINED RELEASE TABLETS**” has been prepared by me under the supervision of **Dr. Surajpal Verma**, Assistant Professor, Delhi Pharmaceutical Sciences and Research University, New Delhi and co-supervision of **Dr. Narendra Kumar Pandey**, Professor, School of Pharmaceutical Sciences, Lovely Professional University, Phagwara, Jalandhar, India. No part of this thesis has formed the basis for the award of any degree or fellowship previously.

Mohit Kumar

Research Scholar (41600044),
School of Pharmaceutical Sciences,
Lovely Professional University,
Phagwara, Jalandhar, Pb., India 144 411

Date:

CERTIFICATE

This is to certify that **Mohit Kumar** has prepared his thesis entitled “**FORMULATION, OPTIMIZATION AND EVALUATION OF MICROWAVE ASSISTED ACRYLAMIDE GRAFTED COPOLYMER AS NOVEL MATRIX FOR SUSTAINED RELEASE TABLETS**” for the award of Ph.D. degree of Lovely Professional University, under our guidance. He has carried out the work at the School of Pharmaceutical Sciences, Lovely Professional University and Pharmaceutical Research Lab, Rajendra Institute of Technology and Sciences, Sirsa, Haryana.

Dr. Surajpal Verma

(Supervisor)

M. Pharm. Ph.D.,

Assistant Professor,

School of Pharmaceutical Sciences,

Delhi Pharmaceutical Sciences and

Research University, New Delhi

INDIA 110017

Dr. Narendra Kumar Pandey

(Co-Supervisor)

M. Pharm. Ph.D.,

Professor,

School of Pharmaceutical Sciences,

Lovely Professional University,

Phagwara, Jalandhar, Pb.,

INDIA 144 411

Date:

ABSTRACT

Natural polysaccharides have been widely used as food and pharmaceutical excipients because of their biodegradability, biocompatibility, ease of availability, and low cost. They do, however, have some constraints that limit their use, such as inconsistent hydration, viscosity fluctuations during storage, pH-dependent solubility and a reduced shelf life. Chemical modification of natural polymers can address these disadvantages. Natural polymers can be chemically modified in a variety of ways, including etherification, graft copolymerization and cross-linking. Natural polysaccharide modification has recently gained a lot of interest. Among the methods of polysaccharide modification, grafting is one of the most promising strategy for imparting a variety of functional groups to polysaccharides. Gum grafting with synthetic polymers can be used to develop new materials with improved release properties.

The purpose of this research was to synthesize, describe, and assess the drug release behavior of a graft copolymer comprising acrylamide and natural gum from Rumi mastagi and banana peel. Furthermore, the in vitro release pattern of graft copolymer was compared to that of ungrafted gum by employing the model drug to create sustained release matrix tablets.

Acrylamide grafted Mastic gum and banana peel gum were prepared by Microwave assisted method. The optimization of acrylamide grafting on Mastic and banana peel gums was achieved using a box behnken design where acrylamide amount, temperature and initiator concentration were used as independent variables and % yield, % grafting and grafting efficiency were used as dependent variables. The lamivudine sustained release matrix tablets were made by combining the drug, polymer, diluent, and lubricant.

The randomly selected tablets from each batch of grafted and ungrafted gum were evaluated for weight variation, hardness, friability and drug content. All the parameters were found within specified limits. The results revealed that grafting formed sustained release system.

The results also revealed that the grafted mastic gum found to be more suitable candidate as compared to grafted banana peel gum.

The data obtained from dissolution profile was fitted into various mathematical models and data was found fit best into Korsmeyer-Peppas model, indicates that drug release is mostly caused by polymer disentanglement and erosion.

Overall, recent advancements in the field of polysaccharide grafting under microwaves have enhanced awareness of the possibility of improving material performance using such techniques.

ACKNOWLEDGEMENTS

We do not accomplish anything in this world alone... and whatever happens is the result of the whole tapestry of one's life and all the weaving of individual threads from one to another that create something. The thread initiates with my supervisor **Dr. Surajpal Verma**, Assistant Professor, Delhi Pharmaceutical Sciences and Research University, New Delhi, to whom I will always be grateful for embellishing me with all his knowledge and valuable guidance. His scientific approach, patient hearing, all his appreciation and constructive criticisms made this work, to reach the goal. I owe him lots of gratitude for providing all big or small facilities required for this project and for showing me the way to true research. I am immensely grateful to my co-supervisor **Dr. Narender Kumar Pandey**, Associate Professor, School of Pharmaceutical Sciences, Lovely Professional University, Jalandhar, for his excellent scientific guidance, valuable suggestions and constructive criticism and above all for his morale boosting attitude during the period of project work. I thank him whole-heartedly for trusting me and finding me worthy to assign a project and correcting my flaws throughout my project.

My work would have been a mission unaccomplished without the facilities provided by **Dr. Monica Gulati**, Sr. Dean, Lovely Professional University, Jalandhar for providing me with necessary research experiments under their kind guidance.

I am deeply grateful to honorable chancellor **Mr. Ashok Mittal** and **Pro-chancellor Ms. Rashmi Mittal**, Lovely Professional University, Jalandhar for providing me required facilities to carry out this project.

A special & well deserve token of thanks goes to the most loveable person "**Loveleen (my wife)**" for her moral support to me. She always encouraged me during my work especially when my work was not running well or when I was not getting the result.

I find it difficult to pen down my deepest sense of indebtedness toward my **father and mother** who soulfully provided me their moral support, unbounded love & affection and the right impetus to undertake the challenge of this proportion like all other spheres of life.

My sincere thanks to **Dr. G. D. Gupta**, Director, ISF College of Pharmacy, Moga, **Dr. Shailesh Sharma**, Director, ASBASJSM College of Pharmacy, Bela, Ropar, **Mr. Sanjeev Kalra**, Administrator, Rajendra Institute of Technology & Sciences, **Dr. Vikramdeep Monga**, Assistant Professor, Central University of Punjab, Bathinda, **Mr. Raghuvir Singh**, Principal, PDM College of Pharmacy and **Dr. Neelam Sharma** for their immense support and help at each and every step of my work and teaching me numerous concepts and techniques that I encountered during the course of dissertation.

I express my thanks to **Dr. R. C. Gupta**, Prof & Head (Retd.), Department of Botany, Punjabi University, Patiala for providing me the certificate of authentication for plant specimen.

I acknowledge all my other nears & dears. I shall be failing in my duty without expressing deep sense of faith to GOD, the 'Almighty' who graced me in finishing this task.

Needless to say, errors and omissions are mine.

Date:

Mohit Kumar

LIST OF ABBREVIATIONS

Short Form	Full Form
%	Percent
% RSD	Percent Related Standard Deviation
°C	Degree Centigrade (unit of temperature)
°F	Degree Fahrenheit (unit of temperature)
°	Degree (unit of angle)
ANOVA	Analysis of variance
BP	British Pharmacopoeia
cm	Centimeter (unit of length)
C _{max}	Maximum Concentration
DSC	Differential Scanning Calorimetry
et al.,	Latin term “et alia,” meaning “and others.”
FTIR	Fourier Transform Infrared Spectroscopy
g	Gram (unit of weight)
g/mol	Gram per moles
HPLC	High Performance Liquid Chromatography
h	Hour (unit of time)
IP	Indian Pharmacopoeia
kg	Kilogram (unit of weight)
K _{o/w}	Oil/water Partition Coefficient
min	Minute (unit of time)
ml	Milliliter (unit of volume)
nm	Nanometer (unit of length)
pKa	Dissociation Coefficient
RH	Relative Humidity

s	Second (unit of time)
SD	Standard Deviation
CAN	Ceric Ammonium Nitrate
SEM	Scanning Electron Microscopy
USP	United State Pharmacopoeia
UV	Ultraviolet Spectroscopy
w/v	Weight by Volume
w/w	Weight by Weight
XRD	X-Ray Diffraction
λ_{\max}	Absorption Maxima
μm	Micro Meter (unit of length)

TABLE OF CONTENTS

S. No.	Contents	Page No.
1	Chapter 1: Introduction	1-26
	1.1 Graft Copolymerization	2-8
	1.2 Oral Dosage Forms	8-13
	1.3 Controlled and Sustained Release Systems	13-15
	1.4 Matrix Tablets	15-18
	1.5 Methods of Preparation of Matrix	18-23
	1.6 HIV and AIDS	23-26
2	Chapter 2: Review of Literature	27-59
	2.1 Drug Review	27-29
	2.2 Excipients Review	30-42
	2.3 Review on Grafting	43-51
	2.4 Review on Sustained Release Matrix Systems	52-59
3	Chapter 3: Rationale, Aim & Objectives	60-61
	3.1 Rationale of the Study	60
	3.2 Aim of the Study	60
	3.3 Objectives of the Study	60-61
4	Chapter 4: Materials & Methods	62-86
	4.1 Materials Used	62
	4.2 Equipments Used	63
	4.3 Preformulation Studies	64-67
	4.4 Drug-Excipients Compatibility Studies	67
	4.5 Synthesis and Optimization of Grafted Mastic Gum	67-71
	4.6 Synthesis and Optimization of Grafted Banana Gum	71-74
	4.7 Swelling studies of ungrafted and grafted gums	74-75
	4.8 Viscosity Measurement of ungrafted and grafted gums	75
	4.9 Compatibility studies of ungrafted and grafted	75

		mastic gum with lamivudine	
	4.10	Compatibility studies of ungrafted and grafted banana peel gum with lamivudine	75
	4.11	Preparation and Characterization of Lamivudine Matrix Tablets Using Grafted and Ungrafted Mastic and Banana Peel Gum	76-83
	4.12	Release Kinetics	83-85
	4.13	Stability Studies	85-86
5	Chapter 5: Results & Discussion		87-162
	5.1	Preformulation Studies	87-93
	5.2	Synthesis and Optimization of Grafted Mastic Gum and Banana Peel Gum	93-141
	5.3	Swelling Studies	141-142
	5.4	Viscosity Measurement	142-143
	5.5	Compatibility Studies of Ungrafted and Grafted Mastic Gum with lamivudine	143-144
	5.6	Compatibility Studies of Ungrafted and Grafted Banana Peel Gum with lamivudine	144-145
	5.7	Preparation and Characterization of Lamivudine Matrix Tablets using Grafted and Ungrafted Mastic and Banana Peel Gum	145-158
	5.8	Release Kinetics	158-160
	5.9	Stability Studies	160-162
6	Chapter 6: Summary & Conclusion		163-165
7	Chapter 7: References		166-188
8	Appendices		A1-A8

LIST OF TABLES

Table. No.	Title	Page No.
1.1	Solvents used in microwave grafting process	06
2.1	Marketed strengths and form of lamivudine	29
2.2	Physicochemical Properties of Mastic Gum	31
2.3	Properties of Banana Peel	33
2.4	Mineral composition of banana peel	34
2.5	Physicochemical Properties of Acrylamide	36
2.6	Physicochemical properties of Ceric ammonium nitrate	37
2.7	Specifications of Magnesium stearate	38
2.8	Specifications of Talc	39
2.9	Excipient Profile of Lactose	40
2.10	Excipient Profile of PVP	41
4.1	Research-related materials	62
4.2	Research-related equipments	63
4.3	Levels of Independent Variables in Box Behnken Design for mastic gum	69
4.4	Design Matrix of Box Behnken Design for mastic gum	70
4.5	Levels of Independent Variables in Box Behnken Design for banana peel gum	73
4.6	Design Matrix of Box Behnken Design for banana peel gum	73
4.7 (a)	Formulation table for matrix tablets of ungrafted mastic gum	76
4.7 (b)	Formulation table for matrix tablets of grafted mastic gum	77
4.8 (a)	Formulation table for matrix tablets of ungrafted banana peel gum	77
4.8 (b)	Formulation table for matrix tablets of grafted banana peel gum	78
4.9	Standard values of Angle of repose	79
4.10	Standard values of Carr's index	80
4.11	Standard values of Hausner's Ratio	80
4.12	Weight variation limits as per I.P.	82
4.13	Exponent of diffusion and release mechanism	85

5.1	Melting point determination of lamivudine	87
5.2	FTIR interpretation of Lamivudine	89
5.3	Qualitative solubility data of Lamivudine	89
5.4	Quantitative solubility data of Lamivudine	90
5.5	Absorption Maxima (λ_{\max}) of Lamivudine in different solvents	90
5.6	Calibration data of lamivudine drug in 0.1N HCl	91
5.7	Calibration parameter values in 0.1 N HCl	92
5.8	Calibration data of lamivudine drug in phosphate buffer (pH-6.8)	92
5.9	Calibration parameter values in phosphate buffer pH-6.8	93
5.10	Partition coefficient of Lamivudine	93
5.11	Design Matrix of BBD taking in account three responses for mastic gum	95
5.12	ANOVA Table of % Yield response for mastic gum	96
5.13	Observed and predicted values for % yield	97
5.14	ANOVA Table of % Grafting response for mastic gum	101
5.15	Observed and predicted values for % grafting	102
5.16	ANOVA Table of % Grafting efficiency response for mastic gum	106
5.17	Observed and predicted values for % grafting efficiency	107
5.18	Numerical optimization as per desirability of the process of dependent and independent variables for mastic gum	111
5.19	Optimized solutions for Grafted Mastic gum	111
5.20	Design Matrix of BBD taking in account three responses for banana peel gum	113
5.21	ANOVA Table of % Yield response for banana peel gum	114
5.22	Observed and predicted values for % yield	115
5.23	ANOVA table of % Grafting response for banana peel gum	119
5.24	Observed and predicted values for % grafting	120
5.25	ANOVA table of % Grafting Efficiency response for banana peel gum	124
5.26	Observed and predicted values for % grafting efficiency	125
5.27	Numerical optimization as per desirability of the process of dependent and independent variables for banana peel gum	128

5.28	Optimized solutions for Grafted Banana peel gum	129
5.29	Swelling Capacity of ungrafted and grafted gums	142
5.30	Viscosity of ungrafted and grafted gums	143
5.31	Precompression parameters from formulation UMA1 to UMA5 and GMA1 to GMA5	147
5.32	Precompression parameters from formulation UBA1 to UBA5 and GBA1 to GBA5	147
5.33	Post compression parameters from formulation UMA1 to UMA5 and GMA1 to GMA5	148
5.34	Post compression parameters from formulation UBA1 to UBA5 and GBA1 to GBA5	148
5.35	In-vitro release data of ungrafted mastic gum tablets	150
5.36	In-vitro release data of grafted mastic gum tablets	152
5.37	In-vitro release data of ungrafted banana peel gum tablets	153
5.38	In-vitro release data of grafted banana peel gum tablets	155
5.39	Mean dissolution time for ungrafted and grafted gum tablets	157
5.40	Different kinetic models for grafted mastic gum (GMA5)	159
5.41	Organoleptic property analysis data of sample (GMA5 tablet) kept for different time intervals	160
5.42	Drug content, Hardness and friability of sample (GMA5) kept for different time intervals	160
5.43	Drug release data of sample (GMA5) kept for different time intervals	161
5.44	Values of difference factor (f1) and similarity factor (f2) for drug release of sample (GMA5) kept for different time intervals	161

LIST OF FIGURES

Fig. No.	Title	Page No.
1.1	Structure of Polysaccharide	01
1.2	Conventional grafting techniques	03
1.3	Plasma concentration versus time profile	09
1.4	Flow diagram of direct compression technique	20
1.5	Flow diagram of wet granulation technique	21
1.6	Flow diagram of dry granulation technique	22
1.7	Structure of HIV	24
1.8	Lifecycle of HIV	25
2.1	Chemical Structure of Lamivudine	27
2.2	Mechanism of action of lamivudine	28
2.3	Chemical Structure of some important chemical constituents of Pistacia lentiscus	30
2.4	Chemical Structure of some important chemical constituents of banana peel	35
2.5	Chemical Structure of Acrylamide	35
2.6	Chemical Structure of Ceric ammonium nitrate	37
2.7	Chemical structure of Magnesium stearate	38
2.8	Chemical structure of Talc	39
5.1	DSC thermograph of lamivudine	87
5.2	FTIR spectrum of Lamivudine (Reference)	88
5.3	FTIR spectrum of Lamivudine (Test)	88
5.4	Calibration Curve of Lamivudine in 0.1 N HCl	91
5.5	Calibration Curve of Lamivudine in phosphate buffer pH-6.8	92
5.6	Schematic presentation of preparation of Acrylamide grafted Mastic gum	94
5.7	Contour Plot showing the effect of Acrylamide amount (A), and CAN amount (B) on % Yield (Y1) of mastic gum	98

LIST OF FIGURES

Fig. No.	Title	Page No.
5.8	3D Surface Response Graph showing the effect of Acrylamide amount (A), and CAN amount (B) on % Yield (Y1) of mastic gum	98
5.9	Contour Plot showing the effect of Acrylamide amount (A), and Temperature (C) on % Yield (Y1) of mastic gum	99
5.10	3D Surface Response Graph showing the effect of Acrylamide amount (A), and Temperature (C) on % Yield (Y1) of mastic gum	99
5.11	Contour Graph showing the effect of Initiator amount (B), and Temperature (C) on % Yield (Y1) of mastic gum	100
5.12	3D Surface Response Graph showing the effect of Initiator amount (B), and Temperature (C) on % Yield (Y1) of mastic gum	100
5.13	Contour Graph showing the effect of Acrylamide amount (A), and CAN amount (B) on % Grafting (Y2) of mastic gum	103
5.14	3D Surface Response Graph showing the effect of Acrylamide amount (A), and CAN amount (B) on % Grafting (Y2) of mastic gum	103
5.15	Contour Graph showing the effect of Acrylamide amount (A), and Temperature (C) on % Grafting (Y2) of mastic gum	104
5.16	3D Surface Response Graph showing the effect of Acrylamide amount (A), and Temperature (C) on % Grafting (Y2) of mastic gum	104
5.17	Contour Graph showing the effect of CAN amount (B), and Temperature (C) on % Grafting (Y2) of mastic gum	105
5.18	3D Surface Response Graph showing the effect of CAN amount (B), and Temperature (C) on % Grafting (Y2) of mastic gum	105

LIST OF FIGURES

Fig. No.	Title	Page No.
5.19	Contour Graph showing the effect of Acrylamide amount (A), and CAN amount (B) on % Grafting Efficiency (Y3) of mastic gum	108
5.20	3D Surface Response graph showing the effect of Acrylamide amount (A), and CAN amount (B) on % Grafting Efficiency (Y3) of mastic gum	108
5.21	Contour Graph showing the effect of Acrylamide amount (A), and Temperature (C) on % Grafting Efficiency (Y3) of mastic gum	109
5.22	3D Surface Response Graph showing the effect of Acrylamide amount (A), and Temperature (C) on % Grafting Efficiency (Y3) of mastic gum	109
5.23	Contour Graph showing the effect of CAN amount (B), and Temperature (C) on % Grafting Efficiency (Y3) of mastic gum	110
5.24	3D Surface Response Graph showing the effect of CAN amount (B), and Temperature (C) on % Grafting Efficiency (Y3) of mastic gum	110
5.25	Overlay graph of optimized values of process parameters for mastic gum	112
5.26	Contour Graph showing the effect of Acrylamide amount (A), and CAN amount (B) on % Yield (Y1) of banana peel gum	116
5.27	3D Surface Response Graph showing the effect of Acrylamide amount (A), and CAN amount (B) on % Yield (Y1) of banana peel gum	116
5.28	Contour Graph showing the effect of Acrylamide amount (A), and Temperature (C) on % Yield (Y1) of banana peel gum	117
5.29	3D Surface Response Graph showing the effect of Acrylamide amount (A), and Temperature (C) on % Yield (Y1) of banana peel gum	117

LIST OF FIGURES

Fig. No.	Title	Page No.
5.30	Contour Graph showing the effect of Initiator amount (B), and Temperature (C) on % Yield (Y1) of banana peel gum	118
5.31	Contour and 3D Surface Response Graph showing the effect of Initiator amount (B), and Temperature (C) on % Yield (Y1) of banana peel gum	118
5.32	Contour Graph showing the effect of Acrylamide amount (A), and CAN amount (B) on % Grafting (Y2) of banana peel gum	121
5.33	3D Surface Response Graph showing the effect of Acrylamide amount (A), and CAN amount (B) on % Grafting (Y2) of banana peel gum	121
5.34	Contour Graph showing the effect of Acrylamide amount (A), and Temperature (C) on % Grafting (Y2) of banana peel gum	122
5.35	3D Surface Response Graph showing the effect of Acrylamide amount (A), and Temperature (C) on % Grafting (Y2) of banana peel gum	122
5.36	Contour Graph showing the effect of CAN amount (B), and Temperature (C) on % Grafting (Y2) of banana peel gum	123
5.37	3D Surface Response Graph showing the effect of CAN amount (B), and Temperature (C) on % Grafting (Y2) of banana peel gum	123
5.38	Contour Graph showing the effect of Acrylamide amount (A), and CAN amount (B) on % Grafting Efficiency (Y3) of banana peel gum	126
5.39	3D Surface Response Graph showing the effect of Acrylamide amount (A), and CAN amount (B) on % Grafting Efficiency (Y3) of banana peel gum	126
5.40	Contour Graph showing the effect of Acrylamide amount (A), and Temperature (C) on % Grafting Efficiency (Y3) of banana peel gum	127

LIST OF FIGURES

Fig. No.	Title	Page No.
5.41	3D Surface Response Graph showing the effect of Acrylamide amount (A), and Temperature (C) on % Grafting Efficiency (Y3) of banana peel gum	127
5.42	Contour Graph showing the effect of CAN amount (B), and Temperature (C) on % Grafting Efficiency (Y3) of banana peel gum	128
5.43	3D Surface Response Graph showing the effect of CAN amount (B), and Temperature (C) on % Grafting Efficiency (Y3) of banana peel gum	128
5.44	Overlay graph of an optimized values of process parameters of D6 formulation	129
5.45	FT-IR spectrum of Gum Mastic	130
5.46	FT-IR spectrum of Acrylamide	130
5.47	FT-IR spectrum of Grafted Mastic Gum	131
5.48	DSC of Mastic Gum	131
5.49	DSC of Acrylamide	132
5.50	DSC of Grafted Mastic Gum	132
5.51	XRD spectra of Mastic Gum	133
5.52	XRD spectra of Acrylamide	133
5.53	XRD spectra of grafted mastic gum	134
5.54	SEM images of pure gum mastic	134
5.55	SEM images of grafted gum mastic	135
5.56	FTIR Spectrum of Extracted banana peel gum(test)	136
5.57	FTIR Spectrum of Extracted banana peel gum (Reference)	136
5.58	FT-IR spectrum of Grafted Banana Peel Gum	137

LIST OF FIGURES

Fig. No.	Title	Page No.
5.59	DSC of Banana Peel Gum	138
5.60	DSC of Grafted Banana Peel Gum	139
5.61	XRD spectra of banana peel gum	139
5.62	XRD spectra of Grafted Banana Peel Gum	140
5.63	SEM images of pure banana peel gum	141
5.64	SEM images of grafted banana peel gum	141
5.65	Swelling Capacity of ungrafted and grafted gums	142
5.66	FTIR spectrum of physical mixture of Lamivudine and Gum Mastic	143
5.67	FTIR spectrum of physical mixture of Lamivudine and Grafted Gum Mastic	144
5.68	FTIR spectrum of physical mixture of Lamivudine and Banana Peel Gum	144
5.69	FTIR spectrum of physical mixture of Lamivudine and Grafted Banana Peel Gum	145
5.70	In-vitro release graph for ungrafted mastic gum formulations (UMA1 to UMA5)	151
5.71	In-vitro release graph for grafted mastic gum formulations (GMA1 to GMA5)	153
5.72	In-vitro release graph for ungrafted banana peel gum formulations (UBA1 to UBA5)	154
5.73	In-vitro release graph for grafted banana peel gum formulations (GBA1 to GBA5)	156
5.74	Zero order release graph for grafted mastic gum (GMA5)	158

LIST OF FIGURES

Fig. No.	Title	Page No.
5.75	First order release graph for grafted mastic gum (GMA5)	158
5.76	Higuchi model graph for grafted mastic gum (GMA5)	159
5.77	Koresmeyer Peppas model graph for grafted mastic gum (GMA5)	159

1.0 INTRODUCTION

Polysaccharides are present in nearly every living thing. They can be found in seed tissues, plant stems and leaves, animal bodily fluids, crab shells, and insect wings. They are a renewable source of high-yielding materials, and they can also be present in the walls of cell and extracellular fluids of fungi, yeast and bacteria [1,2].

Polysaccharides, such as guar gum, starch, sodium alginate, xanthan gum and chitosan are utilized as coagulants and flocculants in their natural forms [3,4], While in a modified form, such as guar-graft-poly (sodium acrylate), they can be utilized as a water super sorbent [5]. Derivatization of functional groups is a common method for modifying polysaccharide materials [6,7], polymeric chain grafting [8,9] and by oxidative [10] or hydrolytic [11] degradation.

The monosaccharides combine to form polysaccharides. Polysaccharides are abundant in nature and are less expensive due to their vast range of forms and availability [12]. The polysaccharides are used in targeted systems of drug delivery as they are easy to modify. They are also stable, safe, non-toxic and biodegradable. Most polysaccharides, including as chitosan, pectin, guar gum, inulin and amylose, have already been employed as colon-specific drug delivery systems [13]. Several natural polysaccharides have been used as food and pharmaceutical excipients due to good biocompatibility, degradability, ease of accessibility, and low cost. However, the natural polysaccharides have certain drawbacks like viscosity change during storage, less shelf life, uncontrolled hydration and change in solubility upon changes in pH. The modification by chemical means reduces the above shortcomings. Natural polymers can be chemically modified in a variety of ways, including etherification, graft copolymerization and cross-linking [14,15].

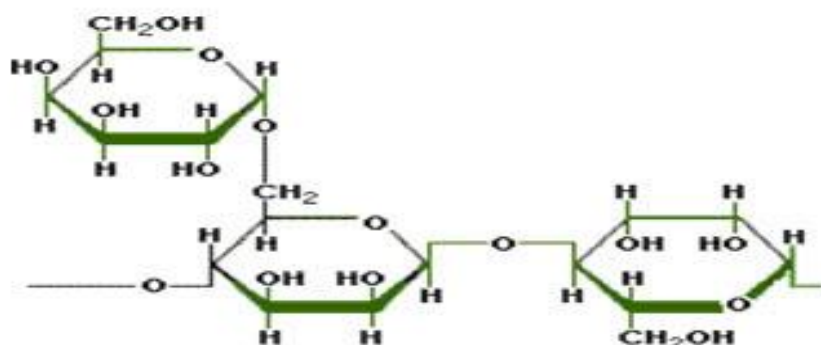


Figure 1.1: Structure of Polysaccharide (Sinha VR et al., 2001)

1.1 GRAFT COPOLYMERIZATION

The process of formation of graft polymer involves one polymer's long sequence with another polymer i.e., polysaccharides [16,17]. With the help of an agent, free radical sites will develop on the surface of a premade polymer. The agent must be powerful enough to generate the requisite free radical sites while remaining gentle enough not to damage the premade polymer chain's structural integrity. Once the polymer backbone's free radical sites have been generated, the chain propagation mechanism allows the monomer to be added up, resulting in grafted chains. Grafting has the advantage of adding new qualities to a natural polymer without sacrificing its original properties. As a starting point, natural polysaccharides are utilised for the graft polymers. Graft polymerisation is achieved by attaching vinyl and acryl monomers to the backbone of the biopolymer [18].

There are three methods which are used in graft copolymerisation process which are as following:

1.1.1 Conventional Grafting

In conventional grafting process, there are 3 strategies for grafting of monomers on surface of polysaccharides [19] which are as following:

A. *Grafting Through*

In case of grafting through technique, copolymerisation with co-monomer materials is done on presynthesised vinyl functionalised polysaccharides.

B. Grafting from

In this technique, there is direct formation of grafts from backbones of polysaccharide materials. This is most widely used technique.

C. Grafting to

In this technique, chemical initiators are used to produce the free radicals along the backbone of polysaccharides [20]. The common initiators which are used like tetra acetic acid/ceric ammonium nitrate [21].

Degradation of the polysaccharide backbone might occur during traditional grafting techniques. Because the traditional grafting procedure has little or no control over the weight distribution of the graft molecule, it can only be employed for a few applications. These problems have been solved by using controlled/living radical polymerizations to make graft-functionalized polysaccharide-based macromolecular materials [22]. The traditional approach was used to graft sterculia gum [23], cashew gum [24], okra mucilage [25], and xyloglucan [26].

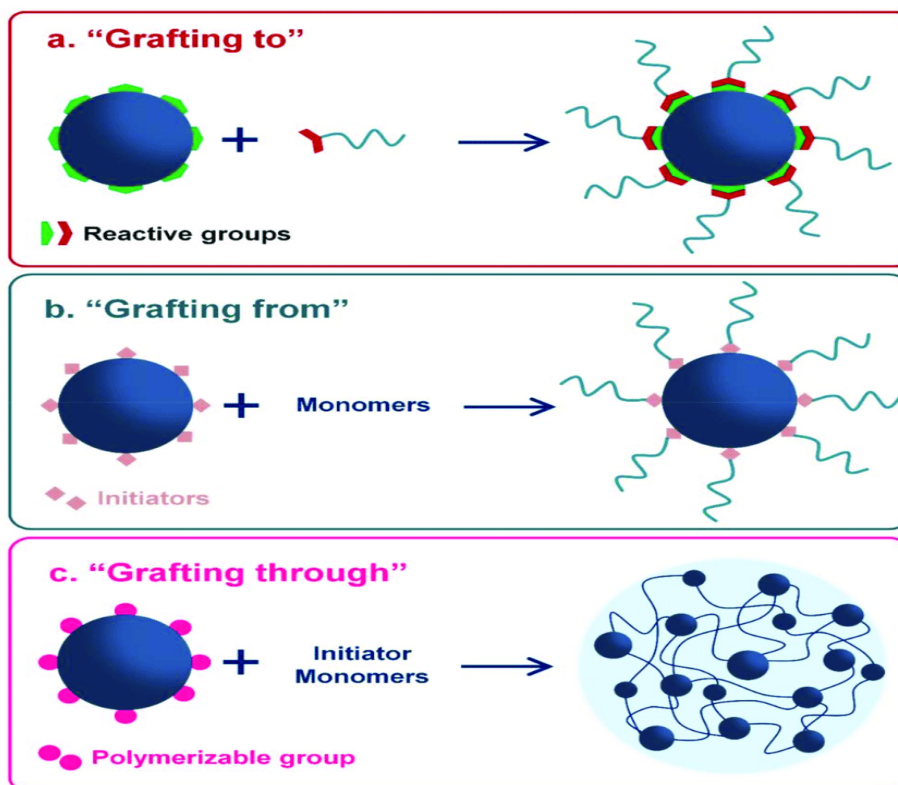


Figure 1.2: Conventional grafting techniques (Macchione MA et al., 2018)

1.1.2 Microwaves

Microwave irradiation for chemical synthesis has increased its popularity in the pharmaceutical and academic worlds [27].

Microwaves have a range of frequency 300 MHz to 300 GHz and produce electromagnetic radiation. When exposed to microwaves, charged particles direct themselves with the microwave's electric field, which reverts their orientation, causing the medium to heat up [28].

Microwave reactions can be carried out in both a solution and a dry medium. The reagents are preadsorbed onto an inorganic substrate. Microwave ovens were popular because of their convenience of use and low cost, but their use was not recommended owing to safety concerns because they didn't have enough control over the temperature and pressure of the reaction. Over the last decade, various changes to residential microwave ovens have been made to address these issues. By varying the microwave oven's power, different percentage grafting can be achieved. The duration of irradiation has an effect on percentage grafting [29,30].

1.1.3 Microwave assisted grafting and its mechanism

In this technique, the aqueous reaction mixture is used with addition of external redox initiators. The redox initiator will produce the ions and the presence of these ions will improve the ability of reaction mixture to convert energy of microwave to heat [31-34]. The grafting reaction will be expedited by the free radicals generated from the initiator with the help of microwave dielectric heating [35]. The acrylamide grafting on locust bean gum by microwave assisted method [36] is an example of this method. In an aqueous media, microwave aided grafting was used to crosslink and graft PVP on k-carrageenan backbone and agar utilising KPS (potassium per sulphate) as an initiator [37].

1.1.4 Microwave initiated grafting

In this process, there is no requirement of initiator for the purpose of grafting. When great repeatability and precise control of percentage grafting are required, the started grafting approach comes in handy. Hydroquinone is used to stop free radicals from forming. When conducted under microwaves, grafting of acrylamide on sodium

alginate [38] and carboxymethyl starch [39] indicated that there is possibility of grafting of polysaccharides without redox initiator and/or catalyst [40].

1.1.5 Microwave technology has a number of advantages over traditional methods

- In comparison to traditional heating, the Microwave (MW) heating rate is quick.
- In the MW approach, the reaction time is quick, whereas in the conventional method, the reaction time is greater.
- High-pressure reactions in MW are no more harmful than ordinary reactions. Because of the longer reaction time, conventional reactions are more harmful.
- In MW heating, a high yield of product is obtained, however in conventional heating, a poor yield is produced.
- In MW methods, it is simple to conduct in a solvent-free environment, whereas in traditional methods, it is impossible to conduct without a solvent.
- MW reactions can be carried out without the use of an initiator or catalyst, whereas conventional procedures cannot.
- In MW approaches, percent G (grafting) and percent E (efficiency) are higher, whereas in traditional methods, they are lower.
- Super heating: Because traditional heating occurs from the outside, the core of the solvent may be 5°C colder than the edge, whereas in the microwave, due to surface cooling, the core is 50°C hotter than the outside, allowing us to increase the boiling point by 5°C, a phenomenon known as super heating [41-43].

1.1.6 Grafting on solid support

Microwave-assisted polymer grafting has seen explosive growth in recent years, particularly when combined with solvent-free techniques, resulting in clean, easy-to-perform, inexpensive, safe, and ecologically friendly circumstances [44]. Polymers are adsorbed on a microwave-transparent support, such as silica or alumina [45-47].

1.1.7 Solvents used in microwave grafting procedures

One of the most important components of the microwave grafting procedure is solvents. They can't have any harmful effects on the polymeric system. In the

microwave grafting technique, the solvent must also give acceptable yields and grafting. The following solvents can be used in microwave grafting method without any harmful effects [48].

Table 1.1: Solvents used in microwave grafting process (Schanche, JS et al., 2003)

S. No.	Solvent	Boiling Point (°C)
1	N,N Dimethyl formamide (DMF)	153
2	Water	100
3	Methanol	65
4	Ethanol	78
5	Acetone	56
6	Acetonitrile	86
7	Xylene	137
8	Toluene	110
9	Pyridine	115
10	Dimethyl sulfoxide (DMSO)	189
11	Diethyl ether	35
12	Ethylene Glycol	197
13	Nitromethane	101
14	Nitrobenzene	202

1.1.8 Application of microwave grafting in various types of drug delivery systems

Polysaccharides and their grafted copolymers have been employed in a variety of medication delivery systems in recent years. Colon targeted systems, buccal systems, controlled systems, and transdermal systems have all made use of them.

A. Colon drug delivery systems

Graft copolymers have been used in colon related systems because of advantages such as pH near to neutral, extended transit duration, and lower enzymatic activity. Bharaniraja B and his colleagues use grafted katira gum to build colon-targeted systems for ibuprofen. Grafting of acrylamide onto katira gum resulted in polyacrylamide-grafted katira gum. Wet granulation was used to make matrix tablets having varying quantities of grafted katira gum. As a model drug candidate, ibuprofen was used. The findings of this investigation showed that Ibuprofen tablets containing 60% of the grafted katira gum would be viable formulation for drug delivery to the colon, where it would be more sensitive to enzymatic breakdown [49].

B. Controlled drug delivery systems

Rattan S and her colleagues investigated the use of grafted soy protein isolate (SPI) in pharmaceuticals. The SPI-g-(AA-co-HPBA) hydrogel was studied as a sustained and regulated drug delivery system for the release of the model drug ciprofloxacin. In oral cavity bacterial infections, the hydrogel has the potential to be employed as a vehicle for regulated drug delivery [50].

C. Buccal drug delivery systems

Tamarind seed polysaccharide (TS) was extracted from Tamarindus indica linn seeds by Shailaja T and her colleagues. It was attempted to graft the Tamarind seed polysaccharide with methyl methacrylate in a suitable manner (MMA). For grafting, the chemical approach of potassium per sulphate was used as initiator. Buccal patches were made with metoprolol succinate, a medication with a low bioavailability (40-50%). The buccal patches containing 2% Tamarind seed polysaccharide and 2.86 percent grafted tamarind seed polysaccharide showed sustained drug release for 12 hours [51].

D. Modified binder properties

In the preparation of diclofenac sodium tablets, Huanbutta and his colleagues used tamarind seed gum as a binder. The carboxymethylation method introduced a carboxymethyl group to the chemical structure of crude gum, according to

physicochemical characterization data. Fourier transformed infrared (FTIR) results proved the success of chemical alteration. The gum in both the crude and modified forms was amorphous, according to a powder X-ray diffractogram. Disintegration time and drug dissolution were both slowed by increasing the concentration of gum in the formulation [52].

E. Super viscosifier

Rani and her colleagues used a microwave-assisted technique to make polymethyl methacrylate grafted sodium alginate. An intrinsic viscosity analysis validated the grafting of PMMA chains onto the backbone of polysaccharide. The intrinsic viscosity of sodium alginate was significantly improved after PMMA chains were grafted on it, resulting in a grafted product that may be used as a superior viscosifier [53].

F. Transdermal drug delivery systems

Skin penetration assays in vitro were used to evaluate nanoparticles of graft copolymer of D, L-tetrahydropalmatine (THP). Franz diffusion cells were used to conduct transdermal permeation investigations in vitro. The results show that THP-loaded PEGECAT NPs can enter the skin of rats. This nanotechnology could be used to administer drugs via the skin [54].

1.2 ORAL DOSAGE FORMS

For the delivery of various drug delivery systems, the most suitable route is oral route. In designing of various dosage forms, the most suitable route is oral route. The mechanism of oral drug delivery systems is mainly diffusion, dissolution or both. The targeted oral delivery systems are better as compared to conventional dosage forms because of achievement of better therapeutic success. Oral route can be used in preparation of both conventional and novel drug delivery systems [55,56].

1.2.1 Downsides of conventional drug delivery systems

- Poor patient assent
- Variations in concentration of drug

- Maintenance of steady state concentration becomes difficult due to formation of peak-valley plasma concentration time profile
- Variations in levels of drug can produce various types of adverse effects mainly in case of drugs have small therapeutic index [57].

1.2.2 Sustained release dosage forms

The disadvantages of traditional dosage forms can be reduced by developing sustained release systems, which give drug release in adequate amounts to maintain therapeutic drug levels for a long time, with release profiles maintained by the system's unique architecture and design [58].

The main goals of these delivery systems are to ensure about the safety of patient and improve treatment effectiveness while improving patient compliance. As a result, these dosage forms are mostly used in the treating acute and chronic illnesses because they keep drug concentrations in plasma above the MEC and below the minimum dangerous level for a longer duration. As a result, continuous medication delivery leads to optimal therapeutic efficacy with reduction in frequency of dosing and side effects. Oral controlled release systems remain the most popular of all drug delivery systems because they offer various advantages over traditional systems, including as [59].

- Improve patient compliance and convenience by reducing medicine dosing frequency.
- The variation of the steady state plasma level is reduced.
- Maximum medication use allows for a reduction in the total dose provided.

Sustained release, sustained action, prolonged action, controlled release, extended action, timed release, depot and repository dosage forms are terms used to identify drug delivery system that are designed to achieve or prolonged therapeutic effect by continuously releasing medication over an extended period of time after administration of a single dose [60, 61].

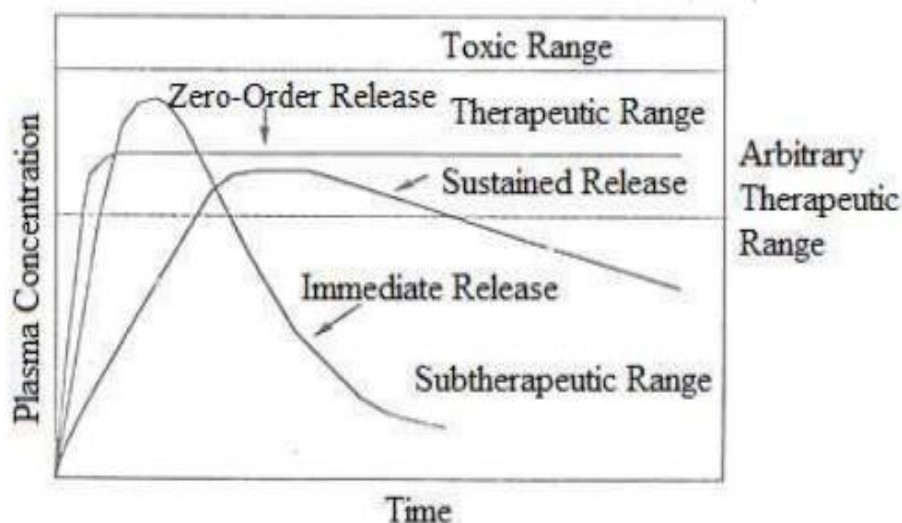


Figure 1.3: Plasma drug concentration vs time profile (Kube RS et al., 2015)

1.2.3 Benefits of sustained release products

- Patient compliance has improved.
 - Fewer dosing intervals.
 - Dosing at night has been reduced.
 - Less time spent caring for patients.
- Side effects are reduced both locally and systemically.
 - GI irritation and other dose-related adverse effects are reduced.
- Treatment efficiency has improved.
 - More effective treatment.
 - Improved blood concentration uniformity.
 - Drug level volatility is reduced, resulting in a more consistent pharmacological response.
 - Quicker cure or control of the illness.
- Use a less amount of total medication.
- On chronic dosage, there is a minimum amount of drug buildup [62, 63].

1.2.4 Disadvantages of sustained release products

- Dose dumping: Dose dumping occurs when a large amount of medication in a sustained release formulation is released abruptly, potentially releasing dangerous levels of drug into the bloodstream. Toxicity may occur if the product dose dumps.
- Reduced ability to make precise dose adjustments.
- Additional patient education is required.
- First-pass metabolism potential has been increased.
- There's a chance that systemic availability will be reduced.
- Variability in dose units has increased.
- Expensive.
- Stability problems: The complexity of sustained release forms can cause problems with stability, leading in either faster or slower drug release than expected [64, 65].

1.2.5 Drug properties relevant to sustained release dosage forms

Variables like the ailment to be treated, the type of patient, duration of therapy, and the drug qualities are all taken into account when designing sustained release delivery systems. The limits imposed by the drug's qualities are of particular importance to the scientist building the system [66].

These characteristics have the most impact on the drug's behavior in body and the delivery system. Because a drug's biological qualities are a result of its physicochemical features, there is no apparent separation between these two groups. Physicochemical properties can be determined in vitro, whereas biological properties are derived from traditional pharmacokinetic investigations of a drug's absorption, distribution, metabolism, and excretion, as well as those that come from pharmacological investigations [67]. These characteristics are categorized as

A. Physicochemical properties**➤ Size of dose**

As the incorporation of the sustaining result in an excessively large volume product. A desirable drug candidate for sustained release systems must have a dose size of less than 500mg.

➤ Solubility in water

The solubility of a medication is also a significant factor in its inclusion into long-acting drug delivery systems. More than 0.1 mg/ml solubility is required. Drugs with a higher water solubility, on the other hand, are more difficult to include into sustained release systems.

➤ Partition Coefficient

Drugs having low partition coefficient are water soluble but have a hard time penetrating lipid membrane; on the other hand, drugs having high partition coefficient are lipid soluble but have poor solubility in water.

➤ Drug Stability

The drugs having instability in stomach can act as suitable candidate for prolonged delivery systems. However, the drugs with instability in intestine cannot be a suitable candidate because most of drug is released in intestine in case of sustained release systems which can further affect the bioavailability of the drug.

➤ Molecular size and diffusivity

The drug ability of diffusion throughout a membrane is known as diffusivity. The diffusivity of a drug depends upon its molecular size. The following equation relates diffusivity to molecular weight:

$$\text{Log } D = -S_v \log V + k_v = -S_M \log M + k_m$$

Where, V = Molecular volume

M = Molecular weight

S_v, S_M, k_v, k_m = Constant

For medications with a molecular weight of 150 to 400, a value of roughly 10^{-6} is normal. The diffusion coefficient in many polymers for medications with a molecular weight more than 500 is frequently so small that it is difficult to quantify. Thus, high molecular weight drugs should be suitable candidate for sustained release systems.

➤ **Protein binding**

A huge number of drugs bind to proteins in plasma, which can impact the duration of the drug's activity. The binding with proteins can affect the distribution of drugs in extravascular space. This drug and protein complex can act as a reservoir in extra vascular space for sustained release systems. A high level of plasma protein binding may result in a longer drug elimination half-life, indicating the need for sustained release systems.

B. Biological properties

➤ **Biological Half Life**

Because the dose frequency is lowered, drug candidates with a suitable half-life are good for formulation of sustained release systems. A drug candidate having a half-life of less than 3 hours is not a good candidate since the dose size will increase. However, the drug candidate with half-life more than 8h will also an unsuitable candidate because its effect is already sustained.

➤ **Absorption**

Absorption is an important aspect in the formulation of sustained release formulations. For an acceptable medication candidate for sustained release systems, the rate of absorption must be quick. In the case of sustained-release systems, $K_r \ll K_a$ becomes particularly important. For absorption, drug must have a maximum $T_{1/2}$ of 3 to 4 hours.

➤ **Distribution**

Two aspects linked to distribution are taken into account in the formulation of sustained release systems: the volume of distribution and the ratio of drug concentration to plasma concentration (T/P ratio). The volume of distribution is a

useful metric for determining drug dosage. The information about drug disposal is also significant in the formulation of sustained release systems.

➤ **Metabolism**

The drugs which are metabolised before absorption in intestine or lumen cannot act as suitable candidate for sustained release formulations. However, the enzymes systems in intestinal walls are saturable. Another feasible option is to use enzymatically susceptible molecules as a prodrug.

➤ **Side effects and margin of safety**

A drug candidate's toxic effect or side effects are determined by its therapeutic concentration in the blood. A drug's therapeutic index (TI) is the most commonly used margin of safety.

$$TI = \frac{TD_{50}}{ED_{50}}$$

Where, TD_{50} = median toxic dose

ED_{50} = median effective dose

In general, the higher the TI value, the less likely they are to be formulated into sustained release formulations [68,69].

1.3 CONTROLLED AND SUSTAINED RELEASE SYSTEMS

These systems are commonly known as continuous release systems. The release of drug from these systems occurs for a prolonged period of time in whole gastrointestinal tract with normal transit. These systems are divided into following categories

1.3.1 Dissolution controlled release systems

Drugs with very slow dissolving rate or high-water solubility and dissolution are used in these types of systems. Controlling the rate of release is difficult with drugs with high solubility. These systems were developed by covering drug candidates with polymers and incorporating the drug into an insoluble polymer. The following equation is used for calculation of the rate of dissolution (dm/dt):

$$Dm/dt = ADS/h$$

Where, S = Aqueous solubility of the drug,

A = Surface area of the dissolving particle or tablet,

D = Diffusivity of the drug and

h = Thickness of the boundary layer.

These systems are divided in following two categories:

A. Matrix (or monolithic) dissolution-controlled systems

Due to the homogenous dispersion of medication throughout the medium, this system is also known as a monolithic system. Waxes such as bees wax and carnauba wax are utilised in this technique to limit the dissolving rate by lowering the wettability of the tablets. In these systems, the release rate is first order.

B. Reservoir (Encapsulation) dissolution-controlled systems

Encapsulation techniques were employed in this system to encapsulate the drug candidate using cellulose and polyethylene glycol. Depending on the thickness of the coating, these compounds will slow down the dissolving rate.

1.3.2 Diffusion controlled systems

The release of drug in these types of systems is determined by its diffusion through the membrane barrier. Diffusion devices are divided into two categories.

A. Membrane Reservoir devices

A diffusion solution or osmotic pump mechanism usually governs the kinetics of drug release from membrane reservoir devices.

The drug candidate is transported via the solution-diffusion process by dissolving first in the reservoir membrane at one surface, then diffusing down a chemical potential gradient across this membrane, and finally being discharged into the external media at the second interface. Non-porous membranes are known to have such a solution diffusion process.

A semipermeable membrane is used to manage the osmotic penetration of water/GI fluid in the osmotic pumping mechanism. The water permeability of the

semipermeable membrane and the osmotic pressure of the drug core formulation determine the delivery rate from such devices.

B. Matrix Systems

The matrix system is the simplest method for producing sustained-release dosage forms. The following is a classification of matrix systems

➤ **Matrix diffusion**

The matrix system has long been the most popular diffusion-controlled delivery technique. The matrix system's intrinsic flaw is its first-order release behavior, which has a steadily decreasing release rate. This is due to a decrease in the area of the penetrating diffusion front and an increase in diffusional resistance. T. Higuchi's equation is as following

$$Q = [Dt (2A - Cs) Cs] \times \frac{1}{2}$$

Where; Q = amount of drug released after time t,

D = diffusivity of the drug in the homogenous matrix media,

Cs = the solubility of the drug in the matrix substance

A = surface area of drug particle.

➤ **Polymer erosion**

The release of a drug either dispersed or dissolved from a polymer matrix can be governed by a various mechanism, ranging from enzymatic cleavage to swelling and dissolving. The case in which a polymer erodes via a purely diverse mechanism, such as erosion from surface, is particularly important.

➤ **Polymer swelling**

During the drug's discharge into the external environment, both hydrophobic and hydrophilic polymer matrices are subjected to swelling processes. [70-73].

1.4 MATRIX TABLETS

The sustained release matrix tablets have given a new breakthrough in the field of pharmaceutical technology by removal of various complex procedural steps during

production. The rate of drug release can be sustained by type and amount of polymer used. In formulation of these formulations mainly hydrophilic polymeric materials are used. In formulation of tablets, matrix systems are mainly used. A matrix may be defined as a complex formulated by mixing of one or more drugs with a suitable polymeric system. By using sustained release systems, a suitable concentration of drug can be reached in blood for a desired period of time which is helpful in attaining the better patient compliance [74].

1.4.1 Advantages of matrix tablets

- Manufacturing of matrix tablets is easy like conventional tablets.
- Cost effective and versatile.
- Drugs with a high molecular weight can also be utilised to make matrix tablets.
- The drug's therapeutic effective concentration is maintained over an extended period of time.
- Improved patient compliance.
- Toxicity is reduced as a result of the drug's delayed absorption.
- Protect the medicine in the GIT to increase its stability.
- Side effects are reduced.
- The treatment's efficacy has improved.
- Drug accumulation has been minimised.
- Improvements in bioavailability in the case of certain medications.
- The capacity to generate special effects has been improved. For example, bedtime dosage relieves arthritic pain in the morning [75-79].

1.4.2 Disadvantages of matrix tablets

- After complete release of drug, matrix has to be removed.
- Depending on the type of matrix, the cost can be quite high.
- The rate of release is influenced by transit rate through the gut and the presence of food [75-79].

1.4.3 Classification of matrix tablets

The types of matrices utilised in the matrix tablets are classed as follows:

A. Hydrophobic Matrices (Plastic matrices)

In this technique, an inactive plastic material such as polyethylene, PVA, or PMA is used to granulate the drug, which is subsequently compressed into tablets. By leaching the medication from the inert plastic matrix into the body fluids, the drug is slowly released. The matrix or plastic form of the tablet is created by compressing it, and it keeps its shape during drug leaching and elimination from the gastrointestinal tract. The substance that was released initially is present on the tablet's surfaces or is merely superficially imbedded. Gradumet (Abbott), is the most common example of this sort of dosage form. The matrix in this scenario decreases the irritating drug's exposure to the GI mucosal tissues. After all of the medication has been leached out, the matrix is normally excreted intact in the stool [80, 81].

B. Lipid Matrices

Lipid waxes and related components are used in this matrix system. Drug release is accomplished through pore diffusion and erosion processes. As a retardant base, carnauba wax is frequently combined with stearic acid in several delayed release formulations [82-85].

C. Hydrophilic Matrices

These are the most common matrix systems utilised in sustained release systems. The hydrophilic matrices give the needed release rate and are widely accepted by regulators. The medication is released in a hydrophilic matrix via two mechanisms: Fickian diffusional release and relaxation release. The total release of a drug from the matrix is aided by the erosion of the matrix during polymer relaxation; diffusion isn't the only way for a drug to exit from the matrix. The mechanisms determining release will be diffusion if the medication is moderately or very hydro soluble. For example, a swelling controlled diffusion method is used to achieve simultaneous water absorption and desorption of a sparingly soluble drug from hydrophilic matrices. The glass transition temperature is lowered as water penetrates a glassy polymeric matrix, as the

polymer expands. The dissolved drug diffuses into the external releasing media through the expanded rubbery zone at the same time.

Methylcellulose 400 and 4000Cps, Hydroxy ethylcellulose, Hydroxypropyl methylcellulose (HPMC), Sodium carboxy methyl cellulose, Agar-Agar, Alginates, Molasses, Polysaccharides of mannose and galactose, Chitosan and Modified starches are used in formulation of hydrophilic matrices [86-89].

D. Biodegradable Matrices

This class of matrix contains polymers that are made up of monomers joined together by functional groups and have an unstable backbone linkage. Enzymatic or non-enzymatic processes degrade them. Natural polysaccharides, modified polysaccharides, and synthetic polymers such as aliphatic poly (esters) and poly anhydrides are examples of matrix building substances [90-92].

E. Mineral Matrices

Polymers derived from seaweeds make up the mineral matrices. Mineral matrixes include things like alginic acid [93-95].

1.4.4 Polymers used in formulation of matrix tablets [96]

A. Hydrogel polymers

- Poly acrylamide (PA)
- Cross-linked polyvinyl pyrrolidone (PVP)
- Cross-linked polyvinyl alcohol (PVA)
- Polyhydroxy ethyl methacrylate (PHEMA)
- Polyethylene oxide (PEO)

B. Soluble polymers

- Polyethyleneglycol (PEG)
- polyvinyl alcohol (PVA)
- Polyvinyl pyrrolidone (PVP)
- Hydroxypropyl methyl cellulose (HPMC)

C. Biodegradable polymers

- Polyglycolic acid (PGA)
- Poly caprolactone (PCL)
- Polylactic acid (PLA)
- Poly anhydrides
- Poly orthoesters

D. Non-biodegradable polymers

- Poly dimethyl siloxane (PDS)
- Polyether urethane (PEU)
- Polyvinyl chloride (PVC)
- Cellulose acetate (CA)
- Ethyl cellulose (EC)

E. Mucoadhesive polymers

- Poly carbophil
- Polyacrylic acid
- Methyl cellulose
- Pectin

F. Natural gums

- Xanthan gum
- Guar gum
- Karaya gum
- Locust bean gum

1.5 METHODS OF PREPARATION OF MATRIX

The medicament and excipients are dispersed in retardant base using one of four techniques.

1.5.1 Solvent evaporation technique

A solution of medicine and excipients is added to a melted wax phase in this approach. Evaporation is then used to remove the solvent [97-99].

1.5.2 Compression technique

Three techniques are involved in compression:

A. Direct compression [100-102]

This technique is most widely used in compression of tablets. It involves direct compression of premixed drug and excipients. This method of production of tablets is very speedy method as it requires less machinery, less labour and less processing time.

Advantages of direct compression are as following

- Direct compression method is economical as compared to other methods due to less processing time, low cost of labours, a smaller number of steps and very less amount of equipment are required.
- Because heat and moisture are removed, this approach is best for moisture-sensitive drugs.
- Uniformity in particle size.
- Dissolution of prime particles.
- Variations between batches are minimal.
- API and excipient chemical stability issues would be avoided.
- Provides stability against the ageing impact, which affects the rate of dissolution.

Disadvantages of direct compression process

- Low-dose drugs are difficult to distribute uniformly.
- Direct compression is not appropriate for drugs with low compressibility and flowability.
- Direct compression is not suited for excipients with weak compressibility and flowability.

- Instability is caused by a large particle size difference between the medication and the excipients.
- Colour distribution in case of direct compression is non-uniform.
- Air entrapment during direct compression is occasionally linked to tablet capping, laminating, splitting, or layering.
- Direct compression equipment is costly.

The steps in the direct compression process are as follows:

- Milling of API and additives
- Mixing of API and additives
- Compression of tablets

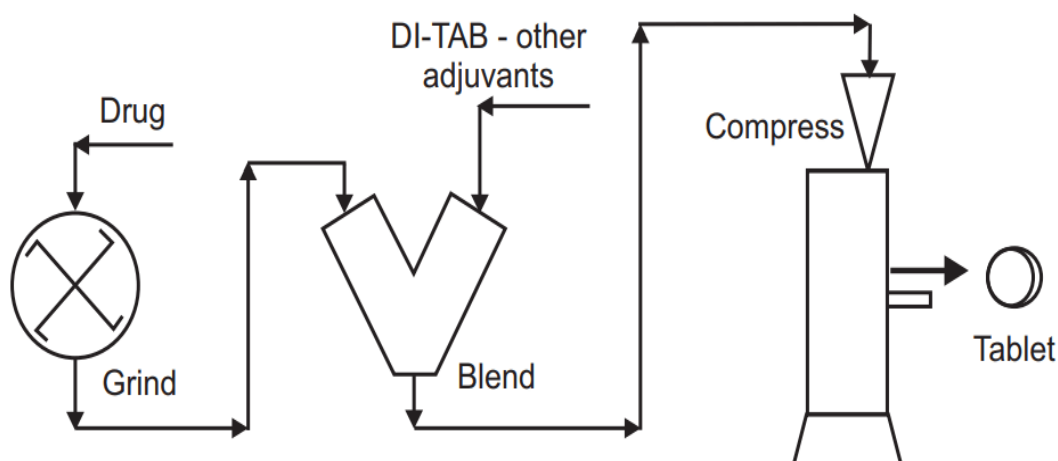


Figure 1.4: Flow diagram of direct compression technique (Ansel's HC et al., 2014)

B. Wet granulation [102-106]

The most common agglomeration method is wet granulation. In this process, the blend of powder is converted into wet mass with a granulating liquid. Wet mass is then sized and dried.

The wet granulation method involves a number of phases:

- Medicament and additives mixed together.
- Binder solution preparation.

- By combining a powder combination with a binder solution, a wet mass is formed.
- Using a coarse sieve to screen moist mass.
- Wet granules drying.
- Dry granule screening.
- Granules mixing with lubricants.

Disadvantages of wet granulation process

- Very expensive process as compared to direct compression process.
- For thermosensitive and moisture-sensitive medicines, this technique is unsuccessful.
- In comparison to the direct compression method, the procedure is more complicated.
- Incompatibilities between several types of formulation components are a possibility.

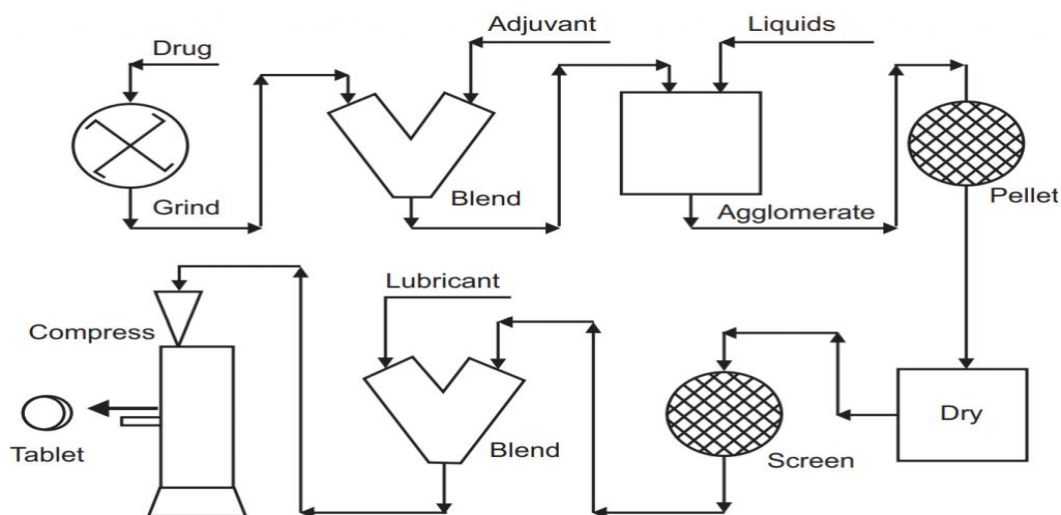


Figure 1.5: Flow diagram of wet granulation technique (Ansel's HC et al., 2014)

C. Dry granulation [102, 107-109]

This method is less used method in formulation of tablets. No binder solution is used in this method.

Advantages of dry granulation process

- Because powder particles are not bound by a wet binder, disintegration is improved.
- In the case of thermosensitive medications, this is useful.
- Useful for medications that are sensitive to moisture.

Disadvantages of dry granulation process

- Colour distribution that isn't even
- Slug creation necessitates the use of a heavy-duty tablet press.

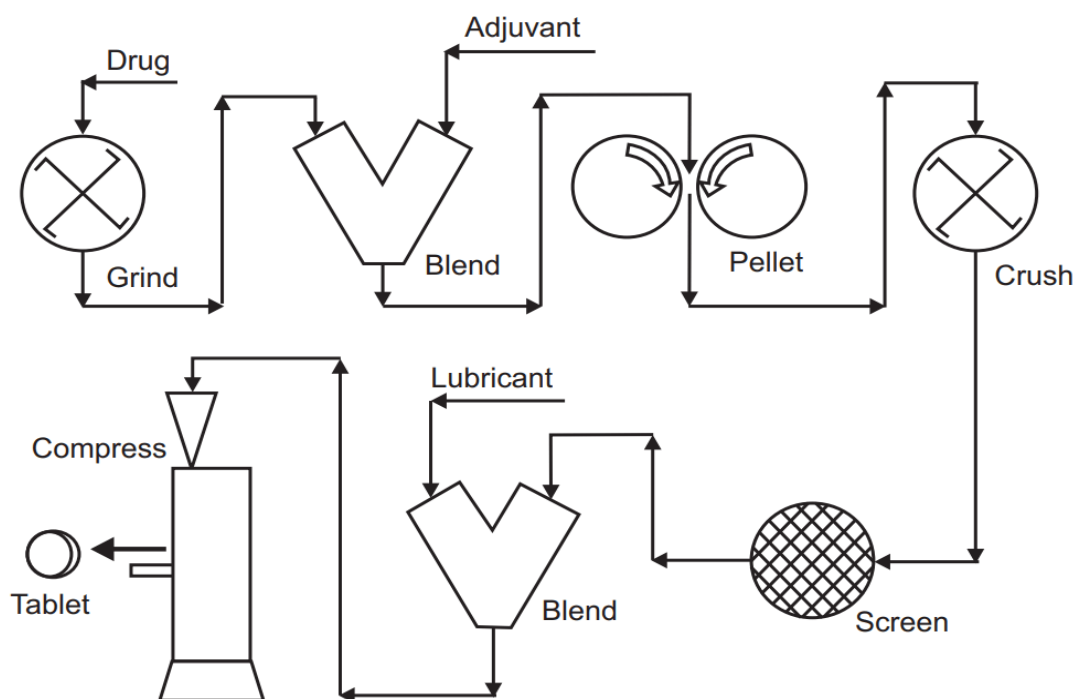


Figure 1.6: Flow diagram of dry granulation technique (Ansel's HC et al., 2014)

1.5.3 Fusion technique

Drugs and excipients are fused into a molten wax matrix in this method. In this procedure, the dispersion becomes more uniform.

The downside of this method is that the rate of medication release decreases over time. This is due to a decrease in surface area and increased diffusional distance at the penetrating solvent front. If the surface area increases with the diffusional distance, a

zero-order release rate can be reached. Drug release from materials can also be controlled with additives like polyvinylpyrrolidone or hydrophilic polymers, and apparent zero-order release can be achieved [110-112].

1.5.4 Melt granulation technique

This technique is mainly used for drugs with poor solubility. The process of transforming a raw material into a finished product is referred to as extrusion through a die under pressure to produce a product with a uniform shape and density [113-115].

Advantages of melt granulation technique

- No requirement of solvent or water for the process.
- In the process, there are fewer steps.
- There are no criteria for active component compressibility, and the overall process is simple, continuous, and efficient.
- The mixture's dispersion becomes uniform.
- Stability is good at varied pH and moisture levels.
- Because they are non-swelling and water insoluble, they are safe to use in individuals.

Disadvantages of melt granulation technique

- High amount of energy is consumed during this process.
- This method can't be used for temperature sensitive products.
- The binders having low melting points can't be used

Applications in the pharmaceutical industry

- This method can be used in improvement of bioavailability and dissolution rate of drugs.
- Modification of drug release rate.
- The taste of bitter drugs can be masked.

1.6 HIV AND AIDS [116-122]

HIV stands for human immunodeficiency virus. AIDS stands for acquired immunodeficiency syndrome.

HIV

H-It infects only human beings and also transmitted between humans not from animals. It is not transmitted from bites of mosquitoes, bats or any other species.

I-The body has immune system whose function is to protect our body from germs, infections etc. But a person suffering from HIV has inability to fight against diseases. However, immune system becomes deficient.

V-Virus is a small, simplest thing which is in inactive form outside the body and becomes active when it goes inside human body.

AIDS

A-It is not inherited means it cannot be transmitting from one generation to another. It is transmitted to healthy person by infected person.

I-It weakens the immune system.

D-Creates a deficiency of CD4+ cells in the immune system.

S-It is a collection of diseases

The HIV virus is the cause of AIDS. Our immune systems fight viruses and bacteria in most cases. The immune system's WBC protect us from infections. White blood cells contain CD4+ cells, often known as T cells. These T cells can be developed by a person who has been infected. These pathogens take advantage of the body's immune system. These infections can cause a variety of health problems and even death. Although there is no cure for AIDS, there are treatments that can help you stay healthier for longer by delaying the disease's progression.

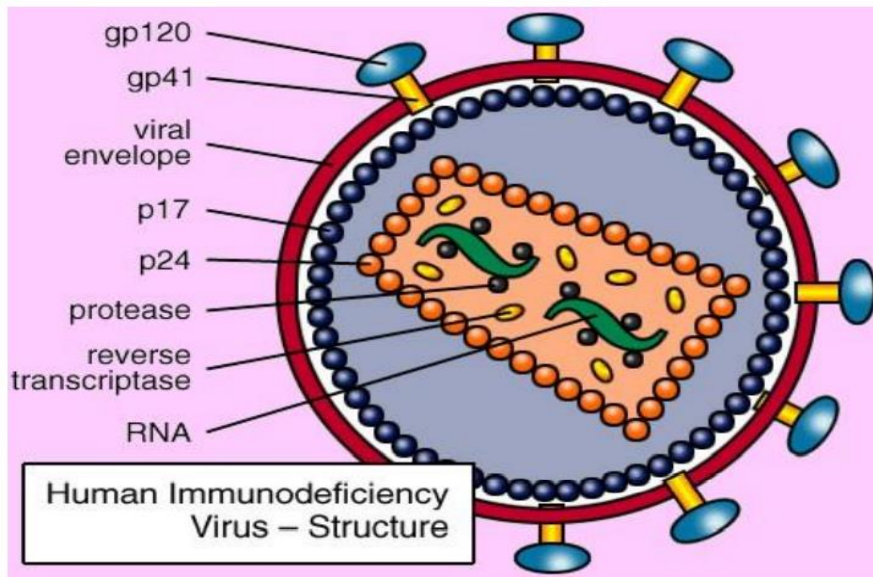


Figure 1.7: Structure of HIV (Kaila A et al., 2016)

1.6.1 HIV structure

A. *Gp120*

Its molecular weight, which is 120 defines its name. It is required for virus entrance into cells because it aids in the attachment of viruses to certain cell surface receptors.

B. *GP41*

It's a component of retroviruses, which includes the human immunodeficiency virus. It's a group of enveloped viruses that employ reverse transcriptase to replicate in their host cells. It is aimed for a host cell.

C. *Viral envelope*

The virus attaches itself to the envelope.

D. *P17*

Protein makes up the viral core. It's in the shape of a bullet. Reverse transcription, integrase, and protease are three enzymes necessary for HIV replication.

E. *P24*

P24 is a protein that is found in the HIV capsid.

F. Protease

It is an enzyme that is required for HIV, the retrovirus that causes AIDS, to complete its life cycle. This enzyme cleaves polyproteins at the proper sites to produce the natural protein components of the HIV virus.

G. Integrase

Retrovirus-produced enzyme that allows the retrovirus' genetic material to be incorporated into the DNA of infected cells.

H. RNA

Long strands of DNA are used by all species, to store their genetic material. Retroviruses are unique in that their genes are made up of RNA.

1.6.2 Life cycle of HIV

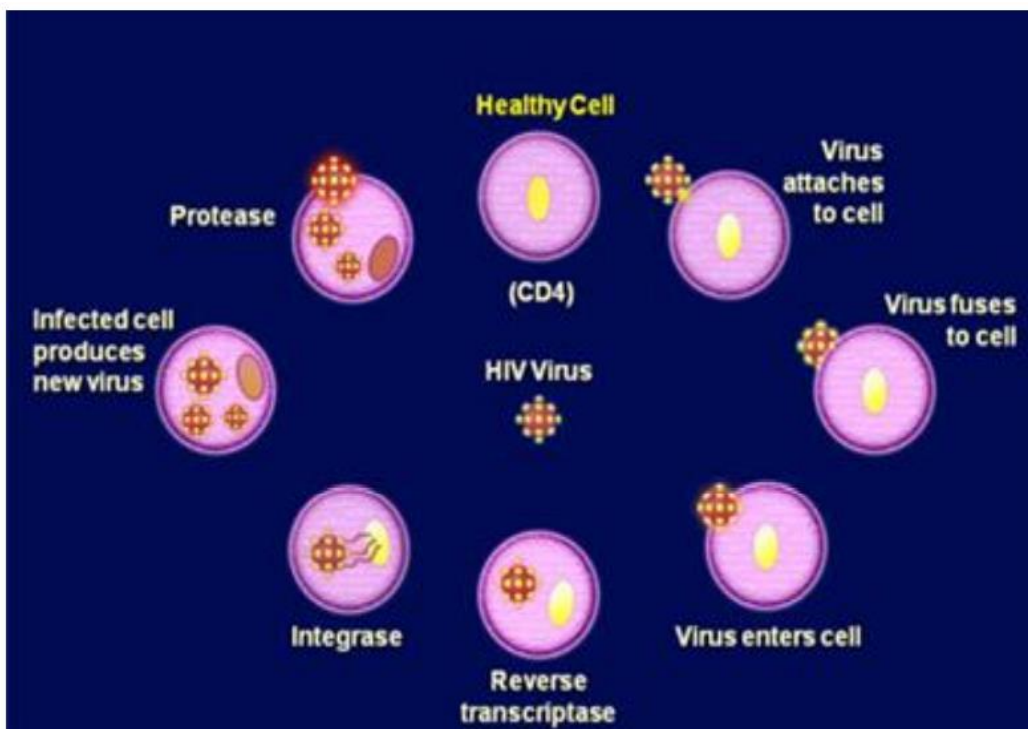


Figure 1.8: Lifecycle of HIV (Kaila A et al., 2016)

1.6.3 Symptoms

- Enlarged or swollen lymph nodes
- Regular fever and sweat

- Short term memory loss
- Breath related problems
- Lack of coordination
- Difficulty in swallowing
- Vomiting and diarrhoea
- Loss in vision
- Unexpected weight loss

1.6.4 Antiviral drugs used in treatment of AIDS

A. Nucleoside reverse transcriptase inhibitors

Zidovudine (ZDV), Didanosine (ddI), Stavudine (d4T), Zalcitabine (DDC), Lamivudine (3TC), Abacavir (ABC), Tenofovir (TDF), Emtricitabine (FTC).

B. Non nucleoside reverse transcriptase inhibitors

Nevirapine (NVP), Efavirenz (EFV), Delavirdine, Rilpivirine, Etravirine.

C. Protease inhibitors

Saquinavir (SQV), Indinavir (IDV), Ritonavir (RTV), Nelfinavir (NFV), Darunavir (DRV), Amprenavir (APV), Lopinavir (LPV/r), Atazanavir (ATV), Fosamprenavir (FPV), Tipranavir (TPV).

D. Fusion inhibitor:

Enfuvirtide T-20.

E. Integrase inhibitor

Raltegravir, Eltegravir, Doultagravir

2.1 DRUG REVIEW

LAMIVUDINE [123-129]

Lamivudine is nucleoside reverse transcriptase inhibitor (NRTI) that is taken orally to treat HIV-type I infection in individuals with AIDS and as monotherapy for hepatitis B virus (HBV) infection.

IUPAC Name: 4-amino-1-[(2R, 5S)-2-(hydroxyl methyl)-1, 3-oxathiolan-5-yl]-1, 2-dihydropyrimidin-2-one.

Proprietary names: EPIVIR, 3TC.

Molecular formula: C₈H₁₁N₃O₃S

Molecular weight: 229.3

Structural formula:

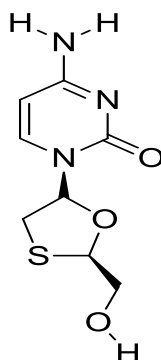


Figure 2.1: Chemical Structure of Lamivudine (Strauch S et al., 2011)

Solubility: It is water soluble, methanol soluble, and nearly insoluble in acetone.

Category: Anti-retroviral drug

Melting point: 160-162⁰C

Volume of distribution: 1.30 L/kg

Protein binding: Less than 36%

Biological half life: 6 h

Bioavailability:	86%
Description:	Lamivudine exists as white crystalline powder. It is odourless.
Storage:	It must be stored in airtight container and protect from sunlight.

Mechanism of action of lamivudine

Lamivudine is a cytidine analogue. It is an inhibitor of both type-1 and type-II reverse transcriptase. It also inhibits the hepatitis B reverse transcriptase. After phosphorylation, it is converted into active metabolites which inhibits the enzyme named reverse transcriptase and terminates synthesis of DNA. The deficiency of 3'-OH group prevents elongation of DNA chain and viral DNA growth is terminated.

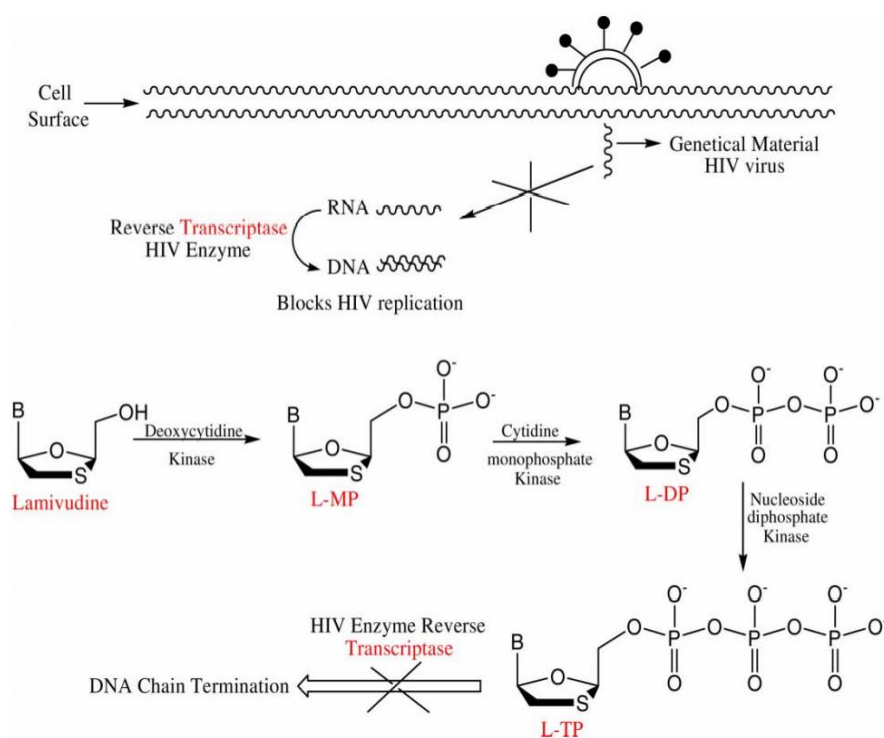


Figure 2.2: Mechanism of action of lamivudine (Vasconcelos, TRA et al., 2008)

Pharmacokinetics

The lamivudine pharmacokinetics is similar in all type of patients. After oral administration, lamivudine is absorbed rapidly. The bioavailability of lamivudine is

82% in adults and 68% in children. The lamivudine is distributed in body fluids with apparent volume of distribution 1.3 L/kg after administration by I.V. route. Breast milk contains it as well.

Adverse effects

Fullness, vomiting, nausea, stomach pain, burning and pain in the feet, arms, and hands are all side effects of lamivudine.

Drug interaction

The use of trimethoprim/sulfamethoxazole (Bactrim, Septra) and vitamins raises lamivudine levels in the body.

Uses

Lamivudine is used to treat HIV infection, prevent HIV infection in persons who have been unintentionally exposed to HIV, and treat hepatitis B infection.

Dosage forms:

The following strengths and formulations are available for this medicine:

Table 2.1: Marketed strengths and form of lamivudine

S. No.	Brand Name	Company	Dose	Form
1	Hepatavir	Hetero Pharma	100 mg	Tablet
2	Lamivir	Cipla	100 mg	Tablet
3	Lamidac	Zydus Cadila	100 mg	Tablet
4	Hepitec	Glaxosmithkline	100 mg	Tablet
5	Virolam	Sun Pharma	100 mg	Tablet
6	Tapivir	Taj Pharma	100 mg	Tablet
7	Lamihope	Macleods Pharma	150 mg	Tablet
8	Epivir	Cipla	300 mg	Tablet
9	Lamivir	Cipla	50mg/5ml	Solution
10	Lavir	Emcure	50mg/5ml	Solution
11	Lavir Syrup	Emcure		Syrup

2.2 EXCIPIENTS REVIEW

2.2.1 Mastic gum [130-135]

Chios Mastiha – Chios Mastiha is the air-dried resinous exudate of *P. Lentiscus* L. (Family Anacardiaceae), a Mediterranean shrub or tiny evergreen tree that is mostly farmed on the Greek island of Chios. Gum Mastic is a 100 percent natural product with a verified origin. It contains no dangerous substances or chemicals that could affect the body.

A. Chemical Constituents in Gum Mastic

The resin of *Pistacia lentiscus* L. was analysed using GC and GC-MS to get -pinene, -pinene, limonene, terpene-4-ol, and terpeno. Caryophylline (31.38 percent), germaerene (12.05 percent), and -cadinene are all present in the oil extracted (6.48 percent). GC-MS analysis of hydrodistilled oil from leaves revealed the presence of -pinene, -terpene, and terpene-4-ol. Gallic acid and galloyl derivatives, flavonol glycoside, and anthocyanins are polyphenols found in the leaves. There are additional traces of myrcetine derivative and catechin. The leaves contain -tocopherol as well. The gum oil includes 90% monoterpene hydrocarbons, including 79 percent - pinene and 3% - myrcene, whereas the leaf oil contains 50% monoterpene hydrocarbons, including 11 percent - pinene and 19 percent - myrcene.

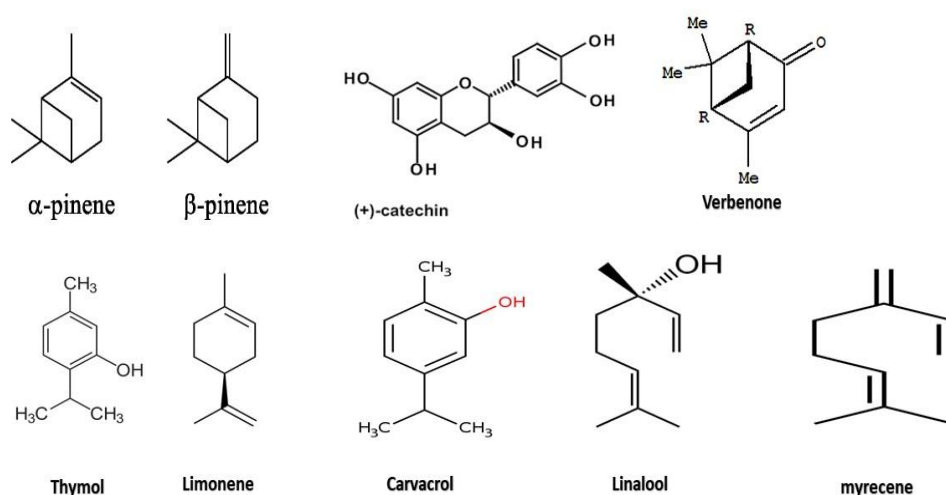


Figure 2.3: Chemical Structure of some important chemical constituents of *Pistacia lentiscus* (Paraschos, S et al., 2012)

Table 2.2: Physicochemical Properties of Mastic Gum [130-135]

S. No.	Type of Physicochemical Property	Inference
1	Density	0.96 – 1.08 g/ml (20°C)
2	Softening Point	45-55 °C
3	Moisture: Max	1.5%
4	Total Ash (550°C)	Max 0.2 %
5	Natural Impurities	Max 1.5 %
6	Chromatic Parameters	L: 60.00 - 70.00 a: 1.00 - 4.00 b: 10 .00 - 20.00
7	Acidity Index	50 - 60
8	Saponification Value	70-85

B. Processing of Mastic Gum cultivation

The mastic tree is a hardy plant with few requirements, which is why it thrives in arid, rocky, and poor soil. Its roots are distributed throughout the surface of the soil and can withstand severe drought. The mastic tree is prepared in the winter by cutting the tree branches to give it a shape that allows people to get under it. A shallow plough is done in the field about the same time. Ploughing is usually done to clear the field of weeds, at a depth of around 10cm, because the mastic tree's roots are just below the soil's surface. The levelling and cleaning of the region surrounding the trunk of the tree, where the mastic will fall, is done around June. The next step is to put white dirt (calcium carbonate powder) on this area to allow dripping mastic resin to dry and facilitate harvesting without changing the chemical composition of the mastic. The tree trunk's bark is "damaged" with wounds 10-15mm long and 2-3mm deep around mid-July. The incisions are made in weekly stages and total 20–100 incisions over a 6–8-week period, depending on the age and size of the tree. Mastic resin will leak out of these incisions in liquid drops that resemble tears. The majority of the mastic drips

to the ground (on the white dirt) and should be left there for 15-30 days before being retrieved.

Mastic collection normally begins in mid-August, and work resumes extremely early the next morning. The larger pieces are recovered from the ground (along with dust, tree leaves, and small stones). They're spread out in large wooden pans and brought into the grower's house to be stored dry and cool. The little bits of mastic are collected from the tree trunk and the ground in mid-September.

Mastic cleansing is a time-consuming process that begins in November. Typically, the entire family is involved, and the cleaning process lasts throughout the winter. The larger fragments of mastic are carefully cleaned one by one with a little pointed knife after being washed. Smaller items are cleaned in a different manner.

C. Applications of Mastic Gum in pharmaceuticals

- Tablets has been prepared by using mastic gum as binder.
- Mastic has also been used in formulation of microcapsules cores.
- Studies have also revealed that mastic gum formulates large particles with no pores, thus it can be used in preparation of controlled release and extended release formulations.
- There is also one report regarding the use of mastic gum in colonic drug delivery systems using compression coating process.

D. Therapeutic applications of Mastic Gum

- Mastic gum is used as dietary supplement and herbal remedy in eastern countries.
- Studies have also revealed that the mastic gum has antacid and cytoprotective effect for gastrointestinal system.
- There are also certain reports regarding treatment of gastric ulcers and reduction in intensity of mucosal damage of stomach caused by ulcers.
- The mastic gum has also been found to have antitumor activity in colorectal tumours.

- Oleanolic acid, a constituent of mastic gum has been found to have anti-inflammatory activity.
- Mastic gum has also been found to have antioxidant effects.

2.2.2 Banana peel [136-145]

Banana is genus of *Musa* and belongs to family *Musaceae*. The banana fruit is cultivated all over the world. The banana plant needs high amount of water to grow and yield the fruits. The main purpose of cultivation of banana plant is collection of fruits as they are easily available with high nutritional value. The banana peels are waste part of banana fruit. The banana peel weighs around 30% of total weight of fruit. The banana peel has not received much attention due to their unknown benefits in commercial applications. The main components of banana peel include dietary fibre, proteins, essential amino acids, polyunsaturated fatty acids and potassium.

Table 2.3: Properties of Banana Peel [136-145]

S. No.	Type of Physical Property	Inference
1	Colour	Pale Brown Colour
2	Odour	Characteristic
3	Solubility	Water - soluble, organic solvents - Insoluble
4	Moisture: Max	1.5%
5	Total Ash (550°C)	Max 8 %

The chemical composition of banana peel includes potassium, iron, sodium, calcium, manganese, bromine, rubidium, strontium, zirconium and niobium. The mineral composition has been confirmed by B.A. Anhwange as shown in table 2.4.

Table 2.4: Mineral composition of banana peel (Anhwange, BA et al., 2009)

S. No.	Element	Concentration (mg/g)
1	Potassium	78.10±6.58
2	Calcium	19.20±0.00
3	Sodium	24.30±0.12
4	Iron	0.61±0.22
5	Manganese	76.20±0.00
6	Bromine	0.04±0.00
7	Rubidium	0.2±0.05
8	Strontium	0.03±0.01

Gallocatechin was discovered in the banana peel by Someya et al. (2002). Other substances found in ripe banana peel include the anthocyanins delphinidin and cyaniding, as well as catecholamines. The antioxidant activity of banana peel has also been assessed, with the effect on lipid autoxidation studied in proportion to gallocatechin concentration.

A. Applications of Banana peel gum in pharmaceuticals

- Banana peel gum has been used in preparation of PCM tablets as binding agent.
- Banana peel gum has also been used as suspending agent in formulation of paracetamol suspension.
- In medicine, banana peel mucilage has been claimed to have features such as thickening, humidifying, dissolving, gelling, and release controlling properties.

B. Therapeutic applications of Banana peel Gum

- Banana peel has been found to have antioxidant properties due to presence of ascorbic acid.
- Banana peel has been found to have antimicrobial properties.
- The major effects of banana peel on mucosal defence factor, which stimulates DNA synthesis and promotes mucosal cell proliferation.

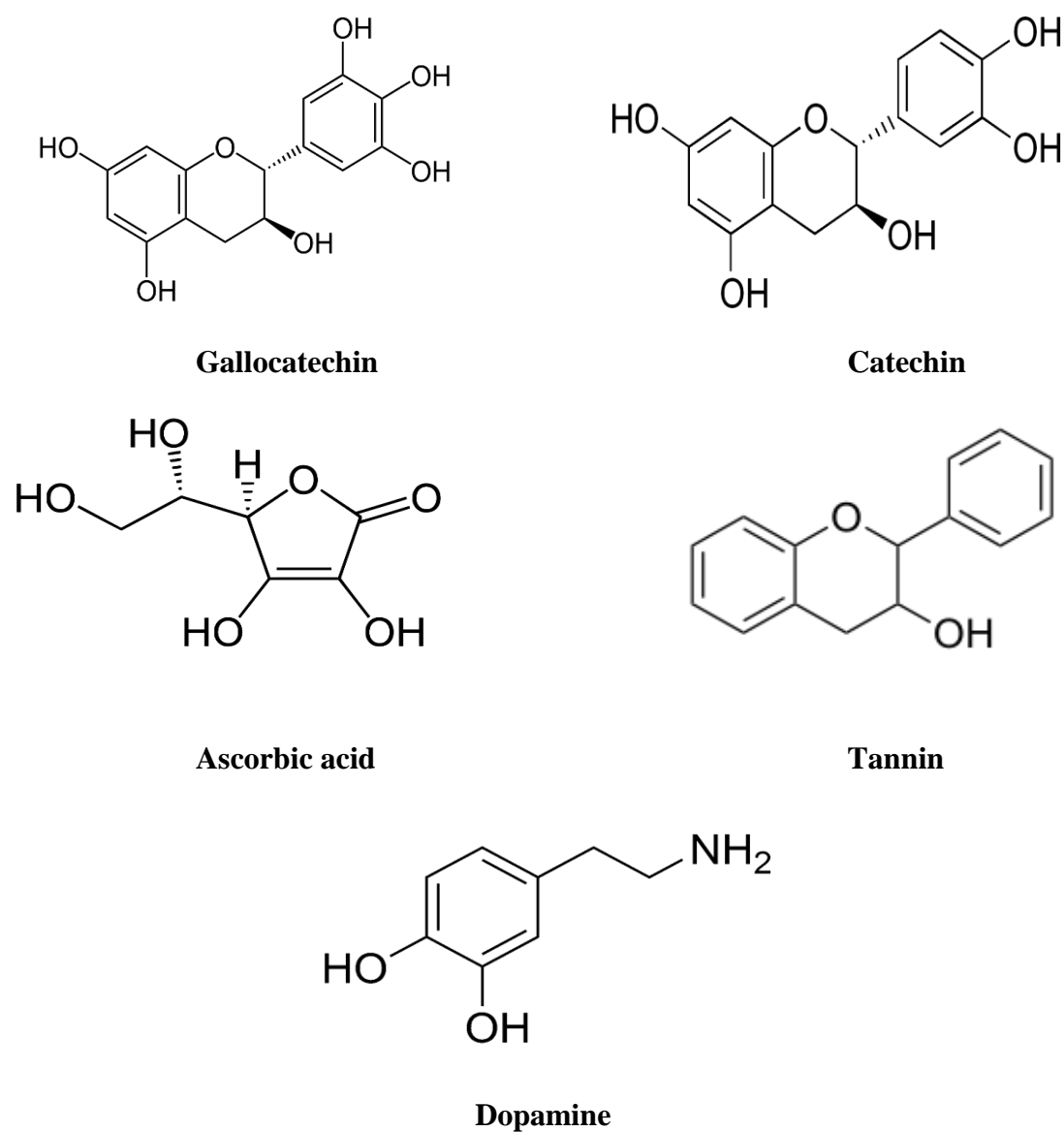


Figure 2.4: Chemical Structure of some important chemical constituents of banana peel (Anhwange, BA et al., 2009)

2.2.3 Acrylamide [146-149]

A. Chemical structure

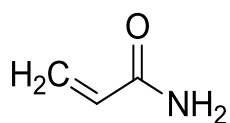


Figure 2.5: Chemical Structure of Acrylamide (Kaity, S et al., 2013)

Table 2.5: Physicochemical Properties of Acrylamide
(<https://pubchem.ncbi.nlm.nih.gov/compound/Acrylamide>)

S. No.	Property	Inference
1	Chemical name	2-propenamide
2	Molecular formula	C ₃ H ₅ NO
3	Molecular weight	71.08
4	Appearance	Flakes that are colourless or white, or crystalline flakes that are practically white
5	Solubility	Water and methanol soluble and in ethanol, freely soluble
6	Odour	Odourless
7	Density	1.122g/cm ³

Uses

- Acrylamide is used in the number of industrial application and in the production of dyes.
- Acrylamide is utilized generally as a precursor in the manufacturing of polyacrylamide. Poly acrylamide has been used to clear drinking water and treat municipal and industrial effluents as flocculants. Cosmetics and toiletries also include poly acrylamide.
- It is used in biotechnology laboratories to prepare polyacrylamide gels.
- Acrylamide is also used to make colours and organic chemicals like N-methylacrylamide, as well as soil stabiliser in tunnels, sewers, wells, and reservoirs.

Storage

Store in a cool, dry, ventilated area. It is stable at room temperature and should keep away from the sources of heat.

2.2.4 Ceric Ammonium Nitrate [150-152]

Ceric ammonium nitrate (CAN) is a one-electron oxidising agent that facilitates the formation of intermolecular and intramolecular carbon-carbon and carbon-heteroatom bonds via oxidative addition of electrophilic radicals to alkenes. Secondary alcohols can be converted to ketones and benzylic alcohols to aldehydes using CAN.

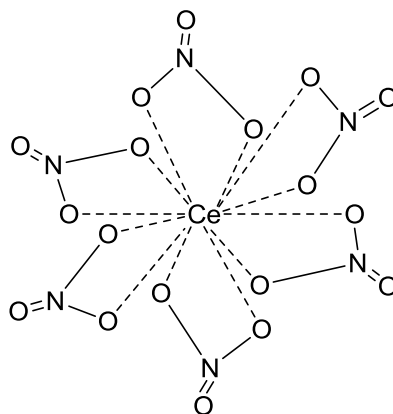


Figure 2.6: Chemical Structure of Ceric ammonium nitrate

(<https://pubchem.ncbi.nlm.nih.gov/compound/Cerium-ammonium-nitrate>)

A. Physicochemical properties

Table 2.6: Physicochemical properties of Ceric ammonium nitrate

(<https://pubchem.ncbi.nlm.nih.gov/compound/Cerium-ammonium-nitrate>)

S. No.	Property	Inference
1	Molecular formula	$((\text{NH}_4)_2\text{Ce}(\text{NO}_3)_6)$
2	Molecular weight	548.26 g/mol
3	Appearance	orange-red
4	Solubility	Freely soluble in water

B. Uses

- CAN has been utilised to liberate organic ligands from metal carbonyls in the past.
- In redox reactions, CAN functions as an oxidant.

2.2.5 Magnesium Stearate [153]

At normal temperature, magnesium stearate is a solid white powder. It's an FDA-approved inactive component that's often utilised as a lubricant in the pharmaceutical business to make tablet, pill, and powder dosage forms. It's used to keep pharmaceutical substances from sticking to equipment in the manufacturing process. Magnesium stearate can come from both animal and plant sources.

A. Chemical structure

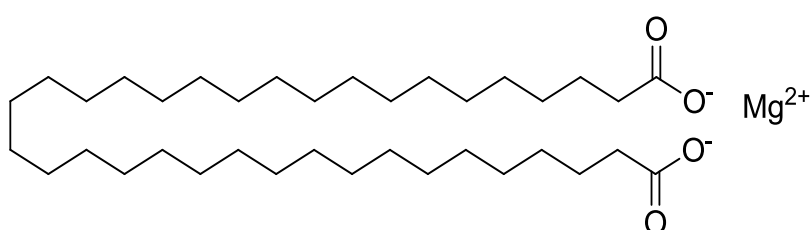


Figure 2.7: Chemical structure of Magnesium stearate (Rowe RC et al., 2006)

Table 2.7: Specifications of Magnesium stearate (Rowe RC et al., 2006)

S. No.	Property	Inference
1	Synonyms	Magnesium Stearate; 557-04-0
2	Chemical names	Magnesium octadecanoate
3	Chemical formula	$C_{36}H_{70}MgO_4$
4	Appearance	White dry powder

B. Uses

- Used as lubricant, flow agent in pharmaceutical formulations.

2.2.6 Talc [153]

Talc is widely utilised in a range of cosmetics, particularly powders. Talc helps to keep the skin smooth and dry. In the pharmaceutical industry, talc serves as a glidant and lubricant. Glidants like talc improve powder flow characteristics by reducing interparticulate friction, van der Waals forces, modifying particle size distribution, and reducing the effect of dampness on host particle surfaces. Its lubricating properties are explained by the loosely connected lattice layers sliding over one other

and forming roller formations. When compared to magnesium stearate, talc has a less negative impact on tablet in vitro properties.

A. Chemical structure

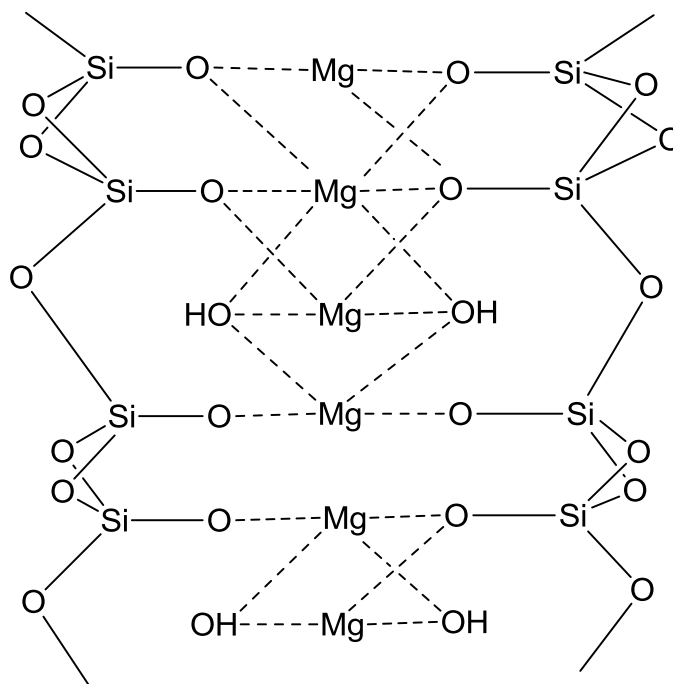


Figure 2.8: Chemical structure of Talc (Rowe RC et al., 2006)

Table 2.8: Specifications of Talc (Rowe RC et al., 2006)

S. No.	Property	Inference
1	Synonyms	Magnesium silicate.
2	Chemical names	Silicates
3	Chemical formula	$Mg_3(OH)_2(Si_4O_{10})$
4	Appearance	White dry powder

B. Uses

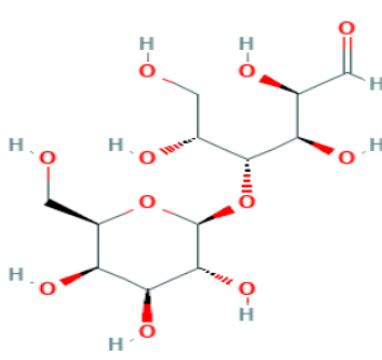
- Used in manufacturing and preparations of paint, plastics, antiperspirants, as pharmaceutical ingredient.

- Talc powder is used as an insecticide and fungicide carrier. It is easy to blast through a nozzle and immediately adheres to plant leaves and stems. The softness of the material decreases wear on the application equipment.

2.2.7 Lactose [153]

Lactose is used in tablets as a diluent and different grades with varying physical qualities are commercially available. Spray-dried lactose was invented 30 years ago and is meant for compression. Small amounts of amorphous lactose bind predominantly β -lactose monohydrate microcrystals into spherical aggregates. Because hydrous lactose monohydrate cannot be compressed directly, it is employed in wet granulation formulations. An examination of the efficiency of six lactose-based excipients as direct compression excipients revealed that anhydrous β -lactose was the most effective, followed by spray-dried lactose.

Table 2.9: Excipient Profile of Lactose (Rowe RC et al., 2006)

Nonproprietary Names	Lactose monohydrate
Description	Crystalline particles or powder, white to off-white, odourless and sweet.
Structure	
IUPAC Name	8-benzyl-7-{2-[ethyl(2-hydroxyethyl)amino]ethyl}-1,3-dimethyl-2,3,6,7-tetrahydro-1H-purine-2,6-dione
Synonyms	<ul style="list-style-type: none"> ➤ D-(+)-Lactose ➤ Lactose, anhydrous [NF] ➤ Lactose – Anhydrous

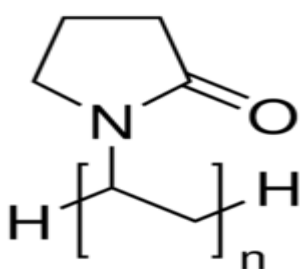
Molecular Weight	385.468 g/mol
Chemical formula	C ₂₀ H ₂₇ N ₅ O ₃
Properties	Density: 1.540 for α-lactose monohydrate Bulk Density: 0.619 g/cm ³ Tapped density: 0.935 g/cm ³ Melting Point: 201-202°C
Category	Diluent
Solubility	Ethanol and water, it's quite soluble.
Stability and Storage Conditions	Growth of mold is possible in humid settings (relative humidity of 80% or higher). Lactose can turn brown when stored, and this reaction is expedited by warm, humid circumstances. Because the purity of different lactose varies, colour analysis may be necessary, especially in case of manufacturing of white tablets. Lactose should be kept cool and dry in a well sealed container.
Applications	Lactose is a popular diluent used in formulation tablets, lyophilized goods, capsules and newborn feed formulas, to a smaller extent. Lactose of various fine grades are typically employed in wet granulation method of tablet manufacture or during milling during processing.
Incompatibilities	Lactose is prone to undergo a Maillard condensation process, resulting in brown-colored products. This reaction is easier to perform with amorphous lactose than with crystalline lactose. Amino acids, aminophylline, and amphetamines are incompatible with lactose.
Safety	As diluent, it is widely utilised in pharmaceutical formulations

2.2.7 Polyvinyl pyrrolidone [153]

PVP stands for polyvinylpyrrolidone, which is a vinylpyrrolidone polymer. It is further divided into soluble PVP and insoluble PVPP depending on the degree of

polymerization (polyvinyl polypyrrolidone). The soluble PVP has a molecular weight of 8,000 to 10,000. PVP (polyvinylpyrrolidone) is one of three novel pharmaceutical excipients that can be utilised as a co-solvent in tablets, granules, and injections.

Table 2.10: Excipient Profile of PVP (Rowe RC et al., 2006)

Nonproprietary Names	BP: Povidone
Description	Povidone is a hygroscopic powder that is white in colour. Spray-drying is used to make povidones with K-values of 30 or less, which appear as spheres.
Structure	
IUPAC Name	1-ethenylpyrrolidin-2-one
Synonyms	<ul style="list-style-type: none"> ➤ Kollidon ➤ Plasdone ➤ Polyvidone ➤ 1-vinyl-2-pyrrolidinone polymer
Molecular Weight	2500–3 000 000 g/mol
Chemical formula	(C ₆ H ₉ NO) _n
Properties	<ul style="list-style-type: none"> ➤ Plasdone has a true density of 1.180 g/ cm³ ➤ Povidone K-15 has a flow rate of 20 g/s, while K-29/32 has a flow rate of 16 g/s. ➤ Melting point: softens at 1508 degrees Celsius ➤ Povidone is extremely hygroscopic

Category	<ul style="list-style-type: none"> ➤ Disintegrant ➤ Dissolution aid ➤ Suspending agent ➤ Tablet binder
Applications	It is predominantly utilised in solid formulations, despite its use in a range of medicinal formulations. Povidone act as solubilizer for poorly water soluble drugs which have to be solubilised to prepare liquid formulations. As a coating agent, povidone solutions can be utilised.
Incompatibilities	Povidone can be mixed with a variety of resins, and other compounds in solution. When it comes in contact with sodium salicylate, salicylic acid, tannins, and other chemicals, it forms molecular adducts. The development of complexes with povidone may reduce the efficacy of various preservatives, such as thimerosal.
Safety	Povidone is a common excipient, especially in tablets and solutions for oral use. Povidone is largely harmless when ingested orally because gastrointestinal system or mucosal membranes will not absorb it. It is also safe to the skin and does not produce any sensitivity reactions.

2.3 REVIEW ON GRAFTING

Attempts of sustaining the release of drug by using naturally obtained polymer has started around two decades ago. Several researchers throughout the world have published their different approaches in this purpose sometimes by using natural gum or sometimes by using natural grafted co-polymers to extend the drug release time. The huge shift in the pharmaceutical industry's focus to these organically produced polymers has attracted people's curiosity. So, here's a quick rundown of the literature in this area.

Chami S et al., (2021) explored the possibility of using xanthan-g-polyacrylamide for polymer flooding in a medium-salinity Devonian oilfield. Microwave-assisted graft copolymerization of acrylamide on xanthan was used to make the graft polymer. Infrared Spectroscopy and Thermal Analysis were used to characterise the produced copolymer with optimal grafting parameters. Under reservoir circumstances, xanthan and grafted xanthan were subjected to rheological investigation using steady shear and oscillatory flow tests. In saline environments, the elastic characteristics of xanthan-g-polyacrylamide solutions have been greatly enhanced over xanthan, and grafted polymer solutions exhibit lower elasticity losses [154].

Oliveira ACJ et al., (2021) proposed a technique including MW-initiated synthesis for the manufacturing of phthalated cashew gum. Benznidazole (BNZ) was employed as a model drug. BNZ is a drug that is used to treat Chagas disease. Size, PDI, zeta potential, AFM, and in vitro release were all used to characterise the nanoparticles. The nanoparticles were 288.8 nm in diameter, with a PDI of 0.27 and a zeta potential of -31.8 mV. The findings revealed that Phat-CG offers intriguing and potential qualities as a new therapy option for Chagas disease [155].

Bal T et al., (2020) created a grafted copolymer of polymeric mix of Fenugreek seed mucilage using acrylamide with an initiator named ammonium per sulphate. To optimise the optimal grade based on greatest percentage grafting efficiency, researchers used intrinsic viscosity testing, FTIR, ¹³C NMR, XRD, elemental analysis, Thermogravimetric analysis and SEM. The optimised sample GF4 has a longer chain length than native mucilage, indicating that it has a very good controlled release, according to the intrinsic viscosity data [156].

Malviya R et al., (2019) formulated acrylamide graft copolymers of neem gum. The grafted neem hydrogels were characterised. Grafted neem gum had a larger index of swelling than the native form in all mediums, including double distilled H₂O, 1 N sodium hydroxide and 0.1 N hydrochloric acid. Data from soil burial biodegradation investigations revealed that neem gum and grafted neem gum biodegraded at 90 percent in 9 and 28 days, respectively [157].

Dan S et al., (2018) used microwave-assisted graft copolymerization to graft acrylamide onto cassia tora (CT). The OECD guidelines were followed for conducting

the oral toxicity (acute) investigation among rats and mice. Metformin and sitagliptin were used as model pharmaceuticals to investigate the pharmaceutical use of the CT grafted with acrylamide tablet formulation. The efficacy of grafting of acrylamide on cassia tora by microwave-assisted method was demonstrated. For pharmacokinetic profiling rats were used to test the suggested formulation. According to guidelines, it was discovered that a bioanalytical approach for determining both drugs in plasma of rat was confirmed [158].

Chaudhary S et al., (2018) developed a grafted Gum xanthan-psyllium hybrid. At an initial concentration of dye EBT and Aur-O with a dosage of 600 mg and a temperature of 323 K, the efficiency of dye removal was 90.53 percent for EBT and 95.63 percent for Aur-O. For both dyes, the kinetics of adsorption showed that pseudo-second order kinetics [159].

Sharma J et al., (2017) employed a free-radical polymerization approach to synthesise semi-IPN with a Psyllium-Gum xanthan hybrid backbone for rhodamine-B dye sequestration from waste water. The synthesised semi-IPN was optimised for optimal liquid absorption efficacy using RSM and CCD. Different adjusted reaction parameters were used to reach the maximum (470.8 percent) liquid absorption efficacy (100 percent). The proposed polymer was characterised using XRD, SEM-EDX, FT-IR, UV-VIS, and BET. The greatest rhodamine-B adsorption (96%) was achieved after 12 hours at 500 mg semi-IPN dosage, 6 mg L⁻¹ dye concentration and at a temperature of 303 K. The natural polysaccharide-based semi-IPN was discovered to be effective for textile industry effluent treatment based on adsorption and kinetic behaviour. [160].

Li B et al., (2017) created an antibacterial superabsorbent. The effect of concentration of HTCC on the swelling ratio was determined. FTIR spectroscopy, SEM and TGA analyses were used to analyse the product. Tara gum was effectively grafted with polyacrylic acid, resulting in a three-dimensional core network. In water and a 0.9 percent sodium chloride solution, the highest swelling ratios were determined. The HTCC addition to superabsorbent improved its antibacterial properties against *Staphylococcus aureus* and *Escherichia coli* [161].

Varma VNSK et al., (2016) chemically modified guar gum (GG) to produce co-polymer to create intestine targeting ESO nanoparticles (NPs). Free radical polymerization was used to create a poly acrylamide-grafted-guar gum co-polymer. Alkaline hydrolysis resulted in the development of PAAm-g-GG after chemical modification. On grafting, the effects of GG and acrylamide (AAM) were investigated. pH-sensitive NPs loaded with esomeprazole magnesium (ESO) were produced and described using a nano-emulsification polymer crosslinking approach. To obtain nanoparticles, sixteen formulations were formulated and the concentrations of process factors were adjusted. The size distribution of the NPs was found to be homogeneous. The drug loading and encapsulation efficiency ranged from 33.2 percent to 50.1 percent and 12.2 percent to 17.2 percent, respectively. Co-polymer concentration enhanced particle size and drug loading. The pH of environment had a significant impact on drug. The pH sensitive grafted nanoparticles resisted the initial release in an acidic pH environment and delayed release in an alkaline pH environment [162].

Mutalik S et al., (2016) developed nanoparticles using grafted-xanthan gum for colonic administration. The optimised nanoparticles (CN20) were spherical and measured 425 nm in diameter on average. In different acidic solutions, CN20 NPs produced a minimal quantity of curcumin (less than 8%). Curcumin release was significantly faster when the pH was raised to 7.2 than when the pH was 1.2 or 4.5. Curcumin released in a pH 6.8 solution was found to be very good. When the contents of rat caeces were combined with a pH 6.8 solution, the highest curcumin release was observed, demonstrating that NPs have a microflora-dependent drug release property. Curcumin nanoparticles lowered nitrite and myeloperoxidase levels, avoided loss in weight and reduced inflammation of colon in rats with acetic acid-induced IBD. Curcumin in nanoparticulate form was better absorbed systemically, with a three fold increase in C_{max} and a 2.5 fold rise in AUC, compared to free curcumin [163].

Mittal et al., (2015) developed biodegradable flocculants and adsorbents using grafted gum-ghatti hydrogels. TGA, FTIR, and SEM were used to examine the hydrogels that had been created. TGA analysis demonstrated that the produced hydrogels were more stable than pure gum, with a high capacity of swelling in pH 7

solution. The best grafted hydrogel was found to be effective in removing saline water from a variety of petroleum fraction–saline emulsions. At 40°C, in an acidic clay suspension with a polymer dose of 15 mg, the maximum flocculation efficiency was attained. Furthermore, the hydrogel absorbed 94 percent and 75 percent of lead and copper ions from water, respectively [164].

Menon S et al., (2014) used both conventional and microwave methods to make guar gum grafted polyacrylic acid/cloisite superabsorbent nanocomposites. The influence of cross-linker and cloisite concentration on swelling was investigated, as well as parameters of reaction such as concentration of initiator, concentration of monomer and time. FTIR, XRD, DSC, and TGA were all used to characterise the produced polymer. In both traditional and microwave procedures, the final optimal percentage grafting was found to be 60% and 63 percent, respectively [165].

Setia A et al., (2014) used a microwave assisted approach to graft poly (acrylamide) onto A. marmelos gum, which was then optimised using a central composite design. They showed the effect of power, time, and concentration on grafting efficiency. The production of acrylamide grafted copolymer and gum was confirmed by characterization. By analysing the release behaviour of drug from the tablet, the graft co-polymer was examined. When compared to the ungrafted A. marmelos, in vitro experiments demonstrated that the drug released from the acrylamide grafted matrix tablet was regulated [166].

Tang XJ et al., (2014) used a polymer for microwave synthesis of graft phullan (D,L-lactide). On the synthesis, the effects of power of microwave, Phullan's catalyst/lactide/OH group and solvents were investigated. These samples were used to load the curcumin model drug. Phullan copolymerization with enhanced yield and conversion of lactide from twenty four hours to five minutes was achieved using microwave-assisted synthesis, as well as some unique physiological effects, when compared to traditional oil heating [167].

Kaity S et al., (2013) used initiator to make locust bean gum copolymer using acrylamide as monomer. By using a consistent amount of gum, the process of grafting was improved by time of irradiation, initiator concentration, and acrylamide amount. FTIR, NMR, SEM, angle of contact and biodegradability were all utilised to

characterise the grafted gum. It was also utilised to make buflomedil hydrochloride controlled-release matrix tablets. In the dissolution profile of the tablet, acrylamide grafted locust bean gum has a rate-controlling property similar to hydroxypropyl methylcellulose [168].

Kaur J et al., (2013) investigated biopolymer modification to enhance physiological, chemical, and thermal qualities. Grafted copolymers of soy protein were prepared in air using an potassium persulphate/ascorbic acid redox initiator technique. FTIR, SEM, and XRD were used to characterise the graft copolymers that were generated. To acquire the best graft yield, multiple reaction parameters were first optimised for graft copolymerization. Binary monomer combinations produce the highest graft yields which were 120.54 percent, 142.38 percent, and 293.58 percent, respectively, with EMA+MMA, EMA+EA, and EMA+MA. The stability was investigated, and it was discovered that they have a good thermal stability. The chemical resistance of the modified protein to acid and base was improved. Furthermore, grafted protein showed improved moisture resistance [169].

Vijan V et al., (2012) used grafting method to make acrylamide-grafted-gellan gum. A series of graft copolymers were created using different concentrations of acrylamide, Ferric ammonium nitrate, and time of microwave irradiation. To eliminate homopolymer generated during the polymerization operation, Methanol (20% v/v) was used to extract the modified gum. Fourier transform infrared spectroscopy, ¹³C Nuclear magnetic resonance, Scanning electron microscopy, rheological investigations, and thermal investigations were utilised to characterise these graft copolymers. Efficiency of grafting, grafting percentage, and conversion percentage were evaluated between different graft copolymer series, and the results were then connected with different investigations. Tablets were made by combining the metformin hydrochloride (MTF) with excipients in grafted gum. In vitro investigations on prepared tablet formulations revealed an 8-hour release time [170].

Pathania D et al., (2012) carried out methacrylic acid graft copolymerization onto gelatinized potato starch. To determine the greatest % grafting, various parameters of reaction such as temperature effect, amount of initiator and monomer were tuned. The temperature of reaction mixture (60⁰C) and monomer concentration (0.81mol L⁻¹)

were tuned for a maximum grafting efficiency of 87.5 percent (0.02 mmol.L⁻¹). Other physico-chemical properties of the grafted samples were assessed, including swelling, moisture absorption, and chemical resistance. FTIR, SEM, XRD, and TGA techniques were used to characterise the grafted samples. The presence of extra peaks in the grafted starch FTIR spectra of samples supported grafting of monomer onto starch. Metal ions and organic dyes have been successfully removed from aqueous systems using grafted co-polymers [171].

Tame A et al., (2011) used Ce⁴⁺ initiator in aqueous medium at 29°C to graft unmodified holocellulose and holocellulose by using acrylamide (AA). The results show that carboxymethylation improves the cellulose substrate's graftability. Grafted polyacrylamide chains on CMC had higher graft levels and molecular weights than those on cellulose. Graft levels were shown to increase by up to 70% and 50% for graft copolymers including Carboxymethyl cellulose. This research focuses on the grafting characteristics of AA on CMC. In relation to ceric ion concentration, degree of substrate substitution, monomer concentration, and reaction duration, the extent and rate of graft copolymerisation of AA onto modified and unmodified cellulose were examined [172].

Kalia S et al., (2011) treated chemically sunn hemp fibres (SHF). To achieve maximal grafting, many reaction parameters were used (91.8 percent). Original and modified fibres were evaluated for morphology, temperature stability, and crystalline behaviour. According to morphological and temperature studies, graft copolymerization makes the surface of sunn hemp fibres rough and amorphous, which improves thermal stability. Microwave-induced grafting had a smaller impact on the crystalline behaviour of sunn hemp fibres than conventional grafting because the time to achieve highest grafting is much shorter. In the manufacture of polyhydroxybutyrate bio composites, synthesised graft copolymers were used as reinforcing material [173].

Sharma AK et al., (2010) used microwave (MW) irradiation to make grafted styrene using chitosan without utilising any catalyst or initiator. Ch-g-sty was synthesised in 40 seconds utilising 187 percent grafting and 80 percent MW power. Cr(VI) absorption was influenced by pH and concentration. According to the Langmuir

isotherm model, the maximum capacities for the grafted copolymer were 526.3 mg/g, 312.5 mg/g, and 166.7 mg/g, respectively [174].

Narkar M et al. (2010) developed and evaluated a controlled release mucoadhesive drug delivery system using gellan gum and amoxicillin as drug candidate. Basic cross-linking medium beads have a high efficacy of entrapment than acidic cross-linking medium beads, according to the study. Entrapment efficiency in acidic media ranged from 32 to 46 percent w/w, increasing from 60 to 90 percent w/w in basic media. Various batches with the low, medium, and high drug entrapment were coated with chitosan to create a polyelectrolyte complex film. Entrapment efficiency and particle size increases as polymer concentration rises. In the acidic cross-linking solution, SEM revealed a spherical but rough surface caused by drug leaching. For up to 7 hours, the Peppas model ($r=0.9998$) was utilised to control in vitro drug release.. *Helicobacter pylori* was completely eradicated in an in vitro growth inhibition research. These findings suggest that amoxicillin gellan beads with a stomach-specific controlled release mucoadhesive system could be effective in the treatment of *Helicobacter pylori* [175].

Kar R et al., (2010) produced isosorbide-5-mononitrate matrix tablets with sustained release. To develop matrix tablets, various drug:polymer ratios were employed containing isosorbide-5-mononitrate. The matrix former was xanthan gum, while the diluent was microcrystalline cellulose. Each formulation complied with pharmacopoeial requirements. F5 had the best sustained release pattern of all the formulations, releasing 92.12 percent of the medication throughout a 12-hour period. The Higuchi model ($r^2 =0.9851$) was shown to be followed by drug release in the kinetic investigations [176].

Ahuja M et al., (2009) using microwave-assisted and ceric graft copolymerization synthesised xanthan-g-poly(acrylamide). To formulate diclofenac sodium tablets utilising matrix of graft copolymer direct compression method was used. The dissolution studies of the graft copolymer was performed. In comparison to ceric induced grafting, microwave assisted grafting delivered grafted copolymer having greater percent grafting in less duration. With increase in power and time of exposure zero order kinetics was found to be mechanism of drug release [177].

Osemeahon SA et al., (2008) created grafted polyacrylamide mix membrane using the sodium alginate and konkoli gum. The effect of various conditions on the percentage yield was investigated. The parameters of grafting such as acrylamide amount, CAN, gum “konkoli”, and time of reaction were found to have a significant impact on copolymer's % graft yield. For all of the characteristics studied, the % graft yield increased at first, then dropped. Changing Acrylamide amount, Ceric ammonium nitrate, reaction time, and gum concentration yielded optimum % graft yields of 83, 85, 86, 84, and 84, respectively. This finding shows the best grafting condition for grafting of acrylamide amount onto konkoli gum [178].

Mishra A et al., (2007) developed new green polymeric materials for specialised applications onto okra mucilage by grafting of monomer acrylamide (AAm). Grafting was done with a redox initiator in a N₂ environment, and hydrogels were made with N,N-methylenebisacrylamide (NN-MBAAm) as a crosslinker. Scanning electron microscopy, fourier transform infrared spectroscopy, and x-ray diffraction techniques were used to characterise the grafted polymers and hydrogels in order to investigate various structural characteristics [179].

Pandey PK et al., (2006) induced grafting of acrylic acid on surface of guar gum. Guar gum was altered using the vanadium (V)–mercaptosuccinic acid system. The grafting parameters were found to rise with increased amount of vanadium (V), but they decreased as the concentration of vanadium (V) was increased further. Efficiency increased with increase in concentration, but decrease when the mercaptosuccinic acid concentration is increased further. The grafting parameters improve as the guar gum concentration rises. It has been discovered that as the temperature rises, the percent G rises as well. The graft copolymer has been analysed by various analytical parameters [180].

Singh V et al., (2004) used a microwave assisted method to synthesise guar-g polyacrylamide and performed a comparative study by grafting with and without presence of redox initiator system. When catalysts and initiator were combined with microwave heating, grafting efficiency increased by up to 20%. In the presence and absence of a catalyst and redox initiator, the influence of microwave power and time of exposure on yield of grafting was investigated. The highest efficiency of grafting

attained with MW was 66.66 percent in 0.22 minutes, against 49.12 percent in 90 minutes using the traditional approach. FTIR, NMR, TGA and XRD were used to characterise a typical MW grafted copolymer [181].

Biswal DR et al., (2004) developed and characterised a polyacrylamide graft copolymer by using CMC (carboxy methyl cellulose), discovering that as the number of PAM chains in the grafted copolymer increases, the viscosity of the grafted copolymer increases. [182].

Taghizadeh MT et al., (2001) revealed the kinetics of grafted copolymer of starch using acrylonitrile initiated by potassium persulfate. Using potassium persulfate can easily initiate graft polymerization of starch with acrylonitrile [183].

2.4 REVIEW ON SUSTAINED RELEASE MATRIX SYSTEMS

Singh P et al., (2021) improved the dissolution rate of aceclofenac and regulated the drug release. Matrix tablets were made using hydrophilic polymers (HPMC/guar gum) and the direct compression method. The in vitro drug release profile of tablets was assessed in phosphatebuffer at pH 6.8. (without enzymes). The gelling feature of polymers slowed drug release when the polymer concentration was increased. Higuchi's model best characterised the in vitro drug release from the suggested system, demonstrating that drug release from tablets followed a diffusion-controlled mechanism. The findings suggest that guar gum could be used as a hydrophilic carrier in the development of oral controlled medication delivery systems. Formulation F8 was chosen as the best formulation on the basis of results [184].

Alam S et al., (2021) used a wet granulation process to create a sustained release dosage form of Metformin Hydrochloride, using both Xanthan Gum and Hydroxy Propyl Methyl Cellulose (HPMC K4M) as rate regulating polymers. Formulation F7 had the best outcomes of all the formulation trial batches. HPMC K4M alone does not provide a suitable drug release profile, however a combination of HPMC K4M with Xanthan gum provides the best drug release kinetics. Fickian diffusion with first order kinetics is used to release the drug from the matrix tablets [185].

Akpabio EI et al., (2020) prepared theophylline tablets with modified release. Three batches of theophylline granules were created utilising three polymers (HPMC,

SCMC, and Sodium alginate) and 95 percent ethanol using the wet granulation method. The granules were compressed into batches of long-acting matrix tablets. Dissolution investigations were conducted using simulated stomach and intestinal liquids at varied agitation speeds, and the tablet batches were assessed for tablet characteristics. The results of the dissolving investigations were then fitted into four different drug release kinetics models. Although there was no substantial difference between the three polymers, their swelling with time was noticeable. The release kinetics followed the Higuchi model, with t_{10} and t_{90} released at 14 minutes and 6.8 hours, respectively, and releasing more than 90% during an 8-hour period. The tablets' mechanical characteristics were within acceptable limits [186].

Yahoum MM et al., (2020) used carboxymethyl xanthan gum derivatives to create hydrophilic matrices for regulated distribution of Piroxicam. An etherification procedure was used to make CMXs with different degrees of substitution. Different tablets were prepared using the direct compression method. The results showed that as the CMX ratio increases, the medication release rate increases. The best options for managing the release profile were determined to be matrices based on CMX2 (DS = 1.7), with the ideal formulation including 40% of CMX2 (F9). The dissolution data revealed that all matrices fit the Korsmeyer–Peppas model well, although F9's release kinetics were non-Fickian type. F9 received the greatest mean dissolution time value. Finally, their findings demonstrated that CMXs can be used as excipients in sustained release dosage forms for up to 20 hours [187].

Pawar SS et al., (2019) investigated the effect of polymers on sustained effect of tablets. Fourier transform infrared spectroscopy and DSC were used to investigate compatibility. Xanthan gum and Ethyl Cellulose were used to make the tablets, which were compressed using a direct compression process. The physicochemical properties of the produced matrix tablets were assessed. The drug release data was applied to various models in order to determine the release kinetics and mechanism of drug release. The optimal formulation was determined to be F4. Formulation F4 can be dissolved in a variety of ways. Mechanism of drug release that's non fickian [188].

Patil CC et al., (2019) developed tizanidine tablets with sustained release. Wet-granulation was used to make tablets, with polymers like Guar gum and Ethyl

cellulose in various ratios. In a conventional dissolution apparatus, the tablets were tested for in vitro release in pH 1.2 and 7.4 phosphate buffer for 12 hours. The data was subjected to First order, Zero order, Pappas and Higuchi diffusion models in order to determine the mode of release. The created Tizanidine sustained-release matrix tablet released the medicine for 12 hours, overcoming the drawback of regular tablets [189].

Latha K et al., (2018) developed sustained release matrix tablets of tolterodine tartrate (for the treatment of hyperactive bladder). The tolterodine tartrate granules were prepared using a wet granulation process, which had good flow characteristics and compressibility. The manufactured tablets were tested for a variety of physicochemical properties. The tolterodine tartrate granules were prepared using a wet granulation process, which had good flow characteristics and compressibility. The manufactured tablets were tested for a variety of physicochemical properties. The drug release of the improved formulation (F6) was fitted to several kinetic models, yielding an R^2 of 0.988 and a n of 0.787. As a result, with non-fickian diffusion, drug release follows zero order. Drug release is a combination of erosion and diffusion. The optimised formulation was tested for stability using ICH guidelines for climatic zone III and found to be stable [190].

Soni P et al., (2018) developed acyclovir sustained release tablets using Colocasia esculenta. The polysaccharide obtained following extraction from a natural source was assessed for colour, viscosity, and pH. The effect of various natural polymers on release from tablets was investigated. Formulation F-1 exhibits up to 97 percent drug release in 720 minutes, whereas Formulation F-6 shows 85 percent drug release in 720 minutes, demonstrating that Formulation F-1 and F-6 demonstrate sustained drug release over an extended period of time. The drug release mechanism from the sustained release tablets was discovered to be Anomalous (non-Fickian) diffusion using Higuchi's Model and the Korsmeyer equation [191].

Li S et al., (2017) used emulsion solvent diffusion to make Sustained-release microcapsules out of EC and PEG-6000. MS dissolution and bioavailability in dogs were compared to a commercially available MS formulation after treatment with novel microcapsules [192].

Kumbhar DM et al., (2017) used xanthan gum as natural polymer and semi synthetic polymers like hydroxypropylmethylcellulose of various grades like HPMCK4M, HPMCK15M and HPMCK100M, and Carbopol to manufacture the tablets of Venlafaxine HCl (VHL) with sustained release effect. To determine compatibility and flow qualities, the VHL and all excipients were tested. Dimensions of tablet, variation in weight test, friability, Uniformity of content, and an dissolution research were all performed on the manufactured tablets. The conclusion was that VHL tablets made with xanthan gum and carbopol have a long-lasting drug release that could be effective in Depressive disorders therapy [193].

Khan H et al., (2017) make bilayer pills with telmisartan as a sustained release (SR) and hydrochlorothiazide as an instant release (IR). Various quality control procedures and dissolution experiments were used to assess the tablets. The amount of drug release investigation was done in a pH 1.2 (0.1N) hydrochloric acid with a USP paddle equipment. By using the established HPLC-UV technique, at different time intervals the release of drug was determined. Telmisartan was released slowly over a 20-hour period in prepared tablets, while hydrochlorothiazide was released quickly within 30 minutes [194].

Sayed MA et al., (2016) developed floating tablets of Itopride hydrochloride (HCl) with sustained-release effect. The floating feature was made with mixing of NaHCO₃ and anhydrous citric acid (1:1 mol/mol). The formulation F10 was found to have a long-term drug release effect [195].

Faria GS et al., (2016) used the effervescence and swelling capabilities of sodium bicarbonate and the HPMC-PEO polymer combination to create an sustained release floating tablets of metformin HCl. The wet granulation process was used to create MTH sustained-release floating tablets. Tablets float in vitro due to CO₂ generation and entrapment of generated CO₂ by swelled polymeric matrix, and the amount of polymer matrix (amount of HPMC and PEO), effervescent agent (sodium bicarbonate), and swelling enhancer all influenced the drug release profile of created tablets (SSG) [196].

Palei NN et al., (2016) studied the effect of mucilage concentration on release of Lamivudine. Acetone was used to remove mucilage from the fruits of Abelmoschus

esclentus. Okra mucilage was taken to prepare Lamivudine matrix tablets. Post compression parameters investigations were all performed on the prepared tablets. The dissolution studies revealed that release of drug candidate from matrix was affected by diffusion of drug and relaxation of polymer, resulting in non-fickian or anomalous release [197].

Ya Zhang et al., (2016) developed sustained-release matrix pellets. Extrusion/spheronization technology was used to create pellets with a solid dispersed capsaicin core mixed using HPMC and MCC and then coated with EC. SEM, DSC, and XRD were used to assess the physicochemical parameters of the pellets (XRD). Additionally, in vivo absorption, release rate were evaluated. All of findings confirmed that successful manufacture of capsaicin sustained-release matrix pellets improved capsaicin oral bioavailability significantly [198].

Mitkare SS et al., (2015) used several grades of HPMC to make diclofenac sodium matrix tablets. The effect of hydrophilic polymers on the release properties of diclofenac matrix tablets was examined. Excipients included dicalcium phosphate and magnesium stearate. Direct compression was used to make the tablets. At a constant polymer content, release of drug from the high viscosity grades (E50) was very slow than that from the low viscosity classes (E15 and E300 LV). The tablet made with HPMC E50 has a longer release time. Drug release was reduced as the Drug: polymer ratio was increased. The greatest viscosity grade HPMC retarded the release most at increasing doses, according to the dissolution results. The model medication took a long time to come out of these HPMC matrix tablets [199].

Sarada A et al., (2015) used a melt granulation process to create matrix tablets of verapamil hydrochloride employing hydrophobic binders such as, carnauba wax, bees wax and stearic acid. The effect of a polymer with hydrophilic nature like PEG (polyethylene glycol) on waxy matrices was investigated. In the preparations, two grades of PEG-4000 and PEG-6000 were utilised. Carnauba wax functions as a good retardant, according to dissolving studies (more than 16 h). PEG 6000 boosts release more than PEG 4000 among the two grades of PEG utilised (4000 and 6000) [200].

Chime SA et al., (2013) developed diclofenac potassium tablets having sustained release effect. SRMS were made with phospholipid and triglyceride mixes in 1:1, 1:2

and 2:1, ratios respectively. An approved plastic mould was used to make SRMS-based tablets. Each tablet was containing 100 mg of diclofenac potassium. For sustained release features, the physicochemical parameters of the tablets were investigated and compared to the marketed tablets [201].

Quinten et al., (2011) used injection moulding of ethyl cellulose (EC) and polyethylene oxide (PEO) mixes to manufacture sustained-release matrix tablets and assess the effect of temperature of process, composition of matrix, and grade of viscosity of EC and PEO on dissolution and processability. Injection moulding was found to be a successful method for developing sustained-release PEO/EC matrix tablets [202].

Shanmugam et al., (2011) used wet granulation to make the sustained release tablets, which were designed with varying polymer drug ratios, resulting in preparations ranging from F1 to F9. HPMC (Hydroxypropyl methylcellulose), EC (Ethyl Cellulose), and natural polymer Gum Xanthan (XG) were used in formulation of tablets. [203].

Ganesh GNK et al., (2010) used Cashew nut tree gum, HPMC, and Carbopol to make diclofenac sodium matrix tablets. Precompression parameters and postcompression parameters were all assessed as part of the preformulation process. The medication was released in vitro for twelve hours in PBS pH 7.2. The produced tablet's physical characteristics were all within permissible limits. The matrix tablet (Batch C-III) composed of carbopol had a greater sustained drug release (50.65 percent) than the cashew nut tree gum and HPMC. The release profile of drug showed that increasing the polymer ratio delayed drug release more [204].

Subramaniam K et al., (2010) used wet granulation and a hydrophilic polymer such HPMC K-100 to develop "once daily" tablets of Aceclofenac (200mg). Preformulation experiments were performed on the medication excipient mixtures. Physicochemical tests, dissolution studies, kinetic studies, and tests of stability were all performed on the tablets. The study's findings suggested that hydrophilic polymers may be used to make formulations of Aceclofenac with sustained release [205].

Li FQ et al., (2006) performed dissolution release of matrix tablets Compritol 888 ATO. The study demonstrated that tablets based on solid dispersion were more successful at delaying the release of Sodium Ferulate than those squeezed from physical mixtures. The drug release from matrix tablets having a physical combination was nearly complete in 12 hours, while the solid dispersion formulation continued for more than 24 hours [206].

Jannin V et al., (2006) studied the effect of polymers like poloxamers on the dissolving performance and stability. Due to the formation of a porous lipid matrix network, the amount of theophylline released was increased [207].

Kuskal A et al., (2006) investigated the influence of combining hydrophilic (Eudragit RLPO and RSPO) and hydrophobic (Ethyl cellulose) polymers on Zidovudine release rate. The Eudragit formulation was only able to sustain release for 6 hours in dissolution study. The release was sustained for 12 hours when Eudragit was combined with Ethyl cellulose [208].

Ochoa L et al., (2005) created hydrophilic matrices for sustained release. Only the formulation with HPMC K4 M and Gelucire 50/13 or PEG 6000 displayed a profile equivalent to the commercial formulation evaluated in terms of dissolution. When lipophilic binders were added, however, the release of Theophylline was significantly reduced [209].

Kamble et al., (2004) used a melt solidification approach to incorporate a higher proportion of wax during the manufacture of Ibuprofen beads for enhanced integrity and sustained drug release. To increase matrix integrity and drug release, a mixture of cetyl alcohol and palmitic acid is utilised. The release was not significantly improved in an in-vitro dissolving test. DSC reveals that waxes' distinct solidification and erosion capabilities are unable to delay drug release even at greater concentrations [210].

Chauhan B et al., (2004) prepared and evaluated floating matrices. Melt solidification matrices were tested for floating ability. Matrix ageing was investigated using DSC, HSPM, SEM, and in-vitro release. The crystal structure of Gelucire changes with age, resulting in increased drug release [211].

Tiwari SB et al., (2003) found the influence of hydrophobic and hydrophilic polymers such as castor oil (hydrogenated) and ethyl cellulose on the Tramadol release. Wet granulation was used to make hydrophilic matrix tablets, while melt granulation was used to make hydrophobic (wax) tablets. Dissolution time was longer for hydrophobic matrix tablets (>20h) than for hydrophilic (14h). The presence of ethyl cellulose slowed the rate of emission. Tablets made from a mix of hydrophobic and hydrophilic polymers failed to last more than 12 hours. Tablets made from hydrogenated castor oil were discovered to be the most effective at modulating the distribution of highly water soluble medications [212].

Makhija SN et al., (2002) developed a matrix system using swellable and non-swellable polymers such as HPMC, cellulose acetate, Eudragit RSPO, and ethyl cellulose. In order to achieve a sustained release profile over 16 hours, non-swellable polymers were combined with HPMC. The impact of the drug-polymer ratio on release rate was investigated [213].

Amaral et al., (2001) investigated the influence of hydrogenated castor oil concentrations on Naproxen release. HPMC and hydrogenated castor oil were used to make matrix tablets. It has been discovered that when concentration rises, release rate decreases. Release of drug can be controlled by using the right diluents. Lipid matrices forming material can be used to formulate sustained-release dosages or modulate the distribution of extremely water-soluble drugs [214].

Barthelemy P et al., (1999) prepared tablets using Compritol 888 ATO as hot melt coating agent. The purpose of this experiment was to study the effect of Compritol 888 ATO coated drug-loaded sugar beads and lactose granules. The coating potential was found to be satisfactory [215].

3.1 RATIONALE OF THE STUDY

The natural polysaccharides have traditionally been utilised as excipients in food and pharmaceuticals because of their biodegradability, bio-compatibility, ease of accessibility and low price. They do, however, have several disadvantages, like hydration that is uncontrollable, solubility based on pH, Variations in viscosity with time and a short lifespan, which limit their applicability. Natural polymers can be chemically modified to overcome these drawbacks. Natural polymers can be modified chemically in a number of ways, which includes etherification, graft copolymerization and cross-linking. Natural polysaccharide modification has recently gained a lot of interest. The modification of polysaccharides can be done by a variety of methods but the best possible method is grafting. In this method, various polymers of synthetic origin may be used to create innovative copolymers with better release characteristics. The various types of synthetic monomers like acrylic acid, acrylamide and acrylonitrile are used to modify the natural polysaccharides. Vinyl treatment increases the polysaccharide's flocculating properties as well as its releasing behaviour.

Grafting copolymerization procedures were traditionally carried out utilising initiator driven reactions, which take a long duration of time to prepare the graft copolymers with lesser grafting efficiency. Microwave assisted method for grafting is an effective approach for transferring energy quickly throughout the reaction mixture with higher grafting efficiency.

3.2 AIM OF THE STUDY

The goal of this study was to manufacture and analyse graft copolymers of acrylamide with Mastic gum and banana peel gum. Furthermore, by formulating sustained release matrix tablets with Lamivudine as the model drug, the in vitro release behaviour of grafted co-polymer was to be compared with of ungrafted gum.

3.3 OBJECTIVES OF THE STUDY

- Synthesis of graft copolymers of banana peel and mastic gums using acrylamide as monomer by microwave assisted grafting technique.
- Optimization of grafted copolymers.

- Characterisation of optimised batch
- Formulation of optimised batch of grafted copolymer and ungrafted copolymer sustained release matrix tablets.
- Comparative drug release studies of grafted copolymer tablets with ungrafted polymer tablets.
- Stability studies.

4.1 MATERIALS USED

Table 4.1: Research-related materials

S. No.	Name	Company/Model
1.	Lamivudine	Yarrow Chem Products, Mumbai
2.	Mastic gum	Chios gum mastic growers' Ass. Greece
3.	Acrylamide	Fisher Scientific Pvt. Ltd., Mumbai
4.	Potassium di-hydrogen- <i>o</i> phosphate	Signet Chemical Corp. Pvt. Ltd., Mumbai
5.	di-Sodium hydrogen phosphate	Central Drug House Pvt. Ltd. New Delhi
6.	Ethanol	Tradewell International Pvt Ltd, Mumbai
7.	Methanol	Fihar Chemical Ltd., Ahmedabad
8.	Hydrochloric Acid	SD Fine-chem. Ltd, Mumbai
9.	Acetone	SD Fine-chem. Ltd, Mumbai
10.	Ceric Ammonium Nitrate	Quali-Tech Chem
11.	Talc	Fisher Scientific India Pvt. Ltd
12.	Lactose	Fisher Scientific India Pvt. Ltd
13.	PVP K-30	Fisher Scientific India Pvt. Ltd
14.	n-octanol	Merk India Ltd.
15.	Magnesium Stearate	Fisher Scientific India Pvt. Ltd

4.2 EQUIPMENT'S USED

Table 4.2: Research-related equipments

S. No.	Name	Company
1.	UV Spectrophotometer	Shimadzu, Japan
2.	Dissolution Test Apparatus	Labindia
3.	Hot air oven	Narang Scientific Works, New Delhi, India
4.	Bath Sonicator	Mesonix, New York, USA
5.	Mechanical Stirrer	REMI Equipment
6.	Magnetic Stirrer	REMI Equipment
7.	pH meter	Shimadzu
8.	Digital Balance	Shimadzu, Japan
9.	Test tube rack	Tarsons Products Pvt. Ltd., Kolkata, India
10.	Melting Point Apparatus	Remi Equipment, Mumbai
11.	Vortex mixer	Genei (SLM-VM-3000), Bangalore
12.	Weighing balance, (CY220)	Denver Instruments, Mumbai
13.	FTIR	ALPHA FTIR, Bruker, Germany
14.	DSC instrument	SDT-Q600® TA Instruments, Tokyo, Japan
15.	FE-SEM	SEM, LEO43 SVP, Cambridge
16.	Humidity chamber	REMI Equipment, Mumbai
17.	XRD instrument	Malvern, UK

4.3 PREFORMULATION STUDIES

The Preformulation studies phase is performed on a drug candidate before preparation of any kind of dosage form. The nature of the medicament has a significant impact on processing factors such as the method of preparation and the formulation's pharmacokinetic response. In the most basic situation, these preformulation experiments may simply confirm that the compound's development is not hindered by any substantial barriers. The preformulation stage provides a basic knowledge about applicant polymers and drugs. The choice made on the data generated during this stage can profoundly affect the resulting improvement of compounds.

FT-IR, UV spectroscopy, solubility, partition coefficient and melting point were used for identification of chemical and physical properties of Lamivudine.

4.3.1 Physical Appearance

The drug's organoleptic characteristics were identified. The drug was characterized for its colour, odour, taste and surface morphology.

4.3.2 Determination of Melting Point

Following techniques were used to determine melting point of lamivudine:

A. Capillary Fusion Method

The melting point apparatus was set up using a small amount of Lamivudine in a one-sided closed capillary tube. The temperature at which Lamivudine starts to melt was noted as melting point. The experiment was performed in triplicate.

B. Differential Scanning Calorimetry

Lamivudine was tested for purity using differential scanning calorimetry, which determined an endothermic peak that must correspond to its melting point. The sample was heated in sealed aluminium crucibles. The temperature with increasing heating range of 10°C/min was used in range of 20-400°C [216, 217].

4.3.3 Fourier Transform Infrared Spectra Analysis

The infrared spectrum of Lamivudine was determined by using potassium bromide dispersion method. The spectrum provides the information regarding the functional

groups present in drug candidate. The infrared spectrum of drug which was obtained and then compared with reference spectra to identify the peaks. The range of 400-4000 cm^{-1} was used for scanning [218, 219].

4.3.4 Solubility determination of Lamivudine in different solvents

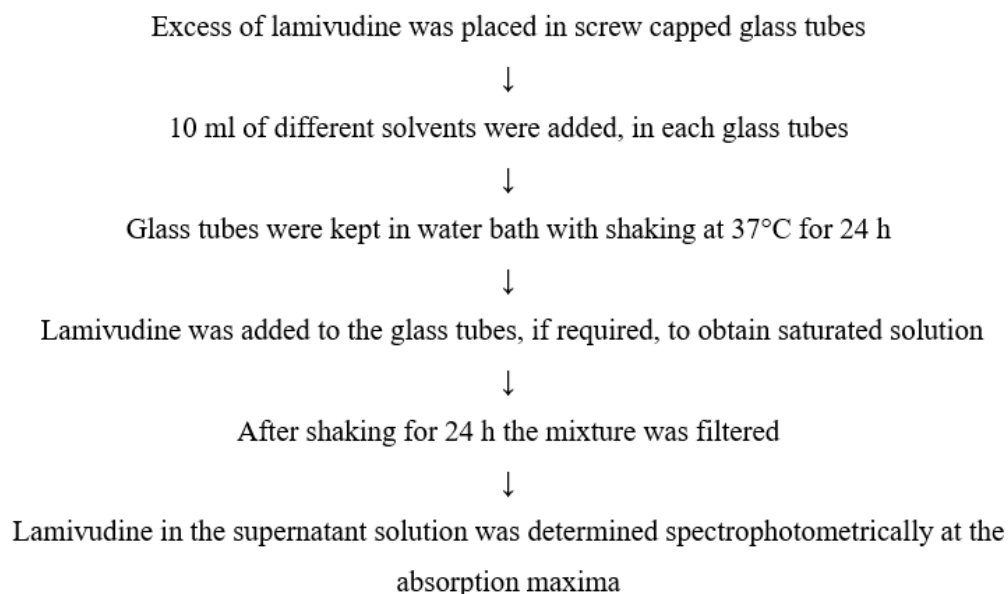
A solid's solubility can be described as its ability to dissolve in a liquid solvent and form a homogenous solution. The definition of solubility as per IUPAC as a saturated solution's analytical composition represented as a fraction of a specific solute in a specific solvent [220-221].

A. Qualitative Solubility of Lamivudine

The solubility studies of lamivudine were carried out in solvents like methanol, water, 0.1N HCl and phosphate buffer of pH-6.8. Lamivudine was added in distinct glass tubes containing 10 ml of solvent. The solubility of Lamivudine was then examined visually.

B. Quantitative Solubility of Lamivudine

An equilibrium solubility approach was used to determine Lamivudine's quantitative solubility in various solvents. Various solvents used in study were purified water, 0.1N HCl and phosphate buffer (pH-6.8). The method followed as:



4.3.5 Absorption Maxima (λ_{\max}) determination by UV Spectroscopy

When drug molecules in a solution are exposed to visible/ultraviolet light, depending on the sort of electric transition involved with absorption, they absorb light of a given wavelength. To obtain detailed information on the chromophoric component of the molecules in solution, a double beam UV-Visible spectrophotometer is commonly used. A graph of absorbance versus wavelength is commonly used to represent the UV spectrum.

The maximum concentration of Lamivudine was determined using a double beam UV-Visible spectrophotometer (Shimadzu, UV-1800, Japan). A 10 μ g/ml Lamivudine solution in various solvents was scanned in the 200-400nm range [222].

4.3.6 Preparation of standard curve of Lamivudine

The standard curve of lamivudine was developed in different solvents (Phosphate buffer pH 6.8 and 0.1 N HCl). The stock solution of 1 mg/ml was made by dissolving 100 mg of lamivudine in 100 ml of solvent. From this above stock solution, 10 ml of sample was taken and diluted up to 100 ml to make the solution of concentration 100 μ g/ml. The concentrations of 5, 10, 15, 20, 25 and 30 μ g/ml were prepared from stock solution by using serial dilution method. A UV-visible spectrophotometer was used to measure the absorbance of these solutions at 270 nm, and the absorbance was plotted against time to obtain a standard curve. The straight-line equation and correlation coefficient were calculated from this curve [222].

4.3.7 Partition Coefficient

A drug's hydrophilicity and lipophilicity, as well as its capacity to cross cell membranes, are measured by the partition coefficient (oil/water). It's the proportion of unionised drug dispersed in the organic and aqueous phases at equilibrium. The partition coefficient can be used to determine if a substance is lipophilic or hydrophilic. An oil phase of n-octanol and phosphate buffer of pH-6.8 is typically used to calculate the partition coefficient.

$$P_{o/w} = C_{n\text{-octanol}}/C_{\text{water}}$$

Thus, partition coefficient ($P_{o/w}$) is the quotient of two drug concentrations in n-octanol and water, and is commonly expressed as a logarithm to base 10 ($\log P$).

Shake flask method was used to determine partition coefficient. Excess amount of the Lamivudine was dissolved in 10 ml of a mixture of two solvents (n-octanol: PBS, pH 6.8) and left for 24 hours. The two layers were separated after 24 hours and centrifuged for 15 minutes. After proper dilution, the absorbance was measured by UV spectrophotometer at the respective maxima [223,224].

4.4 DRUG EXCIPIENT COMPATIBILITY STUDIES

The compatibility of drug with excipients was performed by FTIR. The FTIR was used to find out the interactions between the medicament and the excipients. In a 1:1 ratio, the drug and other excipients were thoroughly combined. FTIR was used to scan the samples in the 400-4000 cm^{-1} range. The spectra of drug with various excipients were examined to check for incompatibility and physical changes [225,226].

4.5 SYNTHESIS AND OPTIMIZATION OF GRAFTED MASTIC GUM

Acrylamide grafted Mastic gum was synthesized using microwave assisted grafting method. When microwave radiation is irradiated on a sample, it causes the dipoles or ions in the sample to align in the direction of electric field. As the applied electric field oscillates, the dipole or ion field strives to realign itself with the alternating electric field, and energy is dissipated as heat owing to molecular friction and dielectric loss. The amount of heat produced by this process is proportional to the matrix's ability to align with the frequency of the applied field.

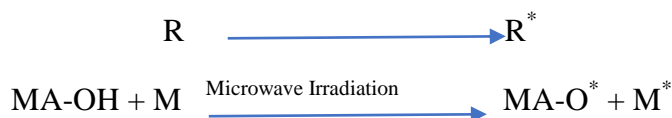
4.5.1 Procedure of grafting of mastic gum

Microwave assisted method was used for the purpose of grafting. In 10 ml of water, an appropriate amount of monomer acrylamide (1.4 g-2.8 g) was solubilized. 0.5 g mastic gum was solubilised in 25 ml distilled water by stirring. Two of above aqueous solutions were mixed and initiator (ceric ammonium nitrate) in varying concentrations (25-75 mg) was added. Microwaves were used to irradiate the above dispersion. After the irradiation time was completed, resulted in formation of mass with properties like a gel. The reaction mixture was then cooled and left undisturbed for 12 hours to allow the grafting process to complete. This gel-like material was added into an excess of acetone after 12 hours. This resulted in precipitation of grafted polymer. These

precipitates were then separated out and dried in hot air oven. Finally, the dried precipitates were pulverised and sieved [227-229].

Synthesis Scheme for microwave assisted synthesis of Mastic-g-acrylamide

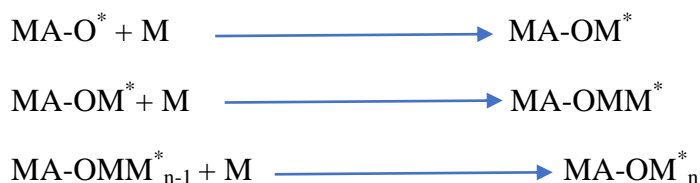
Initiation



Where,

- R is Ceric ammonium nitrate
- MA-OH is gum mastic
- M is monomer (Acrylamide)

Propagation



Termination



Formation of Homopolymer



4.5.2 Optimization of grafting process using box behnken design

For the aim of optimization, the Box Behnken design was selected. The grafted mastic gum copolymer with acrylamide was synthesised and optimised using a 3-factor 3-level response surface design, which required total fifteen runs, with 3 replicates of the centre run and ceric ammonium nitrate was used as initiator to produce free radicals. To generate design space and optimise formulation with the goal of obtaining critical quality attributes (CQA, Y1 = percentage yield, Y2 = percentage

Grafting, Y_3 = percentage grafting efficiency), the critical synthesis and process parameters; CSPP (A = monomer concentration, B = initiator concentration, and C = Reaction Temperature) were used. Different concentrations of three CSPPs were chosen: A = Acrylamide with low (1.4 g), medium (2.1 g), and high (2.8 g) levels; B = ceric ammonium nitrate with low (25 mg), medium (50 mg), and high level (75 mg) levels; and Temperature low (40°C), medium (50°C), and high level (60°C). The software named Design expert was used to develop the box behnken design and the polynomial equation generated was given below:

$$Y = \beta_0 + \beta_1.A + \beta_2.B + \beta_3.C + \beta_4.A.B + \beta_5.A.C + \beta_6.B.C + \beta_7.A_1^2 + \beta_8.B_2^2 + \beta_9.C_2^2$$

Where, Y is the dependent variable, β_0 is the arithmetic mean response of the 15 runs and β_i ($\beta_1, \beta_2, \beta_3, \beta_4, \dots, \beta_9$) is the estimated coefficient for the corresponding factor A, B and C, which represents the average results of changing one factor at a time from its low to high value. The interaction term (A.B, A.C and B.C) depicts the changes in the response when three factors are simultaneously changed. The polynomial terms A^2 , B^2 and C^2 are included to investigate quadratic model. The magnitude of coefficients in polynomial equation has either positive sign indicating synergistic effect or negative sign indicating antagonistic effect. Best fitting experimental model (linear, two factor interaction and quadratic) was taken statistically on the basis of comparison of several statistical parameters like coefficient of variation (CV), multiple correlation coefficient (R^2), adjusted multiple correlation coefficient (adjusted R^2), predicted residual sum of square and graphically by Contour Plot, 3D response surface plot provided by Design Expert software. The level of significance was considered at p-value <0.05 [220,221].

Table 4.3: Levels of Independent Variables in Box Behnken Design for mastic gum

Factor	Name	Units	Low level	Mid-level	High level
A	Acrylamide amount	gm	1.4	2.1	2.8
B	CAN amount	mg	25	50	75
C	Temperature	°C	40	50	60

CAN- Ceric ammonium nitrate

Table 4.4: Design Matrix of Box Behnken Design for mastic gum

Formulation code	Acrylamide amount (g)	Initiator amount (mg)	Temperature (°C)
MA1	2.1	50	50
MA2	1.4	75	50
MA3	2.1	50	50
MA4	1.4	50	40
MA5	1.4	25	50
MA6	2.8	75	50
MA7	2.8	50	60
MA8	2.1	75	40
MA9	2.1	25	60
MA10	2.1	50	50
MA11	2.1	25	40
MA12	2.8	50	40
MA13	2.1	75	60
MA14	1.4	50	60
MA15	2.8	25	50

Where MA -Mastic gum

4.5.3 Characterization of ungrafted mastic gum and optimised grafted mastic gum

The ungrafted mastic gum and optimised grafted mastic gum were further characterised by FTIR, DSC, SEM and XRD analysis.

A. FTIR Analysis

Infrared spectroscopy can provide information on the presence of distinct functional groups as well as molecule structure. FT-IR spectra of native and grafted mastic gum was determined in the region of 4000 to 500 cm^{-1} confirmed the grafting on polymer

backbone. The process of grafting was identified using infrared spectroscopy (FT-IR Bruker, Impact 400 IR spectrophotometer) [232].

B. DSC Analysis

The screening method was differential scanning calorimetry (DSC). The samples of gums were sealed hermetically in an aluminium pan of flat-bottom and heated in instrument (DSC Mettler Toledo, Mumbai, India) in a nitrogen environment at a rate of 25 ml/min. The range of temperature was 25°C to 220°C, with a 10°C/min heating rate. Mastic gum, Acrylamide, and Grafted mastic gum were evaluated using DSC (differential scanning calorimetry) [233,234].

C. Scanning Electron Microscopy

Acrylamide, Mastic gum, and Acrylamide grafted samples were applied to the stubs with double-sided sticky tape, and then fine coat ion sputtering was used to cover them in gold palladium alloy (150-200A0). External surface structure of the samples was checked using SEM [168].

D. XRD Analysis

X-ray diffractometry examination of grafted and native mastic gum and acrylamide samples was performed in powder form using an X-ray Diffractometer. The scanning employed was over the 0.00 to 60.00° diffraction angle (2θ) range [149].

4.6 SYNTHESIS AND OPTIMIZATION OF GRAFTED BANANA PEEL GUM

4.6.1 Screening of banana

The banana species has been screened based on local availability. The plant specimens were taxonomically identified and confirmed by Prof. R. C. Gupta, Department of Botany, Punjabi University, Patiala.

The banana selected for present study are available in north India.

4.6.2 Extraction of banana peel gum

The fresh and ripe bananas were purchased from the local market. The peels were removed from the fruit and washed with water and then dried. The banana peels were

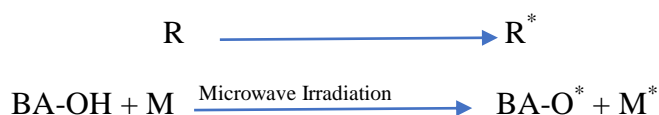
bleached by using 0.02% solution of sodium hypochlorite for 36 h. To prevent the peel from browning when exposed to ambient oxygen, a one percent sodium metabisulphate solution was added and left to stand for 7-8h. After that the solution was boiled for 30 minutes and left to stand for complete removal of gum in water. After filtration the gum was precipitated by addition of acetone and separated by means of filtration. It was then dried in a hot-air oven at 60 °C. After that, the powder was sieved [236].

4.6.3 Procedure of grafting of banana peel gum

Microwave assisted method was used for the purpose of grafting. In 10 ml of water, an appropriate amount of monomer acrylamide (1.4 g-2.8 g) was solubilized. 0.5 g banana peel gum was solubilised in 25 ml distilled water by stirring. Two of above aqueous solutions were mixed and initiator (ceric ammonium nitrate) in varying concentrations (25-75 mg) was added with continuous stirring. The above dispersion was irradiated by microwave. A gel like mass was obtained after completion of irradiation time. The reaction mixture was then cooled and left undisturbed for 12 hours to allow the grafting process to complete [227-229]. This gel-like material was added into an excess of acetone after 12 hours. This resulted in precipitation of grafted polymer. These precipitates were then separated out and dried in hot air oven at 40°C. Finally, the dried precipitates were pulverised and sieved.

Synthesis Scheme for microwave assisted synthesis of Banana-g-acrylamide

Initiation



Where,

- R is Ceric ammonium nitrate
- BA-OH is banana peel gum
- M is monomer (Acrylamide)

Propagation**Termination****Formation of Homopolymer****4.6.4 Optimization of grafting process using box behnken design**

Box Behnken design was used for purpose of optimisation. A 3-factor 3-level response surface Box-Behnken design, which requires 15 runs including three replicates of the central run, was used for the synthesis of graft copolymers of banana peel gum with acrylamide using ceric ammonium nitrate as the free radical initiator [220,221].

Table 4.5: Levels of Independent Variables in Box Behnken Design for banana peel gum

Factor	Name	Units	Low level	Mid-level	High level
A	Acrylamide amount	g	1.4	2.1	2.8
B	CAN amount	mg	25	50	75
C	Temperature	°C	40	50	60

Table 4.6: Design Matrix of Box Behnken Design for banana peel gum

Formulation code	Acrylamide amount (g)	Initiator amount (mg)	Temperature (°C)
BA1	2.1	50	50
BA2	1.4	75	50
BA3	2.1	50	50
BA4	1.4	50	40
BA5	1.4	25	50
BA6	2.8	75	50
BA7	2.8	50	60
BA8	2.1	75	40
BA9	2.1	25	60
BA10	2.1	50	50
BA11	2.1	25	40
BA12	2.8	50	40
BA13	2.1	75	60
BA14	1.4	50	60
BA15	2.8	25	50

Where BA-Banana Peel Gum

4.6.5 Characterization of ungrafted banana peel gum and optimized grafted banana peel gum

The ungrafted banana peel gum and optimized grafted banana peel gum were further characterized by FTIR, DSC, SEM and XRD analysis.

A. FTIR Analysis

Infrared spectroscopy can provide information on the presence of distinct functional groups as well as molecule structure. FT-IR spectra of native and grafted banana peel gum was determined in the region of 4000 to 500 cm^{-1} confirmed the grafting on

polymer backbone. The process of grafting was identified using infrared spectroscopy (FT-IR Bruker, Impact 400 IR spectrophotometer) [232].

B. DSC Analysis

The screening method was differential scanning calorimetry (DSC). The samples of gums were sealed hermetically in an aluminium pan of flat-bottom and heated in instrument (DSC Mettler Toledo, Mumbai, India) in a nitrogen environment at a rate of 25 ml/min. The temperature range was 25°C to 220°C, with a 10°C/min heating rate. Banana peel gum, Acrylamide, and Grafted banana peel gum were studied using differential scanning calorimetry (DSC) [233,234].

C. Scanning Electron Microscopy

Acrylamide, Banana peel gum, and Acrylamide grafted banana peel gum were applied to the stubs with double-sided sticky tape, and then fine coat ion sputtering was used to cover them in gold palladium alloy (150-200A0). External surface structure of the samples was checked using SEM [168,170].

D. XRD Analysis

X-ray diffractometry examination of grafted and native banana peel gum and acrylamide samples was performed in powder form using an X-ray Diffractometer. The scanning employed was over the 0.00 to 60.00° diffraction angle (2θ) range [149].

4.7 SWELLING STUDIES OF UNGRAFTED AND GRAFTED GUMS

When a slightly crosslinked material is soaked in water, it does not dissolve but the water enters into the pre-existing pores in the crosslinked matrix and by the time the material swells. And this swelling pushes the material chains away from each other leading to increased separation between them causing overall segmental motion. The capacity of water absorption by grafted and ungrafted gums was determined. 0.2g of ungrafted mastic, ungrafted banana peel gum, grafted mastic and grafted banana peel gum were soaked separately in 50ml of distilled water for 30, 60, 90, 120, 150, 180, 210 and 240 minutes. After each time period, samples were filtered through a 100-mesh sieve and drained for 15 minutes to remove excess water before being

reweighed [235]. The following formula was used to compute the percentage of swelling:

$$\% \text{ Swelling} = \frac{\text{Weight of swollen polymer} - \text{Weight of dry polymer}}{\text{Weight of dry polymer}} \times 100$$

4.8 VISCOSITY MEASUREMENT OF UNGRAFTED AND GRAFTED GUMS

The viscosity of a fluid can be defined as the resistance generated during flow. In case of linear chain polymer, the viscosity will be less as compared to branched polymer network. During grafting, acrylamide side chains attach with the polymer backbone and form a branched polymer network which leads to increase the viscosity.

The viscosity measurement of ungrafted banana peel gum, ungrafted mastic gum, selected grafted banana peel gum and grafted mastic gums were carried out by using Brookfield viscometer at 32.7°C. The materials were dissolved in hot water and kept at 32.7°C for conditioning. The viscosity was then measured [170].

4.9 COMPATIBILITY STUDIES OF UNGRAFTED AND GRAFTED MASTIC GUM WITH LAMIVUDINE

The compatibility of drug with ungrafted and grafted mastic gum was ascertained by FTIR. FTIR was used as tool to detect any physical and chemical interaction between drug and grafted mastic gum. Drug with ungrafted and grafted mastic gum were mixed separately in ratio of 1:1. Samples were scanned by FTIR under the range of 400-4000 cm⁻¹. To assess for incompatibility and physical changes, the spectra of pure drug and drug with ungrafted and grafted mastic gum were compared.

4.10 COMPATIBILITY STUDIES OF UNGRAFTED AND GRAFTED BANANA PEEL GUM WITH LAMIVUDINE

The compatibility of drug with grafted banana peel gum was ascertained by FTIR. FTIR was used as tool to detect any physical and chemical interaction between drug and grafted banana peel gum. Drug with ungrafted and grafted banana peel gum were mixed thoroughly in ratio of 1:1. Samples were scanned by FTIR under the range of 400-4000 cm⁻¹. To assess for incompatibility and physical changes, the spectra of pure drug and drug with ungrafted and grafted banana peel gum were compared.

4.11 PREPARATION AND CHARACTERIZATION OF LAMIVUDINE SUSTAINED RELEASE MATRIX TABLETS USING UNGRAFTED AND GRAFTED MASTIC AND BANANA PEEL GUM

4.11.1 Preparation of blend of tablets

By manufacturing lamivudine matrix tablets, the release characteristics of grafted and ungrafted mastic and banana peel gums were evaluated and compared. Various batches of lamivudine matrix tablet blends were prepared by using grafted mastic, grafted banana peel, ungrafted mastic and ungrafted banana peel by using lactose as diluent [236,237]. The composition of various formulations is given in following tables

Table 4.7(a): Formulation table for matrix tablets of ungrafted mastic gum

Batches of tablet (mg)	UMA1	UMA2	UMA3	UMA4	UMA5
Lamivudine	100	100	100	100	100
Ungrafted Mastic Gum	25	37.5	50	62.5	75
PVP K30	20	20	20	20	20
Lactose	95	82.5	70	57.5	45
Magnesium stearate	5	5	5	5	5
Talc	5	5	5	5	5

Table 4.7 (b): Formulation table for matrix tablets of grafted mastic gum

Batches of tablet (mg)	GMA1	GMA2	GMA3	GMA4	GMA5
Lamivudine	100	100	100	100	100
Grafted Mastic Gum	25	37.5	50	62.5	75
PVP K30	20	20	20	20	20
Lactose	95	82.5	70	57.5	45
Magnesium stearate	5	5	5	5	5
Talc	5	5	5	5	5

Table 4.8 (a): Formulation table for matrix tablets of ungrafted banana peel gum

Batches of tablet (mg)	UB A1	UB A2	UB A3	UB A4	UB A5
Lamivudine	100	100	100	100	100
Ungrafted Banana Gum	25	37.5	50	62.5	75
PVP K30	20	20	20	20	20
Lactose	95	82.5	70	57.5	45
Magnesium stearate	5	5	5	5	5
Talc	5	5	5	5	5

Table 4.8 (b): Formulation table for matrix tablets of grafted banana peel gum

Batches of tablet (mg)	GBA1	GBA2	GBA3	GBA4	GBA5
Lamivudine	100	100	100	100	100
Grafted Banana Gum	25	37.5	50	62.5	75
PVP K30	20	20	20	20	20
Lactose	95	82.5	70	57.5	45
Magnesium stearate	5	5	5	5	5
Talc	5	5	5	5	5

4.11.2 Precompression evaluation of blend of tablets

A. Angle of repose

The angle of repose was calculated using the funnel method. A funnel was filled with a precisely weighed quantity of powder. The funnel's height was adjusted such that the funnel's tip just touched the powder heap's apex. The powder was permitted to pour freely from the funnel onto the tabletop. A measurement of the diameter of the powder cone was performed [238]. The following equation was used to compute the angle of repose.

$$\tan(\theta) = h/r$$

Where h and r are height and radius of cone of powder respectively.

Table 4.9: Standard values of angle of repose

S. No.	Angle of Repose	Flowability
1	25-30	Excellent
2	31-35	Good
3	36-40	Fair
4	41-45	Passable
5	46-55	Poor
6	56-65	Very Poor
7	>66	Very very Poor

B. Bulk Density

A specific amount of powder material is transferred into a measuring cylinder [239]. Bulk volume refers to the amount of powder in a measuring cylinder, and bulk density is calculated using the formula below:

$$\text{Bulk Density} = \text{Weight of powder} / \text{Bulk Volume}$$

C. Tapped Density

A specific weight of powder material is transferred into a measuring cylinder. The measuring cylinder was tapped until a fixed or constant volume was achieved [239]. This fixed volume is known as tapped volume. The following formula is used to compute the tapped density:

$$\text{Tapped Density} = \text{Weight of powder} / \text{tapped volume}$$

D. Carr's Consolidation Index

It is also known as Carr's compressibility index [240]. This index of powder blend is calculated by following formula:

$$\text{Carr's Compressibility Index} = [(\text{Tapped Density} - \text{Bulk Density}) / \text{Tapped Density}] * 100$$

Table 4.10: Standard values of Carr's index

S. No.	Carr's Index	Type of Flow
1	<10	Excellent
2	11-15	Good
3	16-20	Fair
4	21-25	Passable
5	26-31	Poor
6	32-37	Very Poor

E. Hausner's Ratio

It's mostly used to calculate interparticulate friction and forecast powder flow properties [240]. The following formula is used to calculate the Hausner ratio:

$$\text{Hausner's Ratio} = \text{Tapped Density/Bulk Density}$$

The flowability and compressibility are related by following relationship:

Table 4.11: Standard values of Hausner's Ratio

S. No.	Hausner's Ratio	Type of Flow
1	1.00-1.11	Excellent
2	1.12-1.18	Good
3	1.19-1.25	Fair
4	1.26-1.34	Passable
5	1.35-1.45	Poor
6	1.46-1.59	Very Poor
7	>1.60	Extremely Poor

4.11.3 Preparation of sustained release matrix tablets

All the ingredients which are given in table 4.7 and table 4.8 were separately passed through sieve no 60. The tablets were prepared by wet granulation method and compression was performed by using 8 mm punches in a single station tablet punching machine.

The ratio of lamivudine, polymers (grafted mastic, grafted banana peel, ungrafted mastic and ungrafted banana peel gum) and excipients were selected in such a way that the weight of tablets for all the batches remain constant (250 mg). The ratio of drug and polymers were 1:0.25, 1:0.375, 1:0.5, 1:0.625, 1: 0.75. The talc and magnesium stearate were used as glidant and lubricant. Lactose was used as diluent and PVPK-30 was used as binder [166,177].

4.11.4 Evaluation of sustained release matrix tablets of lamivudine

A. Appearance

The matrix tablets were observed visually for any sign of defects like chipping, capping and lamination [241-243].

B. Thickness of tablets

The thickness of 10 selected tablets was determined by using vernier calliper. Thickness is mainly measured to determine the uniformity in dimension of tablets [241-243].

C. Hardness of tablets

From each batch of tablets, hardness was determined by selecting 10 tablets from each batch. The Monsanto Hardness Tester was used to determine the hardness of the tablets (MHT-20, Campbell Electronics, Mumbai, India). Between the two jaws of the hardness tester, a tablet was held. The reading of meter must be zero at that point. Then the force was applied until the whole tablet get crushed by rotation of knob of hardness tester. At this stage, the value was expressed in kg/m^2 [241-243].

D. Friability of tablets

The strength was measured by a parameter known as friability. This test was performed by using Roche friabilator (FTA-20, Campbell Electronics). The purpose of this test is to examine the effect of shock abrasion on tablets by spinning them at 25 rpm and dropping them from a height of 6 inches after each revolution. Twenty tablets were selected randomly from each batch of tablets and weighed. These preweighed tablets were then placed in a Roche friabilator, which was rotated 100

times in four minutes. After that, the tablets were dusted and reweighed. Weight reduction of less than 1% is generally seen as appropriate [241-243]. The formula for calculating percent friability was as follows:

$$\text{Friability} = \frac{\text{Initial Weight} - \text{Final Weight}}{\text{Initial Weight}} \times 100$$

E. Weight variation test

A total of 20 tablets from each batch of tablets were chosen for the weight variation test. The weight of the 20 tablets was averaged after they had been individually weighed. The weights of the individual tablets were then compared to the average weight. If not more than two tablets fall outside the percentage limits and no tablet differs by more than the percentage restrictions, the test was deemed to be passed. During the compression of tablets, the weight variation test is essential. It must be performed during the specific time intervals in compression process of tablets. If the weight variation is not maintained there will be deviation in drug content as well of yield of tablets [241-243]. The weight variation limits for tablets are as following as per Indian Pharmacopoeia:

Table 4.12: Weight variation limits as per I.P.

S. No.	Weight of tablets	Maximum % deviation allowed
1	80 mg or less	10
2	More than 80 mg but less than 250 mg	7.5
3	More than 250 mg	5

F. Content Uniformity Test

In this test, ten tablets were selected randomly from each batch of tablets. This test was done to see if the amount of medicament in each batch and tablet remained within the label claim's limited range from batch to batch and tablet to tablet. The powder equivalent to 100 mg of lamivudine was triturated and transferred to a 100 ml volumetric flask containing phosphate buffer pH 6.8, followed by a 10-minute

sonication operation. The above mixture was then passed through a whatmann filter paper. The amount of lamivudine was determined by using double beam UV-spectrophotometer at 270 nm after suitable dilution using phosphate buffer pH 6.8 as blank [241-243].

G. In-vitro drug release studies

The in-vitro release tests were performed at 50 rpm using a USP type-II dissolution apparatus. The test was carried out using 900 ml of 0.1 N HCl for the first 2 hours and phosphate buffer of pH 6.8 at $37 \pm 0.5^\circ\text{C}$. After precise intervals of time as shown in the table, a sample of 5 ml of dissolution medium was extracted and replaced with new dissolution media. The samples were then filtered and diluted appropriately using Whatmann filter paper. A double beam UV spectrophotometer set to 270 nm was used to measure the absorbance of the above diluted solutions [240-242]. All of the experiments were repeated 3 times. The drug release kinetics were then calculated using the Zero order, First order, Higuchi, and Koresmeyer Peppas models.

4.12 RELEASE KINETICS

The kinetics of drug release was calculated using the “Zero order, First order, Higuchi, and Koresmeyer Peppas” models [244-247].

A. Zero order release

The zero-order release kinetics is described by the graph of cumulative percent drug release vs time, which is represented by the equation:

$$C=K_0 t$$

Where K_0 is zero order rate constant having units of concentration/time
 t is time in hours.

The slope of above straight-line equation is equal to K_0 . Zero order kinetics is the process of releasing a drug from a drug delivery device at a constant rate while maintaining a constant drug level in the blood throughout the delivery.

B. First order release

The following equation can be used to model medication release that follows first order release kinetics:

$$DC/dt = -K_1C$$

Where K_1 is the first order rate constant, expressed in time^{-1} or per hour.

The first order reaction can be characterised as a process in which the rate is directly proportional to the concentration of drug in the reaction. As a result, the faster the reaction, the higher the drug concentration. The following is the result of integrating and rearranging the previous equation:

$$\text{Log } C = \text{log } C_0 - K_1t/2.303$$

Where K_1 is the first order rate constant, expressed in time^{-1} or per hour

C_0 is the drug's initial concentration

C is the % drug remaining at time t .

The graphical representation of 1st order release kinetics was done by plotting Log % drug remaining vs time. The slope of the plot was the first order rate constant. The correlation coefficient derived from the above plot was used to determine whether the release follows first order kinetics or not.

C. Higuchi Model

Higuchi model is one of most widely used model for describing the release kinetic of sustained release drug delivery systems. The Higuchi equation has become one of most prominent kinetic equations which has been employed in drug dissolution studies in development of various types of drug delivery systems.

The classical basic Higuchi equation is represented by

$$Q = A\sqrt{D(2C_0 - C_s)Cst}$$

where Q is the cumulative amount of drug released in time t per unit area, C_0 is the initial drug concentration, C_s is the drug solubility in the matrix and D is the diffusion coefficient of the drug molecule in the matrix.

When 100% drug depletion is achieved from the dosage form, the above relationship holds true. If, on the other hand, the drug concentration in the matrix is less than its solubility, the porous system is responsible for release, and the equation becomes:

$$Q=A\sqrt{\left(\frac{D\delta}{\tau}\right)(2C-\delta C_s)Cst}$$

where D is the diffusion coefficient of the drug molecule in the solvent; δ is the porosity of the matrix; τ is the tortuosity of the matrix; Q is the cumulative amount of drug released in time t per unit area; C_0 is the initial drug concentration; C_s is the drug solubility in the matrix.

The dimensions of the radius and branching of the pores and canals in the matrix are referred to as tortuosity. Higuchi equation can be expressed in simpler form after simplifying the previous equation.

$$Q=K_H \times t^{1/2}$$

where, K_H is the Higuchi dissolution constant.

In higuchi kinetic model, a graph between cumulative % drug release vs square root of time was plotted. If the correlation coefficient of above plot is higher than the mechanism of drug release will be diffusion-controlled release mechanism. However, following assumptions were taken into account while application of higuchi model:

- The drug concentration was initially much higher than the matrix solubility
- The drug diffusivity remained constant
- Sink conditions were maintained perfectly

D. Korsmeyer-Peppas model

This model is basically used to find out the mechanism of dissolution. Korsmeyer and Peppas proposed a simple relationship that described which sort of dissolution followed drug release from a polymeric system, and he wrote the equation as:

$$\frac{M_t}{M_\infty} = K_{kp} t^n$$

Where, $\frac{M_t}{M_\infty}$ is a fraction of drug released at time t;

K_{kp} is Kores Meyer rate constant

$$\text{Log } (M_t/M_\infty) = \text{Log } K_{kp} + n \log t$$

Where M_t is the amount of drug released in time t; M_∞ is the amount of drug released after time ∞ ; n is the diffusional exponent or drug release exponent.

A graph is plotted between log cumulative percent drug release vs. log time to analyse release kinetics (log t). As a result, for cylindrical shaped matrices, the n value is utilised to characterise different release methods, as shown in Table 4.13.

Table 4.13: Exponent of diffusion and release mechanism

S. No.	Exponent of diffusion	Release Mechanism
1	0.45	Fickian diffusion
2	$0.45 < n < 0.89$	Anomalous diffusion
3	0.89	Case-II transport
4	$n > 0.89$	Super case-II transport

4.13 STABILITY STUDIES

The stability studies were performed to check the quality of formulation with time under the influence of variety of environmental factors like temperature and humidity. At room temperature, the observation of rate of degradation of formulation requires a long time. To prevent this delay, the accelerated stability testing was selected.

As per ICH guidelines, the storage conditions and time of studies are specified. For accelerated stability testing, the temperature and humidity conditions are as following

Temperature: $40^\circ\text{C} \pm 2^\circ\text{C}$,

Relative Humidity: $75\% \pm 5\%$ for 3 months.

In present study the selected formulation was kept at defined conditions for 3 months. The effect of temperature and aging on hardness, drug content, friability and in-vitro

release factors were observed by taking out samples at definite intervals of time. The samples were withdrawn after periods of 1st month, 2nd month, and 3rd month [248-250].

5.1 PREFORMULATION STUDIES

5.1.1 Physical Appearance

Physical appearance of Lamivudine was examined for its organoleptic properties like

Colour: White

Odour: Odourless

Taste: Slightly Bitter

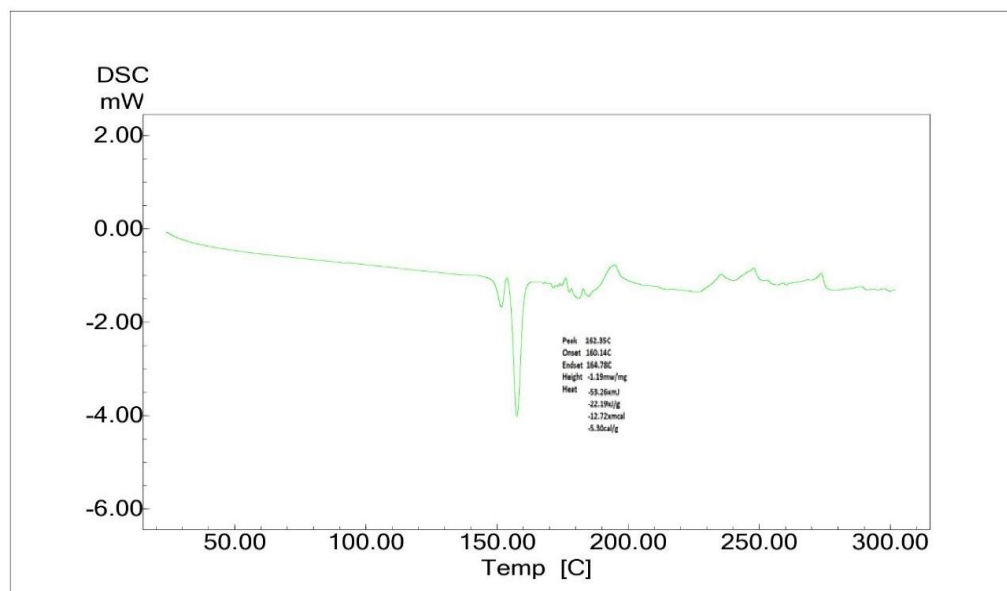
State: Crystalline Powder

5.1.2 Determination of Melting Point

The melting point of the drug was evaluated by method of capillary fusion and the temperature was observed between 160-162°C which is concordant with the official values. Melting point of the lamivudine was also evaluated by DSC. The thermograph of lamivudine was confirmed that melting point was around 160 °C (Figure 5.1).

Table 5.1: Melting point determination of lamivudine

Sample	Reference Melting Point (°C)	Observed Melting Point (°C)	Observed DSC Range (°C)
Lamivudine	160-162°C	161.17±0.76	160.14-164.78



LAM+DR (Lamivudine Drug)

Figure 5.1: DSC thermograph of lamivudine

5.1.3 Fourier-Transform Infrared Spectral Assignment

The FTIR spectrum provides the information regarding the functional groups present in Lamivudine which act as main parameter in identification and purity of drug candidate (Lamivudine). The obtained infrared spectrum of drug was compared with reference spectra to identify the peaks. Scanning of sample was performed by FTIR in the range of 400-4000 cm^{-1} .

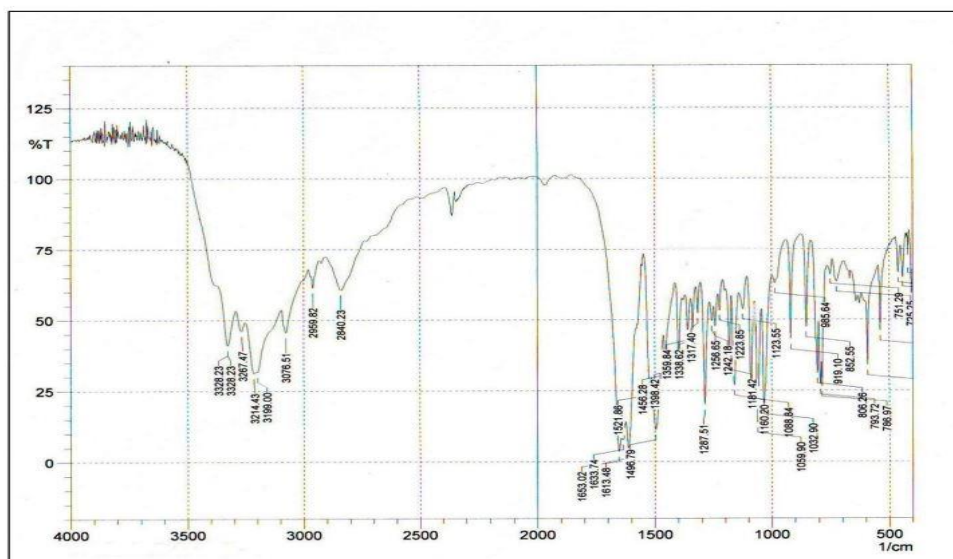
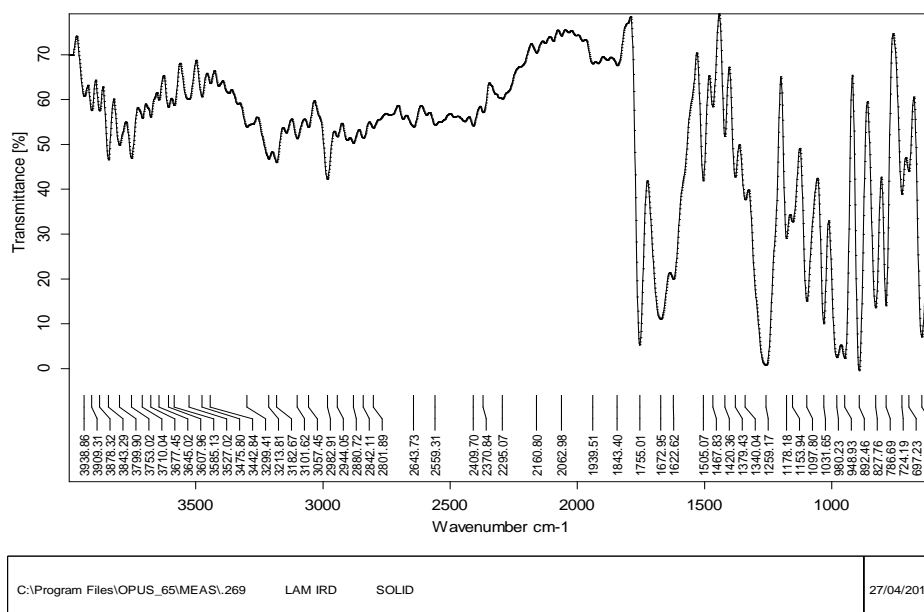


Figure 5.2: FTIR spectrum of Lamivudine (Reference)



C:\Program Files\OPUS_65\MEAS\269

LAM IRD SOLID

27/04/2018

Figure 5.3: FTIR spectrum of Lamivudine (Test)

Table 5.2: FTIR interpretation of Lamivudine

S. No.	Characteristics Peaks	Observed(cm ⁻¹)
1	N-H Stretching	3299.41
2	O-H Stretching	3213.81
3	C-H stretching	2842.11
4	C=O Stretching	1672.95
5	C-O-C Stretching	1259.17 and 1178.18

The principal IR absorption peaks of Lamivudine at 1672.95 cm⁻¹ (C=O stretching), 3299.41 cm⁻¹ (N-H Stretching), 1259.17 and 1178.18 cm⁻¹ (asymmetrical and symmetrical stretching of the C-O-C), 3213.81 cm⁻¹ (O-H Stretching) were all observed in the spectra of Lamivudine. These observed principal peaks confirmed the purity and authenticity of the Lamivudine.

5.1.4 Solubility determination of Lamivudine in different solvents

A. Qualitative Solubility of Lamivudine

The solubility studies of lamivudine were carried out in different solvents like methanol, water, 0.1N HCl and phosphate buffer (pH-6.8). The results were obtained by visual inspection of solutions (Table 5.3).

Table 5.3: Qualitative solubility data of Lamivudine

S. No.	Name of Solvent	Solubility
1	Methanol	+
2	Water	++
3	0.1 N Hydrochloric acid	++
4	Phosphate Buffer (pH 6.8)	++

(+)- Slightly Soluble, (++)- Soluble

B. Quantitative Solubility of Lamivudine

Excess of lamivudine was placed in screw capped glass tubes. 10 ml of different solvents were added, in each glass tubes. Glass tubes were kept in water bath with

shaking at 37°C for 24 h. Lamivudine was added to the glass tubes, if required, to obtain saturated solution. After shaking for 24 h the mixture was filtered. Lamivudine in the supernatant solution was determined spectrophotometrically at the absorption maxima. The quantitative solubility was determined in various solvents.

Table 5.4: Quantitative solubility data of Lamivudine

S. No.	Name of Solvent	Solubility (mg/ml) (mean±SD)
1	Methanol	24.75±1.68
2	Water	156.77±3.14
3	0.1 N HCl	236.73±3.22
4	Phosphate Buffer (pH 6.8)	82.09±1.52

n=3

5.1.5 Absorption Maxima (λ_{\max}) determination by UV Spectroscopy

Double beam spectrophotometer was used to determine the λ_{\max} of Lamivudine. A 10µg/ml solution of Lamivudine in different solvents was prepared and scanned in between 200-400nm. The λ_{\max} of Lamivudine of found to be 270 nm which were concordant with the Pharmacopoeial standards.

Table 5.5: Absorption Maxima (λ_{\max}) of Lamivudine in different solvents

S. No.	Solvent	Absorption Maxima (λ_{\max})
1	Distilled Water	270
2	Phosphate Buffer (pH-6.8)	270
3	0.1 N HCl	270

5.1.6 Preparation of standard curve of Lamivudine

The standard curve of lamivudine was developed in different solvents (0.1 N hydrochloric acid and Phosphate buffer pH 6.8). 100 mg of lamivudine was

solubilised in 100 ml of solvent to prepare a solution of 1 mg/ml which was taken as stock solution for further dilution processes. From this above stock solution, dilutions of 5, 10, 15, 20, 25 and 30 µg/ml were made by serial dilution method. The absorbance of above solutions was recorded at 270 nm and standard curve was prepared by plotting absorbance against concentration. The Lamivudine obeys the Beer-Lambert's law.

Table 5.6: Calibration data of lamivudine drug in 0.1N HCl

S. No.	Concentration of Lamivudine (µg/ml)	Absorbance (at 270 nm)
1	0	0
2	5	0.198±0.001
3	10	0.364±0.002
4	15	0.556±0.001
5	20	0.731±0.002
6	25	0.905±0.001
7	30	1.092±0.001

n=3

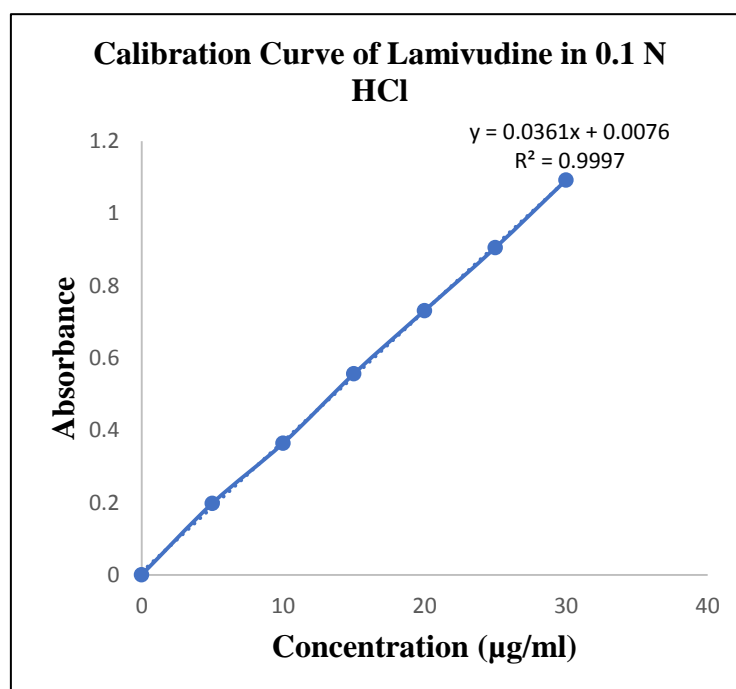


Figure 5.4: Calibration Curve of Lamivudine in 0.1N HCl

Table 5.7: Calibration parameter values in 0.1 N HCl

S. No.	Parameters	Values
1	Correlation Coefficient (R^2)	0.9997
2	Slope (m)	0.0361
3	Intercept (c)	0.0076

Table 5.8: Calibration data of lamivudine drug in phosphate buffer (pH-6.8)

S. No.	Concentration of Lamivudine ($\mu\text{g/ml}$)	Absorbance (at 270 nm)
1	0	0
2	5	0.177 \pm 0.002
3	10	0.332 \pm 0.001
4	15	0.500 \pm 0.001
5	20	0.672 \pm 0.002
6	25	0.854 \pm 0.001
7	30	1.023 \pm 0.002

n=3

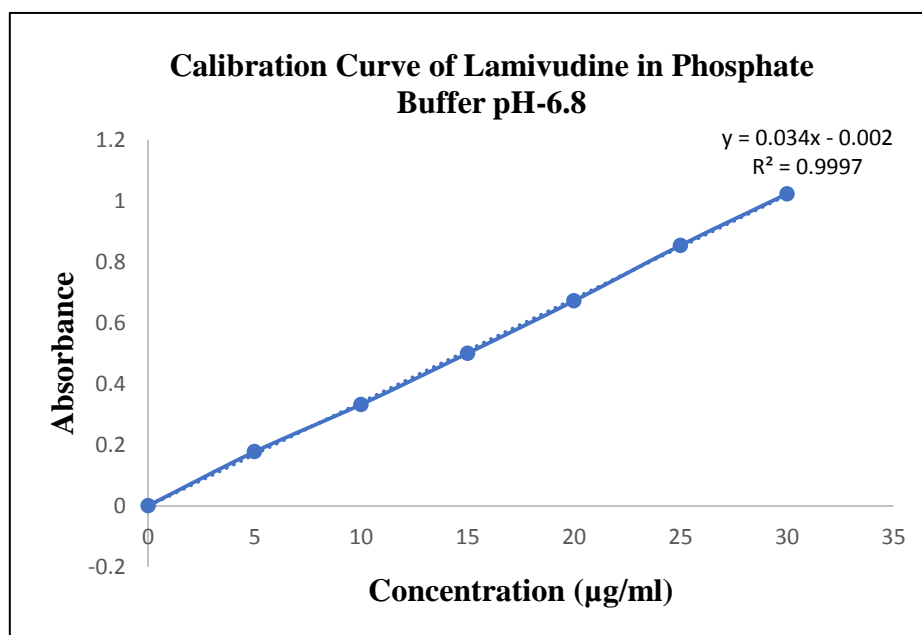


Figure 5.5: Calibration Curve of Lamivudine in phosphate buffer pH-6.8

Table 5.9: Calibration parameter values in phosphate buffer pH-6.8

S. No.	Parameters	Values
1	Correlation Coefficient (R^2)	0.9997
2	Slope (m)	0.034
3	Intercept (c)	0.002

5.1.7 Partition Coefficient

The partition coefficient of lamivudine was determined by using two solvents (n-octanol: PBS of pH 6.8) by using shake flask method. The calculated value of partition coefficient was compared with literature value and reported in table 5.10.

Table 5.10: Partition coefficient of Lamivudine

S. No.	Method Used	Experimental Value	Literature Value
1	n-octanol: PBS of pH 6.8	-1.4±0.002	-1.46

5.2 SYNTHESIS AND OPTIMIZATION OF GRAFTED MASTIC GUM AND BANANA PEEL GUM

5.2.1 Synthesis of grafted mastic gum and banana peel gum

The microwave assisted grafting method was used for the purpose of grafting.

5.2.2 Optimization of grafting process using box behnken design

Box Behnken design was used for purpose of optimisation. A 3-factor 3-level response surface Box-Behnken design, which requires 15 runs including three replicates of the central run, was used for the synthesis of graft copolymers of mastic gum with acrylamide using ceric ammonium nitrate as the free radical initiator. The critical synthesis and process parameters; CSPP (A = concentration of monomer, B = concentration of initiator and C= Temperature) to generate design space and optimize formulation with an aim to obtain critical quality attributes (CQA, Y1 =% Yield, Y2 =% Grafting, Y3 =% grafting efficiency). Different concentration of three CSPP viz., A = Acrylamide with their low (1.4 g), medium (2.1 g) and high level (2.8 g) and B =

ceric ammonium nitrate with their low (25 mg), medium (50 mg) and high level (75 mg) and Temperature low (40°C), medium (50°C) and high level (60°C) were selected.

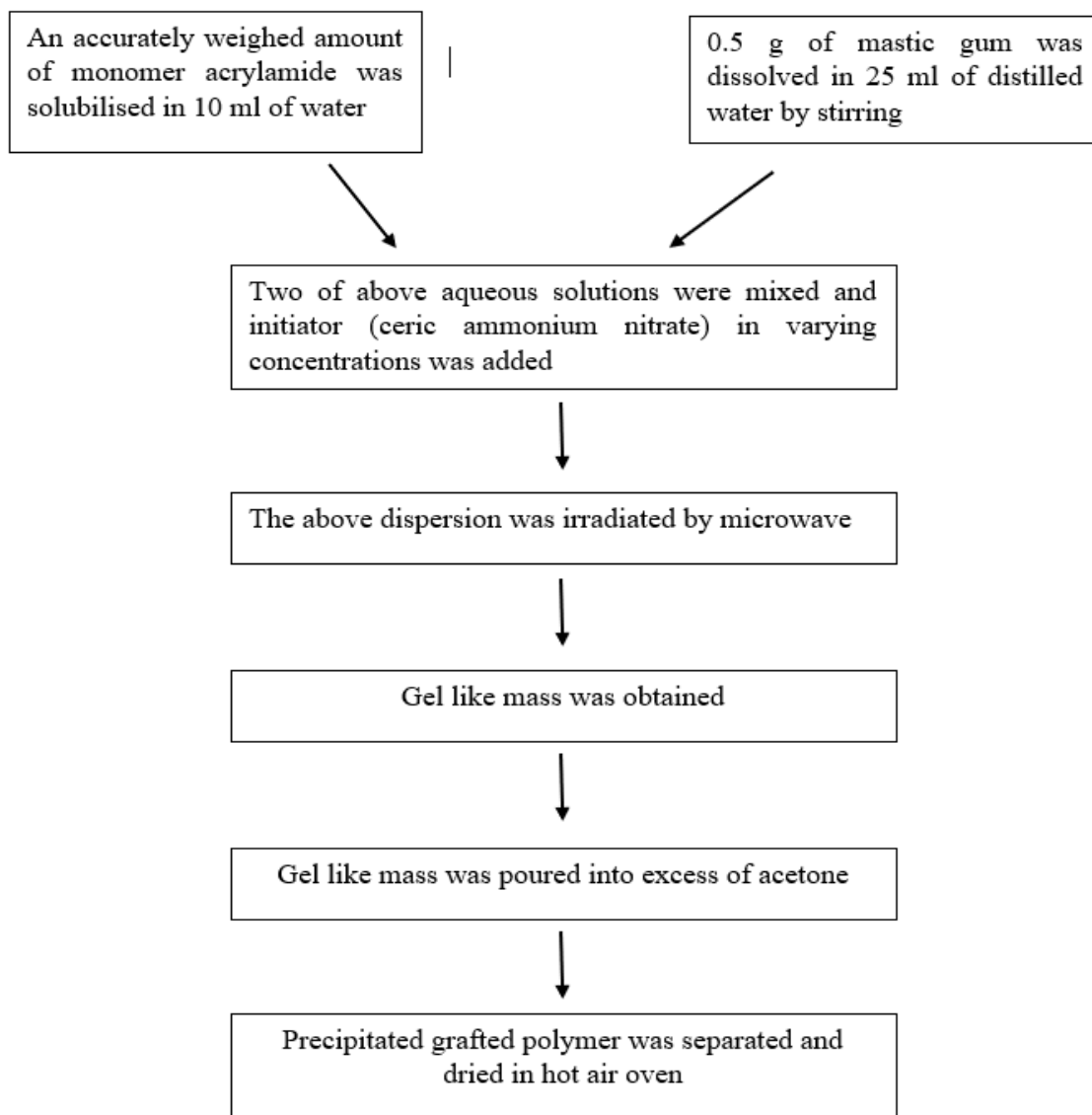


Figure 5.6: Schematic presentation of preparation of Acrylamide grafted Mastic gum

A. Optimization of Mastic Gum

Table 5.11: Design Matrix of BBD taking in account three responses for mastic gum

Formulation code	Acrylamide amount (gm)	Initiator amount (mg)	Temperature (°C)	% Yield	% Grafting	% Grafting efficiency
MA1	2.1	50	50	50.56604	168	32.30769
MA2	1.4	75	50	57.01266	125.2	32.9474
MA3	2.1	50	50	52.07547	176	33.84615
MA4	1.4	50	40	60.51282	136	35.78947
MA5	1.4	25	50	55.16883	112.4	28.5789
MA6	2.8	75	50	50.66667	242	34.6667
MA7	2.8	50	60	48.47761	224.8	34.06061
MA8	2.1	75	40	28.03738	50	9.6154
MA9	2.1	25	60	24	26	5
MA10	2.1	50	50	55.24528	192.8	37.07692
MA11	2.1	25	40	22.09524	16	3.07692
MA12	2.8	50	40	48.62687	225.8	34.21212
MA13	2.1	75	60	41.71963	123.2	23.69231
MA14	1.4	50	60	75.89744	210	51.5789
MA15	2.8	25	50	28.66165	90.6	13.7273

Box behnken design was applied using Design expert software (Version 7.0, Stat-ease. Inc, USA). All the 15 possible combinations were performed in experimental trials. The % yield, % grafting and % grafting efficiency were calculated. The % yield for 15 formulations of grafted mastic gum was found in between 22.09 % to 75.89 %. The % grafting for 15 formulations of grafted mastic gum was found in between 16 % to 242 %. The % grafting efficiency for 15 formulations of grafted mastic gum was found in between 3.07 % to 51.58 %. ANOVA was applied to detect insignificant factors. Fit of model was dependent upon the lower p value, high F value, high level of adjusted R^2 and predicted R^2 .

Table 5.12: ANOVA Table of % Yield response for mastic gum

Source	Sum of Squares	df	Mean Square	F Value	p-value	
					Prob > F	
Model	3163.158	9	351.462	105.6616	< 0.0001	Significant
A-Monomer amount	650.8642	1	650.8642	195.6722	< 0.0001	
B-Initiator amount	282.1573	1	282.1573	84.82618	0.0003	
C-Temperature	118.7523	1	118.7523	35.70102	0.0019	
AB	101.6183	1	101.6183	30.54997	0.0027	
AC	60.32527	1	60.32527	18.13585	0.0080	
BC	34.67727	1	34.67727	10.42518	0.0232	
A ²	561.5261	1	561.5261	168.8141	< 0.0001	
B ²	1077.591	1	1077.591	323.961	< 0.0001	
C ²	159.9763	1	159.9763	48.09439	0.0010	
Residual	16.6315	5	3.326299			
Lack of Fit	5.224353	3	1.741451	0.305326	0.8239	not significant
Pure Error	11.40714	2	5.703572			
Cor Total	3179.79	14				
Std. Dev.	1.823815					
Mean	46.58424					
C.V. %	3.915089					
PRESS	109.2557					
R-Squared	0.99477					
Adj R-Squared	0.985355					
Pred R-Squared	0.965641					
Adeq Precision	35.60381					

Model F-value of 105.6616 implied that the model is significant. Values of "Prob > F" less than 0.0500 indicate model terms are significant. Values greater than 0.1000 indicated that the model terms are not significant. The "Pred R-Squared" of 0.965641

is in reasonable agreement with the "Adj R-Squared" of 0.985355. "Adeq Precision" measures the signal to noise ratio. A ratio greater than 4 is desirable. The ratio of 35.60381 indicates an adequate signal. This model can be used to navigate the design space.

Final Quadratic Polynomial Equation for the process

$$\%Yield (Y1) = 52.66 - 9.01.A + 5.93.B + 3.85.C + 5.04.A.B - 3.88.A.C + 2.94.B.C + 12.33.A^2 - 17.08.B^2 - 6.58.C^2$$

Table 5.13: Observed and predicted values for % yield

Standard Order	Actual Value	Predicted Value	Residual
1	55.16883	55.99879	-0.82996
2	28.66165	27.87846	0.783193
3	57.01266	57.79585	-0.78319
4	50.66667	49.83671	0.82996
5	60.51282	59.66229	0.850532
6	48.62687	49.38949	-0.76262
7	75.89744	75.13482	0.762621
8	48.47761	49.32814	-0.85053
9	22.09524	22.11581	-0.02057
10	28.03738	28.10472	-0.06734
11	24	23.93266	0.067339
12	41.71963	41.69905	0.020572
13	50.56604	52.62893	-2.06289
14	55.24528	52.62893	2.616352
15	52.07547	52.62893	-0.55346

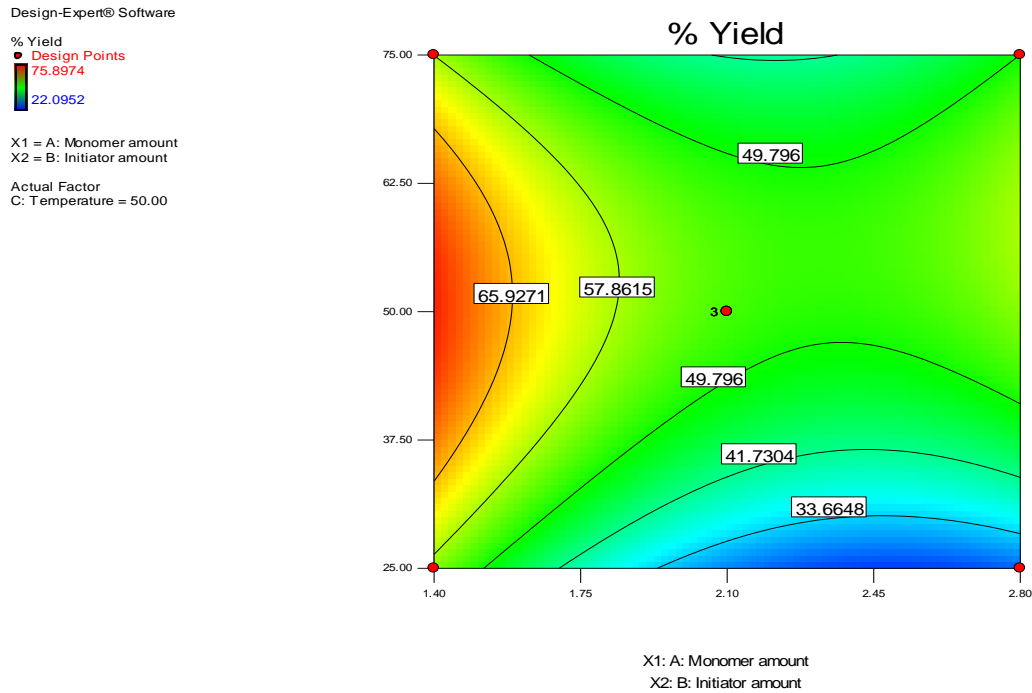


Figure 5.7: Contour Plot showing the effect of Acrylamide amount (A), and CAN amount (B) on % Yield (Y_1) of mastic gum

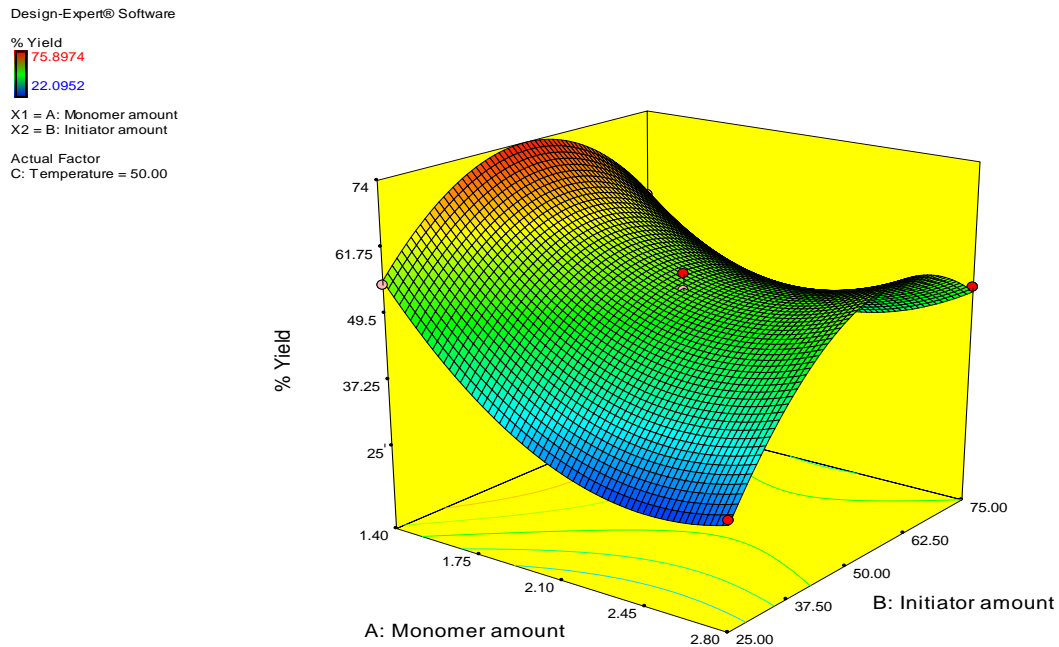


Figure 5.8: 3D Surface Response Graph showing the effect of Acrylamide amount (A), and CAN amount (B) on % Yield (Y_1) of mastic gum

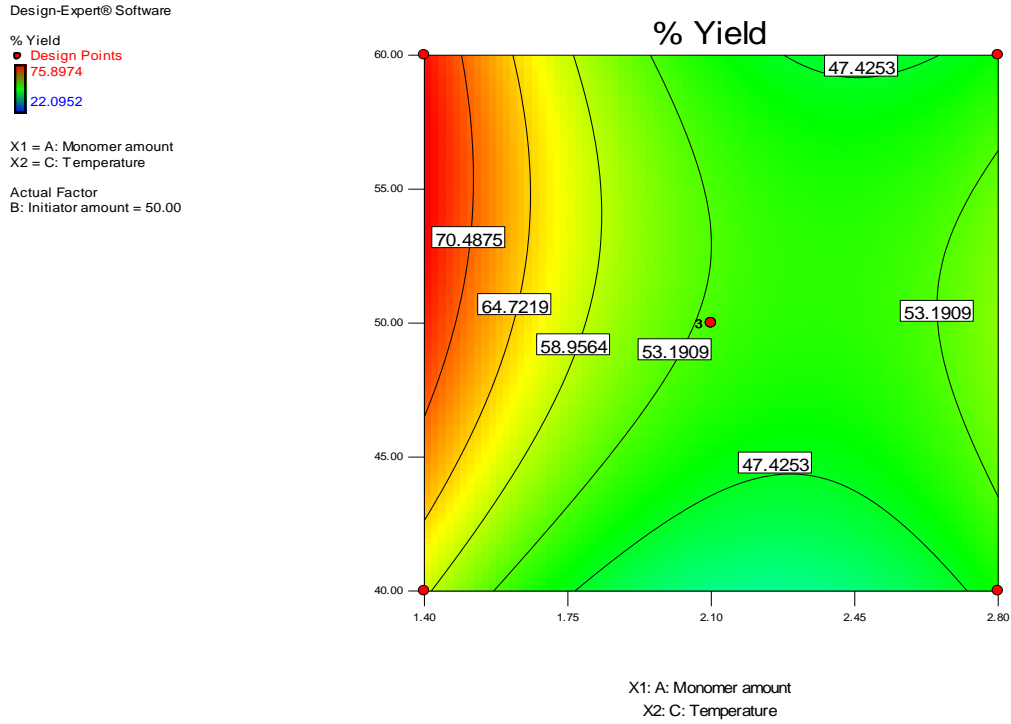


Figure 5.9: Contour Plot showing the effect of Acrylamide amount (A), and Temperature (C) on % Yield (Y_1) of mastic gum

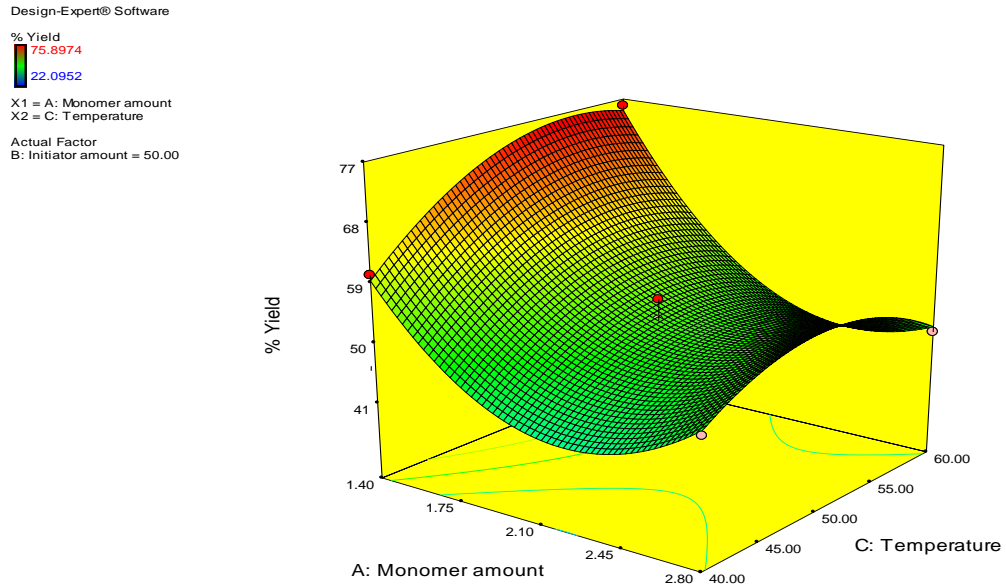


Figure 5.10: 3D Surface Response Graph showing the effect of Acrylamide amount (A), and Temperature (C) on % Yield (Y_1) of mastic gum

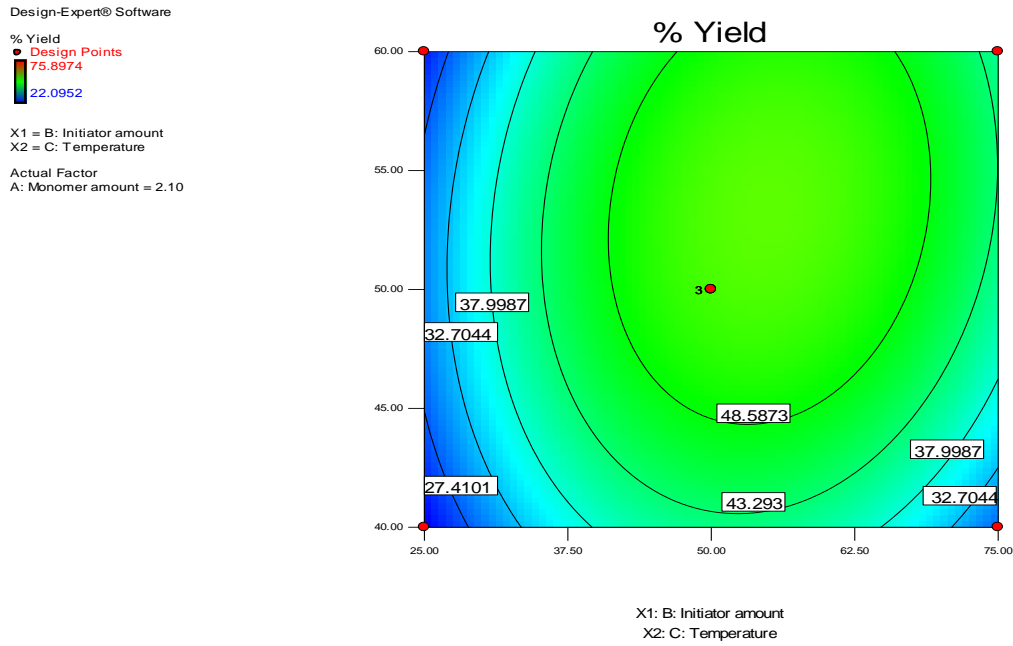


Figure 5.11: Contour Graph showing the effect of Initiator amount (B), and Temperature (C) on % Yield (Y_1) of mastic gum

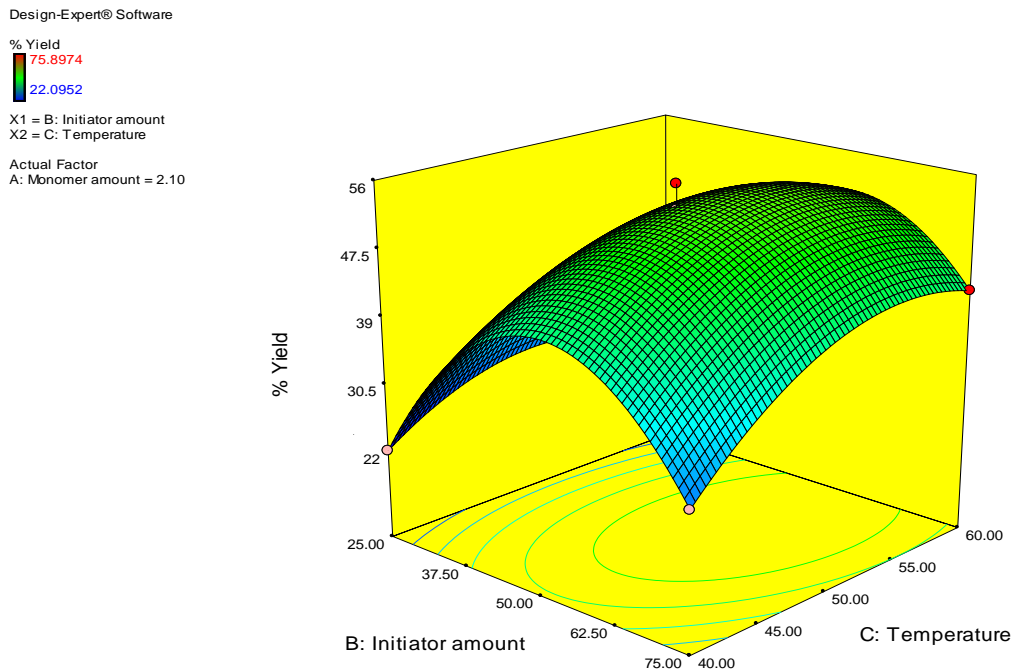


Figure 5.12: 3D Surface Response Graph showing the effect of Initiator amount (B), and Temperature (C) on % Yield (Y_1) of mastic gum

Table 5.14: ANOVA Table of % Grafting response for mastic gum

Source	Sum of Squares	df	Mean Square	F Value	p-value	
					Prob > F	
Model	74411.28	9	8267.92	85.93142	< 0.0001	significant
A-Monomer amount	4980.02	1	4980.02	51.75911	0.0008	
B-Initiator amount	10907.65	1	10907.65	113.367	0.0001	
C-Temperature	3049.805	1	3049.805	31.6977	0.0024	
AB	4802.49	1	4802.49	49.91398	0.0009	
AC	1406.25	1	1406.25	14.61565	0.0123	
BC	998.56	1	998.56	10.37839	0.0234	
A ²	10960.37	1	10960.37	113.915	0.0001	
B ²	30486.47	1	30486.47	316.8566	< 0.0001	
C ²	4335.524	1	4335.524	45.06064	0.0011	
Residual	481.0767	5	96.21533			
Lack of Fit	160.65	3	53.55	0.334242	0.8070	not significant
Pure Error	320.4267	2	160.2133			
Cor Total	74892.36	14				
Std. Dev.	9.808941					
Mean	141.2533					
C.V. %	6.944219					
PRESS	3291.36					
R-Squared	0.993576					
Adj R-Squared	0.982014					
Pred R-Squared	0.956052					
Adeq Precision	28.20901					

Model F-value of 85.93142 implied that the model is significant. Values of "Prob > F" less than 0.0500 indicate model terms are significant. Values greater than 0.1000 indicated that the model terms are not significant. The "Pred R-Squared" of 0.956052 is in reasonable agreement with the "Adj R-Squared" of 0.982014. "Adeq Precision" measures the signal to noise ratio. A ratio greater than 4 is desirable. The ratio of 28.20901 indicates an adequate signal. This model can be used to navigate the design space.

Final Quadratic Polynomial Equation for the process:

%Grafting (Y2)

$$= 178.93 + 24.95.A + 36.92.B + 19.52.C + 34.65.A.B - 18.75.A.C + 15.82.B.C + 54.48.A^2 - 90.86.B^2 - 34.26.C^2$$

Table 5.15: Observed and predicted values for % grafting

Standard Order	Actual Value	Predicted Value	Residual
1	112.4	115.325	-2.925
2	90.6	95.925	-5.325
3	125.2	119.875	5.325
4	242	239.075	2.925
5	136	135.925	0.075
6	225.8	223.325	2.475
7	210	212.475	-2.475
8	224.8	224.875	-0.075
9	16	13.15	2.85
10	50	55.4	-5.4
11	26	20.6	5.4
12	123.2	126.05	-2.85
13	168	178.9333	-10.9333
14	192.8	178.9333	13.86667
15	176	178.9333	-2.93333

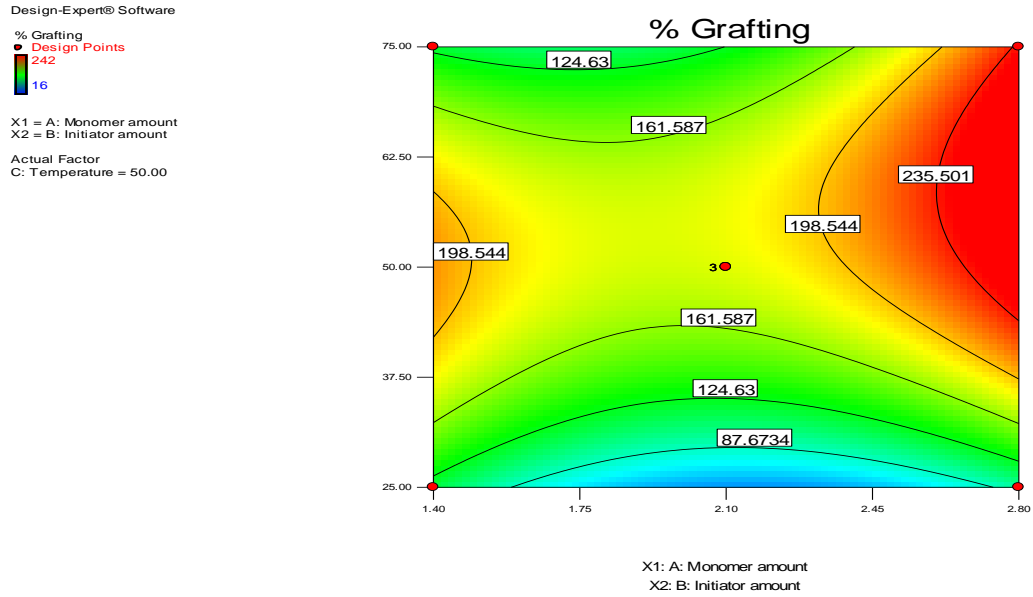


Figure 5.13: Contour Graph showing the effect of Acrylamide amount (A), and CAN amount (B) on % Grafting (Y₂) of mastic gum

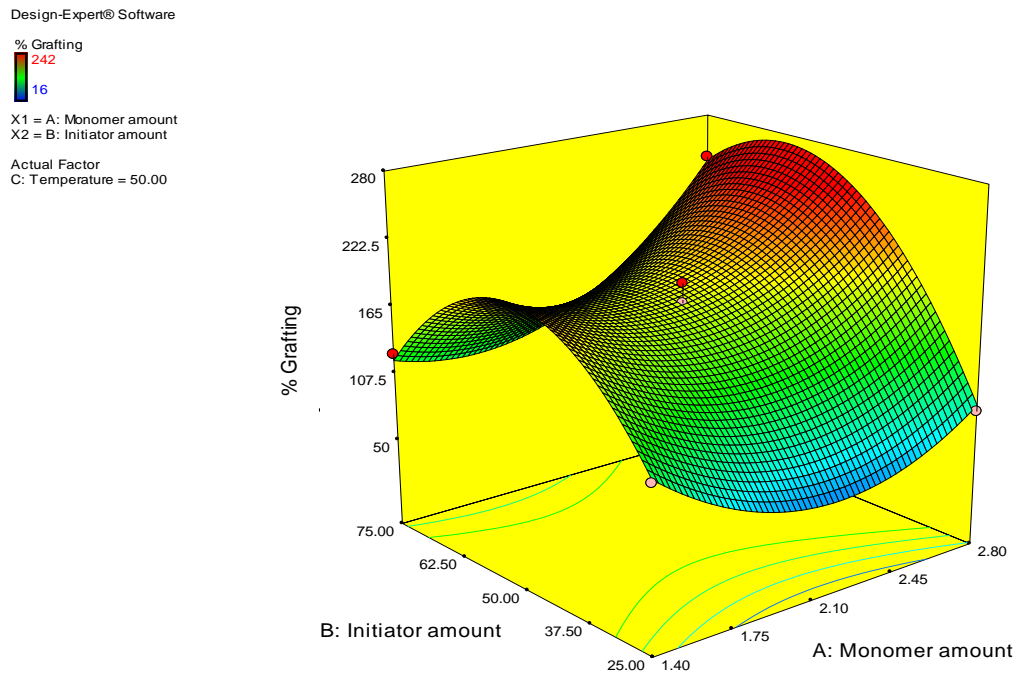


Figure 5.14: 3D Surface Response Graph showing the effect of Acrylamide amount (A), and CAN amount (B) on % Grafting (Y₂) of mastic gum

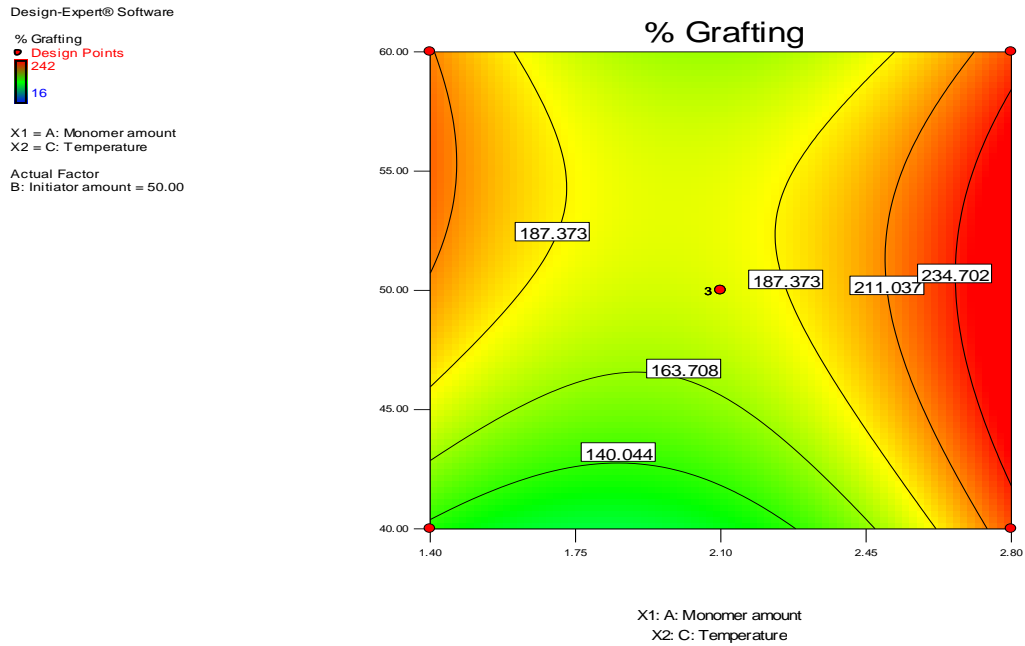


Figure 5.15: Contour Graph showing the effect of Acrylamide amount (A), and Temperature (C) on % Grafting (Y_2) of mastic gum

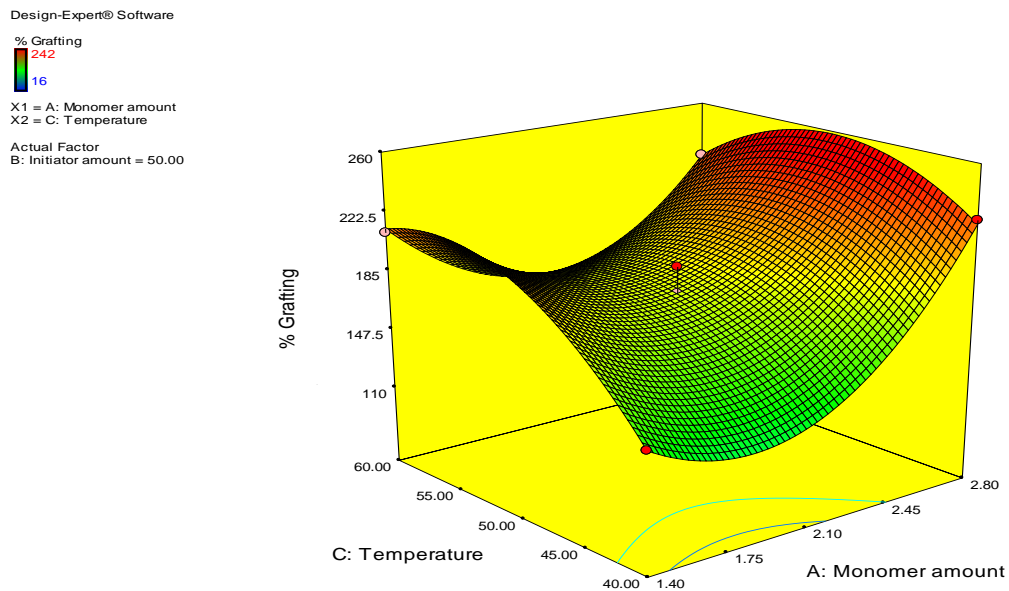


Figure 5.16: 3D Surface Response Graph showing the effect of Acrylamide amount (A), and Temperature (C) on % Grafting (Y_2) of mastic gum

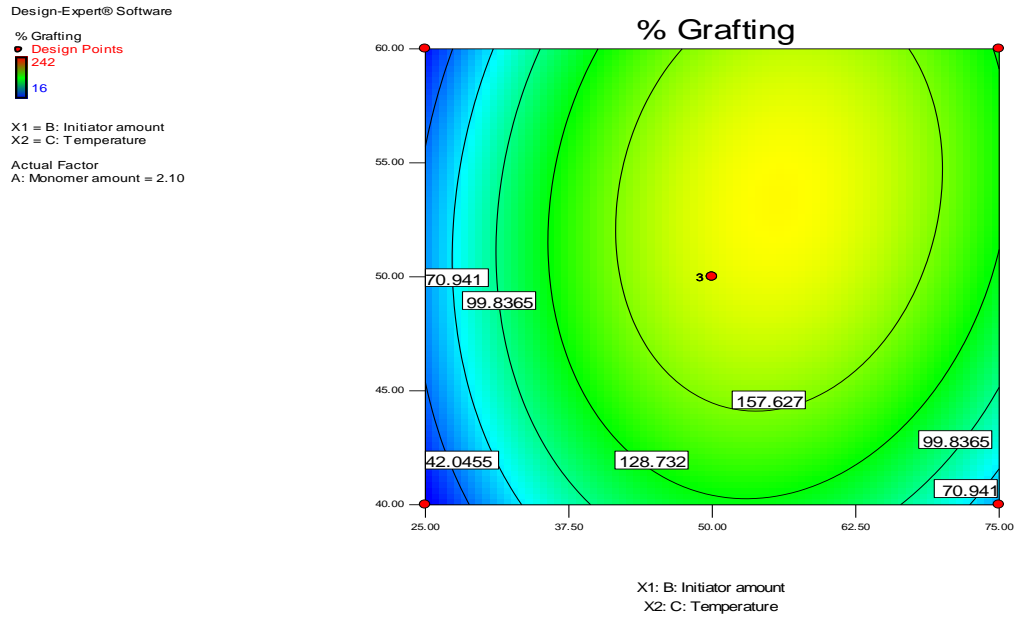


Figure 5.17: Contour Graph showing the effect of CAN amount (B), and Temperature (C) on % Grafting (Y₂) of mastic gum

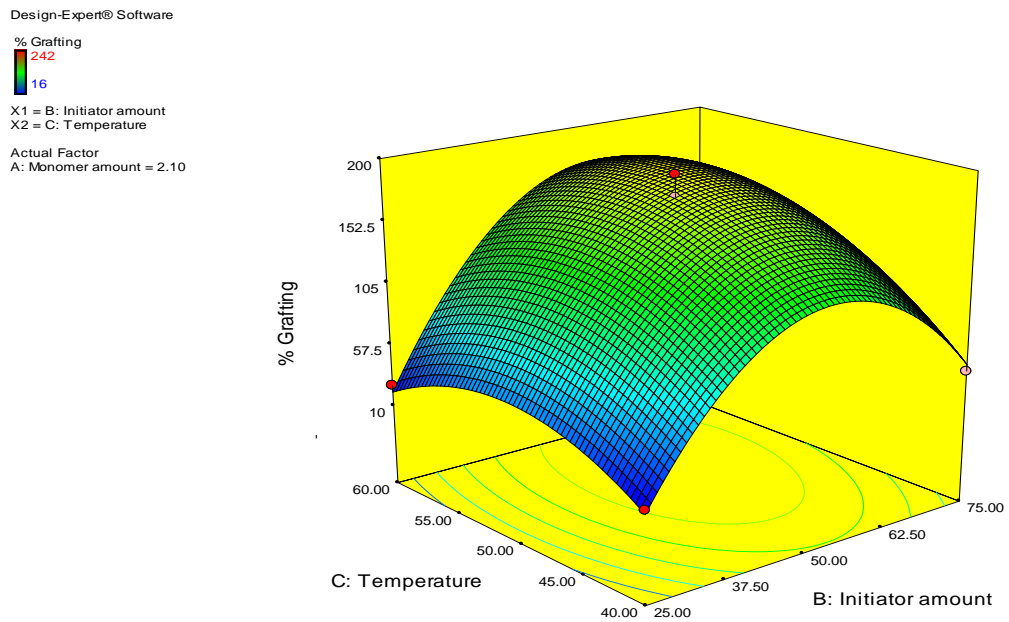


Figure 5.18: 3D Surface Response Graph showing the effect of CAN amount (B), and Temperature (C) on % Grafting (Y₂) of mastic gum

Table 5.16: ANOVA Table of % Grafting efficiency response for mastic gum

Source	Sum of Squares	df	Mean Square	F Value	p-value	
					Prob >F	
Model	2584.017	9	287.113	88.00443	< 0.0001	significant
A-Monomer amount	129.8301	1	129.8301	39.79486	0.0015	
B-Initiator amount	319.2699	1	319.2699	97.86099	0.0002	
C-Temperature	125.1196	1	125.1196	38.35102	0.0016	
AB	68.64868	1	68.64868	21.04185	0.0059	
AC	63.5284	1	63.5284	19.47241	0.0069	
BC	36.92888	1	36.92888	11.31926	0.0200	
A ²	432.0251	1	432.0251	132.4222	< 0.0001	
B ²	1162.934	1	1162.934	356.4567	< 0.0001	
C ²	147.3373	1	147.3373	45.16109	0.0011	
Residual	16.31242	5	3.262483			
Lack of Fit	4.462318	3	1.487439	0.251043	0.8569	not significant
Pure Error	11.8501	2	5.925049			
Cor Total	2600.329	14				
Std. Dev.	1.806235					
Mean	27.34512					
C.V. %	6.605327					
PRESS	98.05981					
R-Squared	0.993727					
Adj R-Squared	0.982435					
Pred R-Squared	0.962289					
Adeq Precision	32.3886					

Model F-value of 88.00443 implied that the model is significant. Values of "Prob > F" less than 0.0500 indicate model terms are significant. Values greater than 0.1000 indicated that the model terms are not significant. The "Pred R-Squared" of 0.962289 is in reasonable agreement with the "Adj R-Squared" of 0.982435. "Adeq Precision" measures the signal to noise ratio. A ratio greater than 4 is desirable. The ratio of 32.3886 indicates an adequate signal. This model can be used to navigate the design space.

Final Quadratic Polynomial Equation for the process:

%Grafting Efficiency (Y3)

$$= 34.41 - 4.02.A + 6.31.B + 3.95.C + 4.14.A.B - 3.98.A.C + 3.03.B.C + 10.81.A^2 - 17.74.B^2 - 6.31.C^2$$

Table 5.17: Observed and predicted values for % grafting efficiency

Standard Order	Actual Value	Predicted Value	Residual
1	28.5789	29.33396	-0.75506
2	13.7273	12.99152	0.735779
3	32.9474	33.68318	-0.73578
4	34.6667	33.91164	0.755057
5	35.78947	34.9988	0.790678
6	34.21212	34.91228	-0.70016
7	51.5789	50.87874	0.700159
8	34.06061	34.85128	-0.79068
9	3.07692	3.112541	-0.03562
10	9.6154	9.670299	-0.0549
11	5	4.945101	0.054899
12	23.69231	23.65669	0.035621
13	32.30769	34.41026	-2.10256
14	37.07692	34.41026	2.666667
15	33.84615	34.41026	-0.5641

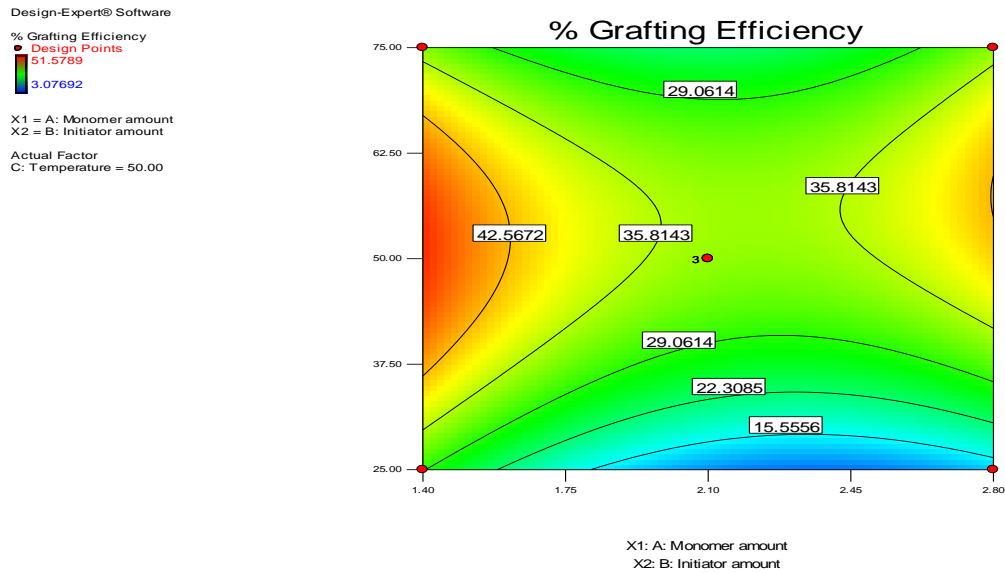


Figure 5.19: Contour Graph showing the effect of Acrylamide amount (A), and CAN amount (B) on % Grafting Efficiency (Y_3) of mastic gum

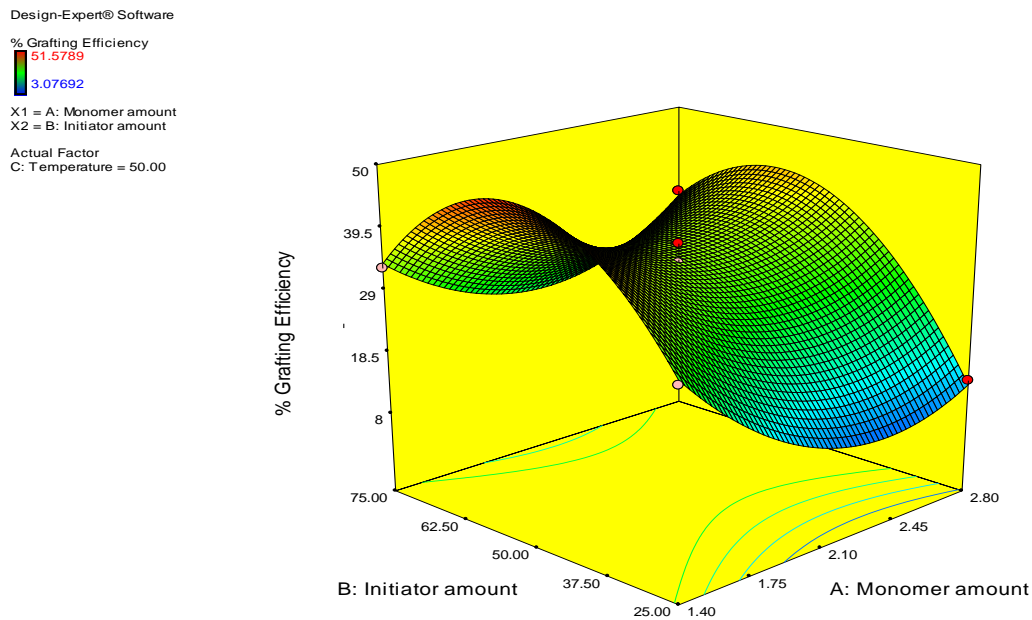


Figure 5.20: 3D Surface Response graph showing the effect of Acrylamide amount (A), and CAN amount (B) on % Grafting Efficiency (Y_3) of mastic gum

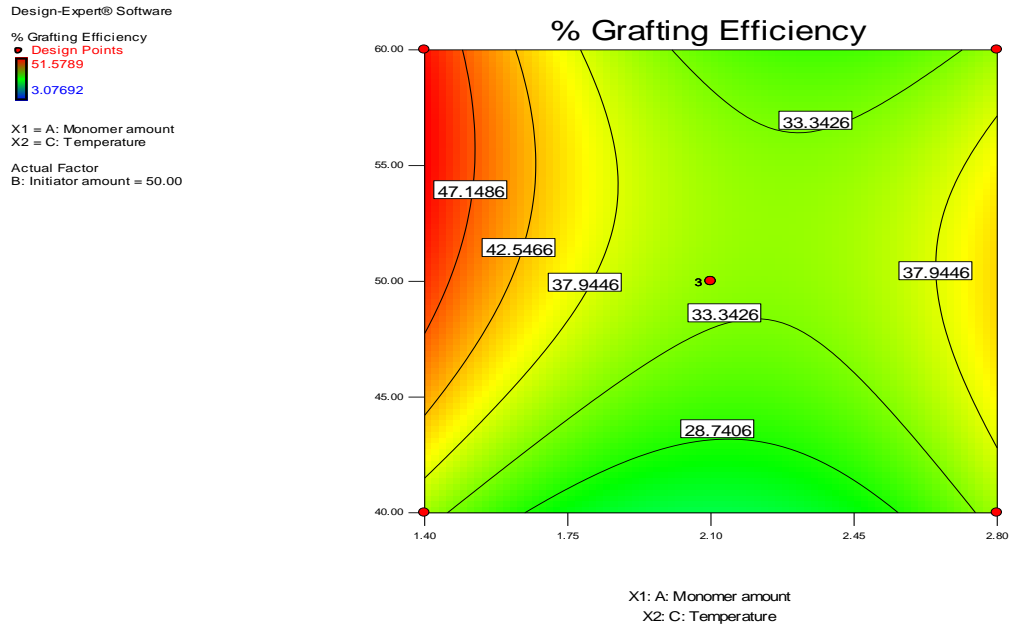


Figure 5.21: Contour Graph showing the effect of Acrylamide amount (A), and Temperature (C) on % Grafting Efficiency (Y_3) of mastic gum

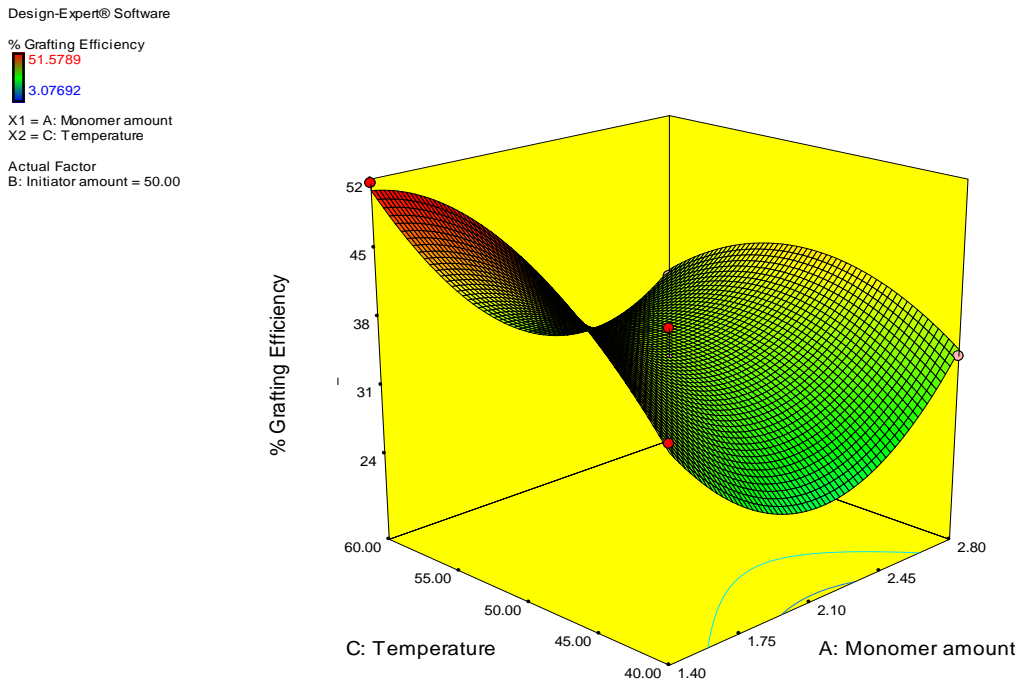


Figure 5.22: 3D Surface Response Graph showing the effect of Acrylamide amount (A), and Temperature (C) on % Grafting Efficiency (Y_3) of mastic gum

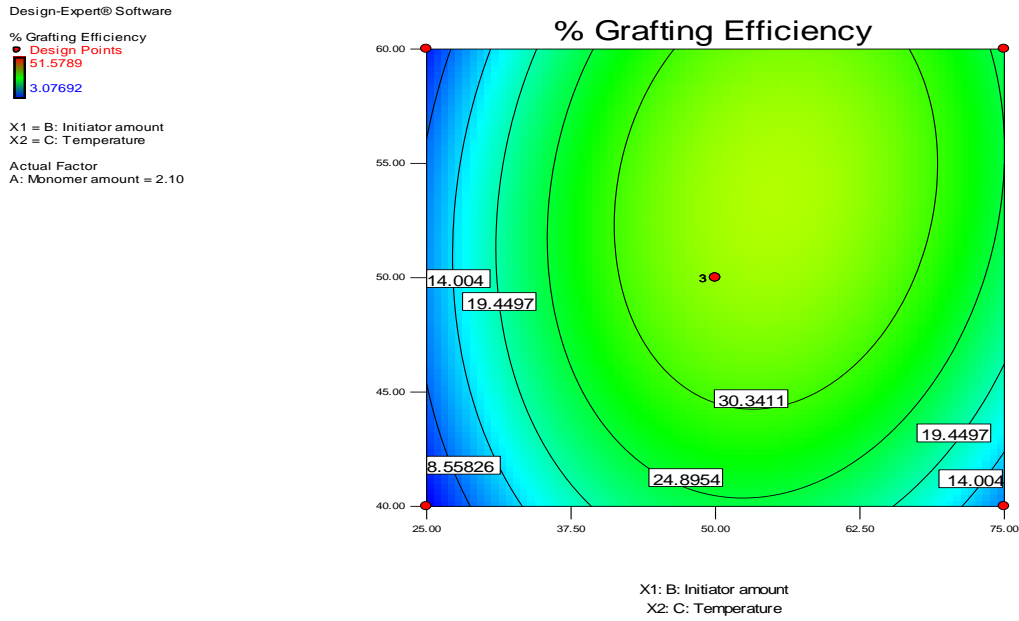


Figure 5.23: Contour Graph showing the effect of CAN amount (B), and Temperature (C) on % Grafting Efficiency (Y₃) of mastic gum

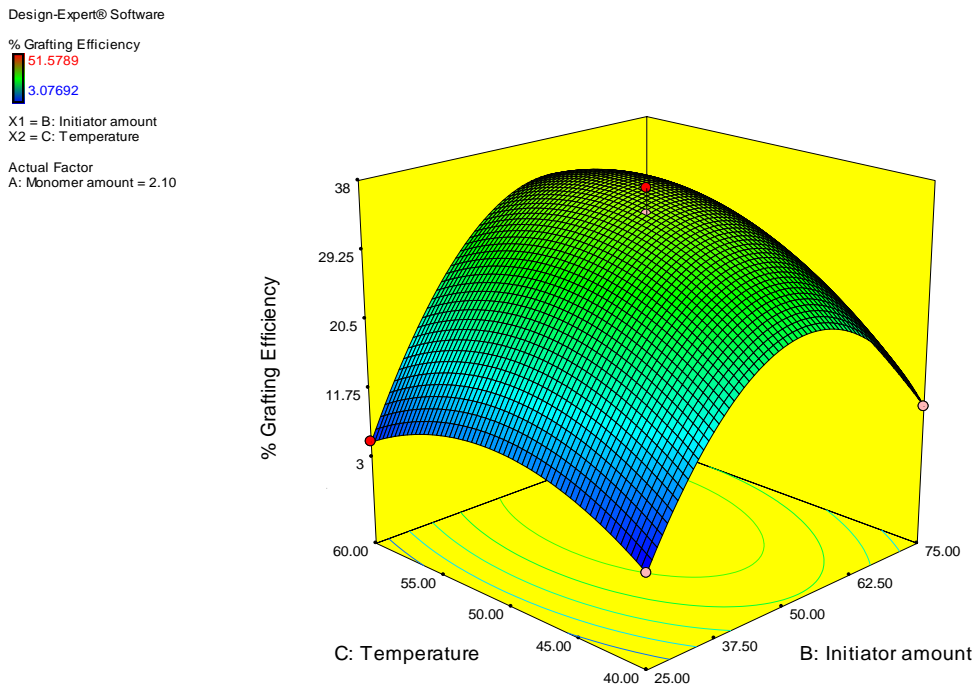


Figure 5.24: 3D Surface Response Graph showing the effect of CAN amount (B), and Temperature (C) on % Grafting Efficiency (Y₃) of mastic gum

Optimized Concentration of Dependent Variables: Data with desirability near to one were run again and calculated for minimum standard deviation between theoretical and experimental response value.

Table 5.18: Numerical optimization as per desirability of the process of dependent and independent variables for mastic gum

Name	Goal
Acrylamide amount	is in range
CAN amount	is in range
Temperature	is in range
% Yield	maximum
% Grafting	maximum
% Grafting Efficiency	maximum

Table 5.19: Optimized solutions for Grafted Mastic gum

Code	M (g)	I (mg)	Temp (°C)	% Y	Exp % Y	% G	Exp % G	% G.E.	Exp % G.E.	D
S1	1.4	75	50	57.79	51.79	119.87	104.6	33.68	27.52	1
S2	2.8	75	50	49.83	45.33	239.07	206	33.91	31.21	1
S3	1.4	50	40	59.66	52.46	135.92	104.6	34.99	27.52	1
S4	1.4	50	60	75.13	73.33	212.47	186	50.87	48.94	1
S5	2.8	50	40	49.38	40.29	223.32	170	34.91	25.75	1

Where,

M-Monomer Amount,

I- Initiator Amount,

% Y- % Yield,

% G- % Grafting,

% G. E. - % Grafting Efficiency,

D- Desirability

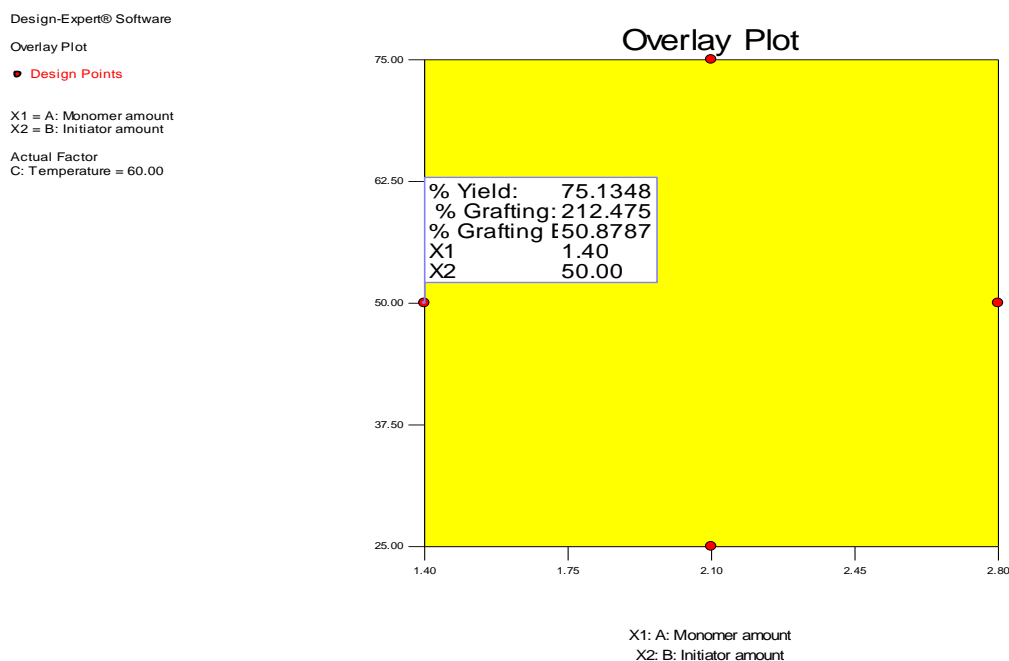


Figure 5.25: Overlay graph of optimized values of process parameters for mastic gum

The optimized process parameters contain 0.5 gm mastic gum, 1.4 gm acrylamide and 50 mg of ceric ammonium nitrate at 60°C. Therefore, the formulation S4 containing 1.4 gm acrylamide and 50 mg of ceric ammonium nitrate at 60°C was selected as optimised formulation.

B. Optimization of Banana Peel Gum

Box behnken design was applied using Design expert software (Version 7.0, Stat-ease. Inc, USA). All the 15 possible combinations were performed in experimental trials. The % yield, % grafting and % grafting efficiency were calculated. The % yield for 15 formulations of grafted banana peel gum was found in between 23.31 % to 70.77 %. The % grafting for 15 formulations of grafted banana peel gum was found in between 22.4 % to 235.2 %. The % grafting efficiency for 15 formulations of grafted banana peel gum was found in between 4.30 % to 46.31 %. ANOVA was applied to detect insignificant factors. Fit of model was dependent upon the lower p value, high F value, high level of adjusted R^2 and predicted R^2 .

Table 5.20: Design Matrix of BBD taking in account three responses for banana peel gum

Formulation code	Acrylamide amount (gm)	Initiator amount (mg)	Temp (°C)	% Yield	% Grafting	% Grafting efficiency
BA1	2.1	50	50	42.434	125	24.03846
BA2	1.4	75	50	51.18987	87.2	26.89474
BA3	2.1	50	50	38.49057	104	20
BA4	1.4	50	40	55.5128	116	30.52632
BA5	1.4	25	50	54.5584	110	28.94737
BA6	2.8	75	50	42.2222	186	28.18182
BA7	2.8	50	60	37.01493	148	22.42424
BA8	2.1	75	40	28.1682	65	10.61538
BA9	2.1	25	60	24.95238	25	5.961538
BA10	2.1	50	50	40.07547	112.4	21.61538
BA11	2.1	25	40	23.31429	22.4	4.307692
BA12	2.8	50	40	50.403	235.2	36.39394
BA13	2.1	75	60	29.15888	56	10.76923
BA14	1.4	50	60	70.7692	180	46.31579
BA15	2.8	25	50	24.2406	82.2	9.272727

Table 5.21: ANOVA Table of % Yield response for banana peel gum

Source	Sum of Squares	df	Mean Square	F Value	p-value	
					Prob > F	
Model	2649.672	9	294.408	118.1584	< 0.0001	significant
A-Monomer amount	750.5324	1	750.5324	301.2204	< 0.0001	
B-Initiator amount	70.23366	1	70.23366	28.18773	0.0032	
C-Temperature	2.401349	1	2.401349	0.963763	0.3713	
AB	115.4051	1	115.4051	46.31693	0.0010	
AC	212.3696	1	212.3696	85.23287	0.0003	
BC	0.066719	1	0.066719	0.026777	0.8764	
A ²	823.4438	1	823.4438	330.4828	< 0.0001	
B ²	548.3717	1	548.3717	220.0847	< 0.0001	
C ²	11.7925	1	11.7925	4.732829	0.0816	
Residual	12.4582	5	2.491639			
Lack of Fit	4.503764	3	1.501255	0.377464	0.7826	not significant
Pure Error	7.954432	2	3.977216			
Cor Total	2662.13	14				
Std. Dev.	1.578493					
Mean	40.85153					
C.V. %	3.863974					
PRESS	89.95769					
R-Squared	0.99532					
Adj R-Squared	0.986897					
Pred R-Squared	0.966208					
Adeq Precision	37.46077					

Model F-value of 118.1584 implied that the model is significant. Values of "Prob > F" less than 0.0500 indicate model terms are significant. Values greater than 0.1000 indicated that the model terms are not significant. The "Pred R-Squared" of 0.966208 is in reasonable agreement with the "Adj R-Squared" of 0.986897. "Adeq Precision" measures the signal to noise ratio. A ratio greater than 4 is desirable. The ratio of 37.46077 indicates an adequate signal. This model can be used to navigate the design space.

Final Quadratic Polynomial Equation for the process:

$$\%Yield (Y1) = 40.339 - 9.685.A + 2.962.B + 0.547.C + 5.371.A.B - 7.286.A.C - 0.129.B.C + 14.933.A^2 - 12.186.B^2 - 1.787.C^2$$

Table 5.22: Observed and predicted values for % yield

Standard Order	Actual Value	Predicted Value	Residual
1	54.5584	55.18083	-0.62243
2	24.2406	25.06637	-0.82577
3	51.18987	50.3641	0.825768
4	42.2222	41.73499	0.48721
5	55.5128	55.33779	0.17501
6	50.403	50.5389	-0.1359
7	70.76923	71.00645	-0.23722
8	37.01493	37.06175	-0.04683
9	23.31429	22.72573	0.588553
10	28.1682	28.90998	-0.74178
11	24.95238	24.07979	0.872595
12	29.15888	29.74743	-0.58855
13	42.434	40.33962	2.09438
14	40.07547	40.33962	-0.26415
15	38.49057	40.33962	-1.84906

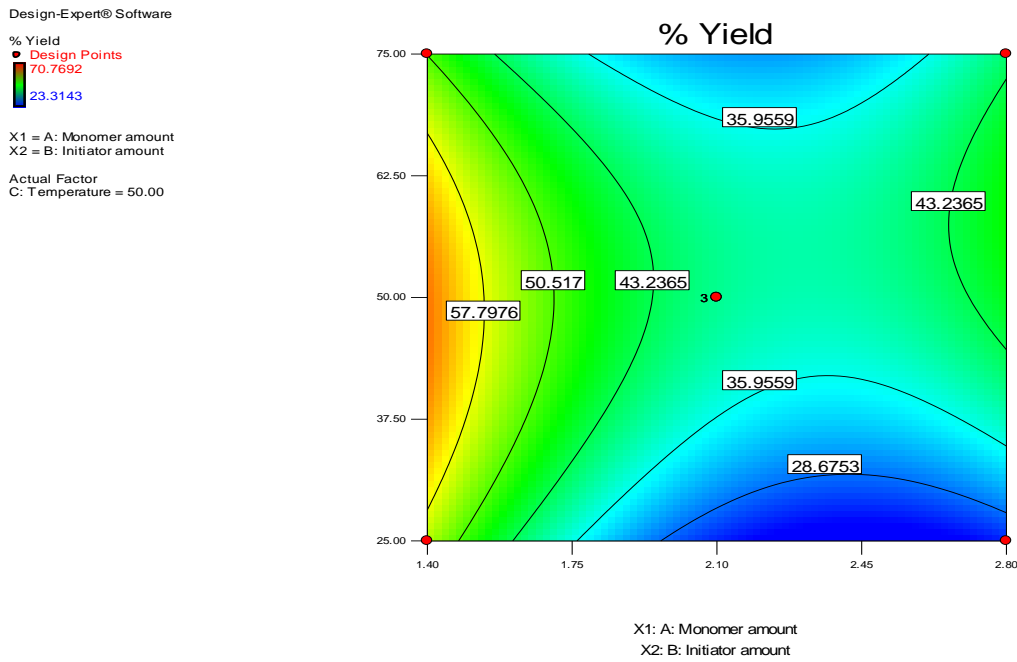


Figure 5.26: Contour Graph showing the effect of Acrylamide amount (A), and CAN amount (B) on % Yield (Y_1) of banana peel gum

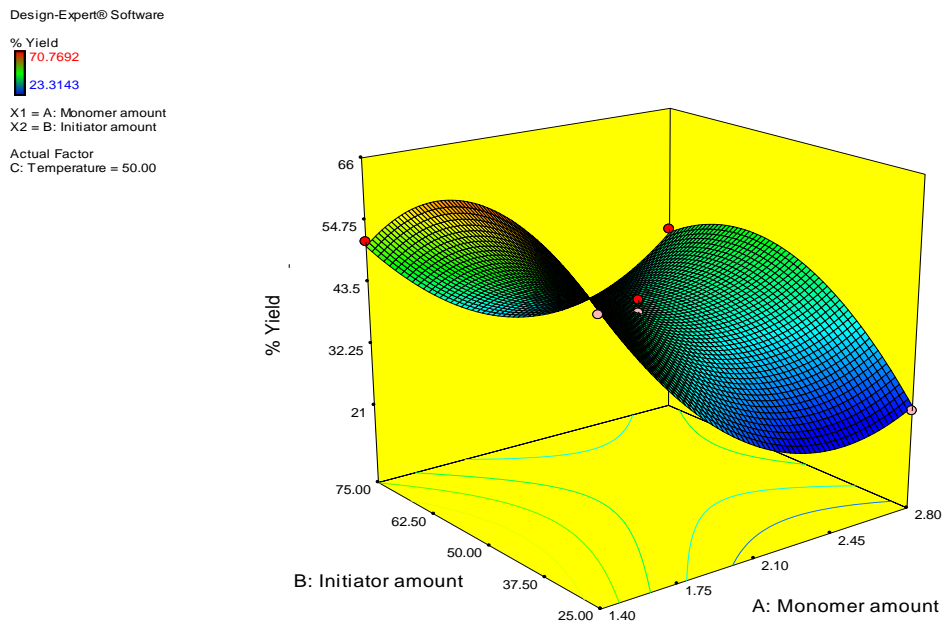


Figure 5.27: 3D Surface Response Graph showing the effect of Acrylamide amount (A), and CAN amount (B) on % Yield (Y_1) of banana peel gum

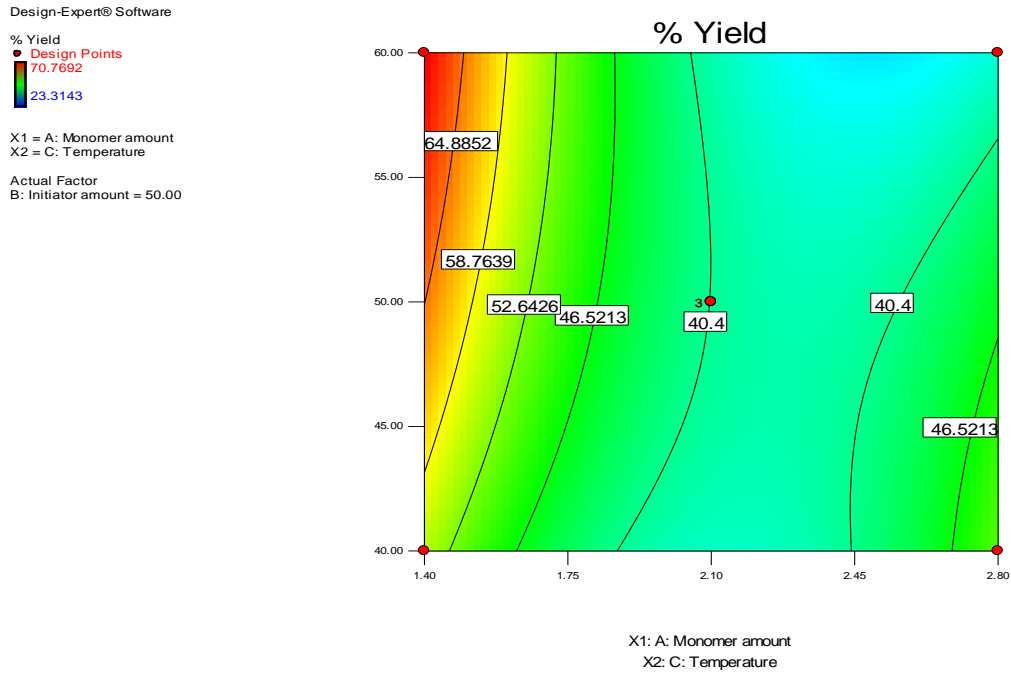


Figure 5.28: Contour Graph showing the effect of Acrylamide amount (A), and Temperature (C) on % Yield (Y_1) of banana peel gum

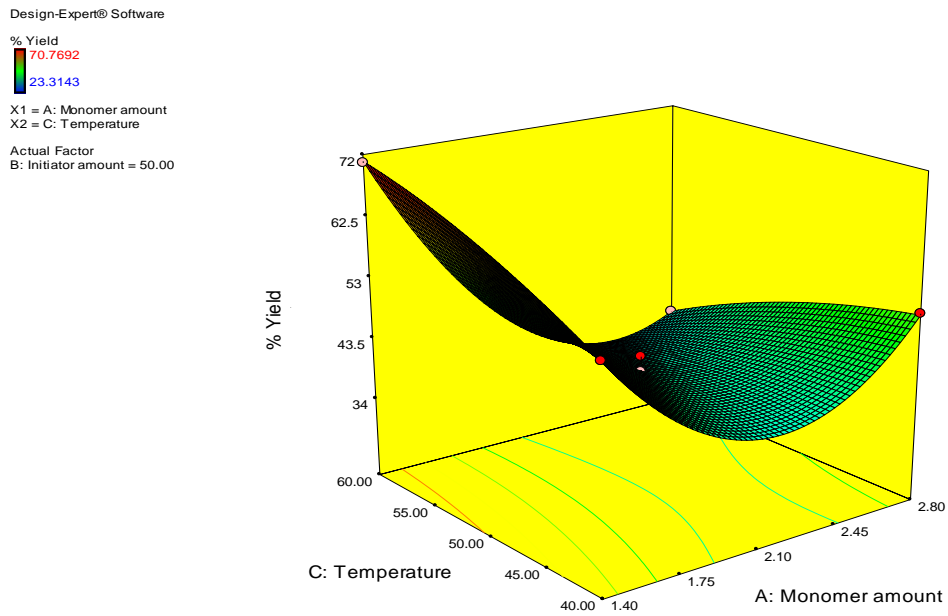


Figure 5.29: 3D Surface Response Graph showing the effect of Acrylamide amount (A), and Temperature (C) on % Yield (Y_1) of banana peel gum

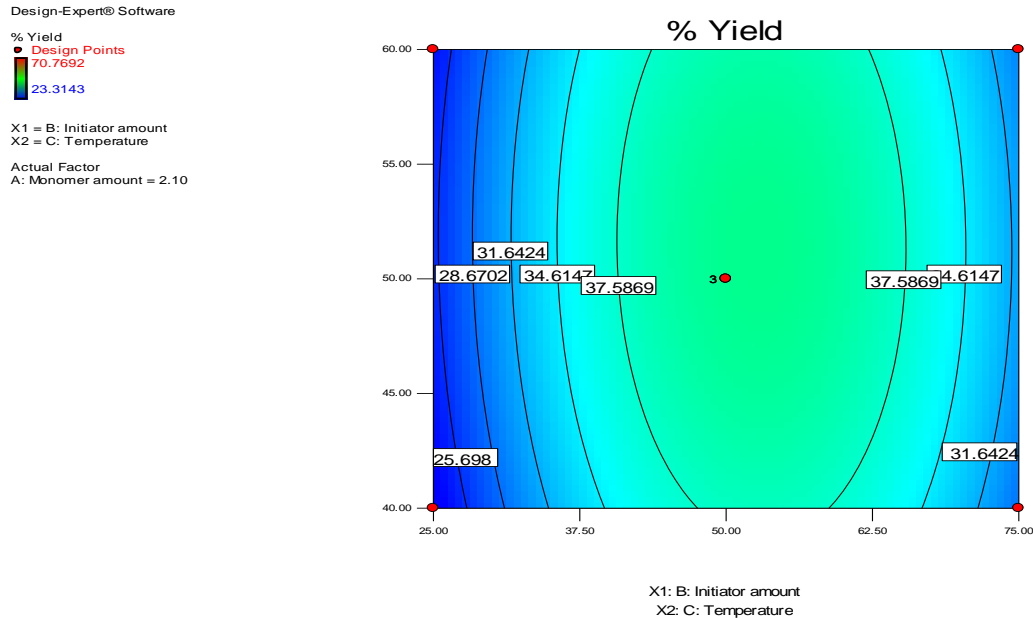


Figure 5.30: Contour Graph showing the effect of Initiator amount (B), and Temperature (C) on % Yield (Y_1) of banana peel gum

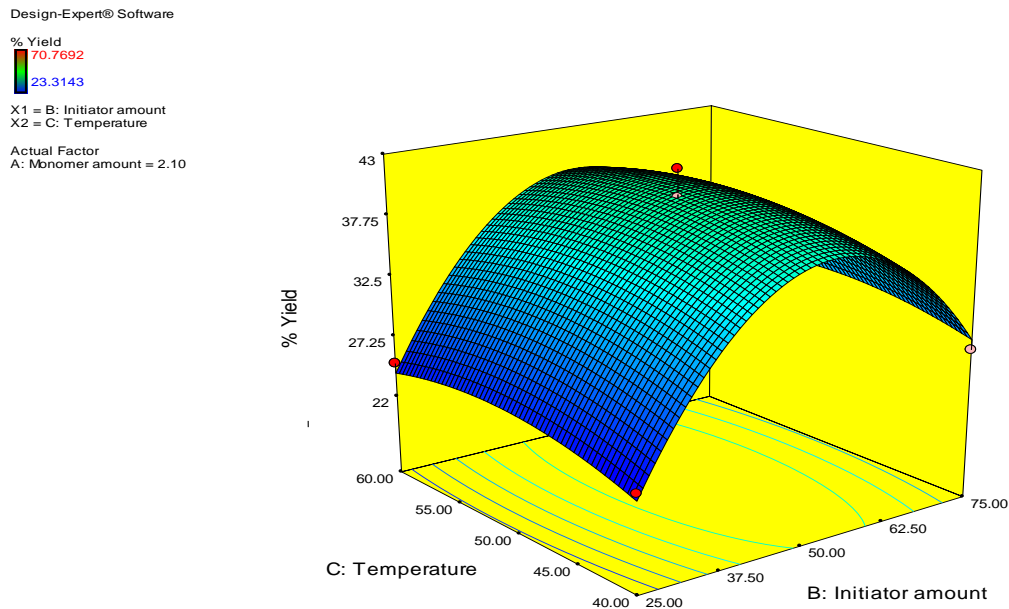


Figure 5.31: Contour and 3D Surface Response Graph showing the effect of Initiator amount (B), and Temperature (C) on % Yield (Y_1) of banana peel gum

Table 5.23: ANOVA table of % Grafting response for banana peel gum

Source	Sum of Squares	df	Mean Square	F Value	p-value	
					Prob > F	
Model	48930.58	9	5436.731	91.1072	< 0.0001	significant
A-Monomer amount	3128.405	1	3128.405	52.42493	0.0008	
B-Initiator amount	2987.645	1	2987.645	50.06611	0.0009	
C-Temperature	109.52	1	109.52	1.835305	0.2335	
AB	4006.89	1	4006.89	67.14633	0.0004	
AC	5715.36	1	5715.36	95.77639	0.0002	
BC	33.64	1	33.64	0.56373	0.4866	
A ²	15660.06	1	15660.06	262.4268	< 0.0001	
B ²	14457.71	1	14457.71	242.2783	< 0.0001	
C ²	307.4423	1	307.4423	5.152031	0.0725	
Residual	298.37	5	59.674			
Lack of Fit	74.93	3	24.97667	0.223565	0.8742	not significant
Pure Error	223.44	2	111.72			
Cor Total	49228.95	14				
Std. Dev.	7.724895					
Mean	110.2933					
C.V. %	7.003954					
PRESS	1701.62					
R-Squared	0.993939					
Adj R-Squared	0.98303					
Pred R-Squared	0.965435					
Adeq Precision	33.1518					

Model F-value of 91.1072 implied that the model is significant. Values of "Prob > F" less than 0.0500 indicate model terms are significant. Values greater than 0.1000 indicated that the model terms are not significant. The "Pred R-Squared" of 0.993939 is in reasonable agreement with the "Adj R-Squared" of 0.98303. "Adeq Precision" measures the signal to noise ratio. A ratio greater than 4 is desirable. The ratio of 33.1518 indicates an adequate signal. This model can be used to navigate the design space.

Final Quadratic Polynomial Equation for the process:

%Grafting (Y2)

$$= 113.8 + 19.775.A + 19.325.B - 3.7.C + 31.65.A.B - 37.8.A.C - 2.9.B.C + 65.125.A^2 - 62.575.B^2 - 9.125.C^2$$

Table 5.24: Observed and predicted values for % grafting

Standard Order	Actual Value	Predicted Value	Residual
1	110	108.9	1.1
2	82.2	85.15	-2.95
3	87.2	84.25	2.95
4	186	187.1	-1.1
5	116	115.925	0.075
6	235.2	231.075	4.125
7	180	184.125	-4.125
8	148	148.075	-0.075
9	22.4	23.575	-1.175
10	65	68.025	-3.025
11	25	21.975	3.025
12	56	54.825	1.175
13	125	113.8	11.2
14	112.4	113.8	-1.4
15	104	113.8	-9.8

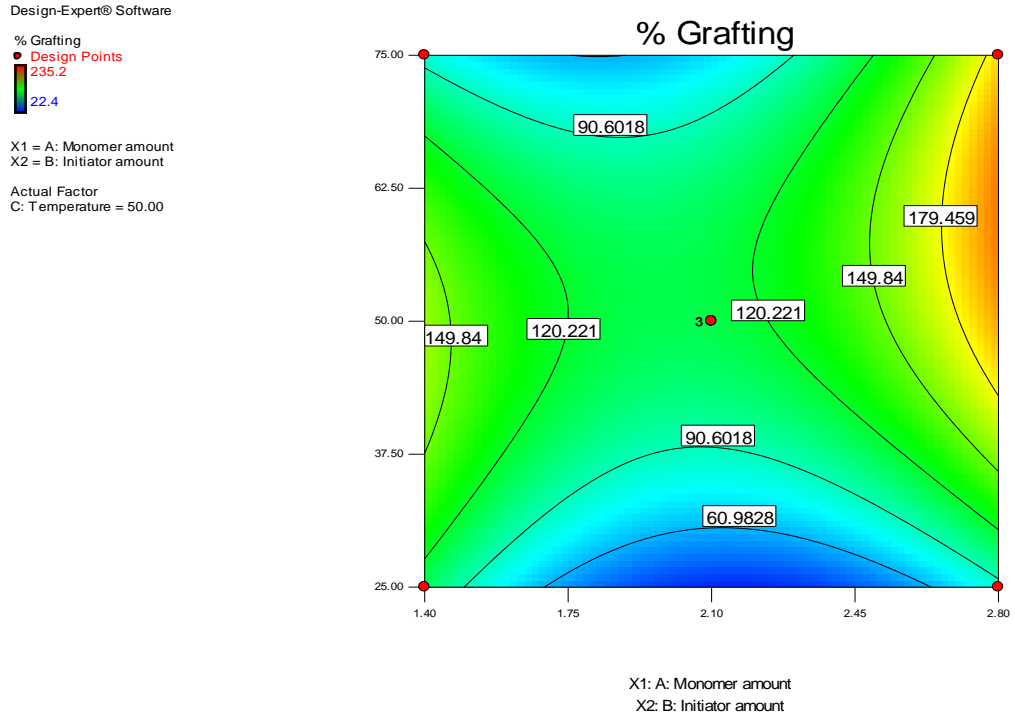


Figure 5.32: Contour Graph showing the effect of Acrylamide amount (A), and CAN amount (B) on % Grafting (Y_2) of banana peel gum

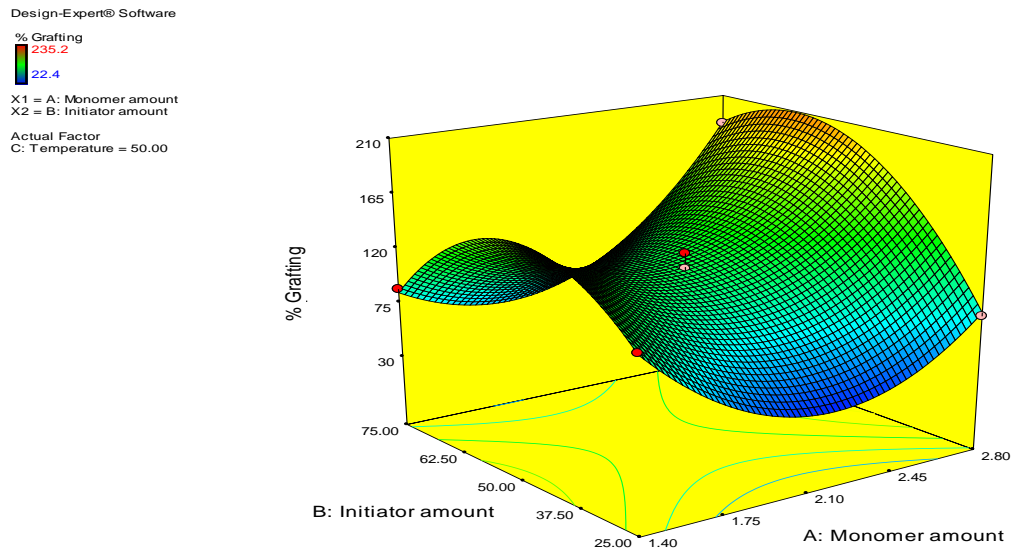


Figure 5.33: 3D Surface Response Graph showing the effect of Acrylamide amount (A), and CAN amount (B) on % Grafting (Y_2) of banana peel gum

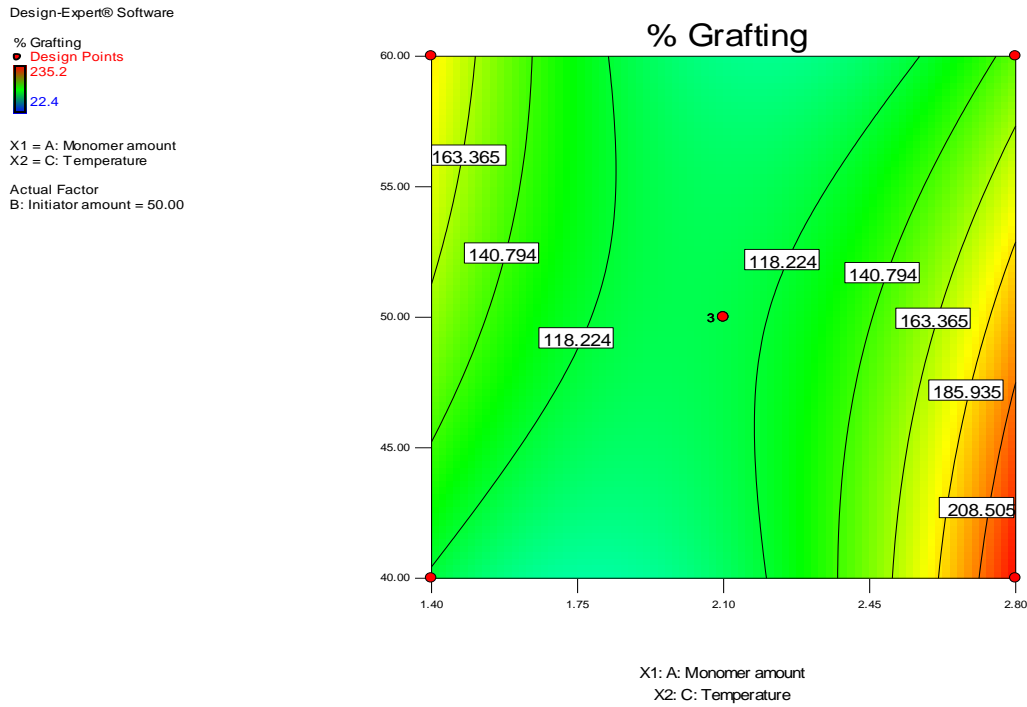


Figure 5.34: Contour Graph showing the effect of Acrylamide amount (A), and Temperature (C) on % Grafting (Y_2) of banana peel gum

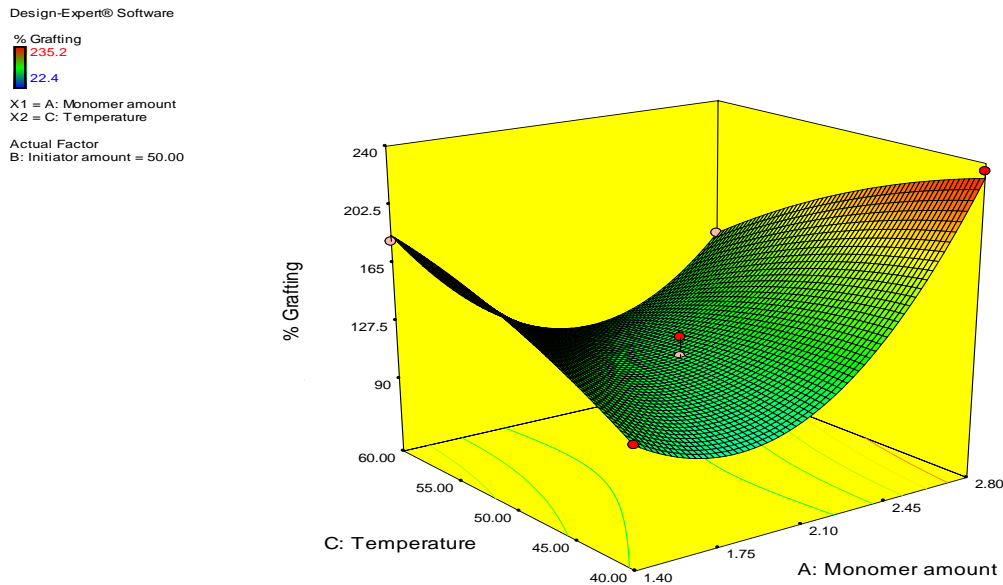


Figure 5.35: 3D Surface Response Graph showing the effect of Acrylamide amount (A), and Temperature (C) on % Grafting (Y_2) of banana peel gum

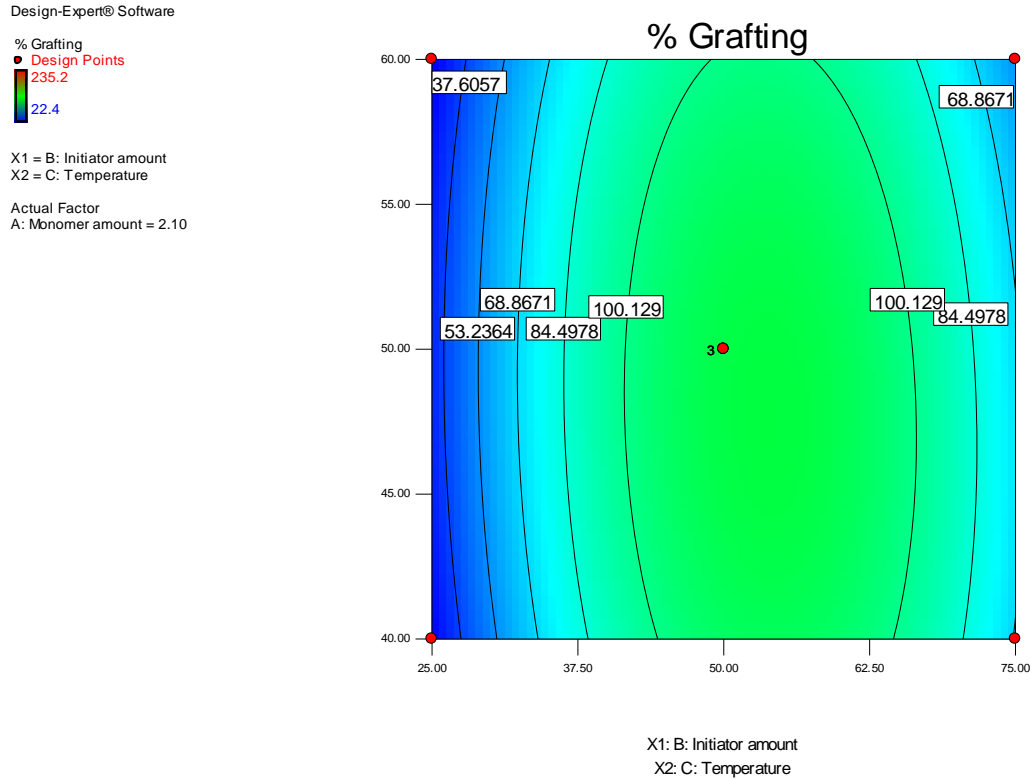


Figure 5.36: Contour Graph showing the effect of CAN amount (B), and Temperature (C) on % Grafting (Y_2) of banana peel gum

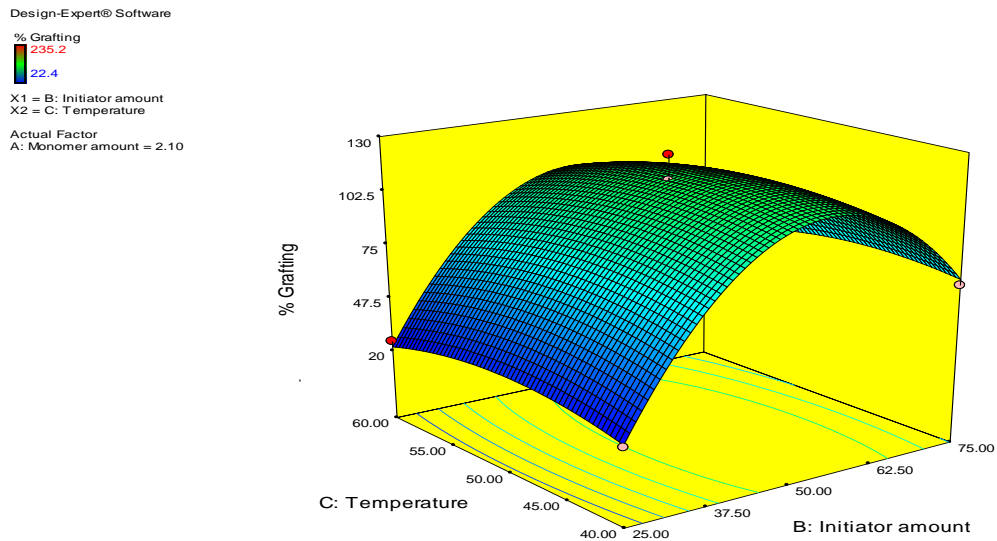


Figure 5.37: 3D Surface Response Graph showing the effect of CAN amount (B), and Temperature (C) on % Grafting (Y_2) of banana peel gum

Table 5.25: ANOVA table of % Grafting Efficiency response for banana peel gum

Source	Sum of Squares	df	Mean Square	F Value	p-value	
					Prob > F	
Model	1964.707	9	218.3008	88.02549	< 0.0001	significant
A-Monomer amount	165.7245	1	165.7245	66.82516	0.0004	
B-Initiator amount	97.80297	1	97.80297	39.43713	0.0015	
C-Temperature	1.644821	1	1.644821	0.663242	0.4524	
AB	109.8485	1	109.8485	44.29423	0.0012	
AC	221.4021	1	221.4021	89.27603	0.0002	
BC	0.562497	1	0.562497	0.226816	0.6540	
A ²	695.0928	1	695.0928	280.2825	< 0.0001	
B ²	556.8877	1	556.8877	224.554	< 0.0001	
C ²	10.54713	1	10.54713	4.252925	0.0942	
Residual	12.39986	5	2.479972			
Lack of Fit	4.136546	3	1.378849	0.333728	0.8073	not significant
Pure Error	8.263314	2	4.131657			
Cor Total	1977.107	14				
Std. Dev.	1.574793					
Mean	21.75098					
C.V. %	7.240101					
PRESS	84.77719					
R-Squared	0.993728					
Adj R-Squared	0.982439					
Pred R-Squared	0.957121					
Adeq Precision	33.26393					

Model F-value of 88.02549 implied that the model is significant. Values of "Prob > F" less than 0.0500 indicate model terms are significant. Values greater than 0.1000 indicated that the model terms are not significant. The "Pred R-Squared" of 0.957121 is in reasonable agreement with the "Adj R-Squared" of 0.982439. "Adeq Precision" measures the signal to noise ratio. A ratio greater than 4 is desirable. The ratio of 33.26393 indicates an adequate signal. This model can be used to navigate the design space.

Final Quadratic Polynomial Equation for the process

%Grafting Efficiency (Y3)

$$= 21.884 - 4.551.A + 3.496.B + 0.453.C + 5.240.A.B - 7.439.A.C - 0.375.B.C + 13.720.A^2 - 12.281.B^2 - 1.690.C^2$$

Table 5.26: Observed and predicted values for % grafting efficiency

Standard Order	Actual Value	Predicted Value	Residual
1	28.94737	29.61955	-0.67218
2	9.272727	10.03582	-0.76309
3	26.89474	26.13165	0.763089
4	28.18182	27.50964	0.67218
5	30.52632	30.57328	-0.04696
6	36.39394	36.34999	0.043945
7	46.31579	46.35973	-0.04394
8	22.42424	22.37728	0.046965
9	4.307692	3.588547	0.719145
10	10.61538	11.3315	-0.71612
11	5.961538	5.245414	0.716125
12	10.76923	11.48838	-0.71914
13	24.03846	21.88462	2.153846
14	21.61538	21.88462	-0.26923
15	20	21.88462	-1.88462

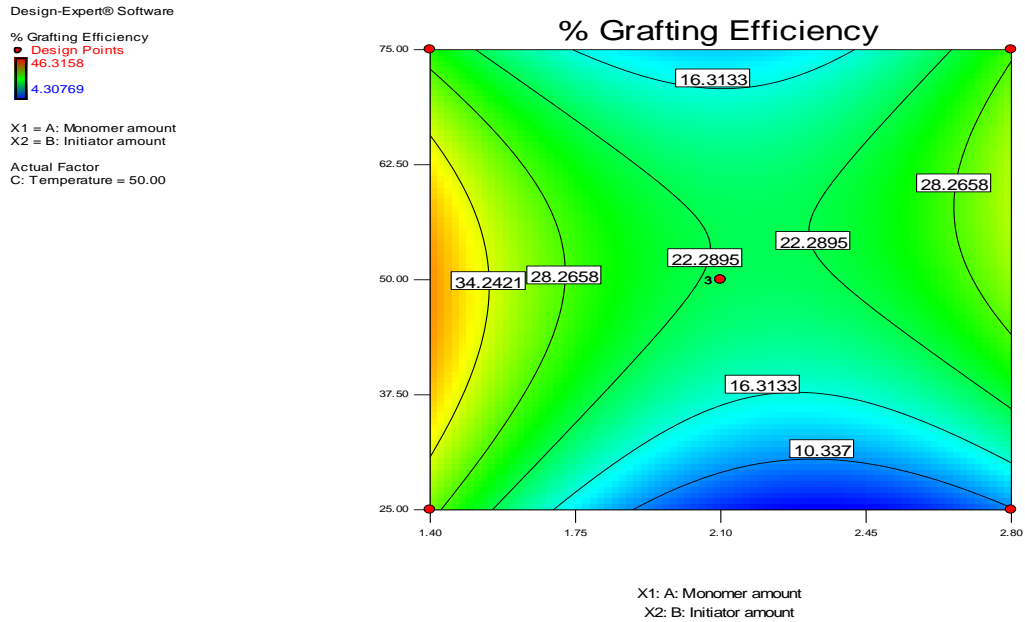


Figure 5.38: Contour Graph showing the effect of Acrylamide amount (A), and CAN amount (B) on % Grafting Efficiency (Y₃) of banana peel gum

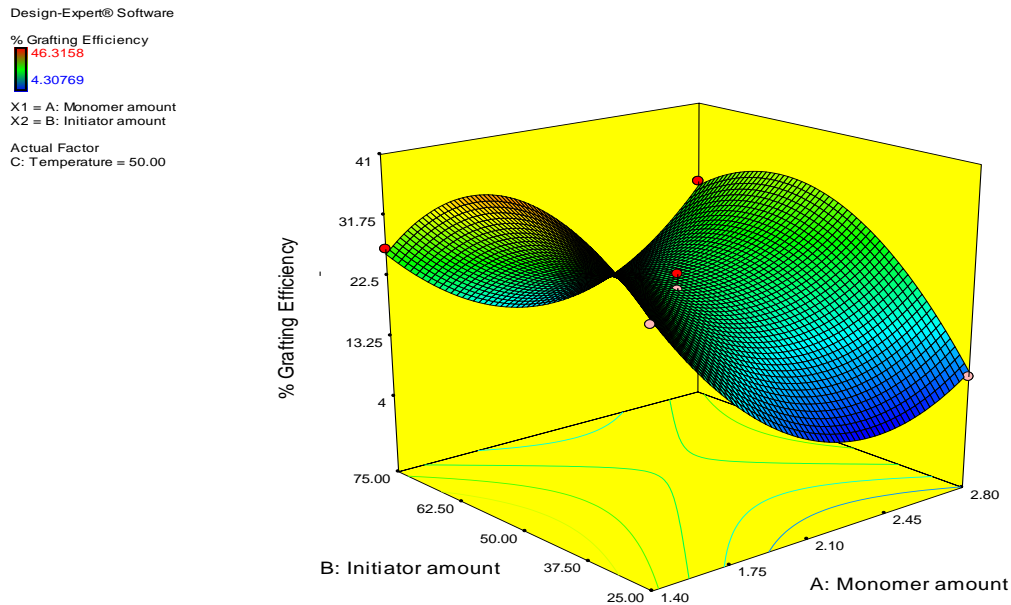


Figure 5.39: 3D Surface Response Graph showing the effect of Acrylamide amount (A), and CAN amount (B) on % Grafting Efficiency (Y₃) of banana peel gum

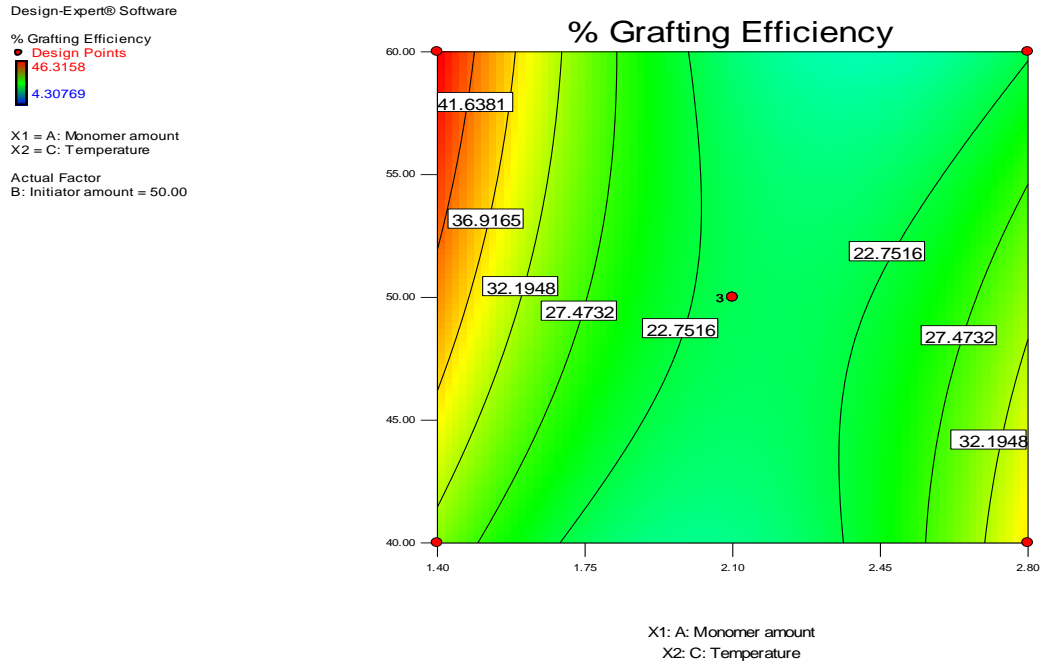


Figure 5.40: Contour Graph showing the effect of Acrylamide amount (A), and Temperature (C) on % Grafting Efficiency (Y₃) of banana peel gum

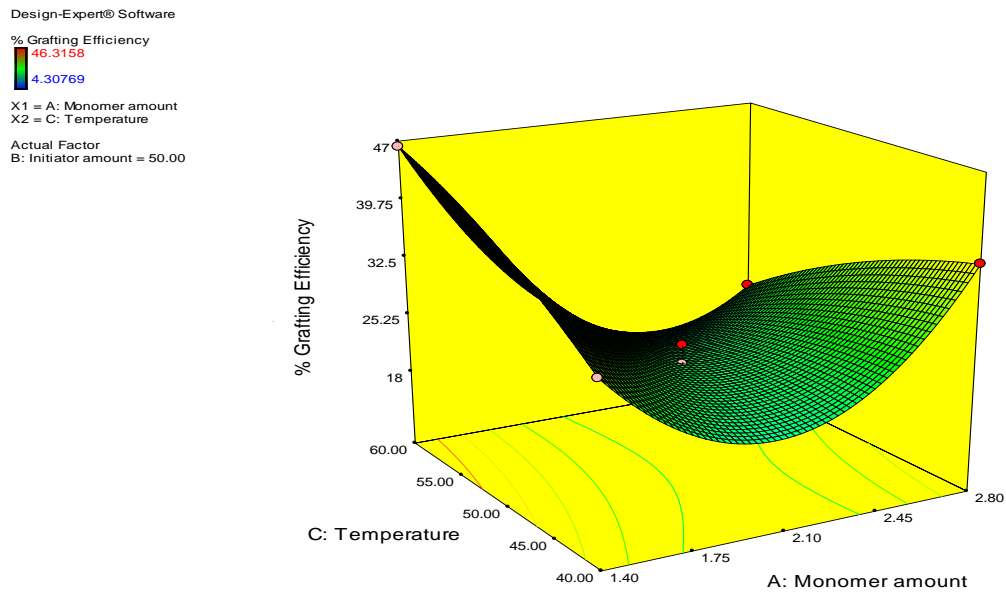


Figure 5.41: 3D Surface Response Graph showing the effect of Acrylamide amount (A), and Temperature (C) on % Grafting Efficiency (Y₃) of banana peel gum

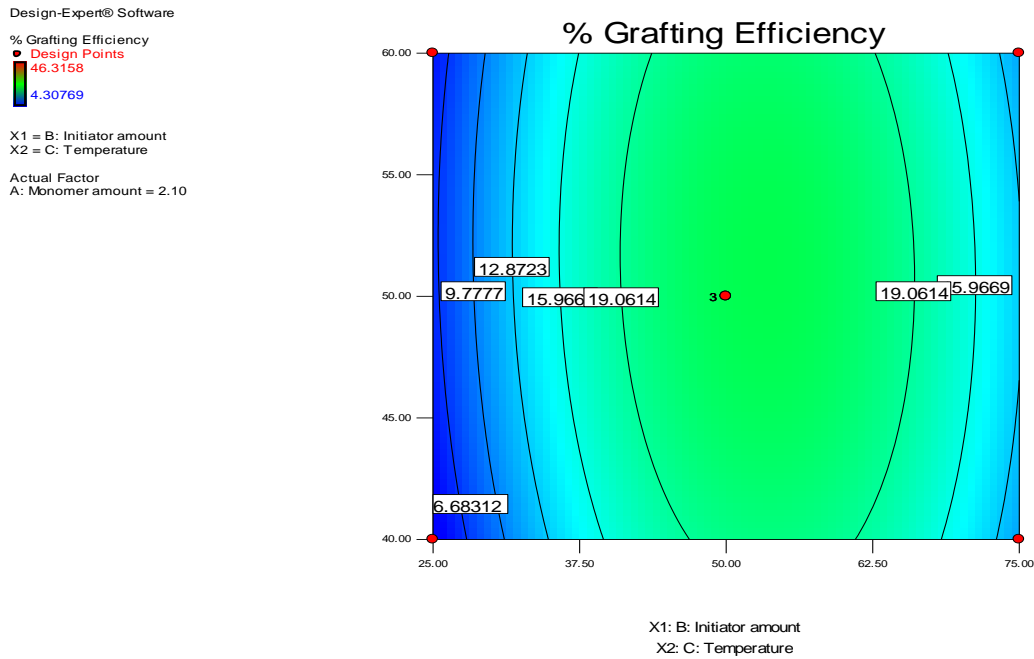


Figure 5.42: Contour Graph showing the effect of CAN amount (B), and Temperature (C) on % Grafting Efficiency (Y₃) of banana peel gum

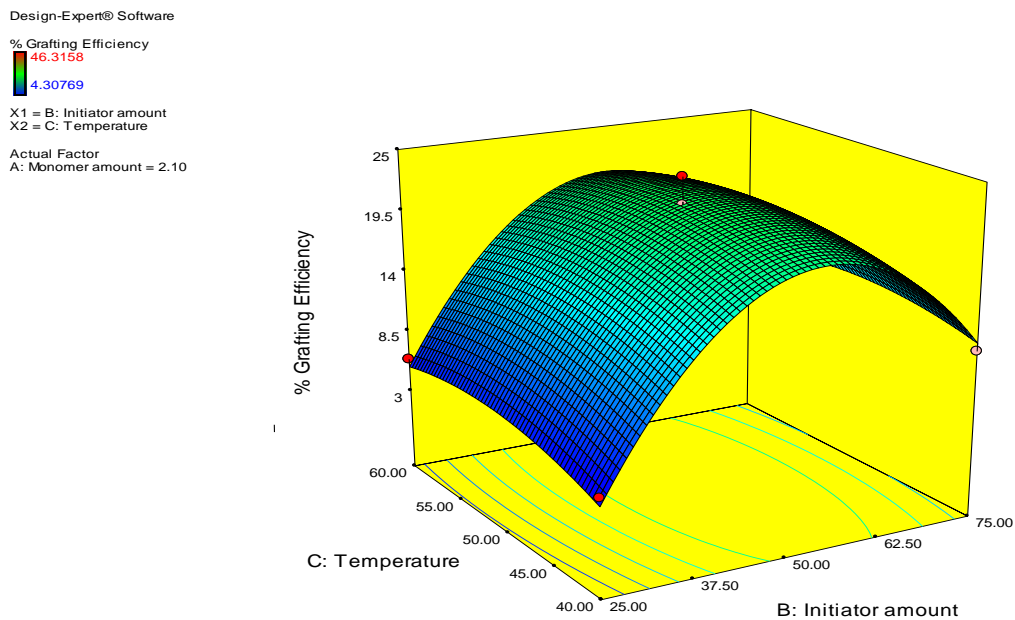


Figure 5.43: 3D Surface Response Graph showing the effect of CAN amount (B), and Temperature (C) on % Grafting Efficiency (Y₃) of banana peel gum

Table 5.27: Numerical optimization as per desirability of the process of dependent and independent variables for banana peel gum

Name	Goal
Acrylamide amount	is in range
CAN amount	is in range
Temperature	is in range
% Yield	maximum
% Grafting	maximum
% Grafting Efficiency	maximum

Table 5.28: Optimized solutions for Grafted Banana peel gum

Code	M	I	Temp	% Y	Exp	% G	Exp	%	Exp	D
	(g)	(mg)	(°C)		% Y		% G	G.E.	% G.E.	
D1	1.4	25	50	55.18	59.74	108.9	130	29.61	34.21	1
D2	1.4	75	50	50.36	56.20	84.25	122	26.13	32.10	1
D3	2.8	75	50	41.73	39.70	187.1	168	27.50	25.45	1
D4	1.4	50	40	55.33	50.30	115.9	96.2	30.57	25.31	1
D5	2.8	50	40	50.53	45.37	184.0	166.3	36.34	30.90	1
D6	1.4	50	60	70.33	68.86	181.7	170	45.74	44.50	1

Where,

M-Monomer Amount,

I- Initiator Amount,

% Y- % Yield,

% G- % Grafting,

% G. E. - % Grafting Efficiency,

D- Desirability

The optimized process parameters contain 0.5 gm extracted gum from Banana peel, 1.4 gm acrylamide and 50 mg of ceric ammonium nitrate at 60°C.

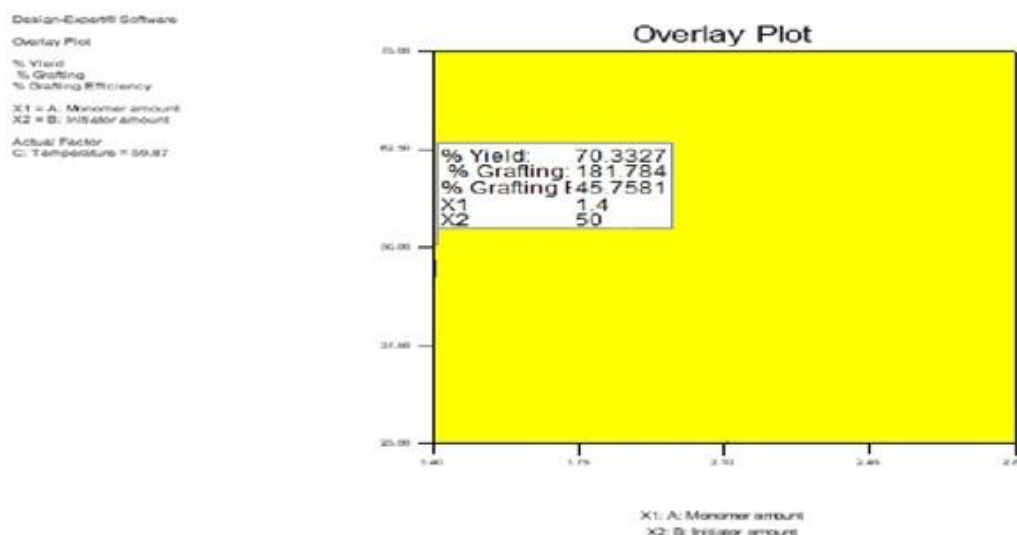


Figure 5.44: Overlay graph of an optimized values of process parameters of D6 formulation

5.2.3 Characterisation of ungrafted mastic gum and optimised grafted mastic gum

The ungrafted mastic gum and optimised grafted mastic gum were further characterized by FTIR, DSC, SEM and XRD analysis.

A. FTIR Analysis

The FTIR spectra (Figure 5.45) of mastic gum showed the characteristic peak of Mastic Gum. The spectrum showed a C-H stretch at 2918.92 cm^{-1} , C=O stretch at 1698.78 cm^{-1} , =C-H bend at 951.12 cm^{-1} . The FTIR spectrum of acrylamide is shown in Figure 5.46. The spectra of acrylamide presented absorption bands at 3355.65 cm^{-1} due to asymmetric and symmetric NH stretching of the NH group. CO stretching appeared at 1647 cm^{-1} . The spectra also showed a bend at 1351.92 cm^{-1} which can be attributed to CN stretching, while the CH stretching appeared at 1613.17 cm^{-1} . The FTIR spectrum of Mastic-g-acrylamide is shown in Figure 5.47. The FTIR spectra of grafted gum showed a broad absorption band at 2926.06 cm^{-1} due to overlap of the OH stretching band of mastic gum and NH stretching band of acrylamide.

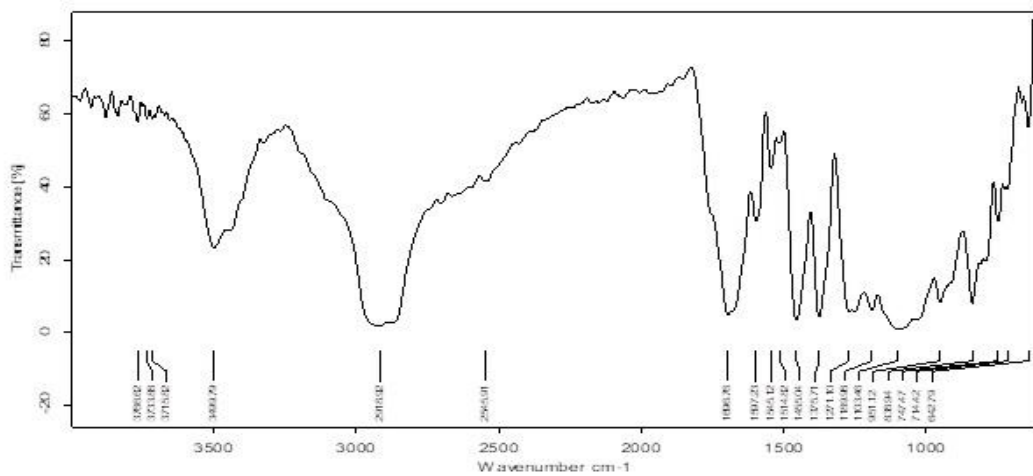


Figure 5.45: FT-IR spectrum of Gum Mastic

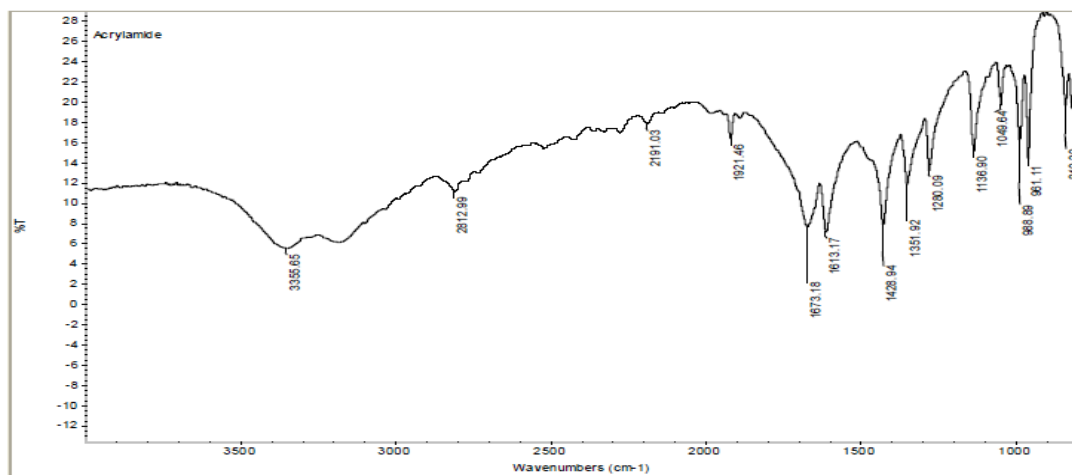


Figure 5.46: FT-IR spectrum of Acrylamide

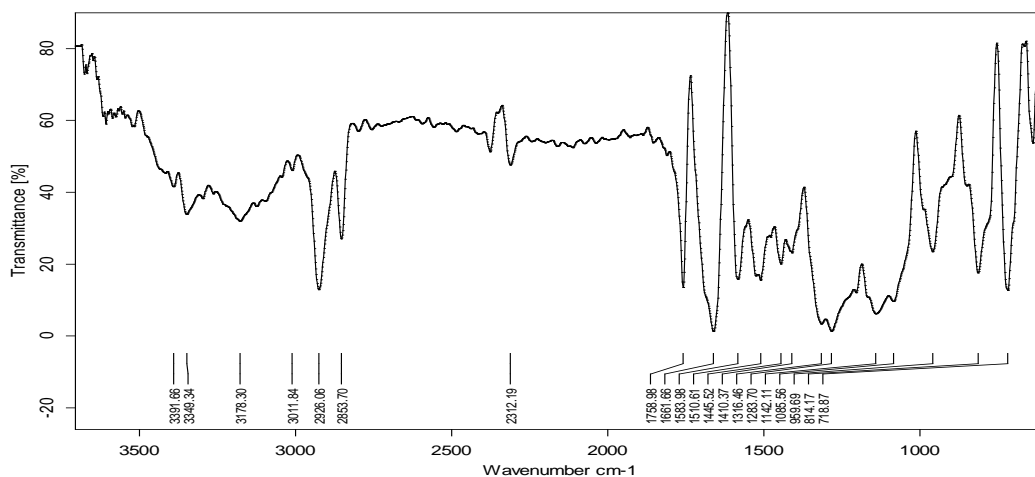


Figure 5.47: FT-IR spectrum of Grafted Mastic Gum

B. DSC Analysis

The Figure 5.48, Figure 5.49 and Figure 5.50 contains the DSC thermogram of Gum mastic, acrylamide and grafted mastic gum. The increase in the glass transition of grafted gum is to be expected because the amine group in acrylamide chains grafted onto gum has more difficulty to interact. The Mastic-g-acrylamide is expected to have longer acryl chains than Gum and acrylamide thus more glass transition temperature.

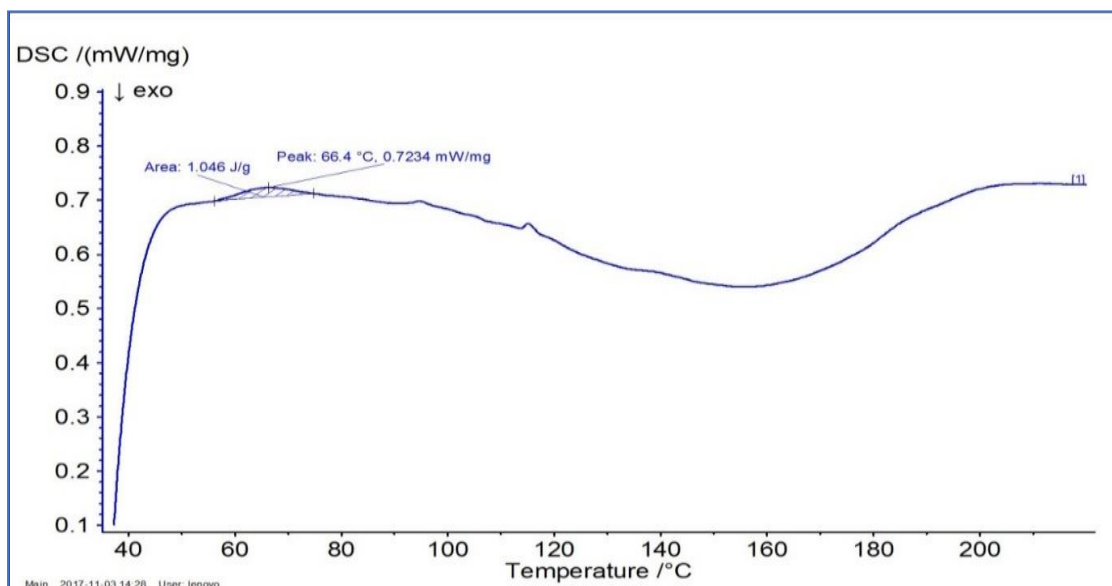


Figure 5.48: DSC of Mastic Gum

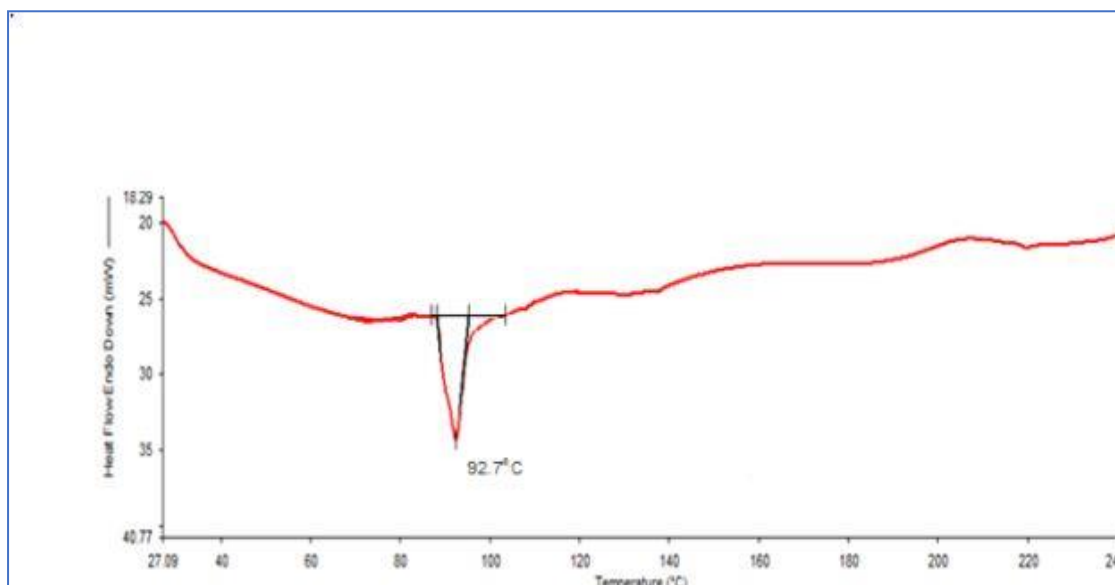


Figure 5.49: DSC of Acrylamide

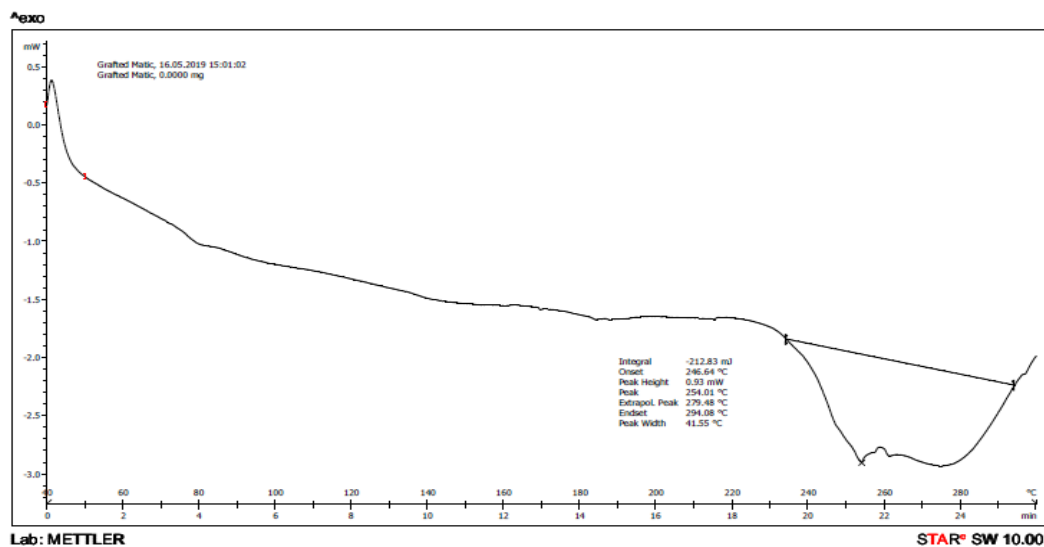


Figure 5.50: DSC of Grafted Mastic Gum

C. XRD Analysis

The XRD spectra (Figure 5.51) showed the amorphous nature of mastic gum as no characteristic peaks in the spectrum were observed while the diffractogram of acrylamide (Figure 5.52) showed the crystalline nature. The XRD spectrum of grafted gum (Figure 5.53) showed the characteristic peaks of acrylamide but with the decreased intensity, which confirmed the formation of graft co-polymer.

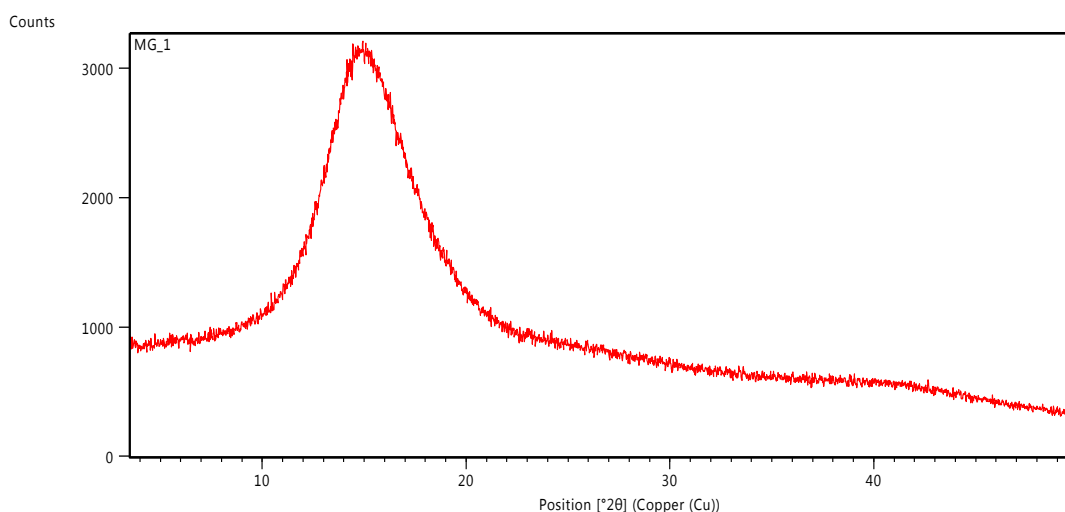


Figure 5.51: XRD spectra of Mastic Gum

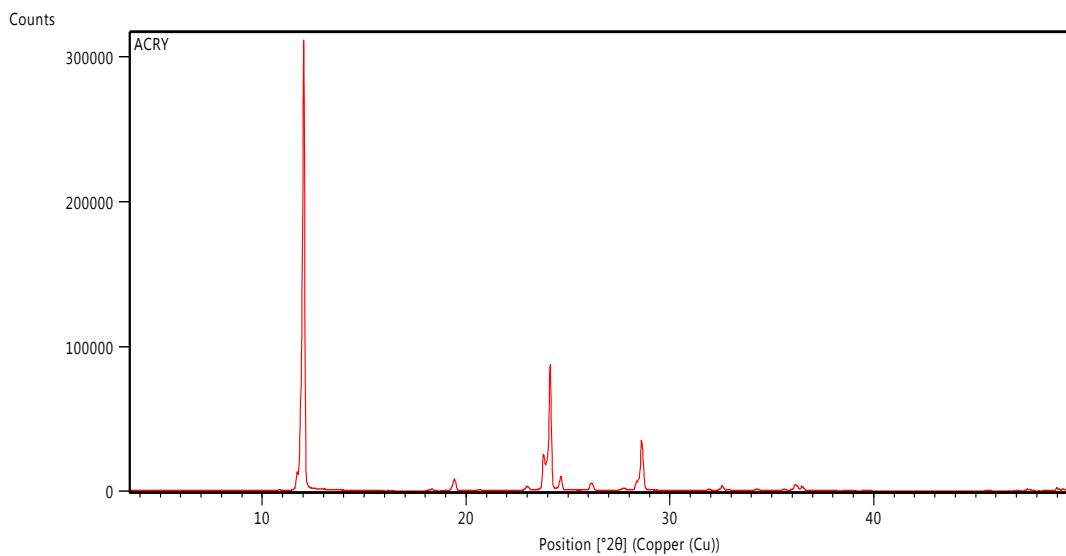


Figure 5.52: XRD spectra of Acrylamide

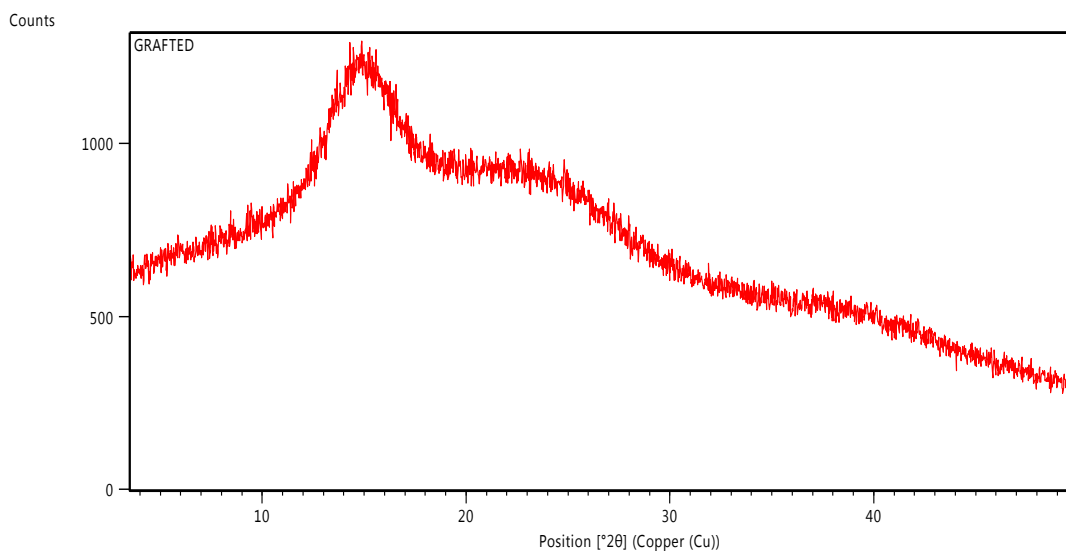


Figure 5.53: XRD spectra of grafted mastic gum

D. Scanning Electron Microscopy

The SEM studies of Mastic Gum (Figure 5.54) and Mastic-g-Acrylamide (Figure 5.55) showed a change in surface morphology after grafting. The more roughness and unevenness on the surface of grafted gum due to deposition of acrylamide was clearly visible.

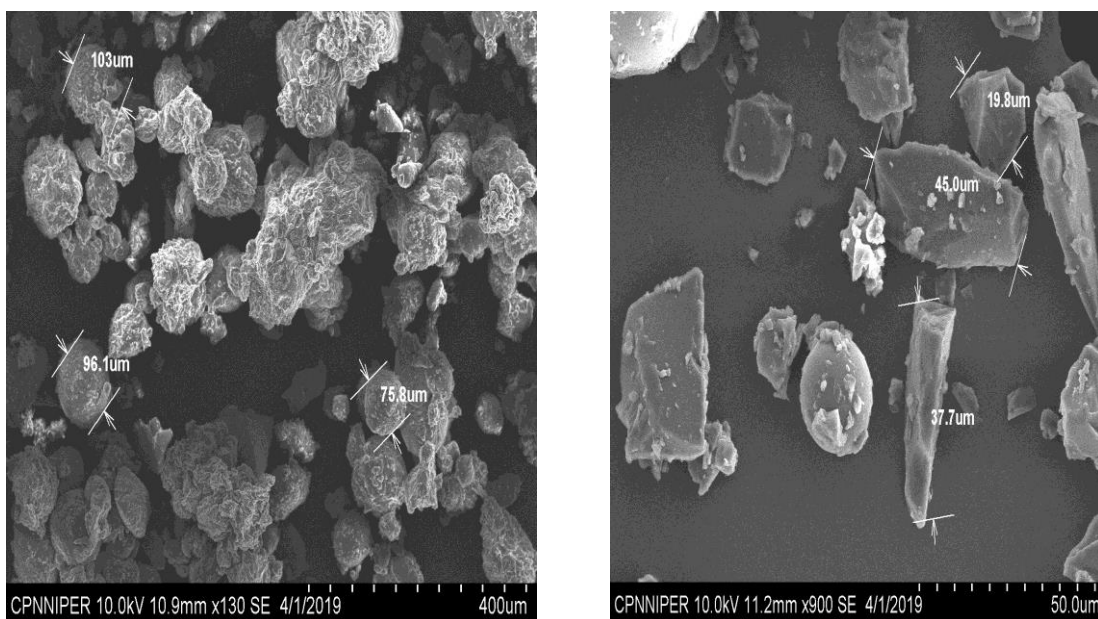


Figure 5.54: SEM images of pure gum mastic

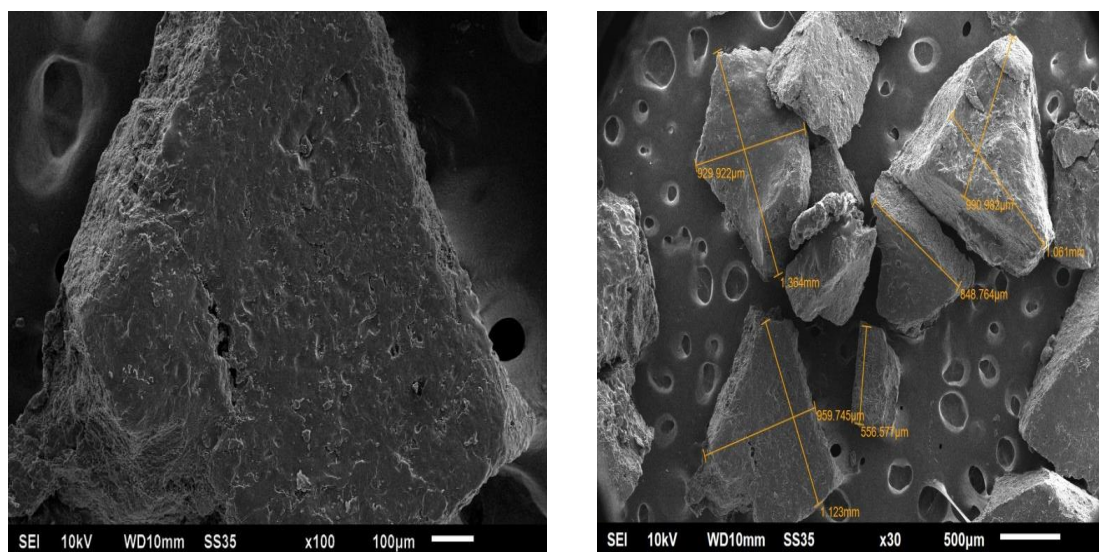


Figure 5.55: SEM images of grafted gum mastic

5.2.4 Characterization of ungrafted banana peel gum and optimized grafted banana peel gum

The ungrafted banana peel gum and optimized grafted banana peel gum were further characterised by FTIR, DSC, SEM and XRD analysis.

A. FTIR Analysis

The FTIR spectra (Figure 5.56) of banana peel gum showed the characteristic peak of banana peel gum. The spectrum showed a C-H stretch at 2918 cm^{-1} , C=O stretch at 1733.58 cm^{-1} , -C=C- stretch at 1636.84 cm^{-1} which was similar to reference FTIR

(Figure 5.57) spectra of banana peel gum. The FTIR spectrum of acrylamide is shown in Figure 5.46. The spectra of acrylamide presented absorption bands at 3340 cm^{-1} and 3200 cm^{-1} due to asymmetric and symmetric NH stretching of the NH group. CO stretching appeared at 1647 cm^{-1} . The spectra also showed a bend at 1300 cm^{-1} which can be attributed to CN stretching, while the CH stretching appeared at 1600 cm^{-1} . The FTIR spectrum of grafted banana peel gum is shown in Figure 5.58. The FTIR spectra of grafted gum showed a broad absorption band at 2924.09 cm^{-1} due to overlap of the OH stretching band of banana peel gum and NH stretching band of acrylamide.

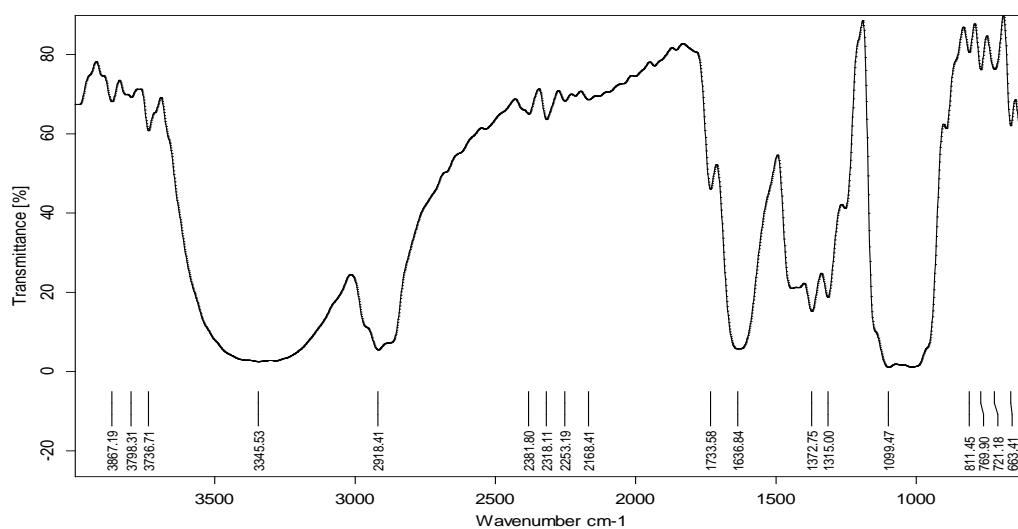


Figure 5.56: FTIR Spectrum of Extracted banana peel gum (test)

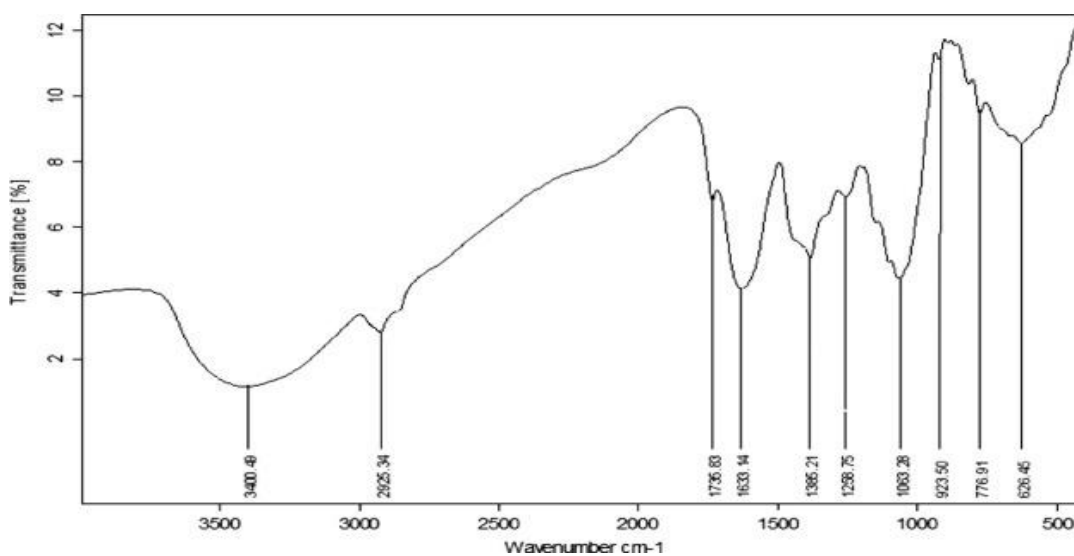


Figure 5.57: FTIR Spectrum of Extracted banana peel gum (Reference) (Alaa El-Din G et al., 2018)

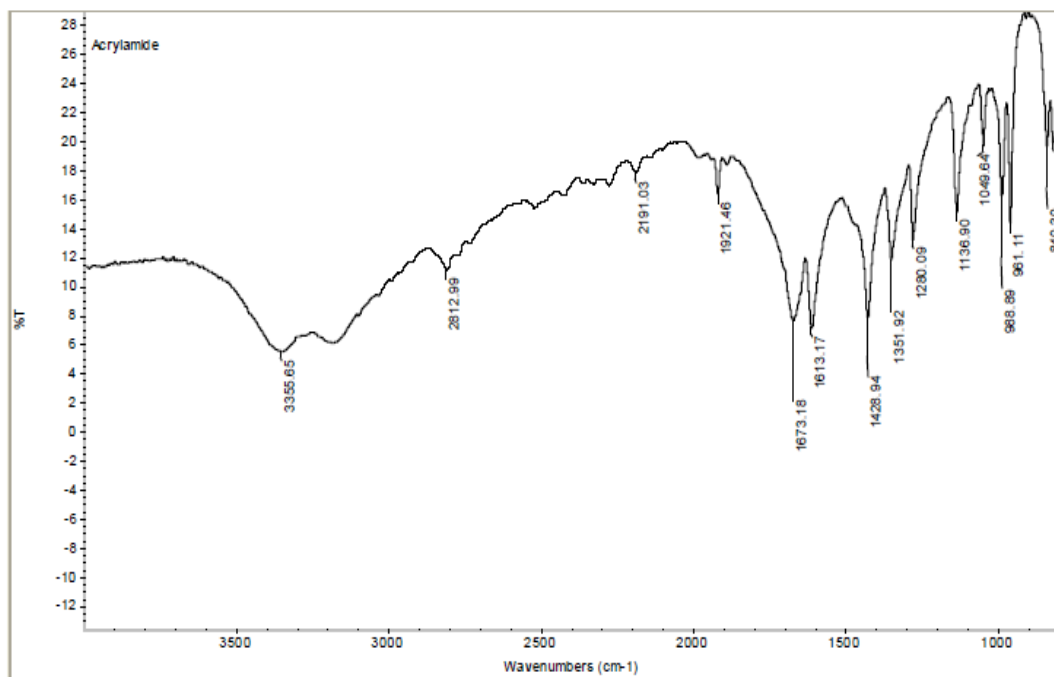


Figure 5.46: FT-IR spectrum of Acrylamide

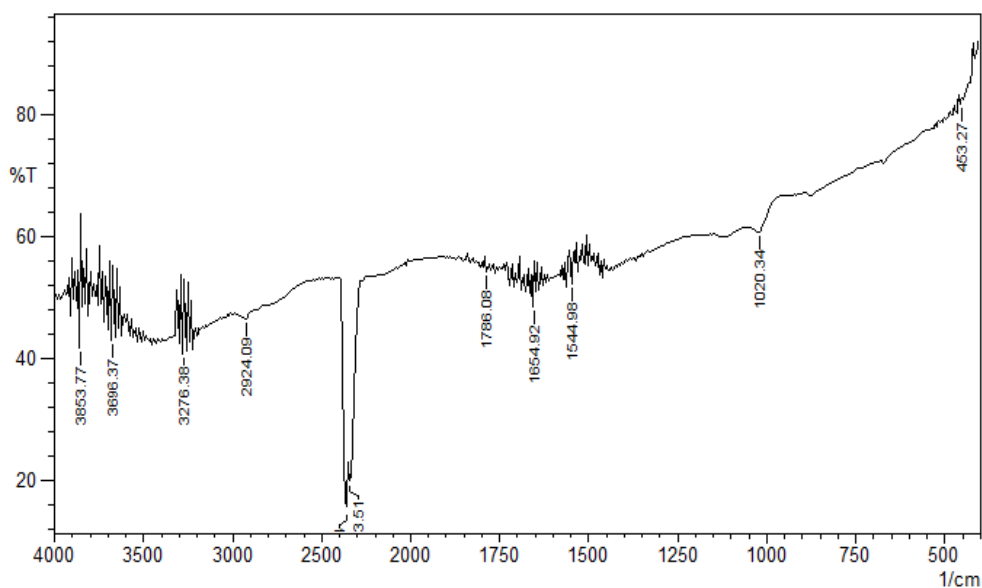


Figure 5.58: FT-IR spectrum of Grafted Banana Peel Gum

B. DSC Analysis

The Figure 5.58, Figure 5.49 and Figure 5.59 contains the DSC thermogram of banana peel gum, acrylamide and grafted banana peel gum. The 3 endothermic peaks were observed at 59°C, 210°C and 272°C in case of banana peel gum. The change in

the glass transition of grafted gum which was expected (peaks were at 189.20 °C and 281.09 °C) because the amine group in acrylamide chains grafted onto gum has more difficulty to interact. The banana-g-acrylamide is expected to have longer acryl chains than Gum and acrylamide thus more glass transition temperature.

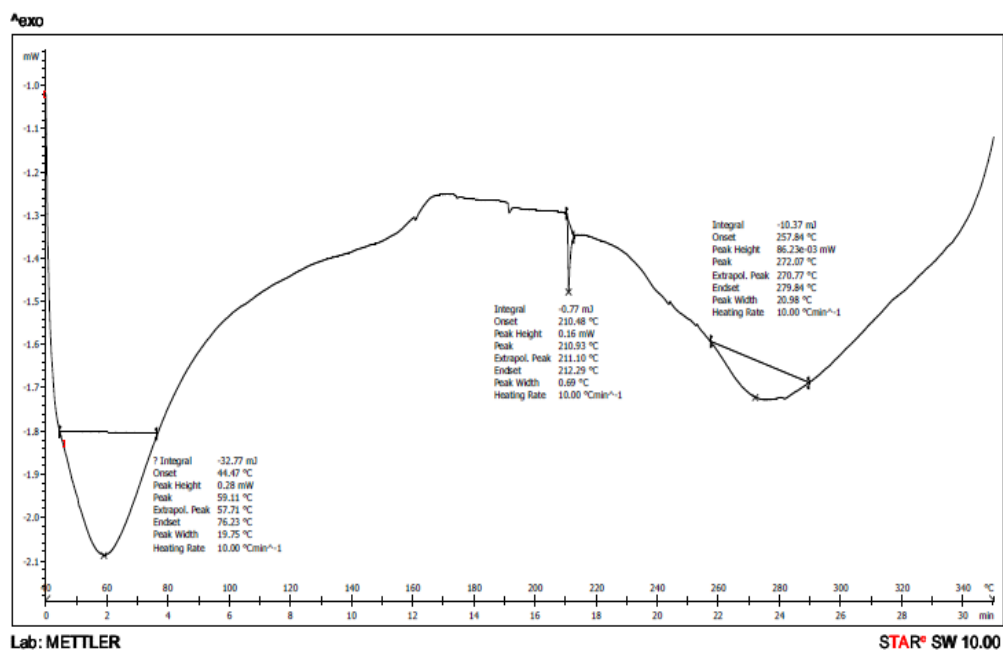


Figure 5.59: DSC of Banana Peel Gum

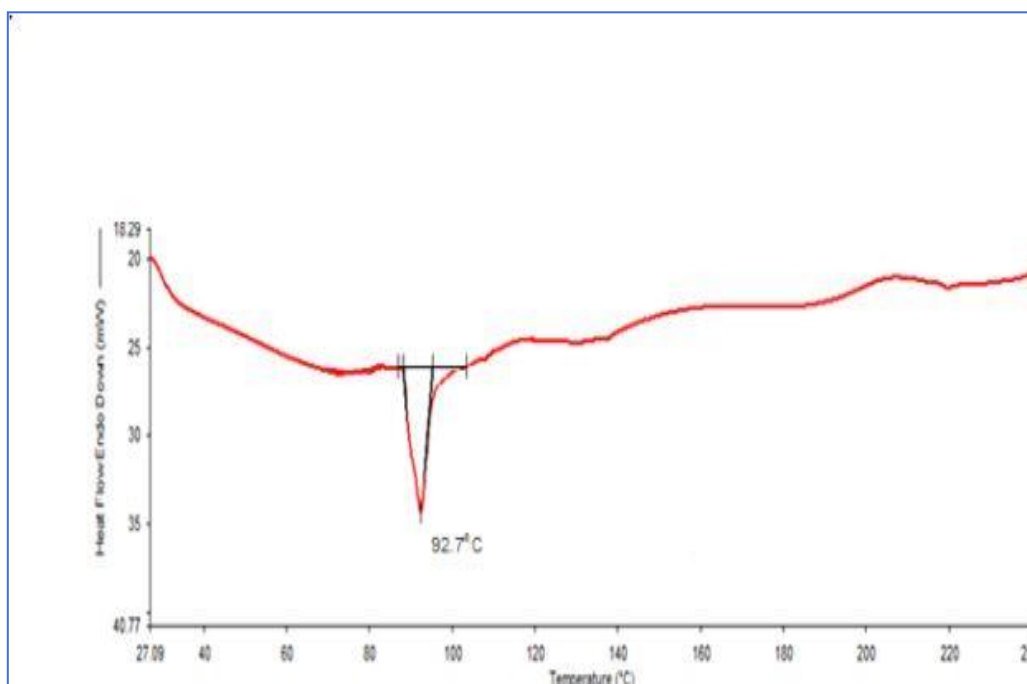


Figure 5.49: DSC of Acrylamide

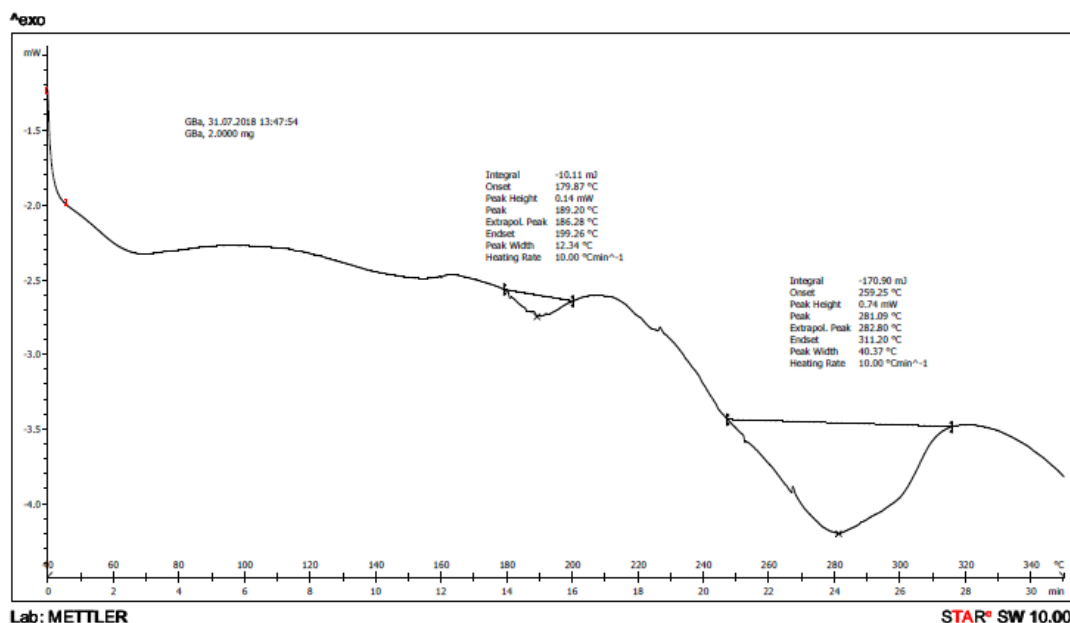


Figure 5.60: DSC of Grafted Banana Peel Gum

C. XRD Analysis

The XRD spectra (Figure 5.60) showed the amorphous nature of banana peel gum as no characteristic peaks in the spectrum were observed while the diffractogram of acrylamide (Figure 5.52) showed the crystalline nature. The XRD spectrum of grafted gum (Figure 5.61) showed the characteristic peaks of acrylamide but with the decreased intensity, which confirmed the formation of graft co-polymer.

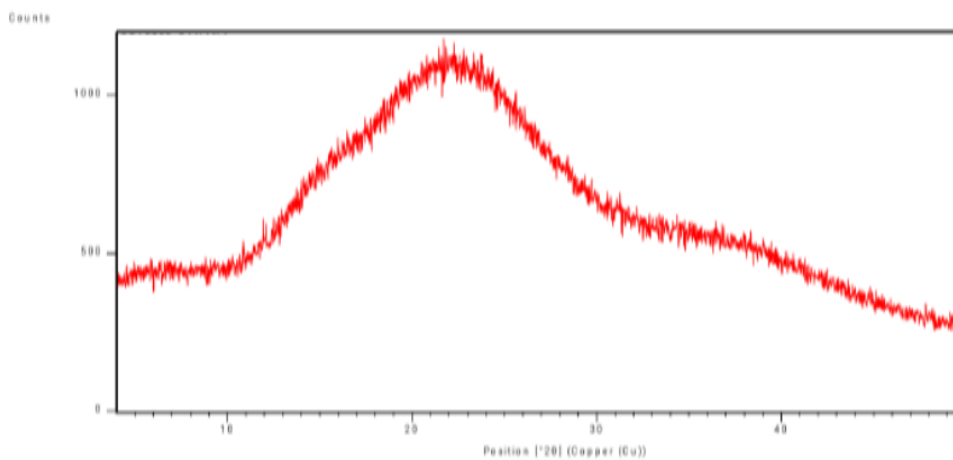


Figure 5.61: XRD spectra of banana peel gum

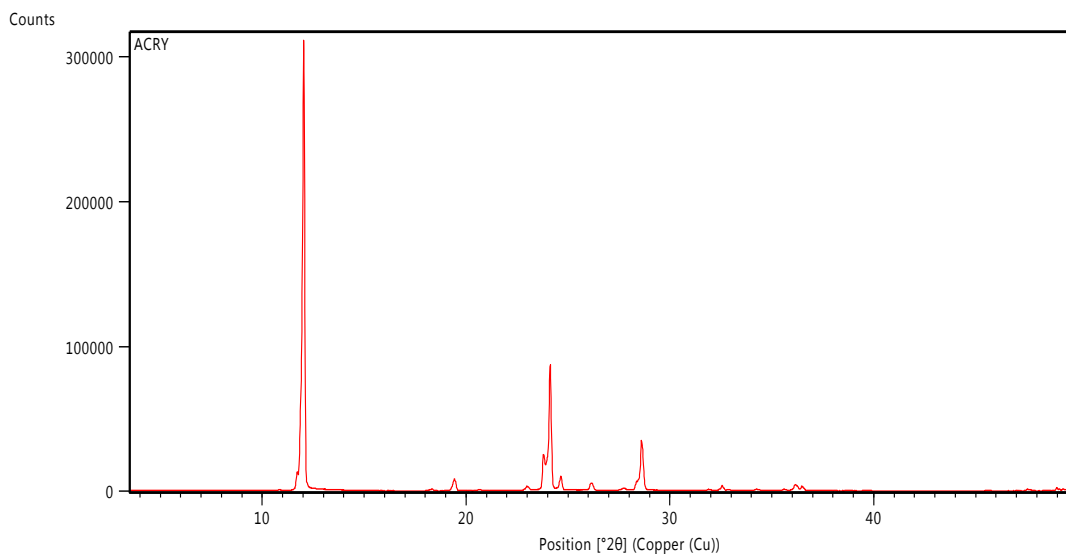


Figure 5.52: XRD spectra of Acrylamide

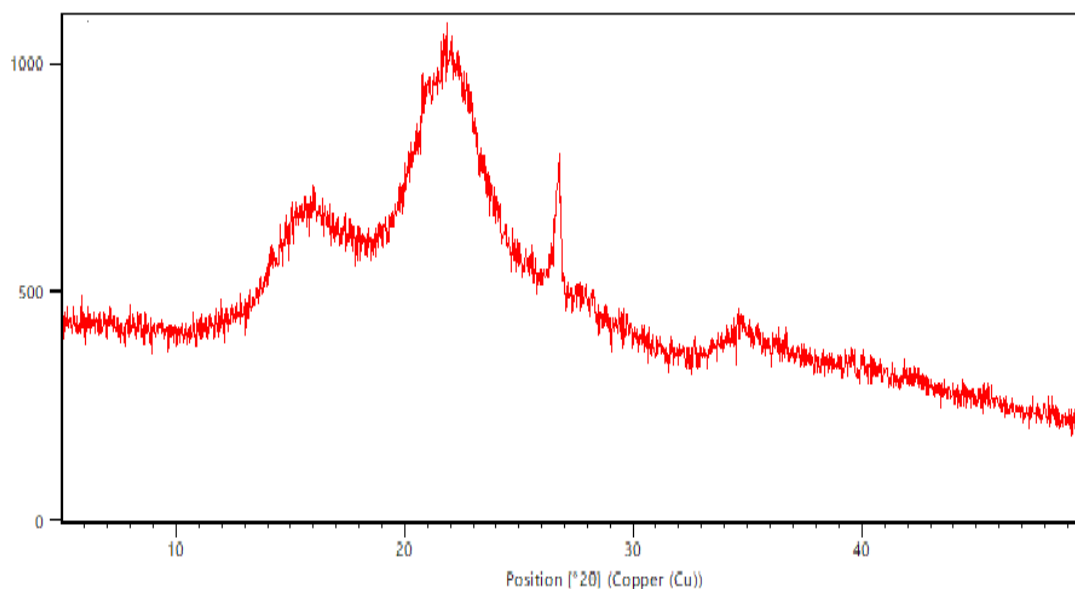


Figure 5.62: XRD spectra of Grafted banana peel gum

D. Scanning Electron Microscopy

The SEM studies of Banana Peel Gum (Figure 5.62) and Banana-g-acrylamide (Figure 5.63) showed a change in surface morphology after grafting. The more roughness and unevenness on the surface of grafted gum due to deposition of acrylamide was clearly visible.

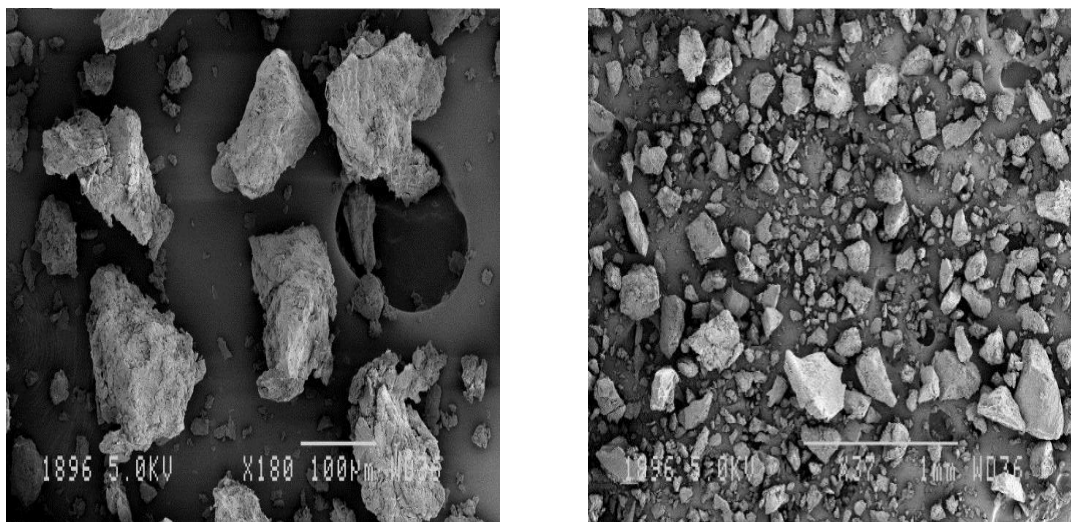


Figure 5.63: SEM images of pure gum banana peel

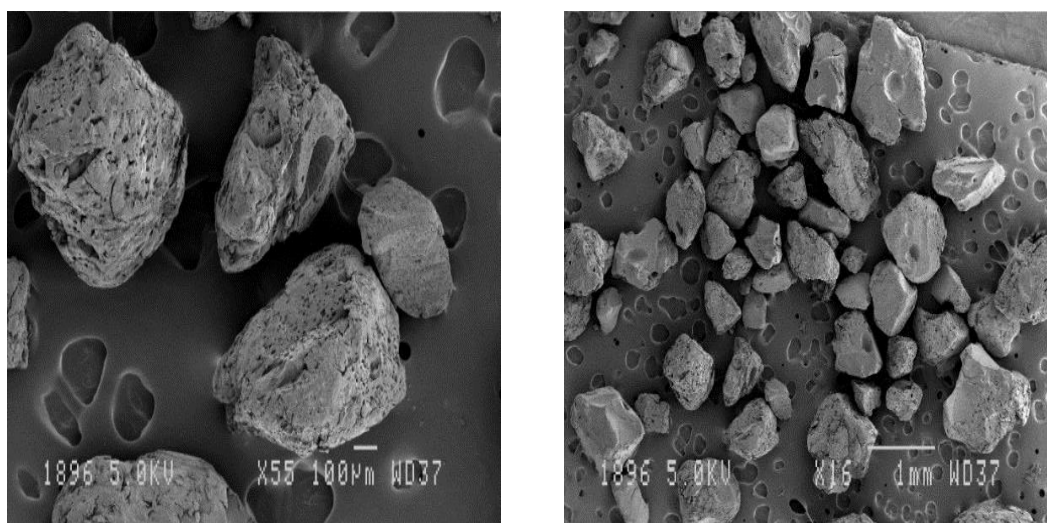


Figure 5.64: SEM images of grafted gum banana peel

5.3 SWELLING STUDIES

The swelling studies were performed for 2 h. The swelling abilities of ungrafted banana peel gum, ungrafted mastic gum, selected grafted banana peel and grafted mastic gums were carried out. All the samples were swelled and adsorbed water as shown by swelling curves as shown in figure 5.64. The results indicated that the grafted copolymers have better swelling capacity as compared to ungrafted copolymers. The enhanced swelling capacity of grafted copolymers may be mainly due to increase in number of polysaccharide chains and more porosity in structure of grafted copolymers as compared to ungrafted copolymers.

Table 5.29: Swelling capacity of ungrafted and grafted gums

S. No.	Time (minutes)	% Swelling			
		Ungrafted Mastic Gum	Grafted Mastic Gum	Ungrafted Banana Peel Gum	Grafted Banana Peel Gum
1	0	0	0	0	0
2	30	96	218.5	83	174
3	60	195	410	177.5	351
4	90	261	551	234	504
5	120	341	655	301	589
6	150	372.5	711	337.5	633
7	180	386.5	712.5	339.5	638.5
8	210	388.5	715	341	641.5
9	240	389.5	716	342.5	644

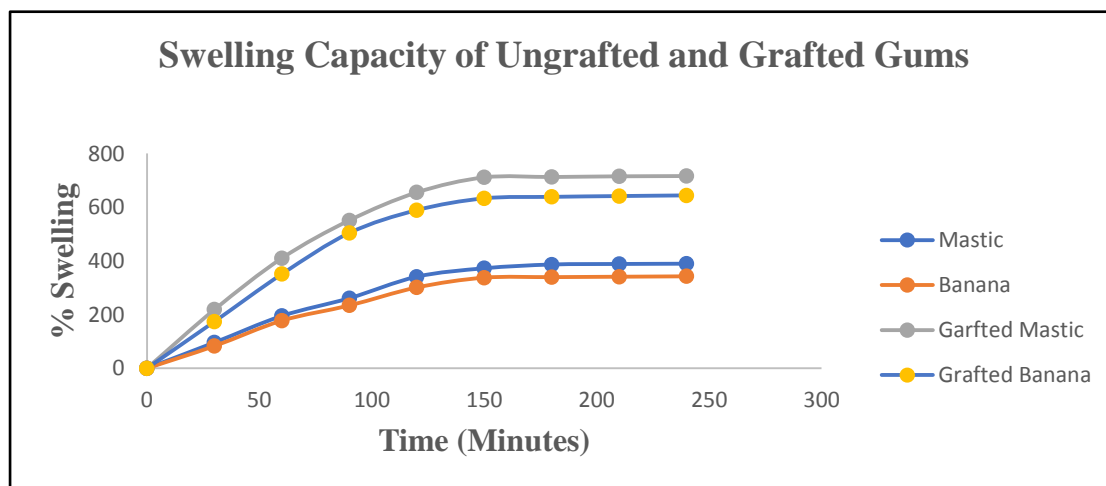


Figure 5.65: Swelling Capacity of Ungrafted and Grafted Gums

5.4 VISCOSITY MEASUREMENT

The viscosity measurement of ungrafted and grafted gums was carried out by using Brookfield viscometer at 32.7°C. The viscosities of grafted gums were found to be more than ungrafted gums. During grafting, acrylamide side chains attach with

polymer backbone and form a branched polymer network which leads to increase in viscosity.

Table 5.30: Viscosity of ungrafted and grafted gums

Viscosity (cps)			
Ungrafted Mastic Gum	Grafted Mastic Gum	Ungrafted Banana Peel Gum	Grafted Banana Peel Gum
621.2±1.1	1188.6±1.4	592.2±1.5	1012.4±2.1

5.5 COMPATIBILITY STUDIES OF UNGRAFTED AND GRAFTED MASTIC GUM WITH LAMIVUDINE

Compatibility study of physical mixture of drug with ungrafted mastic gum and grafted mastic gum along with excipients was performed to ensure that drug is not interacting with the polymer used under experimental conditions for four weeks. No interaction was seen between drug and polymer. The obtained IR spectra of polymer and drug mixtures showed all the substantial peaks of functional groups which present in the standard FT-IR spectra of lamivudine moiety.

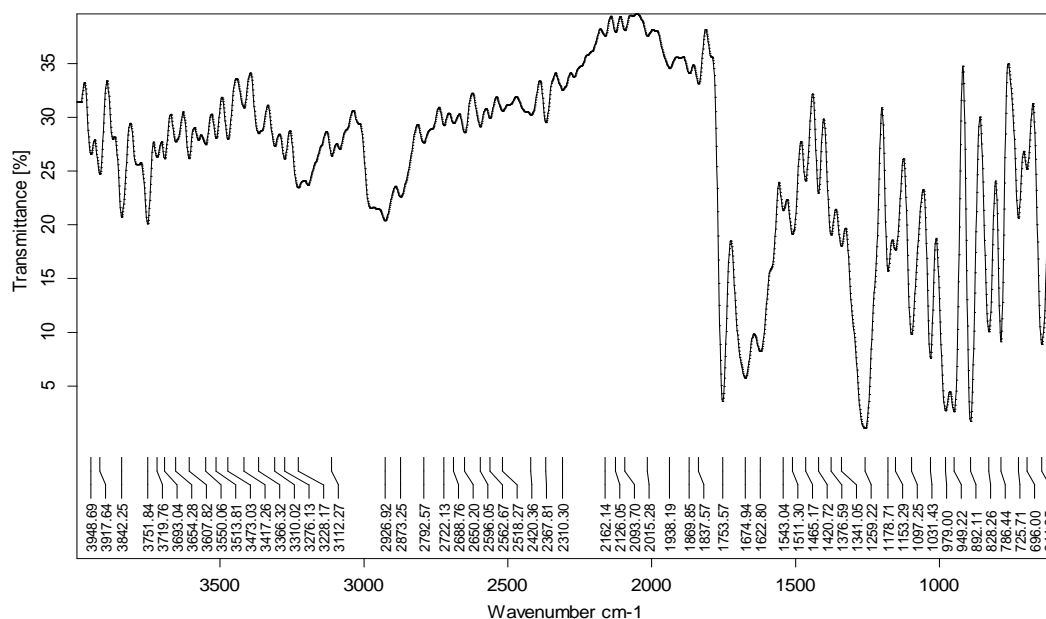


Figure 5.66: FTIR spectrum of physical mixture of Lamivudine and Gum Mastic

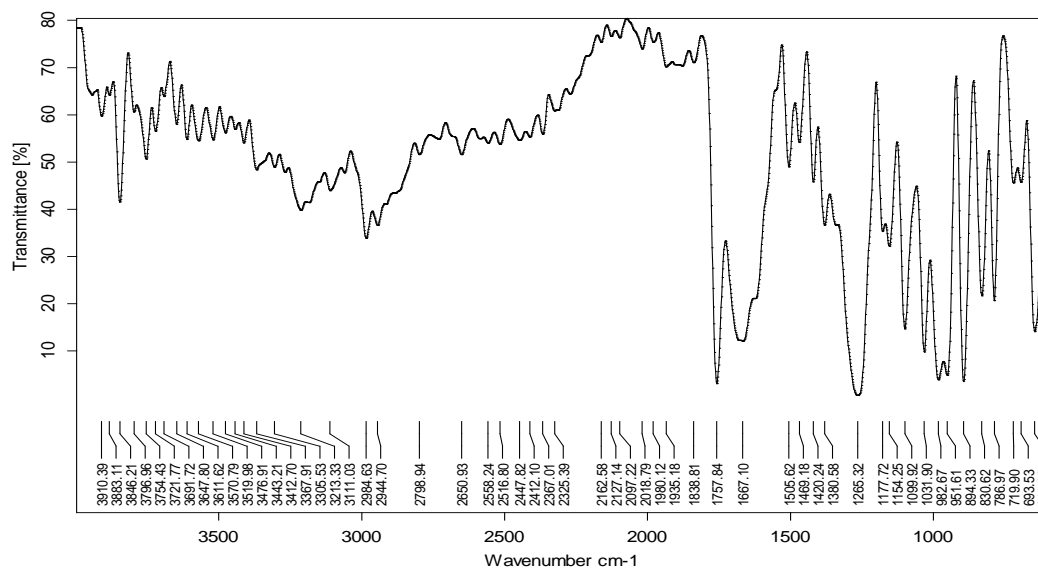


Figure 5.67: FTIR spectrum of physical mixture of Lamivudine and Grafted Gum Mastic

5.6 COMPATIBILITY STUDIES OF UNGRAFTED AND GRAFTED BANANA PEEL GUM WITH LAMIVUDINE

Compatibility study of physical mixture of drug with ungrafted banana peel gum and grafted banana peel gum along with excipients was performed to ensure that drug is not interacting with the polymer used under experimental conditions for four weeks. No interaction was seen between drug and polymer. The obtained IR spectra of polymer and drug mixtures showed all the substantial peaks of functional groups which present in the standard FT-IR spectra of lamivudine moiety.

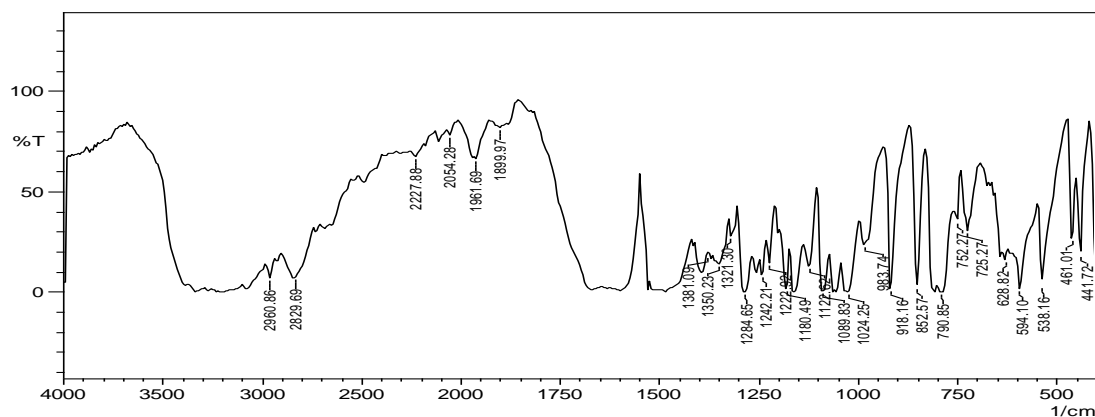


Figure 5.68: FTIR spectrum of physical mixture of Lamivudine and Banana Peel Gum

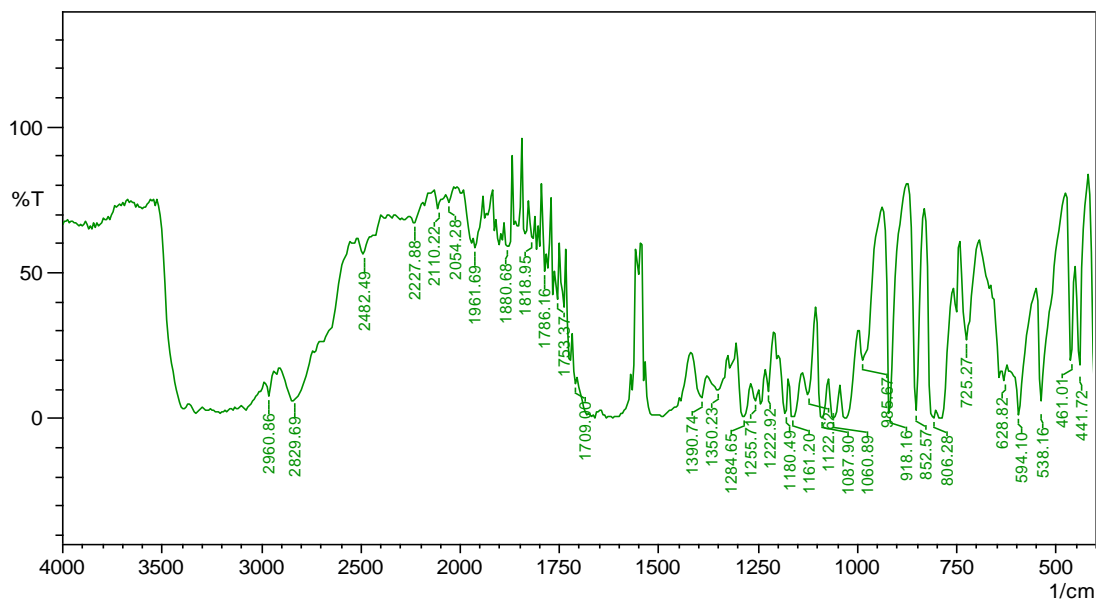


Figure 5.69: FTIR spectrum of physical mixture of Lamivudine and Grafted Banana Peel Gum

5.7 PREPARATION AND CHARACTERIZATION OF LAMIVUDINE MATRIX TABLETS USING GRAFTED AND UNGRAFTED MASTIC AND BANANA PEEL GUM

5.7.1 Preparation of blend of tablets

Various batches of lamivudine matrix tablet blend were prepared by using grafted mastic, grafted banana peel, ungrafted mastic and ungrafted banana peel by using lactose as diluent.

5.7.2 Precompression evaluation of blend of tablets

The various blends of tablets were evaluated for bulk density, tapped density, angle of repose, Carr's index and Hausner's ratio. The results for above evaluations were as following:

A. Angle of repose

The values of angle of repose were found in between 27.084 to 30.823 for ungrafted mastic gum formulations and 27.281 to 29.613 for grafted mastic gum formulations. The values of angle of repose were found in between 26.789 to 29.484 for ungrafted banana gum formulations and 27.130 to 30.222 for grafted banana peel gum

formulations. All the formulations were having the values of angle of repose less than 35. Thus, the blend was found to have good flowability.

B. Bulk Density

The bulk densities of all the powder blends were found in between 0.380 to 0.435 for ungrafted mastic gum formulations and 0.383 to 0.439 for grafted mastic gum formulations. The bulk densities of all the powder blends were found in between 0.395 to 0.423 for ungrafted banana peel gum formulations and 0.381 to 0.421 for grafted banana peel gum formulations as shown in table 5.31 and table 5.32 respectively.

C. Tapped Density

The tapped densities of all the powder blends were found in between 0.419 to 0.484 for ungrafted mastic gum formulations and 0.425 to 0.484 for grafted mastic gum formulations. The tapped densities of all the powder blends were found in between 0.446 to 0.481 for ungrafted banana peel gum formulations and 0.437 to 0.475 as shown in table 5.31 and table 5.32 respectively.

D. Carr's Consolidation Index

The Carr's index was found in between 9.278 to 12.209 for ungrafted mastic gum formulations and 8.475 to 11.596 for grafted mastic gum formulations. The Carr's index was found in between 11.397 to 12.750 for ungrafted banana peel gum formulations and 8.745 to 15.266 for grafted banana peel gum formulations as shown in table 5.31 and table 5.32 respectively. The values of carr's index were found as per the pharmacopoeial limits which confirmed the good flow of blend.

E. Hausner's Ratio

The Hausner's ratio was found in between 1.102 to 1.142 for mastic gum formulations and 1.093 to 1.131 for grafted mastic gum formulations. The Hausner's ratio was found in between 1.129 to 1.146 for ungrafted banana peel gum formulations and 1.099 to 1.181 for grafted banana peel gum formulations as shown in table 5.31 and table 5.32 respectively. The results confirmed the free-flowing properties of powder blend.

Table 5.31: Precompression parameters from formulation UMA1 to UMA5 and GMA1 to GMA5

Code	Angle of Repose (°)	Bulk Density (g/ml)	Tapped Density (g/ml)	Carr's Index (%)	Hausner's Ratio
UMA1	30.823±0.808	0.435±0.0063	0.482±0.0163	9.677±0.809	1.107±0.022
UMA2	29.541±0.989	0.404±0.0136	0.452±0.0103	10.705±1.204	1.121±0.041
UMA3	29.417±0.627	0.425±0.0069	0.484±0.0211	12.209±1.113	1.142±0.069
UMA4	28.509±1.745	0.427±0.0152	0.472±0.0188	9.485±0.866	1.105±0.011
UMA5	27.084±0.981	0.380±0.0048	0.419±0.0034	9.278±0.628	1.102±0.008
GMA1	29.613±1.187	0.402±0.0136	0.439±0.0136	8.475±0.559	1.093±0.007
GMA2	28.807±0.906	0.383±0.0103	0.425±0.0124	9.784±0.412	1.109±0.017
GMA3	29.326±1.419	0.439±0.0037	0.484±0.0078	9.257±1.154	1.102±0.026
GMA4	28.769±1.101	0.429±0.0123	0.469±0.0125	8.480±0.957	1.095±0.058
GMA5	27.281±1.546	0.386±0.0076	0.437±0.0131	11.596±1.364	1.131±0.017

n=3

Table 5.32: Precompression parameters from formulation UBA1 to UBA5 and GBA1 to GBA5

Code	Angle of Repose (°)	Bulk Density (g/ml)	Tapped Density (g/ml)	Carr's Index (%)	Hausner's Ratio
UBA1	29.484±1.510	0.395±0.0156	0.453±0.0238	12.750±1.206	1.146±0.016
UBA2	28.431±0.979	0.413±0.0172	0.467±0.0181	11.461±0.367	1.129±0.005
UBA3	28.312±1.041	0.397±0.0081	0.448±0.0067	11.424±1.535	1.130±0.033
UBA4	26.789±1.096	0.423±0.0060	0.481±0.0117	12.215±0.960	1.139±0.012
UBA5	27.761±1.104	0.395±0.0104	0.446±0.0100	11.397±0.530	1.129±0.007
GBA1	27.415±1.163	0.398±0.0111	0.437±0.0162	8.745±0.787	1.099±0.069
GBA2	28.165±0.809	0.421±0.0069	0.464±0.0042	9.339±0.008	1.103±0.664
GBA3	30.222±2.893	0.381±0.0028	0.450±0.0171	15.266±0.646	1.181±0.037
GBA4	27.130±1.939	0.399±0.0132	0.458±0.0210	12.857±1.156	1.148±0.015
GBA5	27.950±1.682	0.410±0.0195	0.475±0.0262	13.657±0.650	1.158±0.009

n=3

5.7.3 Evaluation of sustained release matrix tablets of lamivudine

A. Appearance

The tablets surface was observed visually. The conclusion of appearance test was that there were not any signs of tablets defects like capping, lamination and chipping.

Table 5.33: Post compression parameters from formulation UMA1 to UMA5 and GMA1 to GMA5

Code	Thickness (mm)	Hardness (kg/cm ²)	Friability (%)	Weight Variation (mg)	Drug Content (%)
UMA1	3.40±0.10	6.93±0.11	0.31	246.05±4.94	93.55±0.85
UMA2	3.43±0.11	7.17±0.29	0.26	249.90±4.92	93.28±0.85
UMA3	3.47±0.11	7.03±0.06	0.34	247.60±5.68	94.94±0.80
UMA4	3.30±0.20	7±0.36	0.32	249.35±6.13	95.86±0.85
UMA5	3.37±0.15	7.13±0.30	0.24	244.85±3.23	93.92±0.58
GMA1	3.40±0.17	6.93±0.15	0.42	250.70±5.29	96.60±0.57
GMA2	3.50±0.17	6.97±0.29	0.43	247.45±6.10	94.85±0.55
GMA3	3.37±0.11	6.90±0.26	0.49	252.75±5.60	96.69±0.89
GMA4	3.33±0.11	7.27±0.32	0.32	248.50±4.95	97.34±0.28
GMA5	3.23±0.11	7.07±0.32	0.45	246.60±4.60	95.59±0.89

n=3

Table 5.34: Post compression parameters from formulation UBA1 to UBA5 and GBA1 to GBA5

Code	Thickness (mm)	Hardness (kg/cm ²)	Friability (%)	Weight Variation (mg)	Drug Content (%)
UBA1	3.43±0.29	6.93±0.35	0.26	247.20±5.35	97.62±1.21
UBA2	3.17±0.15	7.00±0.17	0.42	251.85±6.03	97.52±1.39
UBA3	3.33±0.15	7.10±0.17	0.48	245.95±5.35	95.95±0.48
UBA4	3.43±0.25	7.23±0.15	0.38	248.75±6.02	95.12±1.11
UBA5	3.37±0.06	6.97±0.21	0.36	250.60±5.30	93.74±0.83
GBA1	3.27±0.06	7.37±0.06	0.20	253.25±6.07	96.23±0.83
GBA2	3.23±0.15	7.33±0.25	0.38	247.70±5.50	94.20±0.85
GBA3	3.33±0.23	6.90±0.36	0.31	249.05±5.52	95.59±0.58
GBA4	3.27±0.15	7.03±0.40	0.34	251.05±6.24	97.43±1.39
GBA5	3.43±0.32	7.30±0.26	0.44	248.50±5.30	95.22±1.12

B. Thickness of tablets

The thickness of tablet batches from UMA1 to UMA5 was found to be in between 3.30 to 3.47 mm and from GMA1 to GMA5 was found in between 3.23 to 3.50 mm as shown in table 5.33. Hardness from batches UBA1 to UBA5 was found in between 3.17 to 3.43 mm and from batches GBA1 to GBA5 was found in between 3.23 to 3.43 mm as shown in table 5.34.

C. Hardness of tablets

The hardness of tablet batches from UMA1 to UMA5 was found in between 6.93 to 7.17 kg/cm² and from GMA1 to GMA5 was found in between 6.90 to 7.27 kg/cm² as shown in table 5.33. Hardness from batches UBA1 to UBA5 was found in between 6.93 to 7.23 kg/cm² and from batches GBA1 to GBA5 was found in between 6.90 to 7.37 kg/cm² as shown in table 5.34. The good hardness indicates the good mechanical strength of tablets.

D. Friability of tablets

The % friability of tablet batches from UMA1 to UMA5 was found in between 0.24 % to 0.34 % and from GMA1 to GMA5 was found in between 0.32 % to 0.49 % as shown in table 5.33. Friability from batches UBA1 to UBA5 was found in between 0.26 % to 0.48 % and from batches GBA1 to GBA5 was found in between 0.20% to 0.44% as shown in table 5.34. The friability values indicate the good handling properties of sustained release matrix tablets.

E. Weight variation test

The total tablet weight was 250 mg and the pharmacopoeial limit for 250 mg tablet is 7.5%. All the batches of tablets confirmed that their weight variation test complied with pharmacopoeial limits.

F. Content Uniformity Test

The % drug content of tablet batches from UMA1 to UMA5 was found in between 93.28% to 95.86% and from GMA1 to GMA5 was found in between 94.85% to 97.34% as shown in table 5.33 and the % drug content of tablet batches from UBA1 to UBA5 was found in between 93.74 % to 97.62 % and from batches GBA1 to GBA5 was found in between 94.20% to 97.43% as shown in table 5.34. The drug content of all the batches of tablets was as per pharmacopoeial specifications.

G. In-vitro drug release studies

The *in-vitro* release studies were carried out by using USP type-II dissolution apparatus at 50 rpm. The test was performed by using 900 ml of 0.1 N HCl for first 2 h and phosphate buffer of pH 6.8 at a temperature of $37 \pm 0.5^\circ\text{C}$. The *in-vitro* release graphs for ungrafted mastic gum formulations (UMA1 to UMA5) and grafted mastic gum formulations (GMA1 to GMA5) are given in figure 5.70 and 5.71 respectively and the *in-vitro* release graph for ungrafted banana peel gum formulations (UBA1 to UBA5) and grafted banana peel gum formulations (GBA1 to GBA5) are given in figure 5.72 and 5.73 respectively.

The release from the matrix was largely dependent on the polymer swelling, drug diffusion and matrix erosion. The concentration of polymer in the matrix tablet was a key factor in sustaining the drug release. The variation in drug release was due to different types of polymers and different concentrations of polymer in all the twenty formulations.

The maximum drug released from formulations UMA1 to UMA5 containing ungrafted mastic gum at five concentration ratios to lamivudine (1:0.25, 1: 0.375, 1:0.5, 1:0.625, 1:0.75) were found to be in 8h, 8h, 9h, 9h and 10h respectively as shown in table 5.35

Table 5.35: In-vitro release data of ungrafted mastic gum tablets

Time	UMA1	UMA2	UMA3	UMA4	UMA5
0	0.00	0.00	0.00	0.00	0.00
0.5	5.03±0.13	4.57±0.13	4.15±0.10	4.24±0.20	3.44±0.18
1	7.01±0.11	6.33±0.10	5.67±0.17	5.27±0.17	4.57±0.11
2	9.68±0.14	8.51±0.27	7.68±0.13	6.71±0.20	6.44±0.23
3	22.46±0.47	19.01±0.16	17.41±0.12	15.54±0.12	14.65±0.10
4	36.44±0.98	32.04±0.85	31.00±0.19	29.75±0.19	27.84±0.25
5	49.72±0.38	47.83±0.81	42.20±0.87	40.18±0.04	38.79±0.12
6	65.07±2.16	61.00±0.75	56.53±0.91	54.79±0.36	51.84±0.81
7	88.96±1.9	85.01±2.49	75.66±1.87	72.76±1.57	67.15±1.30
8	98.73±1.87	96.65±0.95	88.75±1.08	84.81±0.95	78.78±1.25
9			97.27±0.95	95.40±1.3	90.21±1.57
10					97.06±1.30

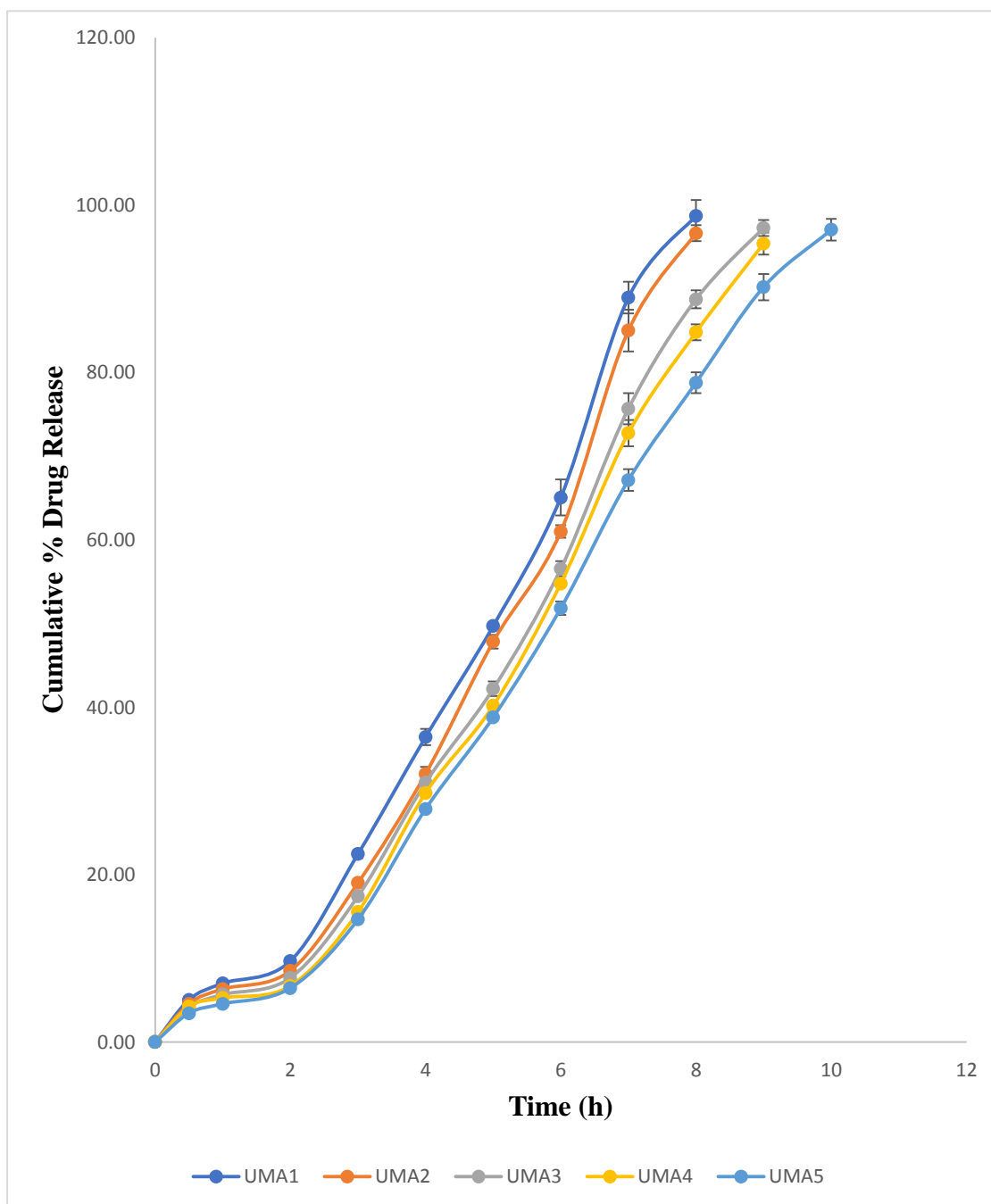


Figure 5.70: In-vitro release graph for ungrafted mastic gum formulations (UMA1 to UMA5)

Table 5.36: In-vitro release data of grafted mastic gum tablets

Time	GMA1	GMA2	GMA3	GMA4	GMA 5
0	0.00	0.00	0.00	0.00	0.00
0.5	3.51± 0.30	2.91± 0.20	2.47± 0.10	2.18± 0.07	1.15± 0.04
1	3.88±0.08	3.75±0.15	3.24± 0.18	2.78± 0.13	1.81± 0.17
2	5.12±0.23	4.92±0.17	4.96± 0.11	3.95± 0.15	3.29± 0.08
3	13.01±1.33	11.47± 0.07	9.58± 0.13	7.48± 0.10	6.96± 0.14
4	18.54±0.19	17.04± 0.22	14.92± 0.19	10.97± 0.10	8.81± 0.16
5	26.53±0.26	23.69± 0.54	19.91± 0.16	15.94± 0.19	12.47± 0.04
6	33.14±0.19	30.75± 1.00	25.23± 0.16	22.77± 0.16	19.55± 0.72
7	39.89± 0.64	36.94±0.65	32.29± 0.91	27.78± 0.26	23.23± 0.81
8	49.64±0.91	44.05±0.69	38.46± 0.97	30.77± 0.84	27.89±0.76
9	55.97±0.87	50.55± 0.91	43.38± 0.82	37.19± 0.78	34.76±0.84
10	65.07±1.65	58.63±1.3	49.93± 0.88	44.07± 0.90	38.71±0.95
11	75.25± 1.30	70.68±2.25	63.20± 1.25	57.89± 1.00	53.25±0.76
12	85.22± 2.19	81.07± 2.96	73.17± 2.49	68.60± 1.44	64.86±2.19
13	93.25± 1.3	89.38± 1.08	84.18± 1.30	79.61± 2.00	74.00±1.57
14		95.82± 2.52	88.75± 1.65	85.43± 2.00	80.86±2.59
15			93.12± 1.65	89.38± 1.87	86.68±1.90
16				94.16± 1.30	90.00±1.25
17					92.70±1.3
18					94.78±1.9

n=3

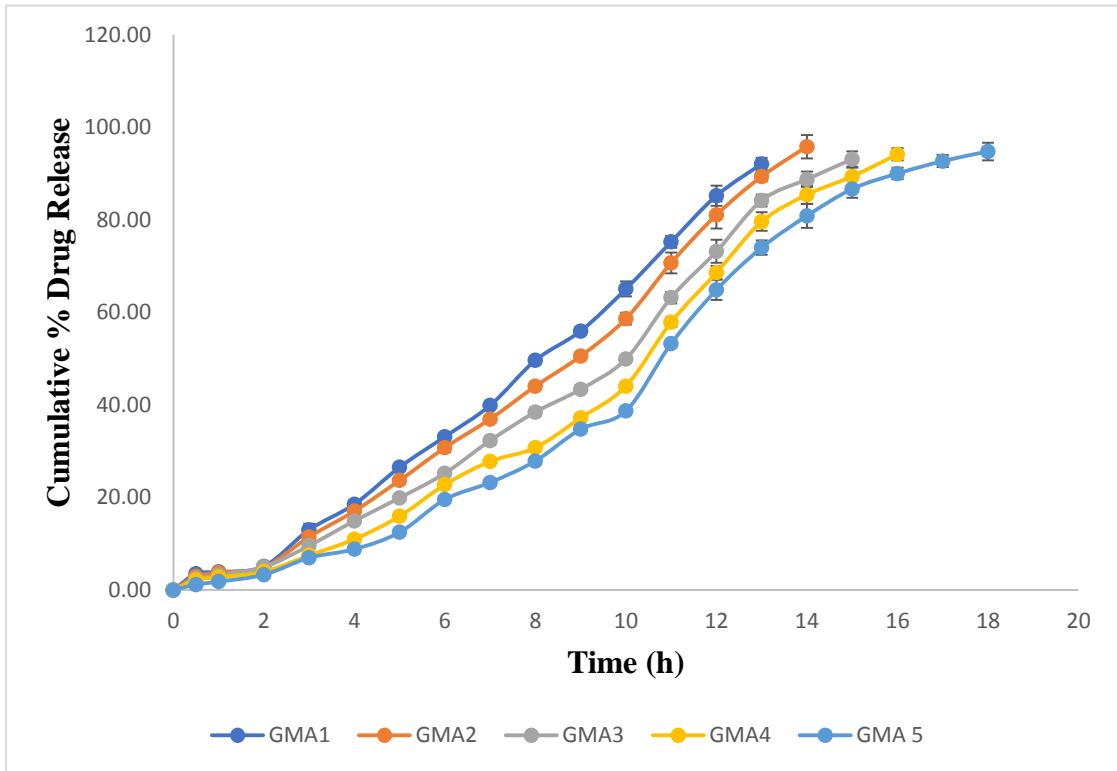


Figure 5.71: In-vitro release graph for grafted mastic gum formulations (GMA1 to GMA5)

Table 5.37: In-vitro release data of ungrafted banana peel gum tablets

Time	UBA1	UBA2	UBA3	UBA4	UBA5
0	0.00	0.00	0.00	0.00	0.00
0.5	7.10± 0.20	7.13± 0.27	6.88± 0.18	5.78± 0.04	5.43± 0.13
1	9.15± 0.15	8.96± 0.19	8.34± 0.11	7.63± 0.19	7.30± 0.23
2	12.33± 0.14	11.96± 0.15	10.92± 0.18	9.71± 0.28	8.60± 0.18
3	25.08± 0.31	23.90± 0.22	22.48± 0.69	20.16± 1.09	18.60± 0.76
4	40.72± 0.97	39.52± 1.09	37.23± 0.81	34.12± 0.93	31.94± 0.97
5	59.59± 0.84	56.62± 1.31	52.23± 0.72	49.95± 0.84	46.94± 0.82
6	80.86± 2.81	75.25± 2.52	70.89± 1.44	66.11± 1.57	60.65± 1.00
7	96.02± 1.57	92.08± 1.30	88.75± 1.25	83.98± 1.57	78.57± 2.36
8			98.10± 1.87	95.19± 0.95	92.66± 1.57

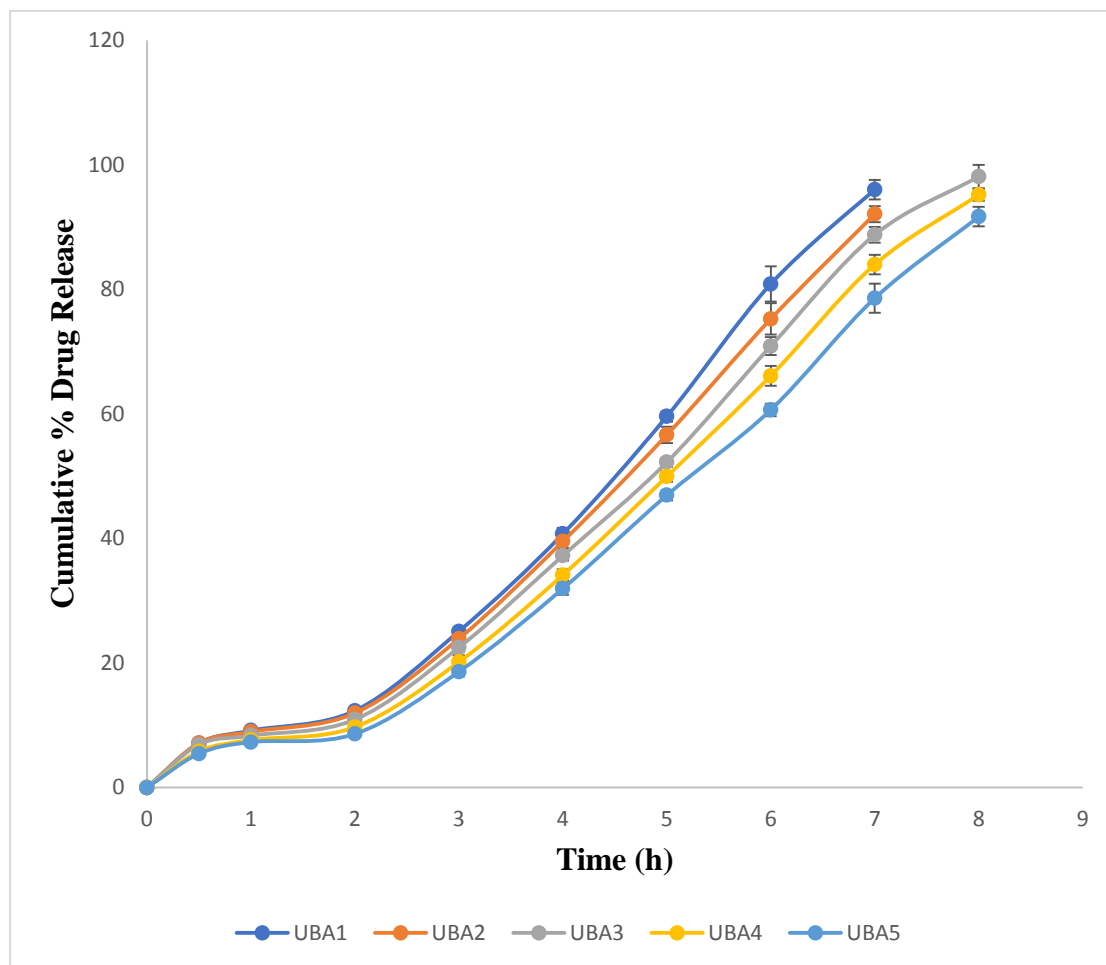


Figure 5.72: In-vitro release graph for ungrafted banana peel gum formulations (UBA1 to UBA5)

The maximum drug released from formulations GMA1 to GMA5 containing grafted mastic gum at five concentration ratios to lamivudine (1:0.25, 1: 0.375, 1:0.5, 1:0.625, 1:0.75) were found to be in 13h, 14h, 15h, 16h and 18h respectively as shown in table 5.36.

The maximum drug released from formulations UBA1 to UBA5 containing ungrafted banana peel gum at five concentration ratios to lamivudine (1:0.25, 1: 0.375, 1:0.5, 1:0.625, 1:0.75) were found to be in 7h, 7h, 8h, 8h and 8h respectively as shown in table 5.37.

Table 5.38: In-vitro release data of grafted banana peel gum tablets

Time	GBA1	GBA2	GBA3	GBA4	GBA5
0	0.00	0.00	0.00	0.00	0.00
0.5	5.03± 0.11	4.46± 0.10	3.31± 0.07	3.04± 0.18	1.65± 0.07
1	6.26± 0.08	5.54± 0.04	5.05± 0.10	4.48± 0.25	3.15± 0.17
2	11.74± 0.23	9.18± 0.08	8.27± 0.11	6.88± 0.13	5.56± 0.13
3	15.07± 0.75	12.82± 0.66	11.47± 0.81	9.85± 0.69	8.31± 0.76
4	21.05± 0.60	19.18± 0.97	17.39± 0.78	14.75± 0.87	13.65± 1.03
5	28.07± 0.78	25.37± 0.90	22.40± 0.75	20.24± 1.11	18.45± 0.86
6	33.29± 0.97	30.32± 0.69	28.40± 1.16	25.29± 0.72	23.56± 0.61
7	40.27± 0.86	37.15± 1.05	35.39± 0.97	31.58± 0.75	28.94± 0.88
8	46.02± 0.93	42.20± 0.91	40.06± 0.97	36.22± 0.69	33.99± 1.22
9	56.45± 1.26	50.20± 0.84	47.77± 0.94	42.64± 1.26	40.06± 0.97
10	68.39± 1.30	58.53± 1.07	52.80± 0.90	49.12± 0.85	46.65± 0.99
11	82.94± 1.44	70.47± 0.95	64.03± 1.30	60.65± 0.63	57.18± 1.04
12	94.83± 0.95	83.56± 1.9	80.03± 1.25	75.66± 1.25	72.55± 1.08
13		93.66± 2.36	90.21± 1.57	86.05± 2.19	82.31± 1.30
14			96.02± 0.95	93.53± 1.3	87.09± 1.80
15					94.16± 2.52

n=3

The maximum drug released from formulations GBA1 to GBA5 containing ungrafted banana peel gum at five concentration ratios to lamivudine (1:0.25, 1: 0.375, 1:0.5, 1:0.625, 1:0.75) were found to be in 12h, 13h, 14h, 14h and 15h respectively as shown in table 5.38.

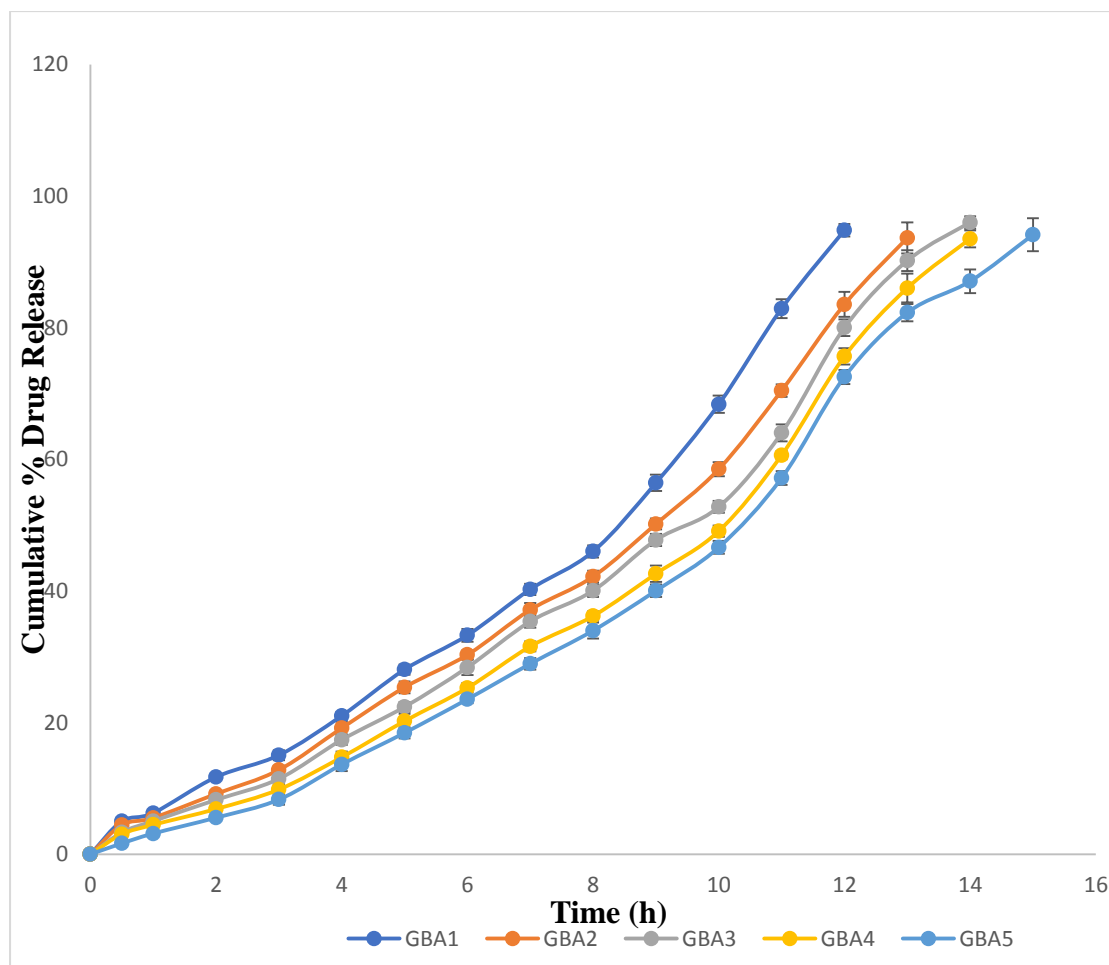


Figure 5.73: In-vitro release graph for grafted banana peel gum formulations (GBA1 to GBA5)

The chemical grafting is one of most effective method to improve the prolonged release. The grafted copolymer has been transformed into highly automatable matrices with hybrid properties. The grafted copolymer of mastic gum showed higher grafting efficiency as compared to banana peel gum. Grafted gums showed more branched network of polymers as compared to ungrafted gum. Branching of polymer plays an important role in prolonged release of drug. More branched polymer network has more prominent effect on prolonged release of drug. The swelling factor also confirmed the more prolonged release behaviour of lamivudine in case of grafted gums as compared to ungrafted gums. The grafted gums showed more swelling as compared to ungrafted gums. There will be formation of more thick gel barrier in case of grafted gums which increases the release retardant effect.

From the *in-vitro* release data it was observed that the high concentration of polymer should be retarding the drug release for longer period of time. It was also observed that the grafted polymer showed drug release for longer period of time as compared to ungrafted polymers.

The *in-vitro* release data also revealed that the both grafted and ungrafted mastic gum formulations were showed slower release rate for longer period of time as compared to grafted and ungrafted banana peel gum formulations.

The mean dissolution time was calculated for all the formulations as shown in following table

Table 5.39: Mean dissolution time for ungrafted and grafted gum tablets

Formulation Code	Mean Dissolution Time (h)
UMA1	4.66
UMA2	4.81
UMA3	5.15
UMA4	5.24
UMA5	5.58
GMA1	7.37
GMA2	8.04
GMA3	8.58
GMA4	9.29
GMA5	9.90
UBA1	4.12
UBA2	4.14
UBA3	4.52
UBA4	4.64
UBA5	4.73
GBA1	6.98
GBA2	7.64
GBA3	8.25
GBA4	8.54
GBA5	8.96

The mean dissolution time confirmed the improved sustained release ability of grafted polymer tablets as compared to ungrafted polymer tablets. From the above study, the formulation GMA5 was concluded as the best formulation among all the twenty formulations of this series. Hence the formulation GMA5 was selected for further stability study.

5.8 RELEASE KINETICS

The drug release data was used to perform the drug release kinetics using Zero order, First order, Higuchi and Koresmeyer Peppas models. The best formulation from all the formulations was selected (GMA5) on the basis of cumulative drug release. The best formulation was further used for application of release kinetics. The regression coefficient values obtained from all four models were compared and best fit model was selected. The results obtained were shown in figures 5.74-5.77.

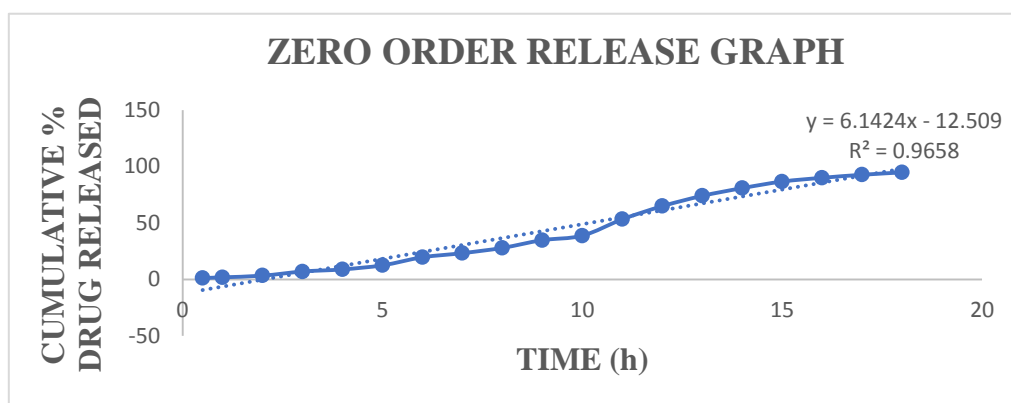


Figure 5.74: Zero order release graph for grafted mastic gum (GMA5)

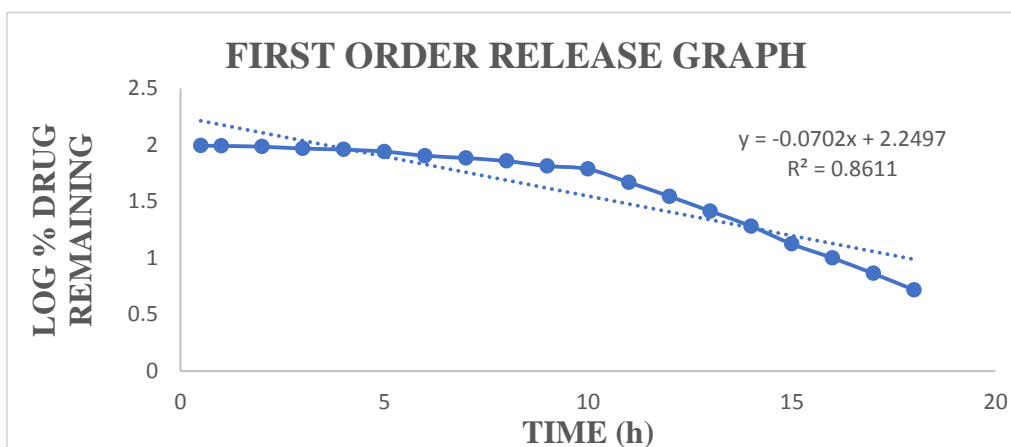


Figure 5.75: First order release graph for grafted mastic gum (GMA5)

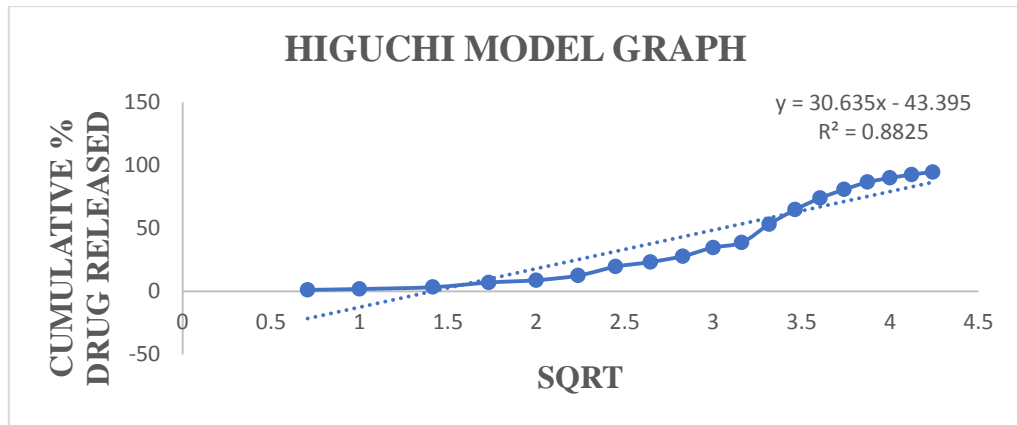


Figure 5.76: Higuchi model graph for grafted mastic gum (GMA5)

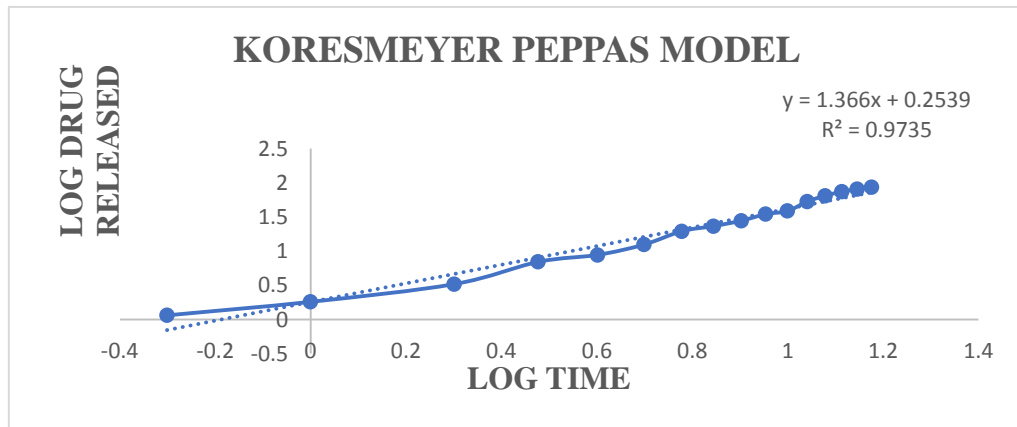


Figure 5.77: Koresmeyer Peppas model graph for grafted mastic gum (GMA5)

Table 5.40: Different kinetic models for grafted mastic gum (GMA5) tablet

Formulation Code	Zero Order	First Order	Higuchi Model	Koresmeyer Peppas model	
	R ²	R ²	R ²	R ²	n
GMA5	0.9658	0.8611	0.8825	0.9735	1.366

From n value more than 1, it was revealed that the mechanism of drug release was a super case-II transport indicating the drug release rate does not change over time and the release is characterized by zero order. The mechanism of the drug release is dominated by the erosion and swelling of the polymer.

5.9 STABILITY STUDIES

The selected formulation GMA5 was exposed to storage conditions as per ICH guidelines. The temperature of storage was $40^{\circ}\text{C} \pm 2^{\circ}\text{C}$ at $75\% \pm 5\%$ of relative humidity. The effect of temperature and aging on hardness, drug content, friability and in-vitro release factors were observed by taking out samples at definite intervals of time as shown in following table:

Table 5.41: Organoleptic property analysis data of sample (GMA5 tablet) kept for different time intervals

S. No.	Time Interval	Colour	Odour
1	Initial month (zero month)	Brown	Odourless
2	First month	Brown	Odourless
3	Second month	Brown	Odourless
4	Third month	Brown	Odourless

Table 5.42: Drug content, Hardness and friability of sample (GMA5) kept for different time intervals

S. No.	Time Interval	Hardness (Kg)	Drug content (%)	Friability (%)
1	Initial month (zero month)	7.30±0.26	95.22±1.12	0.44
2	First month	7.23±0.21	94.94±0.97	0.44
3	Second month	7.20±0.20	94.48±0.85	0.50
4	Third month	7.13±0.21	94.02±0.55	0.54

n=3

Table 5.43: Drug release data of sample (GMA5) kept for different time intervals

Time (h)	Cumulative % Drug Released			
	Zero Month	1 st Month	2 nd Month	3 rd Month
0	0.00	0.00	0.00	0.00
0.5	0.86±0.07	1.37±0.10	1.48±0.36	1.32±0.23
1	1.43±0.14	1.85±0.13	2.12±0.26	1.90±0.38
2	3.04±0.29	3.49±0.23	3.79±0.31	3.95±0.39
3	6.38±0.47	6.51±0.25	7.05±0.65	7.67±0.50
4	8.25±0.38	9.17±0.50	9.91±0.52	9.56±0.65
5	11.31±0.62	13.07±1.56	14.98±1.00	15.44±1.12
6	18.91±0.63	20.01±0.93	21.26±0.89	21.01±0.81
7	21.42±0.91	22.52±1.13	24.37±1.68	25.14±1.29
8	26.78±0.63	27.39±1.24	29.88±1.00	31.42±1.25
9	35.47±0.42	36.30±0.97	39.00±1.70	41.18±1.14
10	40.08±1.73	42.16±1.71	44.17±1.50	46.08±1.55
11	54.29±0.97	55.23±0.75	54.29±1.02	53.15±0.58
12	66.52±1.57	65.69±1.08	67.77±0.95	65.90±1.80
13	76.29±2.49	73.80±3.30	75.04±1.65	74.63±2.36
14	82.31±1.90	78.37±1.90	80.03±1.25	78.78±1.25
15	88.96±2.59	86.68±1.90	88.34±3.43	86.05±3.20
16	91.25±1.08	92.29±1.30	91.66±2.59	92.29±1.57
17	94.16±0.95	94.57±1.57	92.70±1.43	93.74±1.65
18	95.61±1.25	94.99±2.25	93.74±4.36	94.99±2.25

n=3

Table 5.44: Values of difference factor (f1) and similarity factor (f2) for drug release of sample (GMA5) kept for different time intervals

Factor	1st Month	2nd Month	3rd Month
f1	2.73	4.03	5.18
f2	87.23	81.47	75.82

The value of f1 must be in between 0-15 (closer to zero) and value of f2 must be in between 50-100 (closer to 100). The values of difference factor (f1) were found to be 2.73, 4.03, 5.18 after 1st month, 2nd month and 3rd month of stability studies. The values of similarity factor (f2) were found to be 87.23, 81.47, 75.82 respectively. The difference factor (f1) gives the percentage difference between two curves at each reading time and is a measure of the relative error between the two curves. On the other hand, the similarity factor (f2) is the most appropriate method to compare release profiles. The values of both the factors were found to be within acceptance limits.

From the above studies, there was no significance differences between the evaluated data from initial and after stability studies and all the values were found in worth accepting limits. The best formulation showed adequate physical stability at 40°C ± 2°C at 75% ± 5% relative humidity.

6.1 SUMMARY

The goal of this study was to synthesise and analyse graft copolymers of acrylamide with gum Mastic, as well as acrylamide with banana peel gum. Furthermore, by manufacturing sustained release matrix tablets with Lamivudine as the model drug, the in vitro release behaviour of graft co-polymer was compared to that of ungrafted gum.

The complete research work was presented in seven chapters such as introduction, literature review, aim and objective, material and methods, result and discussion, summary and conclusion.

Physical and chemical characteristics of drug molecules were determined through preformulation studies. Identity and purity of drug molecule was confirmed by UV spectrum, FT-IR spectrum and melting point. Log P value of partition coefficient confirmed its hydrophilic nature. The results of preformulation studies suggested that Lamivudine was pure and good in quality for the formulation development. Estimation of Lamivudine was done by UV-Visible spectroscopy. The calibration curve of Lamivudine was found to be linearly regressed. Solubility of Lamivudine was determined by quantitative method. Lamivudine was found to be soluble in water and phosphate buffer pH 6.8.

Acrylamide grafted Mastic gum and banana peel gum were prepared by Microwave assisted method. In the preparation of grafted gums, following steps were taken

- Preparation of preliminary trial batches
- Optimization of grafted gums
- Preparation of optimized graft copolymers
- Evaluation of optimized graft copolymers

The box behnken design was used to optimise acrylamide grafting on Mastic and banana peel gums where acrylamide amount, temperature and initiator concentration were used as independent variables and % yield, % grafting and grafting efficiency were used as dependent variables. Batch having acrylamide concentration (1.4 g), microwave temperature (60%) and initiator amount (50 mg) was selected as

optimized batch of mastic gum. Batch having acrylamide concentration (1.4 g), microwave temperature (60⁰C) and initiator amount (50 mg) was selected as optimized batch of banana peel gum.

Optimized grafted copolymer was further characterized by DSC, SEM, FT-IR and XRD which confirmed the formation of graft copolymer.

DSC graph of mastic gum, acrylamide and grafted mastic gum suggested confirmation of grafting of acrylamide on surface of mastic gum. Similarly, DSC graph of banana peel gum, acrylamide and grafted banana gum suggested confirmation of grafting of acrylamide on surface of banana gum.

FTIR spectra of acrylamide grafted mastic and banana peel gum displayed a wide absorption band due to overlapping of OH stretch band of mastic and banana peel gum with NH stretch band of acrylamide.

The XRD spectra revealed that the mastic gum and banana peel gum exhibit amorphous nature, as no characteristic peaks were observed. The diffractogram of acrylamide, on the other hand, revealed the crystalline nature of the compound, with prominent distinctive peaks. The diffraction spectra of acrylamide grafted banana peel gum and grafted mastic gum showed the frequent peaks which validated the graft copolymer's creation.

The grafting of acrylamide onto the surface of mastic and banana gums was revealed by SEM pictures of grafted copolymer. It was confirmed by change in shape of grafted gums as well as change in surface imperfections.

The lamivudine matrix tablets were made by combining the drug, polymer, diluent, and lubricant and compressing them.

The randomly selected tablets from each batch of grafted and ungrafted gums were evaluated for weight variation, hardness, friability and drug content. All the parameters were found within specified limits.

In-vitro release studies of all the batches were carried out in 0.1 N HCl for first two hours and further in phosphate buffer pH 6.8. From in-vitro release studies it was found that, in case of ungrafted batch 97.06% drug was released in 10 h in case of

mastic gum tablets and 91.66% drug was released in 8 h in case of banana peel gum tablets. In case of grafted batch 94.78% drug was released in 18 h in case of grafted mastic gum tablets and 94.16% drug was released in 15 h case of grafted banana peel gum tablets. The results revealed that grafting formed sustained release system.

The results also revealed that the grafted mastic gum found to be more suitable candidate as compared to grafted banana peel gum for sustained release effect.

The data obtained from dissolution profile was fitted into various mathematical models and data was found fit best into Koresemyer-Peppas model, which suggests that mechanism of drug release is mainly due to polymer disentanglement and erosion.

The stability studies were performed at $40\pm 2^{\circ}\text{C}/75\pm 5\%$ RH for 3 months to assess the stability of batch GMA5. The results of stability studies have shown that no significant changes were observed in drug content and friability. Hence, the selected batch was concluded to be a stable formulation.

6.2 CONCLUSION

Under microwave irradiation, the grafting technique can be a strong strategy for developing useful derivatives with tailor-made features by manipulating natural polysaccharides with fine control over the graft polymer. The characteristics of microwave graft polysaccharides are usually superior to those of traditionally synthesised derivatives.

Overall, contemporary breakthroughs in the field of polysaccharide grafting under microwaves have raised awareness of the possibility of getting improved performance materials through such methods. The microwave technology, which is considerably easier, faster, cheaper, and safer than the existing older methods, helps to achieve the goal of cleaner technologies without sacrificing efficiency or production. The sustained release matrix tablets of lamivudine formulation system by grafted gum include the drug delivery system that achieves slow and extended release of the drug over an extended period of time.

With this study, it is clear that this graft copolymer might be well exploited globally as a potential carrier for drug delivery system. Overall, it may be concluded that the

current advancements in the area of polysaccharide grafting under microwaves have generated awareness on obtaining higher performance materials through such processes. Without having to compromise on efficiency or yield, the microwave methodology works towards achieving the goal of cleaner technologies as it is much simpler, cheaper, quicker and safer than the prevailing traditional methods.

7.0 REFERENCES

1. Bhosale, R. R., Gangadharappa, H. V., Moin, A., et al., *A review on grafting modification of polysaccharides by microwave irradiation- distinctive practice for application in drug delivery*. Int J Curr Pharm Res, 2015. **6**(1): p. 8-17.
2. Bhardwaj, T. R., Kanwar, M., Lal, R., et al., *Natural gums and modified natural gums as sustained release carriers*. Drug Dev Ind Pharm, 2000. **26**: p. 1025-1038.
3. Sanghi, R., Bhattacharya, B., Singh, V., *Cassia angustifolia seed gum as an effective natural coagulant for decolourisation of dye solutions*. Green Chem, 2002. **4**: p. 252–254.
4. Sanghi, R., Bhattacharya, B., *Comparative evaluation of natural polyelectrolytes psyllium and chitosan for decolorization of dye solutions*. Water Qual Res J Can, 2005. **40**(1): p. 97-101.
5. Wang, W. B., Wang, A.Q., *Preparation, swelling and water retention properties of crosslinked super sorbent hydrogels based on guar gum*. Adv Mater Res, 2010. **96**: p. 177–182.
6. Gupta, S., Sharma, P., Soni, P.L., *Carboxymethylation of Cassia occidentalis seed gum*. J Appl Polym Sci, 2004. **94**: p. 1606–1611.
7. Edgar, K. J., Buchanan, C. M., Debenham, J. S., et al., *Advances in cellulose ester performance and application*. Prog Polym Sci, 2001. **26**: p. 1605–1688.
8. Sand, A., Yadav, M., Mishra, D. K., et al., *Modification of alginate by grafting of N-vinyl-2-pyrrolidone and studies of physicochemical properties in terms of swelling capacity, metal-ion uptake and flocculation*. Carbohydr Polym, 2010. **80**: p. 1147–1154.
9. Ramaprasad, A. T., Rao, V., Sanjeev, G., et al., *Grafting of polyaniline onto the radiation crosslinked chitosan*. Synth Met, 2009. **159**: p. 1983–1990.
10. Crescenzi, V., Dentini, M., Risica, D., et al., *C(6)-oxidation followed by C(5)-epimerization of guar gum studied by high field NMR*. Biomacromolecules, 2004. **5**: p. 537–546.

-
11. Galanos, C., Luderitz, O., Himmelspach, K., *The partial acid hydrolysis of polysaccharides: a new method for obtaining oligosaccharides in high yield.* Eur J Biochem, 1969. **8**: p. 332–336.
 12. Shah, N., Shah, T., Amin, A., *Polysaccharides: a targeting strategy for colonic drug delivery.* Expert Opin Drug Deliv, 2011. **8(6)**: p. 779-796.
 13. Sinha, V. R., Kumria, R., *Polysaccharides in colon-specific drug delivery.* Int J Pharm, 2001. **224**: p. 19-38.
 14. Rana, V., Rai, P., Tiwary, A. K., et al., *Modified gums: Approaches and applications in drug delivery.* Carbohydr Polym, 2011. **83**: p. 1031–1047.
 15. Hoogenboom, R., Schubert, U. S., *Microwave-Assisted Polymer Synthesis: Recent Developments in a Rapidly Expanding Field of Research.* Macromol Rapid Commun, 2007. **28**: p. 368–386.
 16. Wiesbrock, F., Hoogenboom, R., Schubert, U. S., *Microwave-Assisted Polymer Synthesis: State-of-the-Art and Future Perspectives.* Macromol Rapid Commun, 2004. **25**: p. 1739-1764.
 17. Sharma, A. K., Mishra, A. K., *Microwave assisted synthesis of chitosan-graft styrene for efficient Cr (VI).* Adv Mat Lett, 2010. **1(1)**: p. 59-66.
 18. Mahdavinia, G. R., Zohuriaan-Mehr, M. J., Pourjavadi, A., *Modified chitosan III, superabsorbency, salt- and pH-sensitivity of smart ampholytic hydrogels from chitosan-g-PAN.* Polym Adv Technol, 2004. **15**: p. 173-180.
 19. Tizzotti, M., Charlot, A., Fleury, E., et al., *Modification of polysaccharides through controlled/living radical polymerization grafting—towards the generation of high-performance hybrids.* Macromol Rapid Commun, 2010. **31**: p. 1751–72
 20. Macchione, M. A., Bilione, C., Strumia, M. *Design, Synthesis and Architectures of Hybrid Nanomaterials for Therapy and Diagnosis Applications.* Polymers, 2018. **10**: p. 1–34.
 21. Zhang, L. M., Tan, Y. B., Huang, S. J., et al., *Water-soluble ampholytic grafted polysaccharides. 1. grafting of the zwitterionic monomer 2-(2-*
-

-
- methacryloethyltrimethylammonio) ethanoate onto hydroxyethyl cellulose. J Polym Sci A Polym Chem, 2000. 37: p. 1247–1260.*
22. Maity, N., Dawn, A., *Conducting polymer grafting: recent and key developments. Polymers, 2020. 12: p. 1-23.*
 23. Singh, B., Sharma, N., *Development of novel hydrogels by functionalization of sterculia gum for use in anti-ulcer drug delivery. Carbohydr Polym, 2008. 74: p. 489-497.*
 24. da Silva, D. A., de Paula, R. C. M., Feitosa, J. P. A., *Graft copolymerisation of acrylamide onto cashew gum. Eur polym j, 2007. 43: p. 2620-2629.*
 25. Mishra, A., Pal, S., *Polyacrylonitrile-grafted Okra mucilage: A renewable reservoir to polymeric materials. Carbohydr Polym, 2007. 68: p. 95-100.*
 26. Mishra, A., Malhotra, A.V., *Graft copolymers of xyloglucan and methyl methacrylate. Carbohydr Polym, 2012. 87: p. 1899-1904.*
 27. Hayes, B. L., *Recent advances in microwave assisted synthesis. Aldrichimica acta, 2004. 37(2): p. 66-76.*
 28. Galema, S. A., *Microwave chemistry. Chem Soc Rev, 1997. 26: p. 233-238.*
 29. Zhang, X., Hayward, D. O., Mingos, D. M. P., *Apparent equilibrium shifts and hot-spot formation for catalytic reactions induced by microwave dielectric heating. Chem Commun, 1999. 11: p. 975-996.*
 30. Kappe, C. O., *Controlled microwave heating in modern organic synthesis. Angew Chem, 2004. 43: p. 6250-6284.*
 31. Gabriel, C., Gabriel, S., Grant, E. H., et al., *Dielectric parameters relevant to microwave dielectric heating. Chem Soc Rev, 1998. 27: p. 213-223.*
 32. Lidstrom, P., Tierney, J., Wathey, B., et al., *Microwave assisted organic synthesis—a review. Tetrahedron, 2001. 57: p. 9225-9283.*
 33. Mingos, D. M. P., Baghurst, D. R., *Applications of microwave dielectric heating effects to synthetic problems in chemistry. Chem Soc Rev, 1991. 20: p. 1-47.*
-

-
34. Kharlamova, T. V., *Characteristics of microwaves, some aspects theory of microwave heating and the field of application of microwaves in organic chemistry and chemistry of natural compounds*. Khim Zh Kaz, 2018. 3(63): p. 37-53.
 35. Singh, V., Tiwari, A., Pandey, S., et al., *Peroxydisulfate initiated synthesis of potato starch-graft-poly(acrylonitrile) under microwave irradiation*. Express Polym Lett, 2007. 1: 51-58.
 36. Tiwari, A., Singh, V., *Microwave-induced synthesis of electrical conducting gum acacia-graft-polyaniline*. Carbohydr Polym, 2008. **74**: p. 427–434.
 37. Prasad K, Mehta G, Meena R, et al., *Hydrogel-Forming Agar-graft-PVP and k-Carrageenan graft-PVP Blends: Rapid Synthesis and Characterization*. J Appl Polym Sci, 2006. **102**: p. 3654–3663.
 38. Sen, G., Singh, R. P., Pal, S., *Microwave-initiated synthesis of polyacrylamide grafted sodium alginate: synthesis and characterization*. J Appl Polym Sci, 2010. **115**: p. 63-71.
 39. Sen, G., Pal, S., *Microwave initiated synthesis of polyacrylamide grafted carboxymethylstarch (CMS-g-PAM): application as a novel matrix for sustained drug release*. Int J Biol Macromol, 2009. **45**: p. 48-55.
 40. Singh, V., Tiwari, A., Tripathi, D. N., et al., *Microwave assisted synthesis of guar-g-polyacrylamide*. Carbohydr Polym, 2004. **58**: p. 1-6.
 41. Sosnik, A., Gotelli, G., Abraham, G. A., *Microwave-assisted polymer synthesis (MAPS) as a tool in biomaterials science: How new and how powerful*. Prog Polym Sci, 2011. **36**: p. 1050–1078.
 42. Singh, V., Kumar, P., Sanghi, R., *Use of microwave irradiation in the grafting modification of the polysaccharides –A review*. Prog Polym Sci, 2012. **37**: p. 340-364.
 43. Singh, I., Rani, P., Kumar, P., *Microwave assisted grafting of gums and extraction of natural materials*. Mini-Rev Med Chem, 2017. **17(16)**: p. 1573-1582.
-

-
44. Arsalani, N., Zare, P., Namazi, H., *Solvent free microwave assisted preparation of new telechelic polymers based on poly(ethylene glycol)*. *Express polym lett*, 2009. **3(7)**: p. 429-436.
 45. Dondi, D., Buttafava, A., Stagnaro, P., et al., *The radiation-induced grafting of polybutadiene onto silica*. *Radiat phys chem*, 2009. **78**: p. 525-530.
 46. Thostenson, E. T., Chou, T. W., *Microwave processing: fundamentals and applications*. *Composites, Part-A*, 1999. **30**: p. 1055-1071.
 47. White, J. B., Hausner, S. H., Carpenter, R. D., et al., *Optimization of the solid-phase synthesis of [¹⁸F] radiolabeled peptides for positron emission tomography*. *Appl radiat isot*, 2012. **70**: p. 2720-2720.
 48. Schanche, J. S., *Microwave synthesis solutions from Personal Chemistry*. *Mol Diversity*, 2003. **7**: p. 293-300.
 49. Bharaniraja, B., Kumar, K. J., Prasad, C. M., et al., *Modified Katira Gum for Colon Targeted Drug Delivery*. *J appl polym sci*, 2011. **119**: p. 2644-2651.
 50. Mehra, S., Nisar, S., Chauhan, S., et al., *Soy Protein-Based Hydrogel under Microwave-Induced Grafting of Acrylic Acid and 4-(4-Hydroxyphenyl)butanoic Acid: A Potential Vehicle for Controlled Drug Delivery in Oral Cavity Bacterial Infections*. *ACS omega*, 2020. **5**: p. 21610-21622.
 51. Shailaja, T., Latha, A., Sasibhusan, P., et al., *A novel bioadhesive polymer: grafting of tamarind seed polysaccharide and evaluation of its use in buccal delivery of metoprolol succinate*. *Pharm lett*, 2012. **4(2)**: p. 487-508.
 52. Fu, H., Xie, L., Dou, D., et al., *Storage stability and compatibility of asphalt binder modified by SBS graft copolymer*. *Constr build mater*, 2007. **21**: p. 1528-1533.
 53. Rani, P., Mishra, S., Sen, G., *Microwave based synthesis of polymethyl methacrylate grafted sodium alginate: its application as flocculant*. *Carbohydr Polym*, 2013. **91**: p. 686-692.
 54. Xing, J., Deng, L., Li, J., et al., *Amphiphilic poly{[α -maleic anhydride- ω -methoxy poly(ethylene glycol)]-co-(ethyl cyanoacrylate)} graft copolymer*
-

-
- nanoparticles as carriers for transdermal drug delivery*. Int j nanomed, 2009. **4**: p. 227-232.
55. Homayun, B., Lin, X., Choi, H. J., *Challenges and Recent Progress in Oral Drug Delivery Systems for Biopharmaceuticals*. Pharmaceutics, 2019. **11(129)**: p. 1-29.
56. Tiwari, S., Batra, N., *Oral Drug Delivery System: A Review*. Am j life sci res, 2014. **2(1)**: p. 27-35.
57. Mandhar, P., Joshi, G., *Development of Sustained Release Drug Delivery System: A Review*. Asian Pac J Health Sci, 2015. **2(1)**: p. 179-185.
58. Khan, G. M., *Controlled release oral dosage forms: some recent advances in matrix type drug delivery systems*. The Sciences, 2001. **1(5)**: p. 350-354.
59. Kube, R. S., Kadam, V. S., Shendarkar, G. R., et al., *Sustained release drug delivery system: review*. Indian J Res Pharm Biotechnol, 2015. **3(3)**: p. 246-251.
60. Mishra, S., *Sustained Release Oral Drug Delivery System: A Concise Review*. Int J Pharm Sci Rev Res, 2019. **54(1)**: p. 5-15.
61. Bose, S., Kaur, A., Sharma, S. K., *A review on advances of sustained drug delivery systems*. Int Res J Pharm, 2013. **4(6)**: p. 1-5.
62. Mali, R. R., Goel, V., Gupta, S., *Novel study in sustained release drug delivery system: a review*. Int J Pharm Med Res, 2015. **3(2)**: p. 204-215.
63. Pundir, S., Badola, A., Sharma, D., *Sustained release matrix technology and recent advance in matrix drug delivery system: a review*. Int J Drug Res Tech, 2013. **3(1)**: p. 12-20.
64. Agarwal, G., Agarwal, S., Karar, P. K., et al., *Oral Sustained Release Tablets: An Overview with a Special Emphasis on Matrix Tablet*. Am J Adv Drug Delivery, 2017. **5(2)**: p. 64-76.
65. Tiwari, G., Tiwari, R., Sriwastawa, B., et al., *Drug delivery systems: An updated review*. Int J Pharm Invest, 2012. **2(1)**: p. 2-11.
-

-
66. Rao, N. G. R., Raj, K. R. P., Nayak, B. S., *Review on Matrix Tablet as Sustained Release*. Int J Pharm Res Allied Sci, 2013. **2(3)**: p. 1-17.
 67. Kambampati, S., Kumar, J. N. S., Sriram, C. H., *A review on sustained release drug delivery system*. Int J Res Pharm Nano Sci, 2013. **2(4)**: p. 441-447.
 68. Karna, S., Chaturvedi, S., Agarwal, V., Alim, M., *Formulation approaches for sustained release dosage forms: A Review*. Asian J Pharm Clin Res, 2015. **7(7)**: p. 16-21.
 69. Alli, P. R., Bargaje, P. B., Mhaske, N. S., *Sustained Release Drug Delivery System: A Modern Formulation Approach*. Asian J Pharm Technol Innovation, 2015. **8(5)**: p. 46-53.
 70. Asija, R., Rathi, H., Asija, S., *Sustained Released Drug Technology: A Review*. Int J Res Pharm Sci, 2012. **2(4)**: p. 1-13.
 71. Gandhi, A., Kumar, S. L. H., *Recent Trends in Sustained Release Drug Delivery System*. Int J Interdiscip Multidiscip Stud, 2014. **1(6)**: p. 122-134.
 72. Subramani, M., Vekatahwaramoorthy, N., Sambathkumar, R., *A Novel Approach on Role of Polymers Used In Sustained Release Drug Delivery System- A Review*. Saudi J Med Pharm Sci, 2021. **7(4)**: p. 170-178.
 73. Senthilkumar, M., Gowramma, B., Kaviarasan, L., et al., *Oral Modified Drug Release Solid Dosage form with Special Reference to Design; An Overview*. Curr Drug Res Rev, 2020. **12(1)**: p. 1-10.
 74. Swaleh, M. M., Nisa, Z., Ali, S. I., Khan, M. A., et al., *A Detailed Review on Oral Controlled Release Matrix Tablets*. Int J Pharm Sci Rev Res, 2020. **64(2)**: p. 27-38.
 75. Alhalmi, A., Altowairi, M., Saeed, O., et al., *Sustained release matrix system: an overview*. World J Pharm Pharm Sci, 2018. **7(6)**: p. 1470-1486.
 76. Jaimini, M., Kothari, A., *Sustained release matrix type drug delivery system: a review*. J Drug Delivery Ther, 2012. **2(6)**: p. 142-148.
 77. Yadav, R. P., Sheeba, F. R., Sharma, M., et al., *The Role of Matrix Tablet in Oral Drug Delivery System*. Asian J Pharm Res Dev, 2021. **9(2)**: p. 80-86.
-

-
78. Mondal, N., *The role of matrix tablet in drug delivery system*. Int J App Pharm, 2018. **10(1)**: p. 1-6.
 79. Shukla, R., Shaikh, S., Damor, Y., et al., *A Review on Sustained Release Matrix Tablet*. EAS J Pharm Pharmacol, 2020. **2(1)**: p. 14-17.
 80. Abdel-Rahman, S. I., Mahrous, G. M., El-Badry, M., *Preparation and comparative evaluation of sustained release metoclopramide hydrochloride matrix tablets*. Saudi Pharm J, 2009. 17: p. 283-288.
 81. Tabandeh, H., Mortazavi, S. A., Guilani, T. B., *Preparation of sustained release matrix tablets of aspirin with ethyl cellulose, Eudragit RS100 and Eudragit S100 and studying the release profiles and their sensitivity to tablet hardness*. Iranian J Pharm Res, 2003. **2**: p. 9-17.
 82. Jennin, V., Leccia, E., Rosiaux, Y., et al., *Evolution of the microstructure of sustained-release matrix tablets during dissolution and storage*. Indian J Pharm Sci, 2018. **80(6)**: p. 1011-1020.
 83. Siepmann, F., Herrmann, S., Winter, G., et al., *A novel mathematical model quantifying drug release from lipid implants*. J Control Release, 2008. **128(3)**: p. 233-40.
 84. Siepmann, J., Siepmann, F., *Mathematical modeling of drug release from lipid dosage forms*. Int J Pharm, 2011. **418(1)**: p. 42-53.
 85. Siepmann, J., Siepmann, F., *Modeling of diffusion-controlled drug delivery*. J Control Release, 2012. **161(2)**: p. 351-62.
 86. Nardi-Ricart, A., Nofrerias-Roig, I., Sune-Pou, M., et al., *Formulation of Sustained Release Hydrophilic Matrix Tablets of Tolcapone with the Application of Sedem Diagram: Influence of Tolcapone's Particle Size on Sustained Release*. Pharmaceutics, 2020. **12(674)**: p. 1-18.
 87. Hiremath, P. S., Saha, R. N., *Controlled Release Hydrophilic Matrix Tablet Formulations of Isoniazid: Design and In Vitro Studies*. AAPS Pharm Sci Tech, 2008. **9(4)**: p. 1171-1178.
-

-
88. Nokhodchi, A., Raja, S., Patel, P., et al., *The Role of Oral Controlled Release Matrix Tablets in Drug Delivery Systems*. Bioimpacts, 2012. **2(4)**: p. 175-187.
 89. Baveja, S. K., Rao, K. V. R., Devi, K. P., *Zero-order release hydrophilic matrix tablets of P-adrenergic blockers*. Int J Pharm, 1987. **39**: p. 39-45.
 90. Avgoustakis, K., Nixon, J. R., *Biodegradable controlled release tablets: III. Effect of polymer characteristics on drug release from heterogeneous poly(lactide-co-glycolide) matrices*. Int J Pharm, 1993. **99**: p. 247-252.
 91. Martínez, A. D. B., Galan, I. C. R., Bellver, M. V. M., *Application of a Biodegradable Polyesteramide Derived from L-Alanine as Novel Excipient for Controlled Release Matrix Tablets*. AAPS Pharm Sci Tech, 2017. **18(8)**: p. 3286-3295.
 92. Dinarvand, R., Moghadam, S. H., Mohammadyari-Fard, L., et al., *Preparation of Biodegradable Microspheres and Matrix Devices Containing Naltrexone*. AAPS Pharm Sci Tech, 2003. **4(3)**: p. 45-54.
 93. Rajakumari, R., Volova, T., Oluwafemi, O. S., et al., *Transformation of essential minerals into tablet formulation with enhanced stability*. Adv Powder Technol. 2020. **31(7)**: p. 2806-2819.
 94. Saini, N., Mathew, G., Lincy, J., *Matrix Tablets: An Effective Way for Oral Controlled Release Drug Delivery*. Iran J Pharm Sci, 2012. **8(3)**: p. 165-170.
 95. Khan, R., Ashraf, M. S., Afzal, M., et al., *Formulation and evaluation of sustained release matrix tablet of rabeprazole using wet granulation technique*. J Pharm Bioall Sci, 2014. **6**: p. 180-184.
 96. Nyamweya, N. N., *Applications of polymer blends in drug delivery*. Future J Pharm Sci, 2021. **7(18)**: p. 1-15.
 97. Iqbal, Z., Nasir, F., Akhlaq, M., et al., *Sustained Release Carbamezapine Matrix Tablets Prepared by Solvent-Evaporation Technique Using Different Polymers*. Middle-East J Sci Res, 2013. **15(10)**: p. 1368-1374.
-

-
98. Urbaniak, T., Musial, W., *Influence of Solvent Evaporation Technique Parameters on Diameter of Submicron Lamivudine-Poly-ε-Caprolactone Conjugate Particles*. *Nanomaterials*, 2019. **9(1240)**: p. 1-18.
 99. Hwisa, N. T., Katakam, P., Chandu, B. R., et al., *Solvent Evaporation Techniques as Promising Advancement in Microencapsulation*. *Vedic Res. Int Biol Med Chem*, 2013. **1(1)**: p. 8-22.
 100. Upadrashta, S. M., Katikaneni, P. R., Hileman, G. A., et al., *Direct compression-controlled release tablets using ethylcellulose matrices*, *Drug Dev Ind Pharm*, 1993. **19(4)**: p. 449-460.
 101. Pandey, N. K., Ghatuary, S. K., Dubey, A., et al., *Formulation and in vitro evaluation of sustained release floating matrix tablet of levofloxacin by direct compression method*, *J Drug Delivery Ther*, 2019. **9(4-s)**: p. 398-403.
 102. Allen, L. V., Ansel, H. C., *Tablets. Ansel's Pharmaceutical Dosage and drug delivery systems*. Philadelphia: Lipincott Williams and Wilkins, 2014. p. 277.
 103. Shanmugam, S., *Granulation techniques and technologies: recent progresses*. *Bioimpacts*, 2015. **5(1)**: p. 55-63.
 104. Khan, R., Ashraf, M. S., Afzal, M., et al., *Formulation and evaluation of sustained release matrix tablet of rabeprazole using wet granulation technique*. *J Pharm Bioallied Sci*, 2014. **6(3)**: p. 180-184.
 105. Radhika, P. R., Pal, T. K., Sivakumar, T., *Formulation and Evaluation of Sustained Release Matrix Tablets of Glipizide*. *Iran J Pharm Sci*, 2009. **5(4)**: p. 205-214.
 106. Kosir, D., Vreser, F., *The performance of HPMC matrix tablets using various agglomeration manufacturing processes*. *Drug Dev Ind Pharm*, 2016. **43(2)**: p. 329-337.
 107. Sandler, N., Lammens, R. S., *Pneumatic dry granulation: potential to improve roller compaction technology in drug manufacture*. *Expert Opin Drug Deliv*, 2011. **8(2)**: p. 225-236.
-

-
108. Wade, J. B., Martin, G. P., Long, D. F., *Controlling granule size through breakage in a novel reverse-phase wet granulation process; the effect of impeller speed and binder liquid viscosity*. Int J Pharm, 2015. **478**: p. 439-446.
 109. Kleinebudde, P., *Roll compaction/dry granulation: pharmaceutical applications*. Eur J Pharm Biopharm, 2004. **58**: p. 317-326.
 110. Barakat, N. S., Elbagory, I. M., Almurshedi, A. S., *Formulation, Release Characteristics and Bioavailability Study of Oral Monolithic Matrix Tablets Containing Carbamazepine*. AAPS PharmSciTech, 2008. **9(3)**: p. 931-938.
 111. Abd El-Halim, S. M., Amin, M. M., El-Gazayerly, O. N., et al., *Comparative study on the different techniques for the preparation of sustained-release hydrophobic matrices of a highly water-soluble drug*. Drug Discoveries Ther, 2010. **4(6)**: p. 484-492.
 112. Wilkins, C. A., du Plessis, L. H., Viljoen, J. M., *Investigating in vitro and ex vivo properties of artemether/lumefantrine double-fixed dose combination lipid matrix tablets prepared by hot fusion*. Pharmaceutics, 2021. **13(922)**: p. 1-17.
 113. Krstic, M., Djuris, J., Petrovic, O., et al., *Application of the melt granulation technique in development of lipid matrix tablets with immediate release of carbamazepine*. J Drug Delivery Sci Technol, 2017. **39**: p. 467-474.
 114. Forster, S. P., Dippold, E., Chiang, T., *Twin-Screw Melt Granulation for Oral Solid Pharmaceutical Products*. Pharmaceutics, 2021. **13(665)**: p. 1-22.
 115. Ramya, S. A., Latha, K., *Formulation and evaluation of zolpidem tartrate layered tablets by melt granulation technique for treatment of insomnia*. Asian J Pharm Clin Res, 2018. **11(6)**: p. 139-147.
 116. Bhatti, A., Usman, M., Kandi, V., *Current Scenario of HIV/AIDS, Treatment Options, and Major Challenges with Compliance to Antiretroviral Therapy*. Cureus, 2016. **8(3)**: p. 1-12.
 117. Kapila, A., Chaudhary, S., Sharma, R. B., *A review on: HIV AIDS*. Indian J Pharm Biol Res, 2016. **4(3)**: p. 69-73.
-

-
118. Simon, V., Ho, D. D., Karim, Q. A., *HIV/AIDS epidemiology, pathogenesis, prevention, and treatment*. Lancet, 2006. **368(9534)**: p. 489-504.
 119. Ligan, K., *A review on various aspects of HIV infection*. HIV Curr Res, 2018. **3(1)**: p. 1-6.
 120. Wable, R., *A review article on HIV and AIDS*. World J Pharm Life Sci, 2020. **6(9)**: p. 146-149.
 121. Bhattacharya, J., *HIV prevention & treatment strategies - Current challenges & future prospects*. Indian J Med Res, 2018. **148**: p. 671-674.
 122. Gunthard, H. F., Saag, M. S., Benson, C. A., *Antiretroviral Drugs for Treatment and Prevention of HIV Infection in Adults*. JAMA, 2016. **316(2)**: p. 191-210.
 123. Johnson, M. A., Moore, K. H. P., Yuen, G. J., et al., *Clinical Pharmacokinetics of Lamivudine*. Clin Pharmacokinet, 1999. **36 (1)**: p. 41-66.
 124. Anonymous, Indian Pharmacopoeia. Government of India Ministry of Health and Family Welfare, Vol-I, II and III, The Indian Pharmacopoeia Commission, Ghaziabad, India, 2007. **142-183**: p. 1276-1285.
 125. Goodman and Gilman's. The Pharmacological Basis of Therapeutics, 10th edn., Harman J.G. and Limbird L.E, New York, 2001, p. 1349-1359.
 126. Strauch, S., Jantravid, E., Dressman, J. B., et al., *Biowaiver Monographs for Immediate Release Solid Oral Dosage Forms: Lamivudine*. J Pharm Sci, 2011. **100(6)**: p. 2054-2063.
 127. Vasconcelos, T. R. A., Ferreira, M. L., Goncalves, R. S. B., et al., *Lamivudine, an important drug in aids treatment*. J Sulphur Chem, 2008. **29(5)**: p. 559-571.
 128. Perry, C. M., Faulds, D., *Lamivudine: A Review of its Antiviral Activity, Pharmacokinetic Properties and Therapeutic Efficacy in the Management of HIV Infection*. Drugs, 1997. **53 (4)**: p. 657-680.
 129. Quercia, R., Perno, C. F., Koteff, J., et al., *Twenty-Five Years of Lamivudine: Current and Future Use for the Treatment of HIV-1 Infection*. J Acquir Immune Defic Syndr, 2018. **78(2)**: p. 125-135.
-

-
130. Nasr, M., Saad, I. E., *Formulation and evaluation of mastic gum as compression coat for colonic delivery of 5-fluorouracil*. Int J Drug Delivery, 2011. **3**. p. 481-491.
131. Dimas, K. S., Pantazis, P., Ramanujam, R., *Chios mastic gum: a plant-produced resin exhibiting numerous diverse pharmaceutical and biomedical properties*. In Vivo, 2012. **26**: p. 777-786.
132. Paraschos, S., Mitakou, S., Skaltsounis, A. L., *Chios Gum Mastic: A Review of its Biological Activities*. Curr Med Chem, 2012. **19**: p. 2292-2302.
133. Huwez, F. U., Thirlwell, D., Dlawer, A. A., *Mastic Gum Kills Helicobacter pylori*. N Engl J Med, 1998. **339(26)**: p. 1946.
134. Panagopoulou, A., Georgarakis, M., *Effect of compression and diluent on drug release from mastix matrix tablets. a statistical analysis*. Drug Dev Ind Pharm, 1990. **16(4)**: p. 637-649.
135. Vrouvaki, I., Koutra, E., Kornaros, M., et al., *Polymeric Nanoparticles of Pistacia lentiscus var. chia Essential Oil for Cutaneous Applications*. Pharmaceutics, 2020. **12(353)**: p. 1-15.
136. Bansal, J., Malviya, R., Malviya, T., et al., *Evaluation of Banana Peel Pectin as Excipient in Solid Oral Dosage Form*. Global J Pharmacol, 2014. **8(2)**: p. 275-278.
137. Sandan, S., Thombre, M., Aher, S., *Isolation and evaluation of starch from musa paradisiaca linn. as a binder in tablet*. Int J Pharm Sci Res, 2017. **8(8)**: p. 3484-3491.
138. Reddy, V. R., Reddy, R. M., *Evaluation of Musa paradisiaca (Banana peel) Mucilage as Pharmaceutical Excipient*. Int J Pharm Chem Sci, 2013. **2(4)**: p. 2055-2064.
139. Anjum, S., Sundaram, S., Rai, G. K., *Nutraceutical application and value addition of banana (musa paradisiaca l. variety "bhusawal keli") peel: a review*. Int J Pharm Pharm Sci, 2014. **6(10)**: p. 81-85.
-

-
140. Mohiuddin, A. K. M., Saha, M. K., Hossian, M. S., et al., *Usefulness of Banana (Musa paradisiaca) Wastes in Manufacturing of Bio-products: A Review*. The Agriculturists, 2014. **12(1)**: p. 148-158.
 141. Ehiowemwenguan, G., Emoghene, A. O., Inetianbor, J. E., *Antibacterial and phytochemical analysis of Banana fruit peel*. IOSR, J Pharm, 2014. **4(8)**: p. 18-25.
 142. Singanusong, R., Tochampa, W., Kongbangkerd, T., et al., *Extraction and properties of cellulose from banana peels*. Suranaree J. Sci. Technol, 2013. **21(3)**: p. 201-213.
 143. Hendrika, Y., Reveny, J., Sumaiyah, S., *Formulation and in vitro evaluation of gastroretentive floating beads of amoxicillin using pectin from banana peel (musa balbisiana abb)*. Asian J Pharm Clin Res, 2018. **11(3)**: p. 72-77.
 144. Rana, G. K., Singh, Y., Mishra, S. P., et al., *Potential Use of Banana and Its By-products: A Review*. Int J Curr Microbiol App Sci, 2018. **7(6)**: p. 1827-1832.
 145. Anhwange, B. A., Ugye, T. J., Nyiaatagher, T. D., *Chemical composition of musa sapientum (banana) peels*. EJEAFChe Electron J Environ Agric Food Chem, 2009. **8(6)**: p. 437-442.
 146. <https://pubchem.ncbi.nlm.nih.gov/compound/Acrylamide> assessed on dated 14-06-2021.
 147. Lande, S. S., Bosch, S. J., Howard, P. H., *Degradation and leaching of acrylamide in soil*. J Environ Qual, 1979. **8(1)**: p. 133-137.
 148. Smith, E. A., Oehme, F. W., *Acrylamide and polyacrylamide: a review of production, use, environmental fate and neurotoxicity*. Rev Environ Health, 1991. **9(4)**: p. 215-228.
 149. Kaity, S., Isaac, J., Kumar, P. M., et al., *Microwave assisted synthesis of acrylamide grafted locust bean gum and its application in drug delivery*. Carbohydr Polym, 2013. **98**: p. 1083-1094.
-

-
150. Shanmugapriya, A., Ramammurthy, R., Munusamy, V., et al., *Optimization of Ceric Ammonium Nitrate Initiated Graft Copolymerization of Acrylonitrile onto Chitosan*. J Water Resour Prot, 2011. **3**: p. 380-386.
 151. Joshi, J. M., Sinha, V. K., *Ceric ammonium nitrate induced grafting of polyacrylamide onto carboxymethyl chitosan*. Carbohydr Polym, 2007. **67**: p. 427-435.
 152. <https://pubchem.ncbi.nlm.nih.gov/compound/Cerium-ammonium-nitrate> assessed on dated 14-06-2021.
 153. Rowe, R.C., Sheskey, P.J, Owen, S.C., Handbook of pharmaceutical excipients. 2006, 5th edition, Published by Pharmaceutical Press, USA.
 154. Chami, S., Joly, N., Bocchetta, P., et al., *Polyacrylamide Grafted Xanthan: Microwave-Assisted Synthesis and Rheological Behavior for Polymer Flooding*. Polymers, 2021. **13(1484)**: p. 1-19.
 155. Oliveira, A. C. J., Ribeiro, F. O. S., Lima, L. R. M., et al., *Microwave-initiated rapid synthesis of phthalated cashew gum for drug delivery systems*. Carbohydr Polym, 2021. **254**: p. 1-32.
 156. Bal, T., Swain, S., *Microwave assisted synthesis of polyacrylamide grafted polymeric blend of fenugreek seed mucilage-Polyvinyl alcohol (FSM-PVA-g-PAM) and its characterizations as tissue engineered scaffold and as a drug delivery device*. DARU J Pharm Sci, 2020. **28**: p. 33-44.
 157. Malviya, R., Sharma, P. K., Dubey, S. K., *Microwave-assisted preparation of biodegradable, hemocompatible, and antimicrobial neem gum-grafted poly (acrylamide) hydrogel using (3)2 factorial design*. Emergent Mater, 2019: **2**: p. 95-112.
 158. Dan, S., Mandal, P., Bose, A., et al., *Microwave Assisted Acrylamide Grafting on a Natural Gum Cassia Tora: Characterization and Pharmacokinetic Evaluation of the Formulation Containing Metformin and Sitagliptin in Rats by LC-MS/MS*, Anal Chem Lett, 2018. **8(5)**: p. 622-641.
-

-
159. Chaudhary, S., Sharma, J., Kaith, B. S., et al., *Gum xanthan-psyllium-cl-poly(acrylic acid-co-itaconic acid) based adsorbent for effective removal of cationic and anionic dyes: Adsorption isotherms, kinetics and thermodynamic studies*. *Ecotoxicol Environ Saf*, 2018. **49**: p. 150-158.
 160. Sharma, J., Anand, P., Pruthi, V., et al., *RSM-CCD optimized adsorbent for the sequestration of carcinogenic rhodamine-B: kinetics and equilibrium studies*. *Mater Chem Phys*, 2017. **196**: p. 270-283.
 161. Bingjie, Li., Shen, J., Wang, L., *Development of an antibacterial superabsorbent hydrogel based on tara gum grafted with polyacrylic acid*. *Int Res J Public Environ Health*, 2017. **4(2)**: p. 30-35.
 162. Varma, V.N. S. K., Shivakumar, H. G., Balmuralidhara, V., et al., *Development of pH sensitive nanoparticles for intestinal drug delivery using chemically modified guar gum co-polymer*. *Iran J Pharm Res*, 2016. **15(1)**: p. 83-94.
 163. Mutalik, S., Suthar, N. A., Managuli, R. S., et al., *Development and performance evaluation of novel nanoparticles of a grafted copolymer loaded with curcumin*. *Int J Biol Macromol*, 2016. **86**: p. 709-720.
 164. Mittal, H., Jindal, R., Kaith, B. S., et al., *Flocculation and adsorption properties of biodegradable gum-ghatti-grafted poly(acrylamide-co-methacrylic acid) hydrogels*. *Carbohydr Polym*, 2015. **67**: p. 427-435.
 165. Menon, S., Deepthi, M. V., Sailaja, R. R. N., et al., *Study on microwave assisted synthesis of biodegradable guar gum grafted acrylic acid superabsorbent nanocomposites*. *Indian J Adv Chem Sci*, 2014. **2(2)**: p. 76-83.
 166. Setia, A., Kumar, R., *Microwave assisted synthesis and optimization of Aegle marmelos-g-poly(acrylamide): Release kinetics studies*. *Int J Biol Macromol*, 2014. **65**: p. 462-470.
 167. Tang, X. J., Huang, J., Xu, L. Y., et al., *Microwave-assisted rapid synthesis, characterization and application of poly (d,l-lactide)-graft-pullulan*. *Carbohydr Polym*, 2014. **107**: p. 7-15.
-

-
168. Kaity, S., Issac, J., Kumar, P. M., et al., *Microwave assisted synthesis of acrylamide grafted locust bean gum and its application in drug delivery*. Carbohydr Polym, 2013. **98**: p. 1083-1094.
169. Kaur, J., Kaith, B. S., Jindal, R., *Evaluation of Physio-chemical and Thermal properties of Soy Protein Concentrate and Different Binary Mixtures Based Graft Copolymers*. Int J Sci Engg Res, 2013. **4(10)**: p. 573-579.
170. Vijan, V., Kaity, S., Biswas, S., *Microwave assisted synthesis and characterization of acrylamide grafted gellan, application in drug delivery*. Carbohydr Polym, 2012. **90**: p. 496-506.
171. Pathania, D., Sharma, R., *Synthesis and characterization of graft copolymers of methacrylic acid onto gelatinized potato starch using chromic acid initiator in presence of air*. Adv Mat Lett, 2012. **3(2)**: p. 136-142.
172. Tame, A., Ndikontar, M. K., Ngamveng, J. N., et al., *Graft copolymerisation of acrylamide on carboxymethyl cellulose (cmc)*. Rasayan J Chem, 2011. **4(1)**: p. 1-7.
173. Kalia, S., Kumar, A., Kaith, B. S., *Sunn hemp cellulose graft copolymers polyhydroxybutyrate composites: morphological and mechanical studies*. Adv Mat Lett, 2011. **2(1)**: p. 17-25.
174. Sharma, A. K., Mishra, A. K., *Microwave assisted synthesis of chitosan-graftstyrene for efficient Cr(VI) removal*. Adv Mat Lett, 2010. **1(1)**: p. 59-66.
175. Narkar, M., Sher, P., Pawar, A., *Stomach-Specific Controlled Release Gellan Beads of Acid-Soluble Drug Prepared by Ionotropic Gelation Method*. AAPS PharmSciTech, 2010. **11(1)**: p. 267-277.
176. Kar, R., Mohapatra, S., Bhanja, S., et al., *Formulation and In Vitro Characterization of Xanthan Gum-Based Sustained Release Matrix Tables of Isosorbide-5- Mononitrate*. Iranian J Pharm Res, 2010. **9(1)**: p. 13-19.
177. Kumar, A., Singh, K., Ahuja, M., *Xanthan-g-poly(acrylamide): Microwave-assisted synthesis, characterization and in vitro release behavior*. Carbohydr Polym, 2009. **76**: p. 261-267.
-

-
178. Osemeahon, S. A., Barminas, T. J., Aliyu, B. A., et al., *Development of sodium alginate and konkoli gum grafted-polyacrylamide blend membrane: optimization of grafting conditions*. Afr J Biotechnol, 2008. **7(9)**: p. 1309-1313.
 179. Mishra, A., Clark, J. H., Pal, S., *Modification of Okra mucilage with acrylamide: Synthesis, characterization and swelling behavior*. Carbohydr Polym, 2008. **72**: p. 608-615.
 180. Pandey, P. K., Srivastava, A., Tripathy, A., et al., *Graft copolymerization of acrylic acid onto guar gum initiated by vanadium (V)–mercaptosuccinic acid redox pair*. Carbohydr Polym, 2006. **65**: p. 414-420.
 181. Singh, V., Tiwari, A., Tripathi, D. N., et al., *Microwave assisted synthesis of Guar-g-polyacrylamide*. Carbohydr Polym, 2004. **58**: p. 1-6.
 182. Biswal, D. R., Singh, R. P., *Characterisation of carboxymethyl cellulose and polyacrylamide graft copolymer*. 2004. **57**: p. 379-387.
 183. Taghizadeh, M.T., Mafakhery, S., *Kinetics and mechanism of graft polymerization of acrylonitrile onto starch initiated with potassium persulfate*. J Sci I R Iran, 2001. **12(4)**: p. 333-338.
 184. Singh, P., Shrivastava, A. K., Kumar, S., et al., *Formulation and evaluation of sustained release matrix tablets of aceclofenac*. Borneo J Pharm, 2021. **4(2)**: p. 99-109.
 185. Alam, S., Bishal, A., Adhyay, B. B., *Formulation and evaluation of metformin hydrochloride sustained release matrix tablets*. Int J Curr Pharm Res, 2021. **13(5)**: p. 82-88.
 186. Ekpabio, E. I., Effiong, D. E., Uwah, T. O., et al., *Sustained -release theophylline matrix tablet using hydrophilic polymers: Effect of agitation rates and pH on release kinetics*. J Adv Med Pharm Sci, 2020. **22(5)**: p. 36-50.
 187. Yahoum, M. M., Lefnaoui, S., Mostefa, N. M., *Design and evaluation of sustained release hydrophilic matrix tablets of Piroxicam based on carboxymethyl xanthan derivatives*. Soft Mater, 2020. **19(2)**: p. 178-191.
-

-
188. Pawar, S. S., Malpure, P. S., Surana, S. S., et al., *Formulation and evaluation of sustained release matrix tablets of captopril*. J Drug Delivery Ther, 2019. **9(4-A)**: p. 260-268.
 189. Patil, C. C., Yogitha, M., Vijapure, V. K., *Studies on development and evaluation of sustained release matrix tablets containing tizanidine*. Indo Am J P Sci, 2019. **6(12)**: p. 16693-16700.
 190. Latha, K., Kranthi, T. C., Shaik, N. B., *Preparation and evaluation of sustained release matrix tablets of tolterodine tartrate using guggul resin*. Bangladesh Pharm J, 2018. **21(1)**: p. 24-34.
 191. Soni, P., Solanki, D., *Formulation and Evaluation of Sustained Release Matrix Tablet of Antiviral Drug by Natural polysaccharide*. Int J Chemtech Res, 2018. **11(11)**: p. 323-328.
 192. Song, Li., He, S., Ping, Q., *Development of a sustained-release microcapsule for delivery of metoprolol succinate*. Exp Ther Med, 2017. **13**: p. 2435-2441.
 193. Kumbhar, D. M., Havaldar, V. D., Mali, K. K., et al., *Formulation and Evaluation of Sustained Release Tablets of Venlafaxine Hydrochloride for the treatment of Depressive disorders*. Asian J Pharm Res, 2017. **7(1)**: p. 1-6.
 194. Khan, H., Ali, M., Ahuja, A., et al., *Formulation and in-vitro evaluation of fdc bilayer matrix tablets containing telmisartan as sustained release and hydrochlorothiazide as immediate release*. Res J Pharm Technol, 2017. **10(4)**: p. 1085-1090.
 195. Sayed, M. A., Ali, A. A., Ali, A. M., et al., *Design and in vitro/in vivo evaluation of sustained-release floating tablets of itopride hydrochloride*. Drug Des Devel Ther, 2016. **14(10)**: p. 4061-4071.
 196. Faria, R. S., Syed, M., Juliana, M. J., Mandal, U. K., *Design and in-vitro evaluation of sustained release floating tablets of metformin HCl based on effervescence and swelling*. Iran J Pharm Res, 2016. **15(1)**: p. 53-70.
-

-
197. Palei, N. N., Mamidi, S. K., Rajangam, J., *Formulation and evaluation of lamivudine sustained release tablet using okra mucilage*. J Appl Pharm Sci, 2016. **6(9)**: p. 069-075.
 198. Zhang, Ya, Huang, Z., Omari-Siaw, E., et al., *Preparation and in vitro–in vivo evaluation of sustained-release matrix pellets of capsaicin to enhance the oral bioavailability*. AAPS PharmSciTech, 2016. **17(2)**: p. 339-349.
 199. Mitkare, S. S., Sarkarkar, D. M., *The effect of different grades polymer blends on release profiles of diclofenac sodium from hydrophilic matrices*. J Appl Pharm Sci, 2015. **5(10)**: p. 142-146.
 200. Sarada, A., Lohithasu, D., Pratyusha, P. V., *Development of Hydrophobic Carriers based tablets for Sustained Release of Verapamil*. J Appl Pharm Sci, 2015. **5(12)**: p. 125-134.
 201. Chime, S. A., Attama, A. A., Kenechukwu, F. C., et al., *Formulation, in vitro and in vivo Characterisation of Diclofenac Potassium Sustained Release Tablets Based on Solidified Reverse Micellar Solution*. Br J Pharm Res, 2013. **3(1)**: p. 90-107.
 202. Quinten, T., Beer, T. D., Almeida, A., et al., *Development and evaluation of injection-molded sustained-release tablets containing ethylcellulose and polyethylene oxide*. Drug Dev Ind Pharm, 2011. **37(2)**: p. 149-159.
 203. Shanmugam, S., Chakrahari, R., Sundaramoorthy, K., et al., *Formulation and evaluation of sustained release matrix tablets of losartan potassium*. Int J Pharm Tech Res, 2011. **3(1)**: p. 526-534.
 204. Ganesh, G. N.K., Kumar, R. S., Senthil, V., et al., *Preparation and evaluation of sustained release matrix tablet of diclofenac sodium using natural polymer*. J Pharm Sci & Res, 2010. **2(6)**: p. 360-368.
 205. Subramaniam, K., Rangasamy, M., Kugalur, G., et al., *Formulation and Evaluation of Sustained Release Tablets of Aceclofenac using Hydrophilic Matrix System*. Int J Pharm Tech Res, 2010. **2(3)**: p. 1775-1780.
-

-
206. Li, F. Q., Hu, J. H., Deng, J. X., et al., *In vitro controlled release of sodium ferulate from Compritol 888 ATO-based matrix tablets*. Int J Pharm, 2006. **324**: p. 52-57.
207. Jannin, V., Pochard, E., Chambin, O., *Influence of poloxamers on the dissolution performance and stability of controlled-release formulations containing Precirol® ATO 5*. Int J Pharm, 2006. **309**: p. 6-15.
208. Kuskal, A., Tiwary, A. K., Jain, N. K., et al., *Formulation and In Vitro, In Vivo Evaluation of Extended- release Matrix Tablet of Zidovudine: Influence of Combination of Hydrophilic and Hydrophobic Matrix Formers*. AAPS PharmSciTech, 2006. 7(1): p. E1-E9.
209. Ochoa, L., Igartua, M., Rosa, M., et al., *Preparation of sustained release hydrophilic matrices by melt granulation in a high-shear mixer*. J Pharm Pharmaceut Sci, 2005. **8(2)**: p. 132-140.
210. Kamble, R., Maheshwari, M., Paradkar, A., et al., *Melt solidification technique: incorporation of higher wax content in ibuprofen beads*. AAPS PharmSciTech, 2004. **5(4)**: p. 1-9.
211. Chauhan, B., Shimpi, S., Mahadik, K. R., et al., *Preparation and evaluation of floating risedronate sodium Gelucire® 39/01 matrices*. Acta Pharm, 2004. **54**: p. 5-14.
212. Tiwari, S. B., Murthy, T. K., Pai, M. R., et al., *Controlled release formulation of tramadol hydrochloride using hydrophilic and hydrophobic matrix system*. AAPS PharmSciTech, 2003. **4(3)**: p. 1-6.
213. Makhija, S. N., Vavia, P. R., *Once daily sustained release tablets of venlafaxine, a novel antidepressant*. Eur J Pharm Biopharm, 2002. **54**: p. 9-15.
214. Amaral, M. H., Lobo, J. M. S., Ferreira, D. C., *Effect of hydroxypropyl methylcellulose and hydrogenated castor oil on naproxen release from sustained-release tablets*. AAPS PharmSciTech, 2001. **2(2)**: p. 1-8.
-

-
215. Barthelemy, P., Laforet, J. P., Farah, N., et al., *Compritol 888 ATO: an innovative hot-melt coating agent for prolonged-release drug formulations*. Eur J Pharm Biopharm, 1999. **47**: p. 87-90.
216. Canbay, H. S., Doğantürk, M., *Application of Differential Scanning Calorimetry and Fourier Transform Infrared Spectroscopy to the Study of Metoprolol-Excipient and Lisinopril-Excipient Compatibility*. Eurasian J Anal Chem, 2018. **13(5)**: p. em39.
217. Meira, R. Z. C., Biscaia, I. F. B., Nogueira, C., et al., *Solid-State Characterization and Compatibility Studies of Penciclovir, Lysine Hydrochloride, and Pharmaceutical Excipients*. Materials (Basel), 2019. **12(19)**: p. 3154.
218. Lankalapalli, S., Tenneti, V. S. V. K., Adama, R., *Preparation and evaluation of liposome formulations for poorly soluble drug itraconazole by complexation*. Der Pharmacia Lettre, 2015. **7 (8)**: p. 1-17.
219. Bhaskar, B., Sarin, G.S., Sharma, B.K., et al., *Process for the preparation of highly pure bexarotene*, 2011-11-17, Patent Number: WO2011141928A1.
220. Rani, T. N., Muzib, Y., Neeharika, M. S., et al., *Solubility enhancement of poorly soluble drug ezetimibe by solid dispersion technique*. J Adv Pharm, 2013. **4(2)**: p. 75-81.
221. Pobudkowska, A., Domanska, U., *Study of pH-dependent drugs solubility in water*. Chem Ind Chem Eng, 2014. **20(1)**: p. 112-126.
222. Sudha, T., Saminathan, J., Anusha, K., et al., *Simultaneous U.V. spectrophotometric estimation of lamivudine and abacavir sulphate in bulk and in tablet dosage form*. J Chem Pharm Res, 2010. **2(5)**: p. 45-51.
223. Walter, J., Jr. Weber, Chin, Yu-Ping., *Determination of partition coefficient and aqueous solubility by reverse phase chromatography-1*, WAT Res, 1986. **20(11)**: p. 1422-1442.
-

-
224. Strauch, S., Jantratid, E., Dressman, J. B., et al., *Biowaiver Monographs for Immediate Release Solid Oral Dosage Forms: Lamivudine*. J Pharm Sci, 2011. **100(6)**: p. 2054-2063.
225. Pavia D.C., Lampman G.M., Kriz G.S., Vivian J.R., *Spectroscopy*, 2nd edition, Cengage learning India Pvt. Ltd. New Delhi, 2009: p. 37-40.
226. Gupta, K. R., Pounikar, A. R., Umekar, M. J., *Drug Excipient Compatibility Testing Protocols and Characterization: A Review*. Asian J Chem Sci, 2019. **6(3)**: p. 1-22.
227. Sen, G., Mishra, S., Rani, G. U., et al., *Microwave initiated synthesis of polyacrylamide grafted Psyllium and its application as a flocculant*. Int J Biol Macromol, 2012. **50**: p. 369-375.
228. Malik, S., Ahuja, M., *Gum kondagogu-g-poly (acrylamide): Microwave-assisted synthesis, characterisation and release behaviour*. Carbohydr Polym, 2011. **86**: p. 177–184.
229. Singh, A. V., Nath, L. K., Guha, M., *Microwave assisted synthesis and characterization of Phaseolus aconitifolius starch-g-acrylamide*. Carbohydr Polym, 2011. **86**: p. 872–876.
230. Abbas, G., Hanif, M., Khan, M. A., *pH-responsive alginate polymeric rafts for controlled drug release by using box behnken response surface design*. Des Monomers Polym, 2017. **20**: p. 1-9.
231. Sharma, G. N., Kumar, C. H. P., Shrivastava, B., *Optimization and characterization of chitosan-based nanoparticles containing methylprednisolone using box behnken design for the treatment of crohn's disease*. Int J Appl Pharm, 2020. **12**: p. 12-23.
232. Xie, W., Xu, P., Wang, W., et al., *Preparation and antibacterial activity of a water-soluble chitosan derivative*. Carbohydr Polym, 2002. **50**: p. 35–40.
233. Singh, V., Kumar, P., Sanghi, R., *Use of microwave irradiation in the grafting modification of the polysaccharides—a review*. Prog Polym Sci, 2012. **37**: p. 340–364.
-

-
234. Malviya, R., Kumar, P., Kumar, S., *Modification of polysaccharides: pharmaceutical and tissue engineering applications with commercial utility (patents)*. Mater Sci Eng C Mater Biol Appl, 2016. **68**: p. 929–938.
235. Shi, Z., Jia, C., Wang, D., et al., *Synthesis and characterization of porous tree gum grafted polymer derived from prunus cerasifera gum polysaccharide*. Int J Bio Macromol, 2019. **133**: p. 964-970.
236. Osonwa, U. E., Majekodunmi, S. O., Onwuzuligbo, C. C., *Potential use of musa sapientum peel gum as adhesive in paracetamol tablets*. African J Pharm Sci Pharm, 2017. **5(1)**: p. 30-58.
237. Soumya, M., Chowdary, Y.A., Naga Swapna, V., et al., *Preparation and optimization of sustained release matrix tablets of metoprolol succinate and taro gum using response surface methodology*. Asian J Pharm, 2014. **8(1)**: p. 1-7.
238. Pawar, S. S., Malpure, P. S., Surana, S. S., et al., *Formulation and Evaluation of Sustained Release Matrix Tablets of Captopril*. J Drug Delivery Ther, 2019. **9(4-A)**: p. 260-268.
239. Sahu, S., Dangi, R., Patidar, R., et al., *Formulation and evaluation of sustain released matrix tablet of atenolol*. J Drug Delivery Ther, 2019. **9(1)**: p. 183-189.
240. Satyanarayana, K., Sahoo, C. K., Bhargavi, G., et al., *Formulation and optimization of olanzapine sustained release matrix tablets for the treatment of schizophrenia*. Pharm Lett, 2015. **7(4)**: p. 266-273.
241. Varma, M. M., Kumar, M. S., *Formulation and evaluation of matrix tablets of ropinirole hydrochloride for oral controlled release*. Indian J Pharm Pharmacol, 2015. **2(1)**: p. 27-42.
242. Madaan, R., Bala, R., Vasisht, T., et al., *Formulation and characterisation of matrix tablets using mucilage of tinospora cordifolia as natural binder*. Int J Pharm Pharm Sci, 2018. **10(7)**: p. 22-27.
-

-
243. Mathur, V., Nagpal, K., Singh, S. K., et al., *Comparative release profile of sustained release matrix tablets of verapamil HCl*. Int J Pharm Invest, 2013. **3(1)**: p. 60-66.
244. Shah, K. U., Khan, G. M., *Regulating drug release behavior and kinetics from matrix tablets based on fine particle-sized ethyl cellulose ether derivatives: an in vitro and in vivo evaluation*. Sci World J., 2012. **1**: p. 1-8.
245. Nokhodchi, A., Raja, S., Patel, P., et al., *The role of oral controlled release matrix tablets in drug delivery systems*. BioImpacts, 2012. **2(4)**: p. 175-187.
246. Karthikeyan, M., Deepa, M. K., Bassim, E., et al., *Investigation of kinetic drug release characteristics and in vitro evaluation of sustained-release matrix tablets of a selective cox-2 inhibitor for rheumatic diseases*. J Pharm Innov, 2020. p. 1-8.
247. Gouda, R., Baishya, H., Qing, Z., *Application of Mathematical Models in Drug Release Kinetics of Carbidopa and Levodopa ER Tablets*. J Develop Drugs, 2017. **6(2)**: p. 1-8.
248. Oliveira, P. R., Mendes, C., Klein, L., et al., *Formulation Development and Stability Studies of Norfloxacin Extended-Release Matrix Tablets*. Biomed Res Int, 2013. **4**: p. 1-8.
249. Haider, M., *Development, in vitro characterisation and stability study for matrix tablets containing chlorphenamine maleate prepared by direct compression*. Am J Drug Discov Dev, 2015. **5(1)**: p. 1-12.
250. Venugopalarao, G., Gowtham, M. S., Sarada, N. C., *Formulation evaluation and stability studies of hydrogel tablets containing Cefditoren Pivoxil*. J Pharm Res, 2013. **7**: p. 230-234.

LIST OF PUBLICATIONS

S. No.	TITLE OF PAPER WITH AUTHOR NAMES	NAME OF JOURNAL / CONFERENCE	PUBLISHED DATE	ISSN NO/ VOL NO, ISSUE NO
1.	Development and Evaluation of Buccoadhesive Film of Ropinirole Hydrochloride for the Treatment of Parkinson's Disease	International Journal of Drug Delivery Technology	2017	7(2)
2.	Mastic-g-poly (acrylamide): microwave-assisted synthesis and characterisation	International Journal of Applied Pharmaceutics	2021	13(2)
3	Design and evaluation of sustained release mucoadhesive film of sumatriptan succinate containing grafted co-polymer as the platform	Saudi Pharmaceutical Journal	2022	Article in press
4.	A novel graft copolymer of natural gum for delivery of pharmaceutically active agents	PATENT	29 June., 2018	201811024277
5.	One Day National Conference on advanced bioanalytical techniques, artificial intelligence and health sciences	ISF College of Pharmacy, Moga	24 December., 2018	
6.	Two Days national conference on Recent trends in radiopharmaceuticals in drug discovery- quality, safety and regulatory perspectives	Himachal College of Pharmacy, Nalagarh, H.P.	12-13 September., 2019	

Development and Evaluation of Buccoadhesive Film of Ropinirole Hydrochloride for the Treatment of Parkinson's Disease

Himanshu², Rahul Bhaskar³, Neelam Sharma¹, Mohit Mehta¹, Amrik Singh¹, Yashwant⁴,
 Narendra Singh Yadav⁵, Gopal Lal Khatik¹, Surajpal Verma^{1*}

¹School of Pharmaceutical Sciences, Lovely Professional University, Phagwara-144411, Punjab, India.

²Overseas healthcare ltd., Punjab, India.

³Wockhardt Research Centre, Aurangabad, India.

⁴Himachal Institute of Pharmacy, Paonta Sahib, Himachal Pradesh, India.

⁵Jacob Blaustein Institutes for Desert Research, Ben-Gurion University of the Negev, Midreshet Ben-Gurion, 84990, Israel.

Received: 25th Aug, 16; Revised 22nd March, 17, Accepted: 12th June, 7; Available Online: 25th June, 2017

ABSTRACT

The present research article represents the formulation and evaluation of buccoadhesive film of ropinirole hydrochloride. This drug is an oral non-ergoline dopamine agonist with the greater affinity at D3 receptor. This drug having low molecular weight (296.84 g/mol), and short biological half-life (4-6 hrs) which necessitates for multiple dosing for maintaining therapeutic effect throughout the day. Moreover, drug is metabolized in liver forming several inactive metabolites which decrease its oral bioavailability upto 50% making it a suitable candidate for administration of drug through buccal mucosa. Buccal films of ropinirole hydrochloride were prepared using various polymers (HPMC, EC, PVA and Carbopol) by solvent casting method using propylene glycol as plasticizer. These films were evaluated for various parameters such as appearance, surface texture, weight uniformity, thickness, folding endurance, surface pH, drug content and swelling index. All the formulations were subjected to *in vitro* drug release study which were carried out using egg membrane as semi permeable membrane.

Keywords: Ropinirole hydrochloride, buccoadhesive film, dopamine agonist, solvent casting, swelling index, *in vitro*.

INTRODUCTION

Parkinson's disease is a chronic progressive age related neurological disorder associated with the degeneration and destruction of neurons in the substantia nigra pars compacta (SN-PC) and nigrostriatal (dopaminergic) tract which result in deficiency of dopamine in the striatum¹. Parkinson's disease has four cardinal symptoms include bradykinesia (slowness and poverty of movement), muscular rigidity, resting tremor (which usually abates during voluntary movement), and an impairment of postural balance leading to disturbance of gait and falling. It is second most common neurodegenerative disease after Alzheimer's disease². There are several treatment options available to reduce signs and symptoms of Parkinson's disease and improve overall quality of life. These include monoamine oxidase type B (MAO-B) inhibitors, anticholinergic that shown to have mild effect, primarily tremors. Carbidopa/levodopa is the most effective treatment options for Parkinson's disease but the effectiveness of dopaminergic therapy is eventually limited by motor fluctuation and dyskinesia³. Non-ergoline dopamine receptor agonist ropinirole is currently recommended and shown to be efficacious in the treatment and reduction of motor fluctuation in patient with advanced Parkinsonism disease¹.

Ropinirole hydrochloride is a 4-[2-(dipropylamino)ethyl]-1,3-dihydro-2H-indol-2-one; 4-[2-(di-n-propylamino)ethyl]-2(3H)-indol-2-one monohydrochloride⁴ (Fig. 1). It is a non-ergoline D2/D3 dopamine agonist that binds to central and peripheral dopamine receptor. It has greatest affinity at D3 receptor^{1,3}. It is weakly active at the 5-HT₂ and α_2 receptors and is said to have virtually no affinity for the 5-HT₁, benzodiazepine, GABA, muscarinic, α_1 , and β -adrenoreceptors⁵. It is used to treat the signs and symptoms of idiopathic Parkinson's disease⁶. It is effective both as monotherapy as well as combination therapy with the reduced dose of levodopa². It is present as oral immediate and prolonged release conventional dosage forms which are effective in treatment, suffers with the problem of frequent dosing due to short half-life (4-6 hrs) and low oral bioavailability^{1,7} that decreases its therapeutic efficacy. To resolve these issues effectively an effective route and dosage form is required.

Among the various routes of drug administration oral route is the most preferred and convenient route for systemic delivery of drug. Several advantages associated with it includes, painless, self-administration and reduced cost as compared to parenteral delivery⁸.

*Author for Correspondence: surajpal_1982@yahoo.co.in

ARTICLE IN PRESS

Saudi Pharmaceutical Journal xxx (xxxx) xxx



Contents lists available at ScienceDirect

Saudi Pharmaceutical Journal

journal homepage: www.sciencedirect.com



Original article

Design and evaluation of sustained release mucoadhesive film of sumatriptan succinate containing grafted co-polymer as the platform

Surajpal Verma^{a,*}, Rajiv Kumar Tonk^a, Mohammed Albratty^b, Hassan Ahmad Alhazmi^{b,c}, Asim Najmi^b, Ravi Kumar^d, Mohit Kumar^d, Mohamad Taleuzzaman^e, Gourav Swami^f, Md Shamsheer Alam^{b,**}

^a School of Pharmaceutical Sciences, Delhi Pharmaceutical Sciences and Research University, Delhi 110017, India

^b Department of Pharmaceutical Chemistry and Pharmacognosy, College of Pharmacy, Jazan University, P.Box No. 114, Jazan, Saudi Arabia

^c Substance Abuse and Toxicology Research Centre, Jazan University, P.Box No. 114, Jazan, Saudi Arabia

^d School of Pharmaceutical Sciences, Lovely Professional University, Phagwara 144411, Punjab, India

^e Department of Pharmaceutical Chemistry, Faculty of Pharmacy, Maulana Azad University, Village Bujhwar, Tehsil Luni, Jodhpur 342802, Rajasthan, India

^f Ananta Medicare Ltd., Sriganaganagar 335001, Rajasthan, India

ARTICLE INFO

Article history:
Received 19 April 2022
Accepted 23 July 2022
Available online xxxx

Keywords:
Migraine
Sumatriptan succinate
Grafted copolymer
Plasticizers
CCD

ABSTRACT

Purpose: The primary goal of this research is to improve the bioavailability and efficacy of Sumatriptan succinate by incorporating it in the mucoadhesive film for the treatment of migraine. Mucoadhesive film offers an excellent substitute to deliver the drug in the systemic circulation and eliminate the chance of first-pass metabolism.

Method: Using central composite design (CCD), various formulations were created by incorporating polymer, plasticizer, and water, and an optimized preparation was created using statistical screening. The optimization has been performed by applying a 3⁴ factorial method based on dependent variables such as Drug content (%), Swelling index (%), Folding endurance (Number of times), and Mucoadhesive strength (g).

Results: The actual experimental values obtained were compared with those predicted by the mathematical models. Formulation S9 was selected as an optimized formulation because it showed the lowest standard deviation between predicted and actual values compared to other formulations. In the case of the S9 formulation, approximately 77.12% of the drug was released within 24 h, but initially, it showed burst release. In addition, the *in-vitro* release of pure drug suspension showed 99.32% drug release within 2 h. That signified that the developed formulation provides sustained release due to presence of grafted co-polymer.

Conclusion: Formulation holding drug-loaded grafted film showed decent sustained and controlled drug release characteristics compared to a pure drug suspension. S9 formulation showed better results than other formulations in drug content, swelling index, folding endurance, and mucoadhesive strength, which is further used to treat migraine.

© 2022 Published by Elsevier B.V. on behalf of King Saud University. This is an open access article under the CC BY-NC-ND license (<http://creativecommons.org/licenses/by-nc-nd/4.0/>).

* Corresponding author at: School of Pharmaceutical Sciences, Delhi Pharmaceutical Sciences and Research University, Delhi 110017, India.

** Corresponding author at: Department of Pharmaceutical Chemistry and Pharmacognosy, College of Pharmacy, Jazan University, P.Box No. 114, Jazan, Saudi Arabia.

E-mail addresses: drsujpalverma@dpsru.edu.in, mosalam@jazanu.edu.sa (M.S. Alam).

Peer review under responsibility of King Saud University.



Production and hosting by Elsevier

<https://doi.org/10.1016/j.jsps.2022.07.014>

1319-0164/© 2022 Published by Elsevier B.V. on behalf of King Saud University.

This is an open access article under the CC BY-NC-ND license (<http://creativecommons.org/licenses/by-nc-nd/4.0/>).

1. Introduction

Migraine is a conjoint neurological or chronic illness categorized by occasional attacks of severe headache enduring 4–72 h associated with vomiting, nausea, photophobia, and phonophobia. It is more common in women with symptoms such as depression, anxiety, and severe pain (Jensen and Stovner, 2008; Diener et al., 2019; Vetvik and MacGregor, 2017). This disease is more common in women, and 14.7 percent of adults in the United States suffer from migraine. The novel approach for the therapy identified cervical nerves and neuropeptides (Antonaci et al., 2016; Charles, 2018). Migraines usually have a family history and affect people aged

Please cite this article as: S. Verma, R.K. Tonk, M. Albratty et al., Design and evaluation of sustained release mucoadhesive film of sumatriptan succinate containing grafted co-polymer as the platform, Saudi Pharmaceutical Journal, <https://doi.org/10.1016/j.jsps.2022.07.014>



MASTIC-G-POLY (ACRYLAMIDE): MICROWAVE-ASSISTED SYNTHESIS AND CHARACTERISATION

MOHIT KUMAR¹, SURAJPAL

School of Pharmaceutical Sciences, Lovely Professional University Phagwara, Jalandhar, Punjab, India
Email: mohitmehta9@gmail.com

Received: 18 Dec 2020, Revised and Accepted: 04 Feb 2021

ABSTRACT

Objective: The objective of the present investigation was the synthesis of grafted co-polymer gum mastic using acrylamide as the monomer.

Methods: 3-factor 3-level response surface Box-Behnken design, which requires 15 runs including three replicates of the central run, was used for the synthesis of graft copolymers of mastic gum with acrylamide using ceric ammonium nitrate as the free radical initiator. The critical synthesis and process parameters; CSPP (A = concentration of monomer, B = concentration of initiator and C= Temperature) to generate design space and optimize formulation with an aim to obtain critical quality attributes (CQA, Y1 =% Yield, Y2 =% Grafting, Y3 =% grafting efficiency).

Result: Formulation F14 having a maximum % yield of 75.89% with % grafting of 210% and % grafting efficiency 51.57% was selected as best.

Conclusion: The microwave-assisted grafted mastic gum was prepared successfully and optimized by using Box Behnken design.

Keywords: Mastic Gum, Microwave-assisted grafting, Acrylamide, Box Behnken design

© 2021 The Authors. Published by Innovare Academic Sciences Pvt Ltd. This is an open access article under the CC BY license (<https://creativecommons.org/licenses/by/4.0/>)
DOI: <https://dx.doi.org/10.22159/ijap.2021v13i2.40551>. Journal homepage: <https://innovareacademic.in/journals/index.php/ijap>

INTRODUCTION

Polymeric materials are widely used in pharmaceutical formulations, especially for making modified release formulations. Their specialty of controlling drug release rate is because of their structure and composition. These are long-chain compounds formed by monomers. These chains can be linear, branched and cross-linked [1, 2].

Grafted co-polymer includes a previously formed polymer backbone onto which the other species of polymer chains, which are of varying chemical nature, are attached at different sites of the polymeric backbone. The connected side chains may be comprising of a monomeric unit or of a binate mix. The one which is having one monomer only is easier to synthesize and generally happens in a solitary step; nevertheless grafting in the case of binate blend requires to be done in continuous and stepwise addition of the monomers [3-5].

A grafted co-polymer shows macromolecular series with single or multiple types of block molecule series associated with core polymeric backbone chain as various side chains. Graft polymerization is one of the most convenient methods to use various natural polysaccharides in extended drug delivery systems [6, 7]. Nowadays in polymer science the synthesis and use of these grafted copolymers in various applications is a major area for researchers. Employment of a peculiar or selected functional groups into the polymer affects the various chemical, physical as well as rheological properties of the compound. In comparison with other Asian countries, India is a rich source for these because of the inherent biodiversity [8-10].

The aim of the study was the development of a modified polymer from a natural gum by using a monomer and initiator.

MATERIALS AND METHODS

Materials

Mastic gum was obtained from Mastic grower association (Greece), acrylamide was purchased from Fisher Scientific Pvt. Ltd. (India), ceric ammonium nitrate was purchased from Qualikem Laboratories (India). Ethanol, petroleum ether and methanol were purchased from Merck, Mumbai, India.

Method

Grafting copolymerization of mastic gum

Mastic-g-poly(acrylamide) was prepared by redox initiator method. An accurately weighed 1.4 gm-2.8 gm of acrylamide was solubilized

in 30 ml of ethanol in a beaker and in another beaker, 0.5 gm of fine powder of mastic gum was dissolved in 10 ml of ethanol. Both these above solutions were mixed and an initiator i.e. ceric ammonium nitrate (CAN) of different concentrations (25 mg-75 mg) was added. This uniform solution was allowed for stirring at 60 °C for 4 h followed by solvent evaporation under reduced pressure. The residue was washed with methanol: water (70:30) to remove any homopolymers. The precipitated gum was dried under vacuum at 40 °C to obtain the dried product [11, 12].

Experimental design

A 3-factor 3-level response surface Box-Behnken design, which requires 15 runs, including three replicates of the central run, was used for the synthesis of graft copolymers of mastic gum with acrylamide using ceric ammonium nitrate as the free radical initiator. The critical synthesis and process parameters; CSPP (A = concentration of monomer, B = concentration of initiator and C= Temperature) to generate design space and optimize formulation with an aim to obtain critical quality attributes (CQA, Y1 =% Yield, Y2 =% Grafting, Y3 =% grafting efficiency). Different concentration of three CSPP (as shown in table 1) viz., A = polyacrylamide with their low (1.4 g), medium (2.1 g) and high level (2.8 g) and B = ceric ammonium nitrate with their low (25 mg), medium (50 mg) and high level (75 mg) and Temperature low (40 °C), medium (50 °C) and high level (60 °C) were selected. Box behnken design was applied using design expert software [13, 14] (version 7.0, Stat-ease, Inc, USA) and the polynomial equation generated was given below:

$$Y = \beta_0 + \beta_1 A + \beta_2 B + \beta_3 C + \beta_4 A.B + \beta_5 A.C + \beta_6 B.C + \beta_7 A_1^2 + \beta_8 B_2^2 + \beta_9 C_2^2$$

Where Y is the dependent variable, β_0 is the arithmetic mean response of the 15 runs and β_1 ($\beta_1, \beta_2, \beta_3, \beta_4, \beta_5, \beta_6, \beta_7, \beta_8, \beta_9$) is the estimated coefficient for the corresponding factor A, B and C, which represents the average results of changing one factor at a time from its low to high value. The interaction term (A, B, A, C and B, C) depicts the changes in the response when three factors are simultaneously changed. The polynomial terms A^2 , B^2 and C^2 are included to investigate the quadratic model. The magnitude of coefficients in the polynomial equation has either a positive sign indicating a synergistic effect or a negative sign indicating an antagonistic effect. Best fitting experimental model (linear, two factor interaction and quadratic) was taken statistically on the basis of comparison of



Office of the Controller General of Patents, Designs & Trade Marks
Department of Industrial Policy & Promotion,
Ministry of Commerce & Industry,
Government of India



Application Details

APPLICATION NUMBER	201811024277
APPLICATION TYPE	ORDINARY APPLICATION
DATE OF FILING	29/06/2018
APPLICANT NAME	Lovely Professional University
TITLE OF INVENTION	A NOVEL GRAFT COPOLYMER OF NATURAL GUM FOR DELIVERY OF PHARMACEUTICALLY ACTIVE AGENTS
FIELD OF INVENTION	CHEMICAL
E-MAIL (As Per Record)	dip@lpu.co.in
ADDITIONAL-EMAIL (As Per Record)	dip@lpu.co.in
E-MAIL (UPDATED Online)	
PRIORITY DATE	
REQUEST FOR EXAMINATION DATE	26/02/2020
PUBLICATION DATE (U/S 11A)	26/07/2019
REPLY TO FER DATE	15/01/2021

Application Status

APPLICATION STATUS	Application in Hearing
--------------------	-------------------------------

[View Documents](#)

FORM 5
THE PATENTS ACT, 1970
(39 OF 1970)
&
THE PATENT RULES, 2003
DECLARATION AS TO INVENTORSHIP



[See Section 10(6) and Rule 13 (6)] Lovely Professional University

1. Name of Applicant

hereby declare that the true and first inventor(s) of the invention disclosed in the Complete specification filed in pursuance of our application numbered **IN201811024277** dated are:

2. Inventor(s)

a. Name: **VERMA, Surajpal**

b. Nationality: Indian

c. Address: Lovely Professional University, Jalandhar-Delhi G.T. Road, Phagwara 144411, Punjab, India

a. Name: **KUMAR, Mohit**

b. Nationality: Indian

c. Address: Lovely Professional University, Jalandhar-Delhi G.T. Road, Phagwara 144411, Punjab, India

a. Name: **VYAS, Manish**

b. Nationality: Indian

c. Address: Lovely Professional University, Jalandhar-Delhi G.T. Road, Phagwara 144411, Punjab, India



ONE DAY NATIONAL CONFERENCE ON Advanced Bioanalytical Techniques, Artificial Intelligence and Health Sciences

Organized by
ISF College of Pharmacy, Moga
In collaboration with
Society of Pharmaceutical Education & Research (ISPER)

24th DECEMBER 2019

Certificate

This is to certify that Dr./Mr./Ms. Mohit Kumar.....
from L.P.U. Phagwara (Punjab).....has
participated in Poster Presentation / Kahoot Online Quiz Competition and awarded
prize in One Day National Conference on "Advanced Bioanalytical Techniques, Artificial Intelligence &
Health Sciences" organized by ISF College of Pharmacy, Moga.

ORGANIZING SECRETARY
Prof. (Dr.) Goutam Rath
ISFCP, Moga

ORGANISING SECRETARY
Dr. Upendra Nagaich
Secretary, SPER

CONVENER & PRESIDENT (SPER)
Prof. (Dr.) G. D. Gupta
Director-cum-Principal
ISFCP, Moga

Prof. (Dr.) Y. K. Gupta
President (GB), AIIMS, Bhopal
Chairman, RAC
ISFCP, Moga

PATRON
Parveen Garg
Chairman
ISFCP, Moga







Centre for
Research Degree Programmes

LPU/CRDP/PHD/EC/20170926/001392

Dated: 19 Nov 2021

Mohit Kumar
Registration Number: 41600044
Programme Name: Doctor of Philosophy (Pharmaceutics)

Subject: Letter of Candidacy for Ph.D.

Dear Candidate,

We are very pleased to inform you that the Department Doctoral Board has approved your candidacy for the Ph.D. Programme on 04 Mar 2017 by accepting your research proposal entitled: "FORMULATION, OPTIMIZATION AND EVALUATION OF MICROWAVE ASSISTED ACRYLAMIDE GRAFTED COPOLYMER AS NOVEL MATRIX FOR SUSTAINED RELEASE TABLETS" under the supervision of Dr. Surajpal Verma.

As a Ph.D. candidate you are required to abide by the conditions, rules and regulations laid down for Ph.D. Programme of the University, and amendments, if any, made from time to time.

We wish you the very best!!

In case you have any query related to your programme, please contact Centre of Research Degree Programmes.

Head
Centre for Research Degree Programmes

Note:-This is a computer generated certificate and no signature is required. Please use the reference number generated on this certificate for future conversations.